THE UNIVERSITY *of* EDINBURGH

Targeting Bone-Microenvironment-Tumour Cell Interactions:

IGF-1 Receptor Kinase Inhibitors.

John Logan MSc

A thesis submitted for the degree of Doctor of Philosophy

University of Edinburgh

2012

To my parents for all their support

DECLARATION

I hereby declare that this thesis has been composed by myself and the work described within, except where specifically acknowledged, is my own and that it has not been accepted in any previous application for a degree. The information obtained from sources other than this study is acknowledged in the text or included in the references.

John Logan

Contents

ACKNOWLEDGEMENTS

Firstly I would like to give my most profound thanks to my primary supervisor Dr. Aymen Idris. His enthusiasm for science in general and this project in particular has been an inspiration to me as I begin my academic career and without him this project could never have been a success. I will miss his help, his insight and our long and almost daily chats both on and off the topic of my research. I would also like to extend my gratitude to my co-supervisor Dr Val Brunton for her invaluable advice and support. Our meetings were always a pleasure.

I am most grateful to Prof. Stuart Ralston for finding time to be on my thesis committee and for the direction and encouragement he gave me. Dr. Rob van't Hof was always willing to give his excellent technical advice, his support, and to put up with me whenever I came to tell him something wasn't working. Special thanks must also go to Morwenna Muir and Lorraine Rose for their help with the *in vivo* side of the project and Dr Antonia Sophocleous for her friendship and help with the histology. I would like to extend my thanks to all past and present members of the Bone Group and the Brunton/Frame group. Of particular note are Dr. Omar Albagha, Dr. Anna Daroszewska, Dr. Philip Riches, Dr. Alan Serrels, Dr Brian Serrels, Ken Rose, Sarah Alison, Micaela Rios, Leila Shaw, Sam Gray, Dr Arek Welman, and Euphemie Landao. A special thank you to Belinda Stephens for all the work she does.

Thank you to my friends both in the group and without for all you did for me over the years and for keeping me sane. Dr Manu Coste, Roslynn McConnell, Rosie Walker, Gareth Briggs, Lowri Hughes, Silvia Marino, Nerea Alonso, Niki and Stephan Meerman and all the other students at the IGMM whose company I enjoyed.

Finally I would like to thank my family and most importantly of all, my girlfriend Rebecca without whom I could never have achieved anything.

This work was supported by the University of Edinburgh, Cancer Research UK, the MRC and the Institute of Genetics and Molecular Medicine.

PUBLICATIONS FROM THESIS

Papers

Frantzias,J., **Logan,J.G.,** Mollat,P., Sparatore,A., Del,Soldato P., Ralston,S., and Idris,A.I (2012) Hydrogen sulphide-releasing diclofenac derivatives inhibit breast cancer-induced osteoclastogenesis *in vitro* and prevent osteolysis *ex vivo*. *British Journal of Pharmacology* 165(6): 1914

Logan,J.G., Sophocleous,A., Muir,M., Brunton,V.G., and Idris,A.I. Selective tyrosine kinase inhibition of insulin-like growth factor-1 receptor inhibits human and mouse breast cancer induced bone cell activity, bone remodelling and osteolysis.*(Submitted)*

Sophocleous,A., **Logan,J.G**., Mackintosh,A., Landao-Bassonga,E., Ralston,S. and Idris,A.I. The CB2 receptor regulates osteoclast formation, breast cancer cell migration and osteoclast - tumour cell interaction via PI3K/Akt pathway. *(In preparation)*

Marino, S., **Logan J.G.,** Mollat, P., Mognetti, B., Ralston, S.H., Idris,A.I. Pharmacological and genetic inhibition of IKKβ activity inhibits breast cancer-induced osteoclastogenesis, promote osteoblast activity and prevent osteolysis. *(In preparation)*

Abstracts, Oral Presentations & Awards

10th International Conference on Cancer-Induced Bone Disease Sheffield 2010

Poster presentation **Logan,J.G.** *et al* Bone 48, Issue1, Jan 2011, Page S43

Awarded: **Travel Award**

3rd Joint Meeting of the ECTS and IBMS Athens 2011

Oral and Poster presentation **Logan,J.G.** *et al* Bone 48, Supp2, May 2011, Page S257

Awarded: **New Investigator Presentation Prize**

3rd Joint Meeting of the ECTS and IBMS Athens 2011

Oral presentation (by Sophocleous) Sophocleous,A and **Logan,J.G.** *et al* Bone 48, Supp2, May 2011, Pages S73-S74

Awarded: **Travel Award**

ABBREVIATIONS

1,25-$(OH)_2$ vitamin D_3	1,25-dihydroxyvitamin D_3
aa	Amino acid
AEA	Anandamide
ALP	Alkaline Phosphatase
αMEM	Alpha-Minimum Essential Medium
ANOVA	Analysis of variance
BCA	Bicinchoninic acid
BFR	Bone formation rate
β-GP	Beta-glyderol phosphate
BM	Bone Marrow
BMD	Bone mineral density
BMP	Bone morphogenetic protein
BMPR	Bone morphogenetic protein receptor
bp	Base pair
BSP	Bone sialoprotein
BV/TV	Trabecular bone volume to total volume
C57BL/6	An inbred mouse strain
Ca^{2+}	Calcium ions
cAMP	Cyclic AMP
Cbfα1	Core-binding factor α1
CDS	Coding sequence
c-Fms	Receptor of M-CSF
CFU-GM	Colony forming unit granulocyte-macrophage
Cl^-	Chloride ions
CNS	Central nervous system
COLIA1	Type I collagen
C-terminus	Carboxyl-terminus
CTX	C-terminal telopeptides of type I collagen
DEPC	Diethyl Pyrocarbonate
dH_2O	Distilled water
DMSO	Dimethyl sulfoxide
ECM	Extracellular matrix
EDTA	Ethylenediaminetetraacetic acid
EP2	PGE2 receptor
ER	Oestrogen receptor
ERK	Extracellular regulated kinase
ET1	Endothelin-1
FCS	Fetal Calf Serum
FGF	Fibroblast growth factors
FSH	Follicle stimulating hormone
FSHR	Follicle stimulating hormone receptor
G	Gauge
g, mg, µg, ng	Gram, milligram, microgram, nanogram
GM-CSF	Granulocyte-macrophage colony stimulating factor
H^+	Hydrogen ions
HBSS	Hank's balanced salt solution

HCO_3^-	Bicarbonate ions
HRP	Horseradish peroxidase
IC_{50}	Half maximal inhibitory concentration
IFNγ	Interferon gamma
IGF	Insulin growth factor
IκB	Inhibitor of NFκB
IKK	IκB kinase
IL (R)	Interleukin (receptor)
JNK	c-Jun N-terminal kinase
K^+	Potassium ions
kb	Kilobase
kg	Kilogram
l, ml, µl	Litre, millilitre, microlitre
LEF	Lymphoid-enhancer binding factor
LRP	LDL receptor-related protein
M, mM, µM, nM	Molar, millimolar, micromolar, nanomolar
mA,	Milliampere
MAPK	Mitogen activated protein kinase
MAR	Mineral apposition rate
M-CSF	Macrophage colony stimulating factor
µCT	Micro computed tomography
MEA	2-Methoxyethyl acetate
MEK	MAPK kinase/ERK kinase
Mϕ	Macrophages
Mm, nm	Millimetre, nanometre
MMA	Methyl methacrylate
MMP	metalloproteinase
MSC	Mesenchymal stem cells
Na^+	Sodium ions
NFATc1	Nuclear factor of activated T cells 1
NF-κB	Nuclear factor κB
N-terminus	Amino-terminus
OA	Osteoarthritis
OB	Osteoblast
Ob.N/BS	Osteoblast number per bone surface
OC	Osteoclast
Oc.N/BS	Osteoclast umber per Bone Surface
Oc.S/BS	Active resorption area per bone surface
OCN	osteocalcin
OPG	Osteoprotegerin
OPN	Osteopontin
OSN	Osteonectin
Osx	Osterix
p	Probability
PBS	Phosphate buffered saline
PDGF	Platelet-derived growth factors
PGE2	Prostaglandin E2
PI3K	Phosphatidylinositol-3-Kinase

PINP	N-terminal propeptide of type I procollagen
PKA/B/C	Protein kinase A/B/C
PPARγ2	Peroxisome proliferator-activated receptor γ2
PTH	Parathyroid hormone
PTHR1	Type 1 PTH/PTHrP receptor
qPCR	Real time quantitative PCR
RANK	Receptor activator of NF-κB
RANKL	Receptor activator of NF-κB ligand
RGD	Arg-Gly-Asp tripeptide
RNA	Ribonucleic Acid
ROI	Region of interest
RPM	Revolutions per minute
Runx2	Runt-related transcription factor
sd	Standard deviation
sem/SEM	Standard error of mean
SNP	Single nucleotide polymorphism
SOST	Sclerostin
Sox	DNA-binding SRY box
Tb.N	Trabecular number
Tb.Pf	Trabecular pattern factor
Tb.Sp	Trabecular separation
Tb.Th	Trabecular thickness
TE	Tris EDTA
TGF-β	Transforming growth factor-β
TNF (R)	Tumour necrosis factor (receptor)
TRAcP	Tartrate-resistant acid phosphatase
TRAF	TNF receptor-associated factor
Trizol®	Total RNA Isolation reagent
UPL	Universal Probe Library
UTR	Untranslated region
UV	Ultraviolet
v/v	Volume to volume
VEGF	Vascular endothelial growth factor
w/v	Weight to volume

LIST OF FIGURES

LIST OF TABLES

Targeting Bone-Microenvironment-Tumour Cell Interactions:

IGF-1 Receptor Kinase Inhibitors.

John Logan
Institute of Genetics and Molecular Medicine
University of Edinburgh

ABSTRACT

Bone metastases are a frequent clinical complication associated with cancer. The aim of this PhD thesis was to set up a model system for the study of tumour cell – bone cell interactions *in vitro*, *ex vivo* and *in vivo* and to use this system to test the efficacy of a novel therapeutic agent for the treatment of osteolytic bone disease.

Co-culture or conditioned medium studies using human or mouse cancer cell lines were used to develop an *in vitro* model system of tumour cell – bone cell interactions. This showed that osteolytic tumour cells enhance osteoclast formation, fusion and resorption through the production of various factors that act directly on osteoclasts and their precursors. And in addition, that osteolytic tumour cells also enhance osteoclastogenesis indirectly via increasing the production of RANKL in osteoblasts. Other effects on osteoblasts included reductions in differentiation, migration and adhesion. Successful *ex vivo* and *in vivo* models for the study of tumour – induced osteolysis were created using adapted organ cultures and intratibial injection techniques respectively.

IGF-1 and its receptor are known to play important roles in both bone metabolism and breast cancer. Therefore a study of the effects of IGF-1 receptor inhibition on tumour cell – bone cell interactions was performed. *In vitro* studies showed that the novel IGF-1 receptor tyrosine kinase inhibitor PQIP significantly inhibited IGF-1 and breast cancer enhanced osteoclast formation. Western blot analysis suggested this may be due to the inhibition of both IGF-1 and cancer conditioned medium induced PI3k/Akt activation. Moreover, treatment of osteoblasts with PQIP inhibited cancer cell conditioned medium induced increases in RANKL production. *Ex vivo* studies using human MDA-MB-231 – mouse calvarial organ co-cultures demonstrated that MDA-MB-231 cells caused osteolysis and this was completely prevented by PQIP without affecting cancer cell viability. Furthermore,

once daily oral administration of PQIP significantly decreased trabecular bone loss and reduced the size of osteolytic bone lesions following mouse 4T1 breast cancer cell intratibial injection in mice. Quantitative histomorphometry showed a significant reduction in breast cancer-induced osteoclast number and activity. Consistent with the significant inhibition of osteoblast differentiation, spreading, migration and bone nodule formation observed *in vitro*, PQIP also inhibited osteoblast number and bone formation *in vivo*. No inhibition of *in vivo* tumour volume was observed. These findings clearly suggest that oral PQIP treatment reduced the rate of cancer associated bone turnover.

In conclusion, this thesis successfully demonstrates a model system for investigating tumour cell-bone cell interactions *in vitro, ex vivo* and *in vivo*. Using this model system I showed that pharmacologic inhibition of IGF-1 receptor kinase activity using PQIP inhibits osteoclast and osteoblast changes induced by breast cancer cells *in vitro* and *in vivo* and prevents osteolysis *ex vivo* and *in vivo*. This indicates that PQIP and its novel derivatives which are now in advanced clinical development may be of value in the treatment of osteolytic bone disease associated with breast cancer.

Chapter 1

Introduction

1 Introduction

1.1 Bone

Bone is a specialised connective tissue that together with joint tissues makes up the skeleton. The structure and functions of bones differs greatly from the lay view of them as fixed rigid organs simply providing structure to the body. In fact the bone microenvironment is a highly dynamic and constantly redeveloping region that not only supports structure but has a variety of other functions including; aiding mobility, providing protection for internal organs, storing minerals and growth factors, and allowing haematopoiesis (1).

The skeleton is traditionally thought to contain two types of bone, flat bones such as the skull, scapula or ilium, and long bones such as the tibia, femur and radius. These two types differ both in structure and the way they are formed during development. Flat bones are derived entirely by intramembranous ossification, where bone forms by direct mineralization of mesenchyme tissue. Long bones, on the other hand, form mainly through the process of endochondral ossification, where a pre-existing cartilage structure is digested by chondroclasts and replaced with bone (1). Three further sub-categories of bone also exist, which accomadate bones that do not fit exactly into either the long bone or flat bone categories. These are short bones which are similar to long bones but are as wide as they are long; examples include tarsals and carpals, irregular bones which have complex, irregular shapes such as the vertebrae or sacrum, and sesamoid bones such as the patella, which are embedded in tendons.

Once formed, long bones have a cylindrical shape with a central medullary cavity that hosts the haematopoietic bone marrow. They consist of a long bony tube called the diaphysis attached to wider extremities, the epiphyses, by an intermediary zone called the metaphysis (Figure 1.1). A layer of hyaline cartilage, known as the growth plate, separates the metaphysis and epiphysis during growth. Once growth is complete this also mineralises leaving behind the epiphyseal line. Flat bones consist of two layers of bone enclosing a thin, flattened medullary cavity filled with bone marrow (1).

Structurally, bone consists of two tissues types; cortical or compact bone and trabecular or cancellous bone. Cortical bone forms the dense outer shell of bones, while the more metabolically active trabecular bone consists of interconnected 'spongy' trabeculae adding strength by spanning across the medullar cavity of flat bones and at the end of the long bones (Figure 1.1).

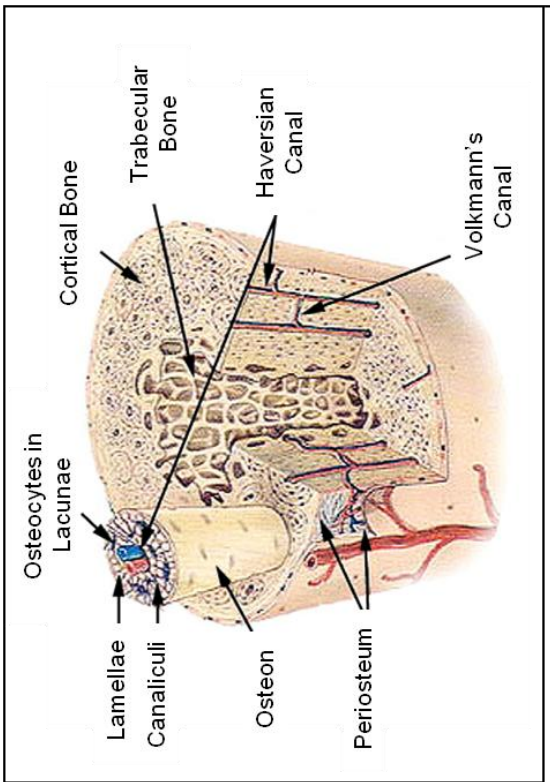

Figure 1.1 Diagram displaying the basic structure of long bones

See text for details. Adapted from National Cancer Institute SEER training module A) http://training.seer.cancer.gov/anatomy/skeletal/classification.html B) http://training.seer.cancer.gov/anatomy/skeletal/tissue.html

Cortical bone, or compact bone, is highly mineralized bone that makes up around 85% of the skeleton and undergoes minimal remodelling (1). It forms the cortex of most bones and is there to protect organs, allow movement and store minerals. In humans and other large mammals, cortical bone is found as a series of cylindrical structures parallel to the long axis of the diaphysis called osteons or Haversian systems (Figure 1.1). Each osteon is several millimetres long and consists of compact repeated layers of calcified bone matrix, called lamellae, concentrically surrounding a central vascular canal known as the Haversian canal (2, 3). At the edges of cortical bone the series of osteons are surrounded by multiple external and sometimes internal circumferential lamellae layers as well as the outer periosteum membrane. The Haversian canals allow blood and nerve vessels to pass through the bone and to the cells within. They are connected to one another and the periosteum blood and nerve vessels by transverse or obliquely situated canals that perforate the concentric lamellae, these are called perforating canals or Volkmann's canals. As layers of successive lamellae are layed down osteocytes become trapped between the concentric layers in lacunae. The osteocytes are connected to one another and the Haversian canal by numerous minute interconnecting cannals called canniculi which contain fine cytoplasmic extensions of the osteocytes (2, 3).

The 'spongy' trabecular bone makes up the remaining 15% of the skeleton, and is found throughout flat bones, but only at the extremities of long bones. It is surrounded and filled by bone marrow, which makes it metabolically more active (1). Trabecular bone is also composed of osteons but, as opposed to cortical bone, the lamellae run parallel to each other. In addition, while 80-90% of the cortical bone is mineralized, only 15-25 % of trabecular bone is mineralized (Figure 1.1).

Bone matrix comprises of two components, the organic matrix and the inorganic mineralised matrix. 90% of the organic bone matrix is made of type I collagen fibres found in the osteons mentioned above (1). The remaining 10% consists of non-collagenous proteins, including proteoglycans, osteopontin (OPN), osteonectin (OSN), osteocalcin (OCN), and fibronectin. The main purpose of these highly specialized proteins is either to aid in ossification or to allow bone cells to adhere to the bone matrix.

The main component of the inorganic mineralised matrix is crystals of hydroxyapatite [$Ca_{10}(PO_4)_6(OH)_2$] orientated in the same direction as the organic collagen fibres (1). It has dual purposes; firstly it adds strength to the organic matrix allowing bone to serve its roles of providing structure and protection. Secondly, the inorganic mineralised matrix is a major body reserve of a variety of minerals including magnesium, phosphate and calcium.

1.2 Bone Cells

Bone cells are highly specialised cells that develop skeletal structure by bone modelling and maintain the integrity of this structure through a constant cycle of bone remodelling. The main bone cell types are the bone-resorbing osteoclasts, the bone-forming osteoblasts, osteocytes and the bone lining cells.

1.2.1 Osteoblast

Osteoblasts are mononuclear bone cells that produce the matrix constituents required for bone formation. They are found as clusters of cuboidal cells along the bone surface and are characterised by a round nucleus opposite the bone surface, extensive endoplasmic reticulum and an enlarged Golgi complex (1). This allows osteoblasts to produce and secrete large amounts of connective tissue matrix (1).

Osteoblasts are mesenchymal cells derived from mesodermal and neural crest progenitor cells called mesenchymal stem cells (MSC) found in the bone marrow. These cells also give rise to a range of other cell types, including, chondrocytes, adipocytes and myocytes (1, 4). A combination of various hormones, growth factors and transcription factors control the osteoblast lineage pathway transforming MSCs into osteoprogenitors, preosteoblast, mature osteoblasts, and finally bone lining cells or osteocytes (Figure 1.2).

While Bone Morphogentic Proteins (BMP) are thought to initiate the initial transformation from MSC to osteoblast, the major transcription factor responsible for the commitment of MSCs towards the osteoblastic lineage is Runt-related transcription factor 2 (Runx2) (5). Mice deficient in Runx2 do not develop mature osteoblasts, and as a result these mice are unable to form mineralised bone (6, 7). Runx2 regulates a variety of osteoblast specific genes including the gene coding another protein essential for osteoblast differentiation, the zinc finger transcription factor Osterix (Osx). This controls the expression of a variety of osteoblastic genes, including type 1 collogen (Col1a1), and causes osteoprogenitor cells to further differentiate into osteoblasts (Figure 1.2) (8, 9). Both Runx2 and Osx also modulate the Wnt signalling pathway in osteoblasts and their pre-cursors (10,

11). This promotes osteoblast differentiation at the expense of other progeny cells of MSC's, particularly adipocytes.

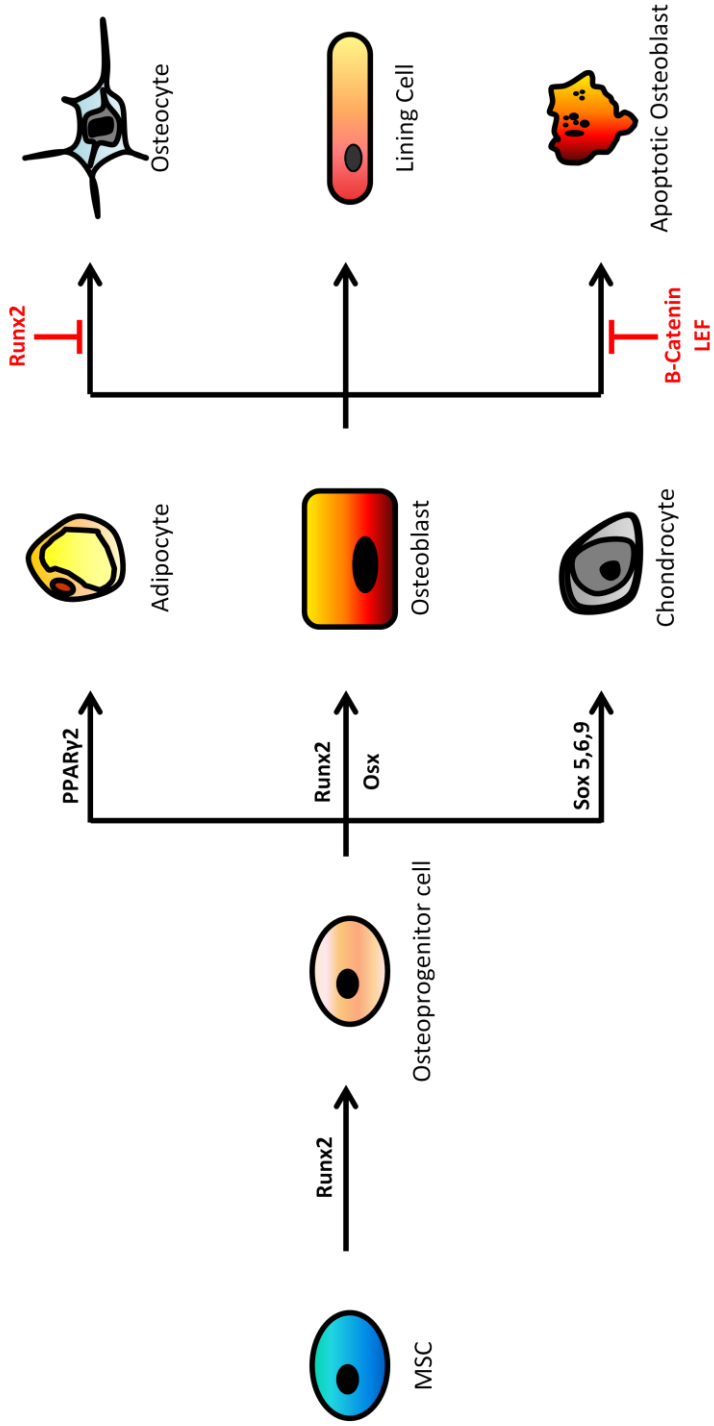

Figure 1.2 Diagram showing the differentiation of cells of the osteoblast lineage. Mesenchymal Stem Cells (MSC) require the expression of Runx2 and Osterix (Osx) to differentiate into osteoblasts. Expression of PPARγ2 or Sox 5, 6, 9 cause differentiation of osteoprogenitors into adipocytes or Chondrocytes respectively. Mature osteoblasts can differentiate into Osteocytes, Lining cells, or undergo apoptosis. Runx2 expression inhibits osteocyte differentiation while β-Catenin and LEF expression inhibit apoptosis. See text for more details.

A variety of external factors influence the differentiation, survival and function of osteoblasts by either altering the expression of Runx2 or Osx, or by reducing activity of the pro-adipogenesis factor PPARγ2 (12). Factors that up regulate osteoblast differentiation include several endocrine system proteins such as parathyroid hormone (PTH) and its related protein (PTHrP) (13-15), oestrogen (16), and vitamin D3 (17, 18), as well as growth factors and cytokines (12) including Insulin-like Growth Factor 1 (IGF-1) (19), BMPs (20-22), Transforming Growth Factors (TGFs) (23), Fibroblast Growth Factors (FGFs) (24) and Indian hedgehog (Ihh) (25). Conversely, pro-inflammatory cytokines, including Tumour Necrosis Factor Alpha (TNFα), inhibit Runx2 expression and so down regulate osteoblastagenesis through the activation of the NFκB signalling pathway (26, 27) (Figure 1.3).

Osteoblasts serve two physiological functions, one direct and anabolic and the other indirect and catabolic. Osteoblasts anabolically synthesize new bone through the secretion of the unmineralised organic bone matrix called osteoid (28). Osteoid consists of type 1 collagen, but also contains some specialised bone matrix proteins, including OCN, OPN and BSP that aid in ossification, regulate bone formation, and allow other osteoblasts to adhere to the matrix. Importantly, osteoblasts also produce alkaline phosphatase (ALP) which aids bone formation by breaking down pyrophosphate and other such inhibitors of bone matrix mineralisation. ALP is also used as a serum marker for osteoblast activity (1).

The catabolic role of osteoblasts is to support osteoclastogenesis through the stimulation of the differentiation of osteoclast pre-cursors and the activation of mature osteoclasts. This is achieved through the production of the key osteoclastic factors, Macrophage Colony Stimulating Factor (M-CSF) and Receptor Activator of Nuclear Factor Kappa-B Ligand (RANKL) (1). Osteoblasts also produce Osteoprotegerin (OPG), a decoy receptor for RANKL, which negatively regulates osteoclastogenesis (1). Through the expression of these proteins, osteoblasts are able to use paracrine signalling to control osteoclast formation and bone resorption (29).

Osteoblasts are not terminally differentiated, despite their non-proliferative status. Once their have performed their primary role they have three different possible fates. They can become buried within the bone matrix as osteocytes, they can undergo apoptosis, or they can become quiescent bone lining cells (30). These bone lining cells cover 95% of intracortical and 75% of trabecular bone (31), and while their functions have not been fully

elucidated, are thought to protect bone from either resorption or formation as well as play a role in initiating bone remodelling (32) (Figure 1.2).

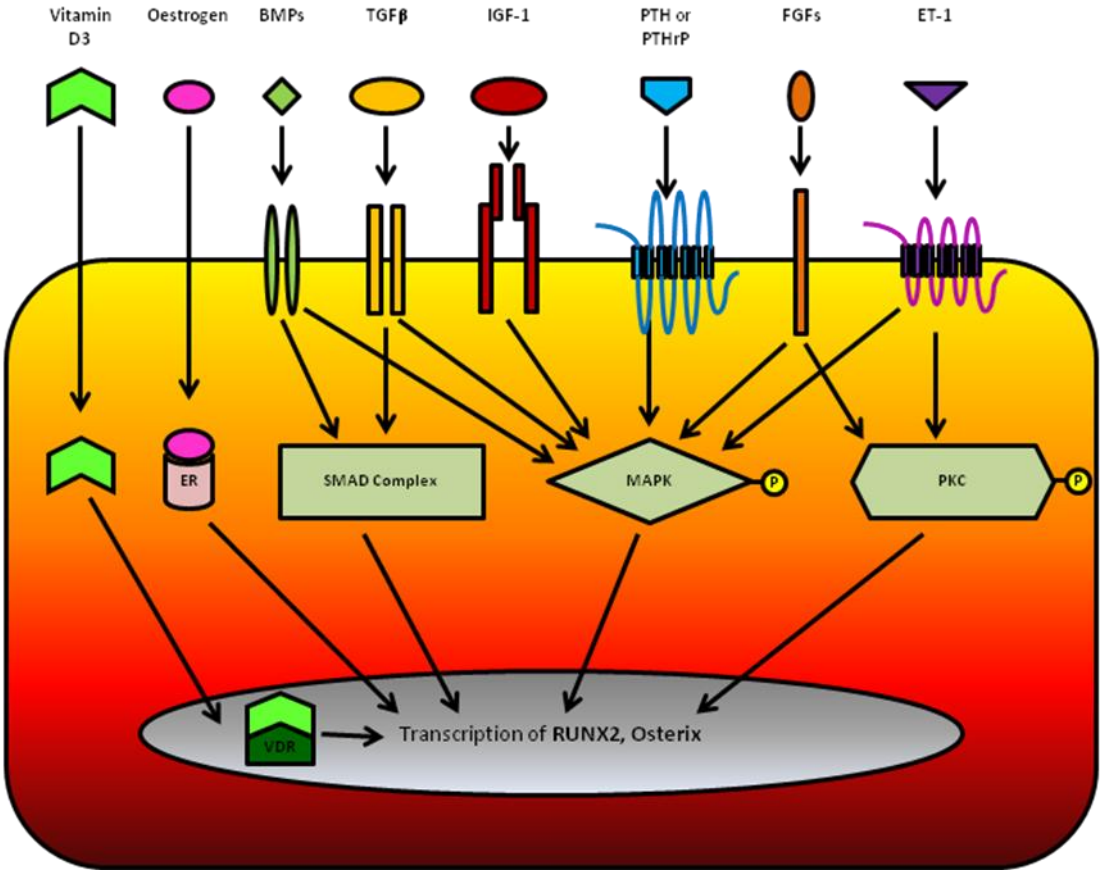

Figure 1.3 Diagram demonstrating key signalling pathways involved in osteoblast differentiation and function. See text for more details. *Abbreviations*: ER is oestrogen receptor, BMPs is Bone Morphogenic Proteins, TGFβ is Tumour Growth Factor Beta, IGF-1 is Insuilin-like Growth Factor 1, PTH is ParaThyroid Hormone, PTHRP is ParaThyroid Hormone Related Protein, FGFs is Fibroblast Growth Factors, ET-1 is EndoThelin 1, MAPK is Mitogen Activated Protein Kinase, PKC is Protein Kinase C, VDR is 1,25-$(OH)_2$ vitamin D_3 receptor, RUNX2 is Runt-related transcription factor 2.

1.2.2 Osteocyte

Osteocytes are terminally differentiated cells of the osteoblast lineage located within the bone matrix and account for more than 90% of bone cells found in the adult skeleton (33, 34). During the bone formation phase, 10-20% of mature osteoblasts become encased in the newly formed osteoid (1). These cells then begin to transform from polygonal cells, forming dendritic process which extend towards the mineralising front, followed by further dendrites which extend in the opposite direction, to either the vascular space or the bone surface (35). As the developing osteocyte becomes embedded deeper into bone it also undergoes various biochemical changes; alkaline phosphatase production declines, while osteocalcin and casein kinase II increase (35), transitioning its function away from that of the osteoblast. Currently there is debate over whether the recruitment of cells to become osteocytes is a passive process, and it is the act of being encased in osteoid that initiates the transformation (36), or an active process with signalling from existing osteocytes driving the conversion of active osteoblasts into osteocytes (37).

While osteocytes are becoming embedded in bone their dendritic processes have been extending through the new and old bone. This allows the osteocyte to join the "so-called" lacunocanalicular system. This system consists of osteocytes in lacunae connected to each other and bone lining cells through their dendrites, which pass through the bone in a network of fluid filled canaliculi tunnels (1, 38-40). The main functions of this system are thought to include a mechanosensory function and regulatory control of mineral homeostasis, as well as some control over both bone resorption and formation (reviewed in (33)).

Osteocytes are thought to regulate bone remodelling in a number of ways. Living osteocytes have been shown to support osteoclast formation by expressing RANKL, as well as supporting osteoblast differentiation (41). However, it is regulation of their death that is thought to give osteocytes greatest control over remodelling. Upon undergoing apoptosis, apoptotic bodies are released that express RANKL, therefore leading to the recruitment of osteoclasts (42). Osteocyte apoptosis occurs in response to microdamage of the bone. At these sites osteocytes express pro-apoptotic factors, while 1-2mm from the site they express protective anti-apoptotic factors, demonstrating that mechanisms exist preventing

the release of osteolytic factors nearby that may cause the resorption of healthy bone (43). It has been hypothesised that the presence of healthy osteocytes also inhibits bone resorption through an unknown mechanism, potentially by releasing anti-resorptive factors such as TGFβ (44). This is supported by work demonstrating that the selective deletion of β-catenin in osteocytes, so preventing the Wnt signalling necessary for their normal function, results in increased osteoclast activity and porous bones (45). The role of osteocytes in regulating bone resorption has recently been shown to be far more important than previously thought as Nakashima *et al* (2011) demonstrated that osteocytes produce a much higher amount of RANKL than osteoblasts, the cells currently thought to be the main regulators of osteoclast formation. In addition, they showed that osteocytes supported osteoclast formation better *in vitro* and that mice with RANKL conditionally knocked out only in osteocytes exhibit extreme osteopetrosis (46).

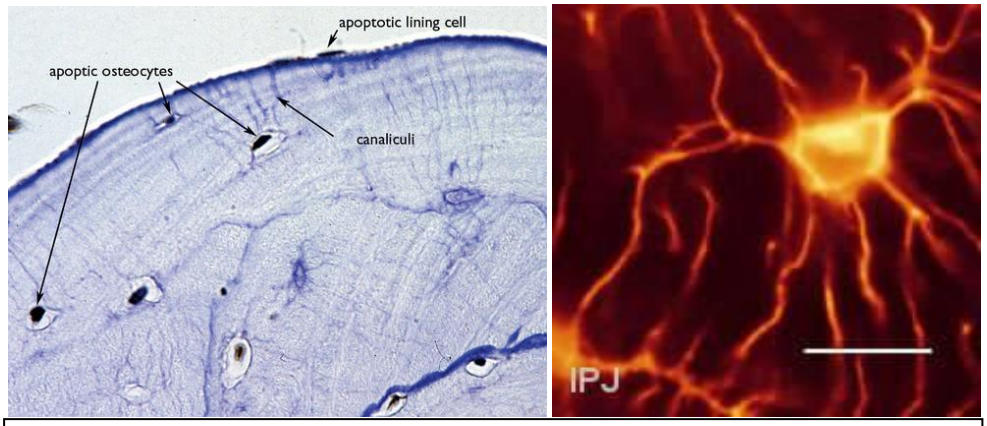

Figure 1.4. Images showing Osteocytes in lacunae and their dendritic network through the lacunocanalicular system. See text for more details.

A)Adapted from Weinstein *et al* Endocrinol Metab. 2000;85:2907-2912. B) Adapted from Meyle *et al* 2001 Int Poster J Dent Oral Med 2001, Vol 3

Osteocytes also regulate bone formation through the expression of Sclerostin (SOST). SOST is a negative regulator of Wnt signalling which is critical for osteoblast differentiation. Osteocyte SOST expression is known to be reduced in response to increased mechanical loading when bone becomes damaged (47-49). Osteocytes are also known to express a number of other factors that promote mineralisation (50), including Phosphate-regulating neutral Endopeptidase on chromosome X (PHEX) (51), Dentin Matrix Protein 1 (DMP1)(52), Matrix Extracellular Phosphoglycoprotein (MEPE)(53), and Fibroblastic growth factor 23 (FGF23) (54). DMP1, PHEX and FGF23 also contribute to controlling the levels of phosphate reabsorbed by the kidney, so regulating mineral homeostasis (55).

In addition to recruiting osteoclasts or osteoblasts, osteocytes are also capable of remodelling their own environment to a limited extent (56). This is achieved through the addition and/or subtraction of mineral within the lacunae and canaliculi by an unknown mechanism thought to be mediated by the PTH type 1 receptor (57).

1.2.3 Osteoclast

Osteoclasts are one of the most distinct and highly specialised cells in the human body. They are terminally differentiated, giant, multinucleated and highly motile cells that express various osteoclasts specific proteins such as tartrate-resistant acid phosphatase (TRAcP) and are formed by the fusion of multiple mononuclear monocyte/macrophage precursor cells (1, 58). Osteoclasts are specialised for one main purpose, the resorption of bone. This is achieved through dissolving the hydroxyapatite mineral component of bone and degrading the organic bone matrix (1).

Over the past three decades, there was much debate over the precise origins and lineage of osteoclasts, but in recent years it has become accepted that they are cells of hematopoitic descent. It has been demonstrated that to become osteoclasts cells must start as hematopoietic stem cells (HSC), which then progress through the colony forming units for granulocytes (CFU-GM) and macrophage (CFU-M) to become pre-osteoclasts and finally mature multinucleated osteoclasts (58, 59). The presence of two key

osteoclastagenic cytokines is required for this differentiation path to reach completion, M-CSF and RANKL (58, 60, 61) (Figure 1.5).

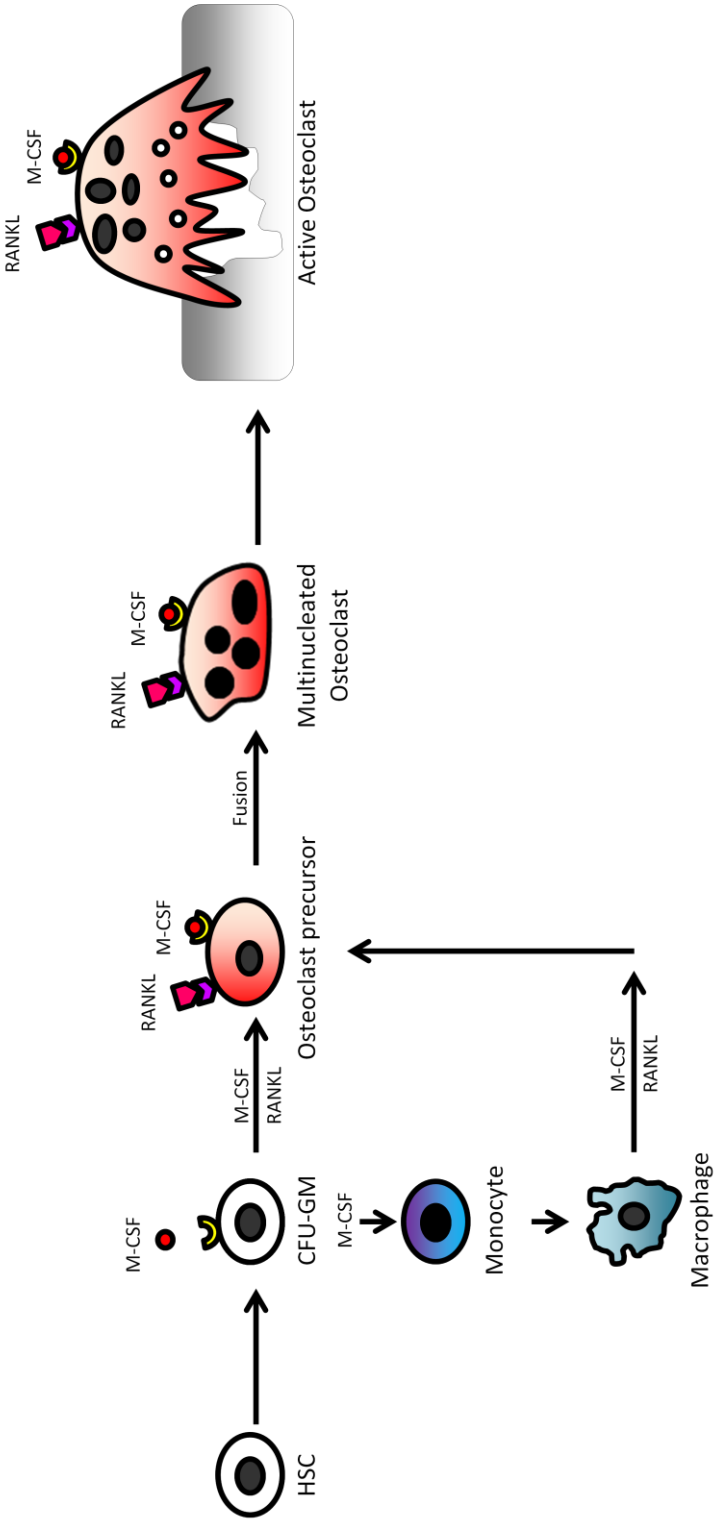

Figure 1.5 A diagram showing the differentiation of cells of the osteoclast lineage from Haematopoietic Stem Cells. Haematopoietic Stem Cells (HSC) differentiate into Colony Forming Units (CFU) of the Granulocyte/Monocyte cells (CFU-GM). When these cells are exposed to M-CSF they differenciate into cells of the Monocyte/Macrophage lineage. If these cells or macrophage are also exposed to RANKL they differentiate into osteoclast precursor cells. These osteoclast precursors then fuse together to form multinucleated osteoclast, which become active osteoclasts when they bind to bone. See Text for more details.

Secreted by osteoblasts and their precursors, M-CSF binds to its receptor, c-Fms, found expressed in all cells of the osteoclast lineage from early pre-cursors to mature osteoclasts (62). This stimulates signalling pathways that promote proliferation, differentiation and survival of osteoclast and their precursors (63, 64).

Once cells have committed to becoming pre-osteoclasts they start to express RANK, the RANKL receptor. The binding of RANKL to RANK stimulates various signalling pathways including the AP-1 and NFκB pathways, which in the absence of granulocyte-macrophage colony stimulating factor (GM-CSF), causes cellular changes that allow the mononuclear pre-osteoclasts to fuse together to form bone resorbing multi-nucleated mature osteoclasts (63, 64). In the presence of GM-CSF osteoclast pre-cursors are driven to become dendritic cells (65). RANKL is found in both soluble and membrane bound components produced by osteoblasts, osteocytes and activated T-cells (66), though it has recently been demonstrated that osteocytes are likely to be the major source of RANKL (46).

Various other factors are known to modulate the formation, fusion, function and survival of osteoclasts. These include Osteoprotegerin (OPG) which is a soluble decoy receptor for RANKL, and completes the RANK/RANKL/OPG axis recognised as the dominant regulator of osteoclastogenesis (1, 67). The rate of osteoclast formation is greatly determined by the ratio of RANKL to OPG present in the bone microenvironment (68). TNFα, IL-1 and PGE2 are known to activate transcription factors that promote osteoclast formation and survival (69, 70), whereas IL-6 and IL-11 act on osteoclast pre-cursors enhancing cell survival and proliferation (71). Finally, TGFβ has been found to increase the expression of RANK in osteoclast precursors (72) (Figure 1.6).

The process of bone resorption involves four key processes after the initial formation of osteoclasts. This starts with the attachment of the cell to the bone surface, followed by polarisation of the cell and the development of ruffled border and a sealing zone, then the secretion of acid and enzymes that resorb bone and finally the removal of resorbed products away from the resorption lacunae (59, 73, 74).

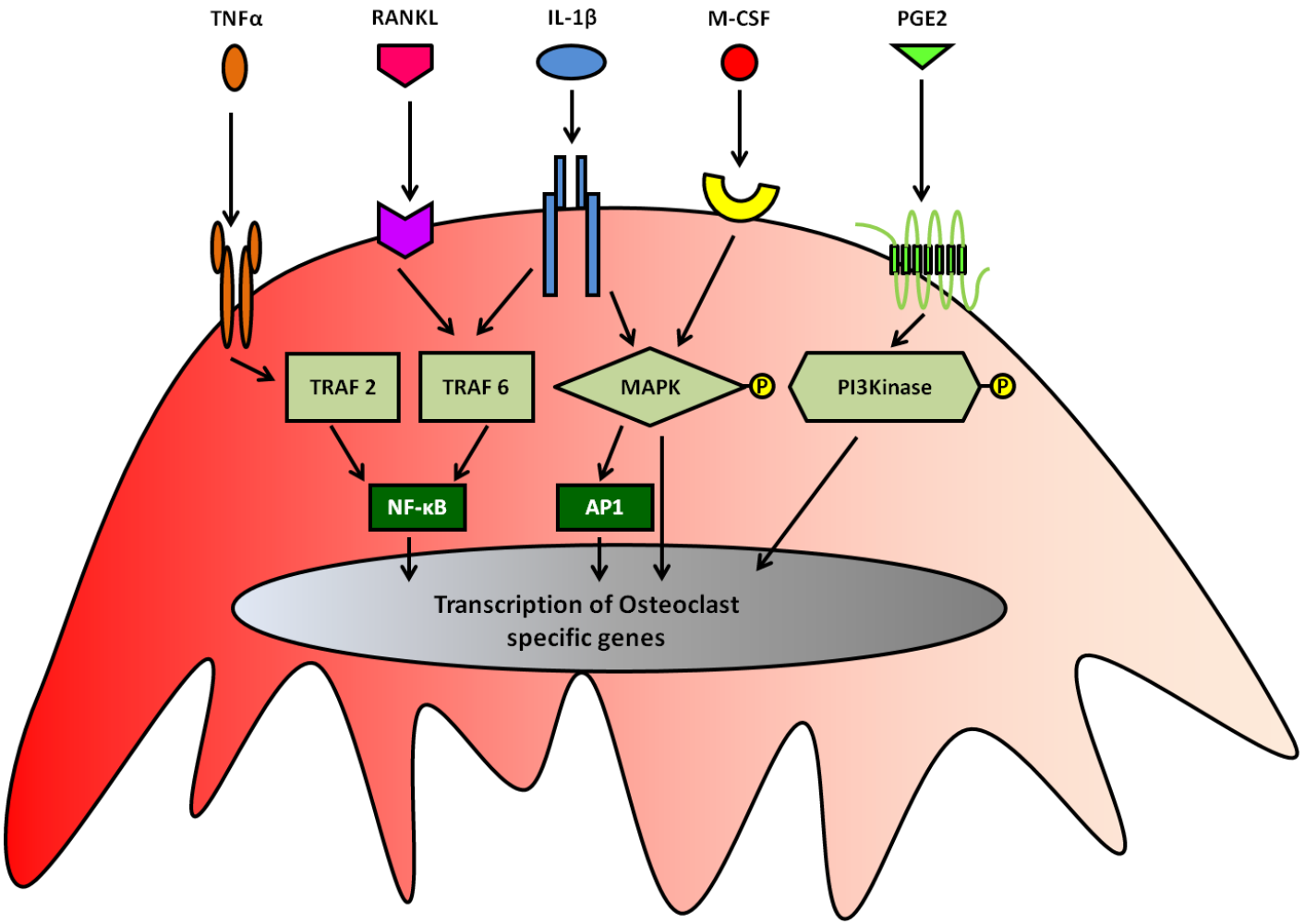

Figure 1.6 a representation of some of the signalling pathways involved in osteoclast differentiation and function.
See text for more details. *Abbreviations :* TNFα is Tumour Necrosis Factor Alpha, RANKL is Receptor Activator of Nuclear factor Kappa-B Ligand, IL-1β is Interleukin-1 beta, M-CSF is Macrophage Colony Stimulating Factor, PGE2 is Prostaglandin E2, TRAF 2/6 is TNF Receptor Associated Factor 2/6, MAPK is Mitogen Activated Protein Kinase, PI3Kinase is Phosphatidylinositol-3 Kinase, NF-κB is Nuclear Factor kappa-light-chain-enhancer of activated B cells, AP1 is Activator Protein 1.

It is not known what attracts osteoclasts to a particular bone site, but some research suggests that this may be linked to osteocyte cell death (42, 75). Once osteoclasts have reached the site to be resorbed, they become polarised and produce actin rich structures called podosomes which fix the cell to bone via an attachment of αvβ3-integrins to Arg-Gly-Asp (RGD) peptides moderated by the activity of c-Src (59, 76). This forms a tight circular 'actin ring' sealed by proteins such as CD44 (77) and known as the sealing zone which is completely isolated from the extracellular space. Within this 'zone' the complex finger-shaped folded membrane projections known as the ruffled border forms; it is this that is the major resorbing organelle (1, 59).

Bone resorption occurs in the isolated compartment of the 'sealed zone' where osteoclasts secrete protons, chloride ions and acidic vesicles containing such proteins as Matrix Metaloprotease 2 (MMP-2) and cathepsin K (63, 78-81). Protons are produced through a two-step reaction; firstly, carbonic anhydrase catalyses the hydration of carbon dioxide into carbonic acid ($H_2O + CO_2 \rightarrow H_2CO_3$). This then dissociates into a bicarbonate ion and proton ($H_2CO_3 \rightarrow HCO_3^- + H^+$), both products of which are useful to osteoclasts (82). The hydrogen ion is taken by the ATP-consuming proton pump known as vacuolar ATPase (V-ATPase) which passes the ion through the ruffled border and into the sealed zone. In contrast, the bicarbonate ion is excreted through the apical membrane. This occurs through a chloride/bicarbonate anion exchanger bringing the chloride ions (Cl^-) required into the osteoclast (83). The secretion of protons out of the cell means that in order to maintain charge equilibrium and intracellular pH the negatively charged chloride ions are soon passively passed out of the cell again and into the sealed zone through the CLCN7 chloride channel.

The presence of large quantities of both H^+ and Cl^- present in the sealed zone causes hydrochloric acid to form. This has the effect of lowering the pH to approximately 4.5 and causes the breakdown of hydroxyapatite mineral component of bone into Ca^{2+}, HPO_4^{2-} and H_2O (59). Once the mineral component has been removed, the organic collagen fibres and other matrix proteins are exposed. Enzymes such as MMP2 and cathepsin K that are released from the ruffled border then degrade the organic bone matrix components (59, 84) completing the resorption of the bone within the sealed zone. Degraded resorption products are endocytosed by the osteoclast and the endocytotic vesicles then fused with a

specialised membrane domain on the opposite side of the cell called the functional secretory domain (FSD). This releases the waste products into the extracellular fluid (85) (Figure 1.7).

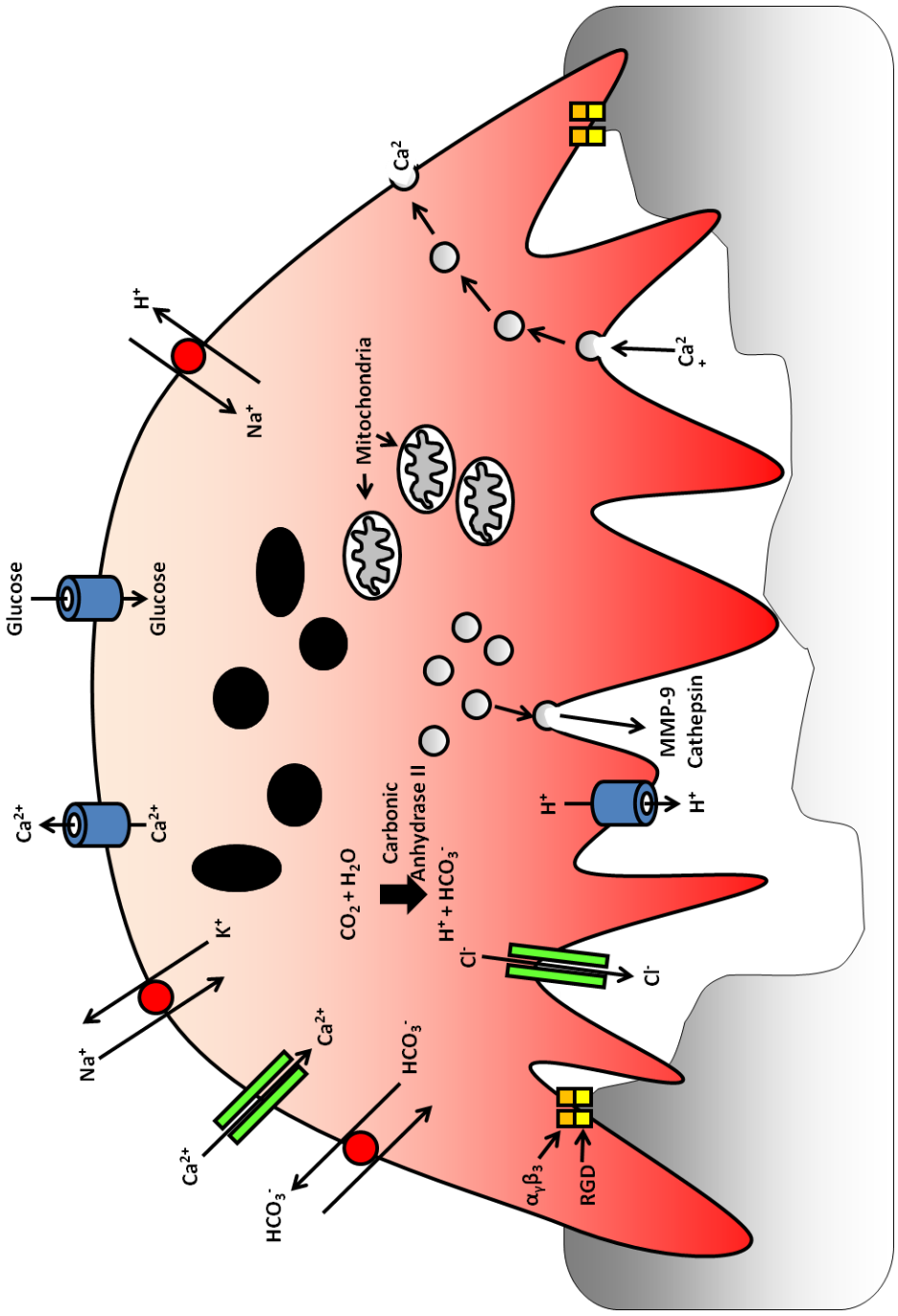

Figure 1.7 A diagram, showing the transport of proteins and ions involved in the resorpbtion of bone by osteoclasts. See text for more details. *Abbreviations:* RGD is Arg-Gly-Asp, MMP-9 is Matrix Metaloprotease 2

Along with visual identification, the most commonly used method of identifying osteoclasts is through stains and antibodies that bind to the TRAcP isoform TRAcP5b (Figure 1.8). It is therefore worth noting that the function of TRAcP is still not fully understood and that other isoforms of the enzyme are highly expressed in other cell types, such as dendritic cells (86). TRAcP -/- mice exhibit only a mild osteopetrotic phenotype and so it is thought that it is unlikely TRAcP plays a vital role in resorption or osteoclast formation and survival (86, 87). One possibility that has been hypothesised that it may in fact play a role in antigen processing and so rather than directly effecting resorption may protect against an auto-immune response to the products of bone resorption (58).

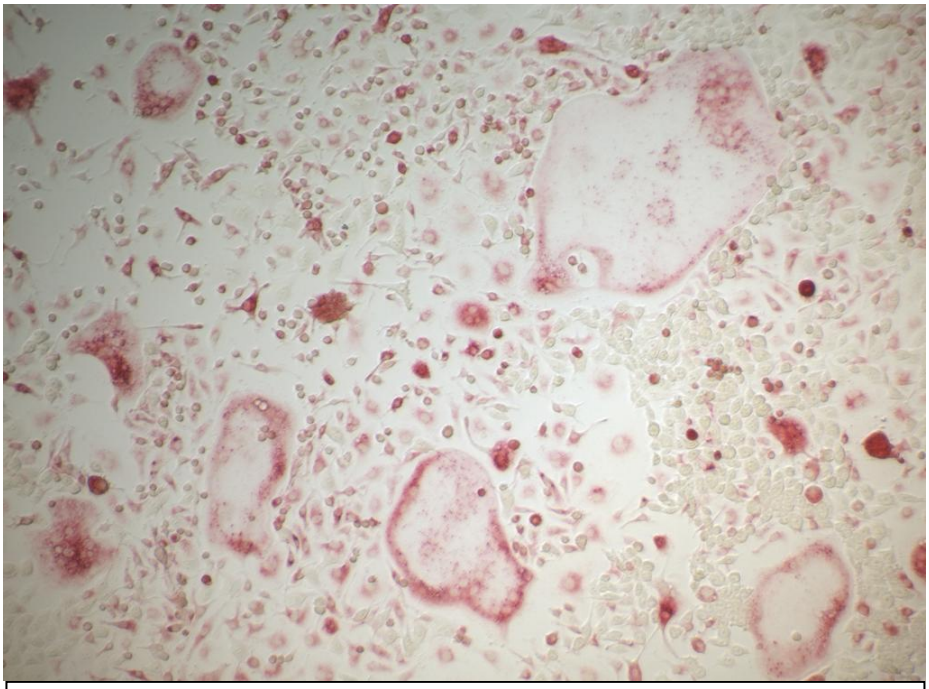

Figure 1.8 A Photomicrograph showing multinucleated osteoclasts stained for tartrate-resistant acid phosphatase (TRAcP). See text for more details. Osteoclasts are stained red by TRAcP stain.

1.2.4 Chondrocyte

In addition to bone, cartilage is also synthesised and deposited by specialised cells found in the bone microenvironment; chondrocytes (Figure 1.9). Like the bone matrix, the basic structure of cartilage is formed from an extracellular matrix mainly consisting of collagen, though this tends to be type II or type X collagen rather than the type I found in bone. Structural proteins such as elastin and proteoglycans, mainly aggrecan, are also present (88, 89). Three distinct types of cartilage are found in the mammalian body, distinguished by their differing extracellular matrix components. Hyaline cartilage is typical cartilage, while elastic cartilage has additional elastin fibres and fibrocartliage contains regions of organised fibrous tissue (89, 90). They are found in various places throughout the body, including for hyaline cartilage the larynx, trachaea, bronchus, articular cartliage and at the growth plates of long bones during development. Elastic cartilage is found in locations such as the ears, the larynx and epiglottis and fibrocartliage in locations such as the intravertebral discs and the meniscus (1).

Chondrocytes are similar to osteoblasts in many ways, but in stead of producing bone, produce cartilage. Chondrocytes and osteoblasts are both derived from MSCs, both secrete an extracellular matrix that forms tissue (osteoid from osteoblasts and the cartliagenous matrix from chondrocytes), both produce matrix vesicles, and both have prominent golgi aparatus, endoplasmic reticulum and large numbers of mitochondria to facilitate their functions. However unlike osteoblasts, chondrocytes are generally found within lacunae in the cartilage, rather than on the surface of bone, and are the only cell types to be found within their environment (91). The Sex determining region Y-Box (Sox) family of developmental transcription factors are the key drivers of chondrocyte development; causing them to be the first skeletal cells to arise during development. Sox9 induces the differentiation of MSCs into chondrocytes and activates the expression of aggrecan and type II collagen (92, 93). Sox 5 and 6 bind to Sox9 and enhance its transactivation function increasing differentiation and proliferation (94). All three also inhibit premature chondrocyte hypertrophy, the final cellular form of chondrocytes and a terminal differentiation that leads to endochondral bone formation. Once cartilage formation is complete, Runx2 and other factors stimulate the chondrocytes to become hypertrophic (95). This causes chondrocytes to express Vascular Endothelial Growth Factor

(VEGF) that stimulates blood vessel development, bringing in haematopoietic and osteoprogenitor cells into the environment and allowing bone development (91). Eventually chondrocytes either undergo apoptosis or are resorbed (91).

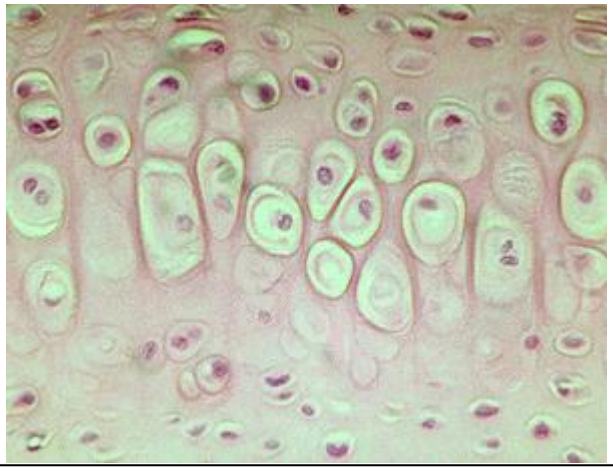

Figure 1.9 Histology image of chondrocytes in their lacunae.

From Develomental Biology Online
http://www.uoguelph.ca/zoology/devobio/210labs/ct2.html

1.2.5 Adipocyte

While not directly involved in bone modelling or remodelling, adipocytes are one of the most numerous cell types found in the bone marrow of long bones. They are derived from the same MSCs as the osteoblast lineage and their differentiation rate directly affects that of osteoblasts. Many studies have shown that as adipocyte differentiation increases, osteoblast differentiation decreases. In undifferentiated MSCs, the pro-adipogenic transcription factors CCAAT-enhancer binding proteins α and β, and peroxisome proliferation-activated receptor γ (PPARγ) counteract each other. PPARγ suppresses osteoblast differentiation by down regulating Runx2 expression, while Runx2 and Osx suppress adipocyte differentiation (12, 96). Once other signals tip the balance of transcription factor expression in one direction or the other MSCs begin to differentiate down either the adipocyte or osteoblast cell lineages.

In addition to PPARγ, a number of factors are known to play an essential role in regulating adipogenesis (97). These factors include the pro-adipogenic cyclic AMP response

element-binding protein (CREB), Kruppel-like factors (KLFs) and various others (reviewed in (96)).

It has long been established that adipocyte number negatively correlates to the amount of haematopoietic activity within bone marrow (98). They were thought to play a simple passive space filling role in bone marrow, forming in response to gaps left where there were fewer haematopoietic cells (98). However, recent work has demonstrated that adipocytes may in fact function as direct negative regulators of haematopoiesis (98-100). In this they would seem to continue their counteraction of the cells of the osteoblast lineage, which are known to support formation of the haematopoietic stem cell niche (99, 100).

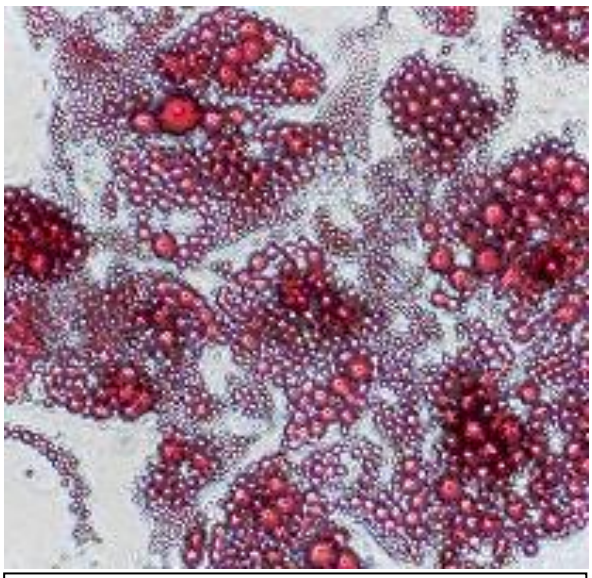

Figure 1.10 A photomicrograph of Adipocytes stained with oil red.

Adapted from Zen-bio.com (http://www.zen-bio.com/products/cells/adult_stem_cells.php)

1.3 Osteogenesis

The formation of bones during development occurs in two different ways: through the conversion of a cartilage template to bone, called endochondral ossification, or by the direct replacement of mesenchyme tissue with bone, called intramembranous ossification. This involves both bone modelling and remodelling, as bone is layed down by osteoblasts and removed by osteoclasts. Bone modelling is the uncoupled action of osteoblasts and osteoclasts which allows the shaping, growth and repair of bones; this means there is a net loss of material in one area, and a net gain in another. Bone remodelling on the otherhand is coupled, with the amount of bone resorbed and the new bone formed being equal in any one location.

1.3.1 Endochondral ossification

During early embryonic development most of what will become the appendicular and axial skeleton consists of a hyaline cartilage template to be replaced by bone. Ossification occurs at ossification sites, of which, in a typical long bone, there are three divided into two distinct types, a primary ossification site in the diaphysis separated from two secondary ossification sites at the epiphysis by the cartilage growth plate (1).

As the type II collagen cartilage template enlarges, chondrocytes at the centre differentiate into hypertrophic chondrocytes that are 5-10 times larger and are known to instead produce type X collagen (91, 101). They also secrete matrix molecules that aid in the recruitment and differentiation of osteoblast and osteoclast precursor cells including OPN, BSP and OSN (102). In addition, these hypertrophic chondroclasts release angiogenic factors, such as VEGF, which cause the vascularisation of the cartilage template (103). This serves two purposes, it allows the transportation of bone cell precursors into the environment and it also reduces the level of hypoxia in the area; a hypoxic environment is known to stimulate chondrocyte proliferation (104).

As the hypertrophic chondrocyte zone is invaded by bone cells and blood vessels, most of the chondrocytes undergo apoptosis. Osteoclasts form and begin to degrade the

provisional cartilage matrix, eventually removing up to 80% of it (105). Newly arisen osteoblasts use the remaining template as the basis for bone formation, producing osteoid that becomes the primary 'woven' bone. This is not yet mature lamellar bone and is repeatedly resorbed and reformed by osteoclasts and osteoblasts until development finishes (106).

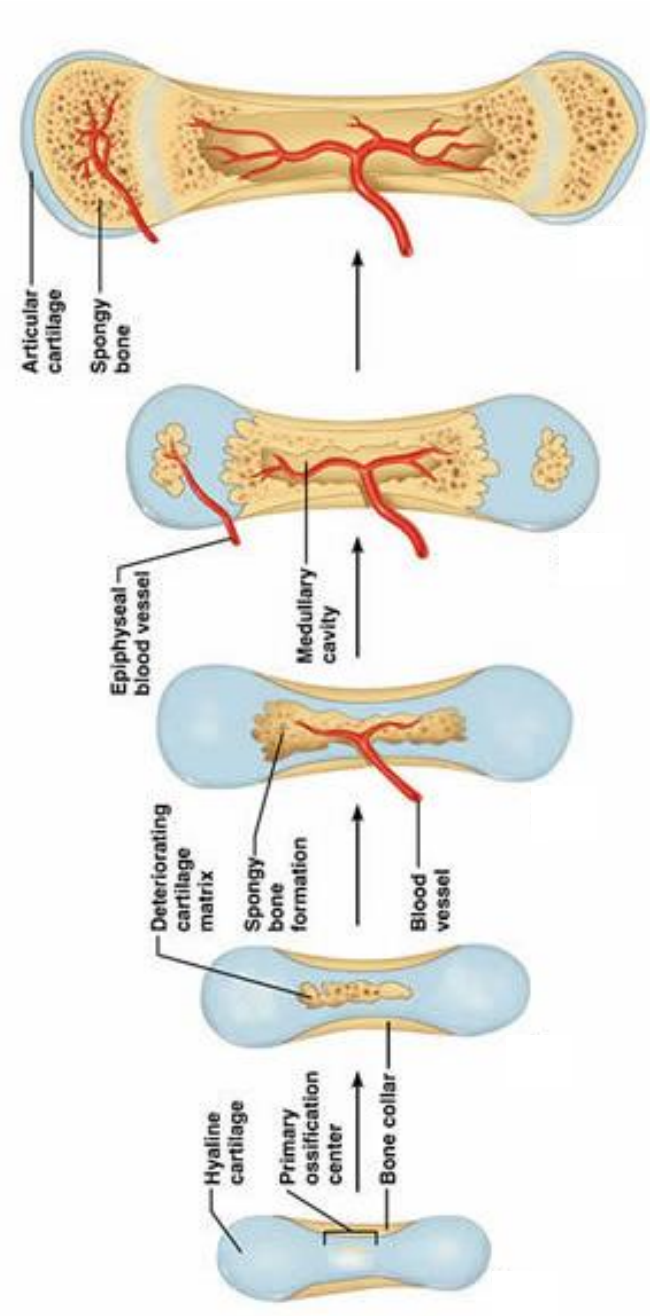

Figure 1.11 A diagram showing the process of endochondral ossification. See text for more details.
Adapted from http://wps.aw.com/bc_marieb_happlace_7_oa/42/10965/2807221.cw/index.html

This conversion of cartilage to bone first occurs at the primary ossification site in the centre of what will become the bone (Figure 1.11). As ossification continues and the bone marrow cavity expands towards the epiphyses, chondrocytes at the epiphyseal margin undergo rapid proliferation. This causes the formation of distinct longitudinal columns of chondrocytes that form a barrier between the epiphysis and the primary ossification site (102). This is known as the growth plate and during growth the rate of chondrocyte proliferation and cartilage production within it balances the replacement of cartilage with bone. This allows the longitudinal growth of the diaphsis of the bone, while maintaining the width of the growth plate. Later in development the secondary ossification centres form within the epiphyses, and are separated from the primary ossification site by the growth plate. This process is dependent on various growth factors stimulating chondrocyte proliferation, and so when the production of these growth factors declines at the onset of puberty the ossification rate begins to overtake the rate of cartilage production. Eventually the growth plate is reached by the 'ossification edge' and the dyaphysis becomes fused to the epiphysis completing bone growth (102, 103, 107).

1.3.2 Intramembraneous ossification

The development of flat bones occurs through the direct conversion of mesenchymal tissue to bone by intramembranous ossification. It should be noted that unlike other flat bones, the cranial bones originate from the neural crests.

While endochondral ossification required a hypoxic environment and is organised into distinct ossification centres, intramembraneous ossification requires vascularisation and occurs across various points of the tissue simultaneously (1). In certain embryonic tissues, MSCs proliferate, condense and form compact nodules of cells. Some MSCs in this nodule differentiate to form blood vessels, while others become the first osteoblasts. The newly formed blood vessels allow the tissue to be further infiltrated by osteoblasts and other bone cell precursors. These osteoblasts then secrete osteoid inside of the nodule which then is mineralised to become the first bone. As the calcification occurs bony spicules radiate out from the point of ossification, and the whole region of bone spicules is surrounded by further compact MSCs that develop into the periosteum. Eventually, the

bone spicules fuse together forming ‘woven’ bone which is then repeatedly remodelled by osteoclasts and reformed by mature osteoblasts to form lamellar bone (108).

Figure 1.12 A photomicrograph of a flat bone undergoing intramembraneous ossification. See text for details.

Adapted from http://www.technion.ac.il/~mdcourse/274203/lect5.html

1.3.3 Mineralisation, the Bone matrix and Matrix vesicles

Whichever of the two ways bones are formed, one of the vital aspects is the way in which tissue becomes mineralised and the inorganic bone matrix forms. As discussed above, osteoblasts produce osteoid, the unmineralised bone matrix, and chondrocytes produce the cartliagenous matrix. The regulation of the production of osteiod and cartliagenous matrix is well understood, however questions remains over precisely how these then become mineralised by the inorganic part of bone or cartliage and whether or not this process occurs via an active and regulated process or simply occurs in an inactive continuous process over time. It now seems likely both processes are involved to some extent.

The organic part of both bone and cartilage consist mainly of collagen fibres but these are interspersed with the non-collageneous proteins that make up ~10% of the bone protein content. These have a wide variety of functions, but are vitally involved in the process of mineralisation and the conversion of cartilage to bone. The non-collagenous proteins can be subdivided into 5 categories, serum derived proteins, the proteoglycans, the glycoproteins, the γ-carboxylated (gla) proteins and other proteins including lipids and enzymes (109, 110).

Serum derived proteins make up 25% of noncollageneous proteins. These are mostly acidic proteins such as albumin that bind to the bone matrix due to a high affinity for hydroxyapatite. While not endogeneously produced by bone cells these can still influence mineralisation, for example albumin can inhibit hydroxyapatite crystal growth (110).

Proteoglycans are heavily glycosylated proteins consisting of a core protein attatched to acidic polysaccharide side chains. Various members are found in the bone matrix including Versican, Decorin, Asporin, Fibromodulin, Biglycan, and Osteoadherin. These seem to have a number of different functions including, the allocation of space to become bone during early bone formation and chondrogenesis (Versican), the regulation of collagen fibrillogenesis and structure (Decorin, Biglycan, Asporin, Fibromodulin), limb patterning (Perlecan), and the attatchment of cells to the bone matrix (Osteoadherin) (109, 110).

The most diverse group of non-collageneous proteins found in the bone matrix are the glycosylated proteins. These include alkaline phosphatase which breaks down pyrophosphate, OSN which binds to growth factors and may influence the cell cycle, and importantly the small integrin-binding ligand, N-glycosylated (SIBLING) proteins. The SIBLING proteins all contain an RGB sequence that allows cells to attatch to them through integrin cell surface receptors. This allows cells, especially osteoclasts, to bind to and interact with bone. SIBLING proteins include OPN, BSP and DMP-1 (109, 110).

The matrix gla-containing proteins are three proteins, matrix gla protein, OCN, and protein S, which undergo post-translational modification by γ-carboxylases. The gla residues enhance calcium binding, but the physiological roles of these proteins are still

unclear. Matrix gla may be involved in the regulation of cartilage metabolism, while OCN is known to act as a hormone in glucose metabolism and may act as a coupling factor in bone remodelling, regulating osteoclast and their pre-cursors (109, 110).

As state above, many of these organic matrix components are thought to facilitate and condition the mineralisation of bone. This process occurs in two steps, starting with the formation of hydroxyapaptite crystals within matrix vesicles. Matrix vesicles are small (20-200 nm) spherical, lipid bilayer bounded, bodies that are formed by polarised budding from the plasma membrane of chondrocytes and osteoblasts (111, 112). These matrix vesicles have a different composistion to their parent membranes with a far higher amount of alkaline phosphatase, as well as other components such as phosphatidylserine, annexins, nucleotide pyrophosphatase phosphodiesterase 1, and the type III Na^{+}/PO_4^{3-} cotransporters Pit1,2 and Phospho-1 (113). These facilitate the accumulation of calcium and phosphates within the matrix vesicles until their concentrations exceeed the solubility point of $CaPO_4$ and this is deposited within the matrix vesicles as hydroxyapatite. This becomes a primary mineral nucleation point and allows secondary mineralisation to build on the existing hydroxyapatite crystal (111-113).

This second stage of mineralisation occurs when the forming hydroxapatite crystals breech the matrix vesicle membrane and expand into the extracellular space. This expansion occurs due to the maintainance of high levels of Ca^{2+} and PO_4^{3-} in the extracellular space by ion pumps on osteoblasts (112). Hydroxapatite crystals then form clustered around the initial matrix vesicle crystals and fill the space between collagen fibrils. This process then continues with clusters from multiple primary nucleation sites combining until the organic bone matrix is fully mineralised (111-113).

1.4 Bone Remodelling

Bone is not dormant once it has been formed through the process of modelling. Instead, throughout life the skeleton is continuously broken down and reformed through the coordinated actions of osteoclasts and osteoblasts. This is called bone remodelling. Over time bone becomes damaged, this may occur through exercise, or in response to mechanical stresses and mechanical loading. In order to maintain the shape, strength and integrity of the whole bone the damaged parts of it must be continuously removed and replaced. This occurs to the extent that the entire adult human skeleton is replaced every ten years (114). To achieve this, discrete packets of remodelling are used, called bone remodelling units (BMU), which are geographically and chronologically isolated from all other remodelling packets (1). Within each BMU the cellular activity of osteoclasts and osteoblasts is coupled so that the net amount of bone remains the same. Outside of bone that is in the resting phase, all bone will be undergoing one of three bone remodelling processes. These are; bone resorption, where bone is digested by osteoclasts, the reversal phase, where bone resorption is coupled to bone formation, and bone formation, where osteoblasts synthesise new bone (1, 115) (See Figure 1.13).

1.4.1 Bone Resorption

The lining cell layer covering quiescent bone is disrupted in response to unknown signals thought to be generated by osteocytes, lining cells themselves, or pre-osteoblasts (116). This initiates the resorption phase. To prepare the bone for resorption MMPs, collagenase and gelatinase are first produced by lining cells (117). This leads to a thinning of the osteoid layer. Next, the key osteoclastogenic factors RANKL and M-CSF are produced by osteocytes (41), osteoblasts and lining cells (61, 118-120). This causes an expansion in the osteoclast progenitor pool and triggers the formation of multi-nucleated osteoclasts. Finally, lining cells detach from the surface of the bone to be resorbed, allowing the forming osteoclasts access to the now osteoid free mineralised bone surface (115, 118).

The multinucleated osteoclasts bind to the bone surface, allowing them to polarise their membranes to form the specialised organelles of active osteoclasts. Extracellular bone

matrix proteins (OPN and vitronectin in particular) are recognised by osteoclast podosomes containing actin filaments and αVβ3 integrin, allowing the formation of an actin ring (115, 121). This actin ring, aided by proteins such as CD44 (77), causes an intimate binding of the cell and the bone surface. The bind is so close that the area beneath the actin ring is completely isolated from the extacellular fluid. This isolated region is known as Howship's lacuna or the sealing zone (122).

The ruffled border of the osteoclast forms inside the sealed zone, allowing the osteoclasts to secrete protons and chloride ions into the area. This is done through V-ATPases and passive chloride channels respectively (82, 83). As a result, a localised extremely acidic environment is created where pH can be as low as 4.5. At such a low pH the mineralised component of the bone matrix breaks down; hydroxyapatite crystals are converted into $Ca^{2+,}$ HPO_4^{2-} and H_2O (59). This exposes the organic bone matrix, which is subsequently degraded by the release of vesicles from the ruffled border. These vesicles contain factors such as Cathepsin K and MMP9 which digest collagen I through the release of carboxyterminal peptides, thereby removing the major organic component of bone (63, 78-81, 123).

By this point, while the bone matrix may have been destroyed, resorption is not over, as the broken down fragments of both the mineral and organic components remain within the lacunae. To complete bone resorption these components must be removed from the freshly resorbed area. To do this osteoclasts ingest these fragments through endocytosis. The vesicles containing the waste products are then secreted through the FSD at the apical membrane and into the extra cellular compartment at the opposite side of the osteoclast to the bone surface (85).

Overall, bone resorption lasts for about ten days and ends when the osteoclasts have achieved the required erosion depth. Once this has occurred, the osteoclasts begin to undergo apoptosis and signal the beginning of the reversal phase (115).

1.4.2 Reversal Phase

The reversal phase is the process that couples the bone resorption phase to the bone formation phase and is thought to last about 9 days in humans. Osteoclasts undergo apoptosis and osteoblast precursors migrate to the newly resorbed bone. Mononuclear macrophage like cells also appear on the bone surface and these cells remove the

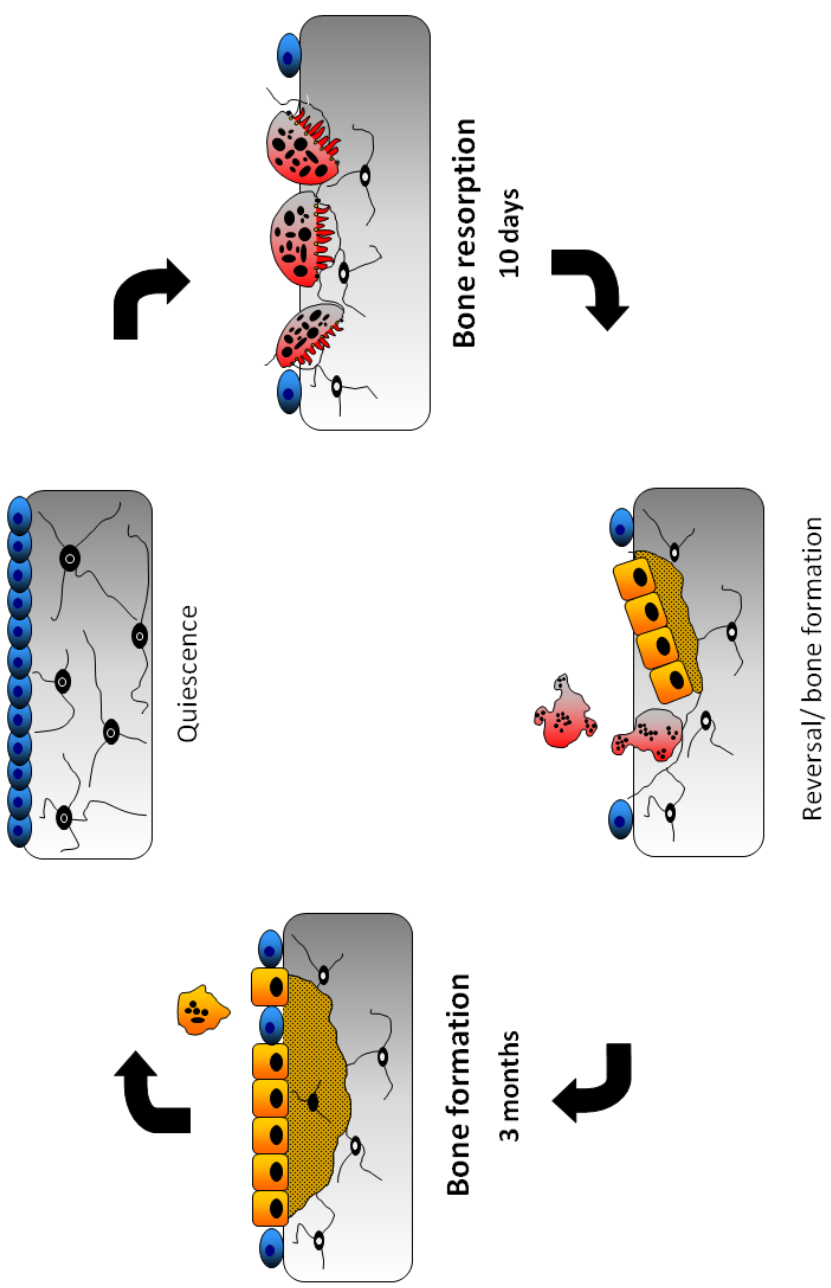

Figure 1.13 A diagram showing the processes involved in the bone remodelling cycle. See Text for more details.

remaining organic residues and causes the formation of the cement line which marks the limits of bone resorption and joins the new bone to the old (1, 115, 124).

The processes that trigger the reversal phase are poorly understood, but several mechanisms have been proposed. First, it may simply be that osteoclasts have a finite lifespan and die after a set amount of time or resorption activity has passed (115). Secondly, it has been observed that a high concentration of calcium builds up in the resorption lacunae over time, this causes an inhibition of osteoclast activity and a reorganisation of actin that leads to podosome disassembly and subsequently cell death (125). Lastly, it may be that the build up of factors released from the bone matrix, such as TGFβ and IGF-1, causes the inactivation of osteoclasts and signals osteoblasts to migrate to the freshly resorbed region (126, 127).

1.4.3 Bone Formation

The final stage of the remodelling cycle is the deposition of new bone to replace that which was resorbed. This is the bone formation phase. The first stage of this is the recruitment of osteoblast precursor cells to the site of resorption. The migration of these cells is mediated by chemotactic agents released from the bone matrix by resorption (128). The most likely factors involved are the pro-osteoblast factors TGFβ and IGF-1, which are abundantly found in the bone matrix.

Once the osteoblast progenitor cells have reached the freshly resorbed site they proliferate and differentiate into mature osteoblasts. This is again mediated by factors released from the bone matrix during resorption, further coupling the bone formation to bone resorption. Factors thought to play roles in osteoblast precursor proliferation include IGF-1 and 2, FGFs, TGFβ and its superfamily, and platelet-derived growth factors (PDGFs) (115). The differentiation to mature osteoblasts is also stimulated by many of these same factors, in particular IGF-1 and BMP2 (a member of the TGFβ superfamily) are important.

The formation of new bone by osteoblasts is initiated by the production of the organic components of the bone matrix. This mostly consists of type I collagen interspersed with the non-collagenous osseous proteins including OCN, OPN, BSP, OSN and

proteoglycans (28). To complete the process, this unmineralised osteoid is transformed into mineralised bone. ALP, produced by osteoblasts, breaks down pyrophosphate inhibitors of mineralisation, which both induces mineralisation and provides inorganic phosphate for the process (1). The extracellular phosphate and calcium ion levels are maintained by osteoblast ion transporters, allowing hydroxyapatite crystals to form continuously within the osteoid. This gives it rigidity and strength as it is converted into fully mineralised bone.

Once the appropriate amount of bone has been formed, the osteoblasts stop producing any new bone. The precise mechanisms by which bone formation is terminated are currently unknown, but it has been hypothesised that it may be due to factors such as SOST released by osteocytes. SOST inhibits osteoblast activity and may lead to osteoblasts becoming lining cells (129). Osteoblast apoptosis, triggered by various bone derived factors, may also be one of the key mechanisms by which bone formation is terminated. Overall the bone formation phase lasts around three months and ends with 65% of osteoblasts undergoing apoptosis while the rest are converted into lining cells or buried in the newly formed matrix as osteocytes (130). The bone then enters the resting phase again, with the quiescent lining cells awaiting the initiation of the next remodelling cycle.

1.4.4 Resting phase

During this phase, lining cells cover the surface of bone and osteocytes are buried within newly filled resorption lacunaes. Bone remains in this state for an indefinite time until a remodelling cycle is signalled (115).

1.5 Cancer and Bone

Cancer cells are groups of cells that have mutated in such a way that they undergo abnormal explosive proliferation and fail to undertake properly controlled apoptosis. Cancer occurs in the bone microenvironment in two different ways. It can originate from bone cells leading to primary bone cancer diseases such as multiple myeloma, osteosarcoma, or Ewing's sarcoma. More commonly though, malignant cancer cells arrive in the bone microenvironment as metastatic cells that have migrated from a primary tumour to form a secondary malignancy within bone. In either case they cause damage to the surrounding bone by either, in the case of some primary tumour, producing abnormal bone tissue, or more commonly through the disruption of the bone remodelling cycle in the surrounding bone. This leads to an imbalance with either excess bone formation, or bone resorption resulting in the formation of osteoblastic, osteolytic or mixed lesions. These can be asymptomatic or cause symptoms ranging from pain and loss of strength or movement, to deformity and pathological fractures.

1.5.1 Primary bone tumours

Primary cancers of bone are relatively rare tumours that appear in two types, benign or malignant. In general, with certain exceptions, most types are far more common among children and juveniles than adults; this is most probably related to the reduction in bone metabolism as bone modelling finishes at the end of growth (131). Symptoms include bone pain, abnormal bone growth and skeletal fractures.

1.5.1.1 Benign primary bone tumours

Benign tumours include neoplasms, such as osteoid osteoma, osteochondroma, and osteoblastoma, as well as a variety of cysts, including enchondroma. Giant cell tumour of bone is also generally considered a benign tumour, but can rarely become malignant. While many benign bone tumours may cause pain or restrict movement, most are not

considered serious and are left to regress on their own or if it is thought necessary may be removed through surgery.

1.5.1.1.2 Osteoid osteoma

Osteoid osteomas are benign bone forming tumours of less than 2cm in size that are found in long bone cortex of young adults (132). They are more common in men than women by a ratio of 3:1 and account for almost 13% of benign bone tumours (133). They consist of a network of 'woven' trabeculae of variable degrees of mineralisation, surrounded by osteoblasts with scattered osteoclast-like multinucleated giant cells (134). Many osteoid osteomas spontaneously regress and they are never life threatening, but they can cause extreme pain. Standard treatments are pain relief by NSAID treatment, or removal through either traditional surgery or advanced minimally invasive techniques such as percutaneous radiofrequency ablation (RFA) (133, 135).

1.5.1.1.3 Osteoblastoma

Osteoblastomas are similar to osteoid osteomas both clinically and histologically but have the potential for progressive growth (132, 136). Like osteoid osteomas they generally occur in young adults and occur more often in men but are characterised as being larger than 2cm in size and cause a dull pain that is not treatable with NSAIDS (136). These tumours consist of woven bone rimmed by osteoblasts and containing abundant osteoclasts. They affect the surrounding cortical bone, leading to either excess bone growth or focal lytic lesions. Overall prognosis is good as with the exception of rare variants metastasis is virtually unknown, and even in these variants metastatic potential is low. Treatment is generally surgical excision using traditional techniques, or rarely using RFA (132, 137).

1.5.1.1.4 Fibrous dysplasia

Fibrous dysplasias (FD) represent between 5 and 7% of benign bone tumours and are caused by a local failure of the ability to produce lamellar bone (132, 138, 139). This results in the formation of immature woven bone that cannot be properly remodelled and becomes enmeshed in dysplastic fibrous tissue. Most cases are identified before the age of 30 and there is no gender preference. It is divided into monostotic (60% of cases) or the more serious polyostotic (40% of cases) which is often a symptom of a more serious underlying condition such as endocrine dysfunction or McCune-Albright syndrome (140). While monostotic FD is often asymptomatic, it generally causes localised thinning of the surrounding cortex and abnormal bone mineralisation which may result in pain, deformity, fractures and loss of strength (132). Generally FD is not life threatening but in 2.5% of cases may progress to become malignant osteosarcoma or fibrosarcoma (138). Bisphosphonates are successfully used to manage the condition in many cases, but surgery followed by bone grafts may be performed to correct deformities and prevent future fractures (138).

1.5.1.1.5 Osteochondroma

Osteochondroma is one of the most common bone tumours, representing over a third of all benign tumours (132). It occurs exclusively in bones formed by endochondral ossification and is generally found within the first two decades of life, most commonly in men (132). Tumours are contiguous with the underlying bone and consist of a cartilage capped bony projection with a marrow cavity that usually points away from the nearest joint due to muscle pull (132). In most cases these tumours are isolated and asymptomatic but can be curatively removed by complete surgical excision if needed (132). In 15% of cases multiple osteochondroma may be present, which can be related to an autosomal dominant condition called Hereditary Multiple Osteochondromas (HMO) (132). This increases the risk of the tumour transforming into malignant chondrosarcomas from 1% to 1-3% (141).

1.5.1.1.6 Enchondroma

Enchondromas are intramedullary masses of hyaline cartilage that comprise 15% of benign bone tumours. These tumours do not appear to have an age or sex preference, but do appear to arise in distinct locations; 41% occur in the small bones of hands or feet (132). Most cases are isolated and only very rarely undergo malignant transformation into a chondrosarcoma. However, certain rare disorders cause multiple enchondromas to arise and hugely increase the risk a malignancy developing; these are Ollier's disease and Maffuci's syndrome (142).

1.5.1.1.7 Chondroblastoma

Chondroblastoma is a neoplasm of cartilage lineage generally found in the epiphysis and representing about 5% benign bone tumours. It is twice as common in men and usually occurs in teenage years (132). They consist of polygonal cells with defined cytoplasmic borders interspersed with randomly distributed giant osteoclast-type cells, and cause lytic lesions that can lead to joint swelling and a reduced range of movement. Surgery is used to remove the neoplasm, but tumours recur in 14-18% of cases and can rarely lead to benign pulmonary metastases (132).

1.5.1.1.8 Chondromyxoid fibroma

One of the least common bone tumours, chondromyxoid fibroma only accounts for 2% of benign bone tumours. It is composed of lobules of loose myxoid stroma separated by fibrous septa that contain giant multinucleated osteoclast-like cells and causes sharply defined lytic lesions. Treatment is surgical removal and bone grafting, though recurrence may occur in 25% of cases (132).

1.5.1.1.9 Giant Cell Tumour of bone

Giant Cell Tumour of bone (GCT) is a common benign bone tumour comprising about 22% of benign bone tumours. The tumour is composed of mononuclear cells surrounding uniformly distributed giant osteoclast-like cells, which cause osteolytic lesions and can lead to reactive bone formation. It is locally highly aggressive and can destroy cortical bone allowing it to extend into local soft tissues causing severe bone pain, swelling and loss of joint movement. Malignant transformation is rare, but benign lung metastasis may occur in 2% of cases. Treatment has typically been surgical removal followed by bone graft, but in recent years adjuvant treatment with anti-resorptive drugs such as bisphosphonates or the anti-RANKL drug denosumab are becoming more common. Clinical trials are currently underway to determine the efficacy of surgery versus adjuvant management.

1.5.1.1.10 Benign notochordal cell tumour

Benign notochordal cell tumours (BNCT) were only characterised in 1999 and so prevalence is unknown. They consist of a small tumour of notochordal origin with sheets of intraossious cells resembling mature adipocytes that do not cause bone destruction, hence many BNCT are asymptomatic. No treatment is normally necessary and often only clinical observation is required (132, 143, 144).

1.5.1.2 Malignant primary bone tumours

Like benign bone tumours, malignant bone tumours are rare cancers accounting for less than 0.2% of cancers in the developed world (145). They are however far more serious illnesses, and can cause severe bone pain, lytic lesions, pathologic fractures, restricted movement and skeletal deformities. Malignant bone tumours commonly metastasise to other skeletal sties, as well as to other organs, most commonly the lungs. All forms are life threatening illnesses with 5 year survival rates ranging from 10% to 90% depending on type of tumour and severity at diagnosis (145). The most common malignant primary bone tumours are osteosarcoma, chondrosarcoma, fibrosarcoma and Ewing's sarcoma. Common treatments are adjuvant chemotherapy followed by surgical removal of the tumour, and regular clinical follow up to check for relapse. No current therapies are effective at treating metastatic malignant bone tumours and much current work is focused on finding appropriate molecular targets for future management (145).

1.5.1.2.1 Osteosarcoma

Osteosarcoma is the most common malignant primary bone tumour and has an estimated incidence of about 4/million/year cases worldwide (146). It occurs most often in young adults, although it can occur at any age (147). Other bone disorders such as Paget's disease of the bone or fibrous dysplasia may increase the risk or an osteosarcoma developing, as does exposure to radiation (145, 148, 149). Osteosarcomas are characterised by the production of malignant osteoid from osteoblastic cells that causes woven bone to be laid down in abnormal locations. Various cartilage or fibrous tissue may also be present as chondroblastic and fibroblastic cells are also found in osteosarcoma in varying amounts. They most often initially form inside the cavity of long bones where they may cause osteolytic, osteoblastic or mixed lesions leading to bone pain and deformity. However, at diagnosis 20% of patients have at least one lung metastasis and a further 40% will develop one or more through the course of the disease (146). 80% of metastases associated with osteosarcoma are found in the lungs and it is these metastases that cause most deaths (146). Isolated osteosarcoma has a relatively good recovery rate, with 65% of patients

surviving at least 5 years. Once a metastasis occurs though this survival rate drops to just 20% (146). Treatments are neoadjuvant chemotherapy followed by surgical excision of the primary tumour and secondary tumours. This is generally followed up by further chemotherapy to lower the risk of relapse. Even so 30-40% of patients will relapse and have metastatic disease within 3 years (150, 151).

1.5.1.2.2 Ewing's Sarcoma

Ewing's sarcoma is the second most common malignant primary bone tumour in young adults, with an estimated 1-3/million/year cases worldwide (145). It exclusively effects adolescents and is 50% more common in men (152). Interestingly, Ewing's sarcoma is extremely rare in children of black African decent (153). It is known to be caused by a specific translocation between chromosomes 11 and 22 that causes a fusion of Friend leukemia integration 1 transcription factor (FLI1) and the EWSR1 gene resulting in the production of a chimeric fusion protein (154). Ewing's tumours consist of small round lumps of uniform round cells of no recognisable bone cell type. They cause pain and deformity of the bone as local osteoblasts and osteoclasts react to the tumour by forming new lamellar bone in abnormal locations (145). This may lead to pathologic fracture. At diagnosis up to 30% of patients have at least one metastasis, most commonly in the lung, though at a far lower rate than seen in osteosarcoma (145, 155, 156). Survival rates are similar to osteosarcoma. If the tumour is restricted to one bone site then 75% of patients will survive 5 years or more, however for patients that present with metastases or distant relapse, current treatments are ineffective and less than 10% will survive for 5 years (155, 157). Treatments are neoadjuvant chemotherapy followed by surgical removal of the tumour and continual adjuvant chemotherapy. Despite this, up to a third of patients relapse after surgery (145).

1.5.1.2.3 Chondrosarcoma

Chondrosarcomas are unusual amongst bone tumours as they are more common in adults than children. They are the third most common malignant bone tumour, but the second most common in adults mainly afflicting those between 30 and 60 with a 2:1 sexual prevalence towards men (145, 158, 159). They occur in cartilage and arise from chondrocytes, generally causing slow growing masses of neoplastic hylaine cartilage tissue that can spread to local tissues, or to the lungs (158). They cause severe bone pain and can lead to loss of movement and deformity. 90% are conventional chondrosarcoma and are not associated with a pre-existing tumour; however 10% are secondary chondrosarcoma and arise due to the transformation of a benign bone tumour such as an osteochondroma (145, 159). Regardless of origin over 90% of chondrosarcoma have low metastatic potential and are usually successfully treated (159). The remaining 10% are more lethal as they are faster growing and commonly metastasize to the lungs and other sites. Treatment is difficult as these tumours are highly resistant to both chemotherapy and radiotherapy. So, while the slow growing nature of most chondrosarcoma means that surgical removal is curative in many cases (90% 5-year survival rate), in cases where metastasis or recurrence occurs prognosis is very poor and survival rates are thought to be as low as 10% of patients living beyond 2 years (158, 160).

1.5.1.2.4 Fibrosarcoma of bone

Fibrosarcomas are a relatively uncommon primary malignant bone tumour with only 0.5/million/year cases occuring worldwide (161). These tumours are more commonly found in adults and have a slight sexual bias towards men (162). As a malignancy of soft tissues fibrosarcoma are not specific to bone and can commonly arise in other tissues. They derive from mesenchymal fibroblasts, the cells that produce the extracellular matrix, and so produce excess collagen fibres. However, this is not the main cause of problems within bone, it is the presence of rapidly proliferating spindle shaped fibroblast-like cells (161, 162). Fibrosarcoma normally occur within the intramedullary cavity of long bones where they lead to osteolytic lesions causing pain, swelling, loss of movement and pathological

fractures. Most (75%) fibrosarcoma of bone are highly metastatic tumours and are not easily treatable. Common treatment is surgical removal combined with chemotherapy. In this case 5 year survival rates are about 20%, with patients who presented with a low grade fibrosarcoma having an increased survival rate of 50%. 18% of patients suffer a relapse after surgery (162).

1.5.1.2.5 Multiple Myeloma

Multiple myeloma arises from plasma cells within the bone marrow and therefore it is not recognised as a true primary bone cancer. Despite this, it is often considered as one as the cancerous cells accumulate within the bone marrow. It is far more common than all other primary bone tumours occurring on average in 4/100,000 people/year and representing approximately 1% of all cancers in the developed world (163). It is more common in men than women at a ratio of 1.5:1 and occurs almost twice as often in patients of black African origin (163, 164). Osteoytic lesions are very commonly associated with multiple myeloma, occurring in 80% of patients due to increased bone resorption and decreased bone formation (165). This loss of bone can cause bone pain, may lead to osteoporosis, and can cause pathological fractures of the long bones and compression fractures in the spine [reviewed in (166, 167)]. Myeloma and stromal cells secrete local factors such as TNF-α, interleukins and RANKL which increase osteoclast formation and activity (168, 168-172). Myeloma cells also inhibit the production of OPG by stromal cells thereby further enhancing bone resorption (171). Multiple myeloma is considered incurable in most cases and median survival rates range between 29 months and 68 months depending on the severity of the cancer at diagnosis (173). Until recently the most common treatment was chemotherapy using drugs such as thalidomide that can suppress or delay the disease, however the vast majority of patients relapse following this treatment, and the drugs have severe side effects (163). Recent advances in stem cell treatments and novel therapeutics have lead to increases in survival times, and the hope of future increases in fully cured disease-free patients (163).

1.6 Bone metastasis

Bone metastasis is the migration of tumour cells from a distant primary site to form a secondary tumour within the bone microenvironment. Secondary bone tumours are far more common than primary bone cancers, in fact representing >99% of malignant bone tumours (174). Metastatic cancers originating in the breast, prostate, kidney, thyroid and lung all have a remarkably high rate of metastasis to bone, and it is thought to cause more than 350,000 deaths every year in the USA (175-177). In fact, bone metastases are the most common metastasis site associated with the three most common human cancers, breast, prostate and lung (178). The cancers that most often metastasise to bone are breast and prostate cancers with an incidence of at least 80% in metastatic breast cancer patients and 68% in prostate cancer patients (176, 177, 179). These are followed by lung and kidney carcinomas, as well as melanomas, which metastasise to bone in 36%, 35%, and 35% of cases respectively (180). Lesser, but still significant, frequencies are found in other cancers.

Bone metastases are associated with increased morbidity, severe bone pain, skeletal fractures, hypercalcemia, nerve compression and in most cases eventually death (181). They are virtually incurable in most cases and as such the majority of current therapies are palliative. These treatments are often designed to prevent pain by reducing tumour burden, inhibiting tumour associated bone pathologies and preventing the progression and further metastasis of the cancer (180, 182, 183). Median survival times are variable and depend on the primary tumour type as well as site and number of bone metastases. On average breast and prostate cancer patients live longer after diagnosis of a bone metastasis, while lung cancer and other primary tumour patients have far shorter survival times. For example, analysis of patients with spinal bone metastases demonstrated median survival times of 14.1 months for breast cancer patients, 9.2 months for prostate cancer patients and only 3.8 months for other cancers and 2.9 months for lung cancer patients (184).

The precise reasons why bone is such a common site of metastasis are not known but it has been hypothesised that it is due to the conditions found within the bone microenvironment. In 1889 the ‘seed and soil’ hypothesis of metastasis was proposed by Stephen Paget (185). This hypothesised that the locations of metastasis are not due to

chance but that when spreading tumour cells grow preferentially in hospitable and habitable environments. He argued that cancer cells are like 'seeds' that are cast onto the 'soil' of the body, while the 'seeds' may land across all of the 'soil', they only grow where the 'soil' is fertile and that different 'seeds' need different types of 'soil'. In other words, metastatic tumour cells spread through all locations in the body, but only form secondary tumours where the environment is 'fertile' and allows them to proliferate.

The anatomical/mechanical hypothesis on the other hand argues that it is the location of organs that explains the patterns of metastasis (186). This maintains that the first organ that metastatic cells come into contact with is the most likely site of metastasis and explains why the lungs, kidneys and liver are common sites for certain tumours due to their locations in the circulatory system. A combination of both hypotheses is likely to be true in reality. However, in the case of bone metastases where the locations of tumours frequently correspond with the most metabolically active areas of bone, the 'seed and soil' theory seems to be the more likely explanation for most cases.

1.6.1 Mechanisms of Metastasis

Before secondary bone tumours can arise, cancer cells must leave the site of the primary tumour and migrate to the bone through the process of metastasis. This process is the same as for other types of metastasis and involves cancer cells undergoing a series of specific steps that facilitate their migration away from the original tumour location. These steps are as follows: invasion of local surrounding tissue, intravasation, translocation through the bloodstream or lymphatic system to distant bones, extravasation into that tissue, adaptation to the bone microenvironment and finally colonisation of the bone (187-189) (Figure 1.14).

The invasion of local tissue, that is the first step in the process of metastasis, is facilitated by changes within the cancer cells that allow them to migrate and invade. These traits allow the malignant cells to degrade and move through the extracellular matrix of the tissue surrounding the primary tumour and local blood or lymphatic vessels. In most cancers, the process of epithelial to mesenchymal transition (EMT) is thought to play the

main role in these cell transformations (189). Over 80% of malignant tumours are of epithelial origin, and these cancers include those that metastasise to bone most frequently (189).

Epithelial tissues generally consist of polarised tightly cohesive thin sheets of epithelial cells separated from stroma by a basement membrane. This tight cohesion allows the barrier function of the epithelium and is due to the actions of intercellular adhesions facilitated by interactions between various factors including cadherin, and catenin proteins (190, 191). In order to become invasive, most cancer cells must lose their epithelial phenotype and become more mesenchymal in nature. This requires mutations that down regulate or remove cadherin expression, particularly of E-cadherin, as well as other structural proteins, causing the cells to lose polarity and the tight bonds to adjacent cells (189). This leads to further changes that give the cancer cells an invasive phenotype. These changes include the up regulation of MMPs (192-194), which allows for stromal matrix degradation, the up regulation of VEGF (189, 195), which stimulates neoangiogenesis attracting new blood vessels to the primary tumour site, and the suppression of responses to apoptotic signals, which allows cells to survive in the blood stream (189, 195). Interestingly, transcriptional repression of various cell-cell adhesion complexes (and so EMT) can be driven by various cytokines and pathways known to be involved in both bone metastases and normal skeletal bone remodelling, including TGFβ, IGF-1 and the Wnt signalling pathway (189). Together, these factors cause cells to undergo EMT and ultimately develop an invasive phenotype.

Once cells have developed an invasive phenotype they are able to successfully invade through local tissues and enter local blood or lymph vessels, a process called intravasation. The blood stream is a hostile environment for most cell types and it is thought that, even with the advantages of a mesenchymal phenotype, less than 1 in 1000 cancer cells that enter the blood stream survive to form a micrometastasis (196). Most malignant cells that do reach the bone do so by arresting their circulation in the sinusoid vessels of the bone marrow, attach to the endothelium of the capillary and undergo extravasation into the bone marrow (189).

Once in the bone marrow, malignant cells do not necessarily then go on to form a bone metastasis. Many of the cells will simply undergo apoptosis once they have

extavasated, while others may become dormant and not proliferate in their new environment (189). Interestingly, tumours that do successfully grow and colonise the bone marrow tend to have mixed phenotypes consisting of both mesenchymal and epithelial cells that are similar to those found in their original primary tumour site. This is often explained by the theory that factors found in the bone microenvironment allow cells to reverse EMT and undergo Mesenchymal to Epithelial transition (MET).

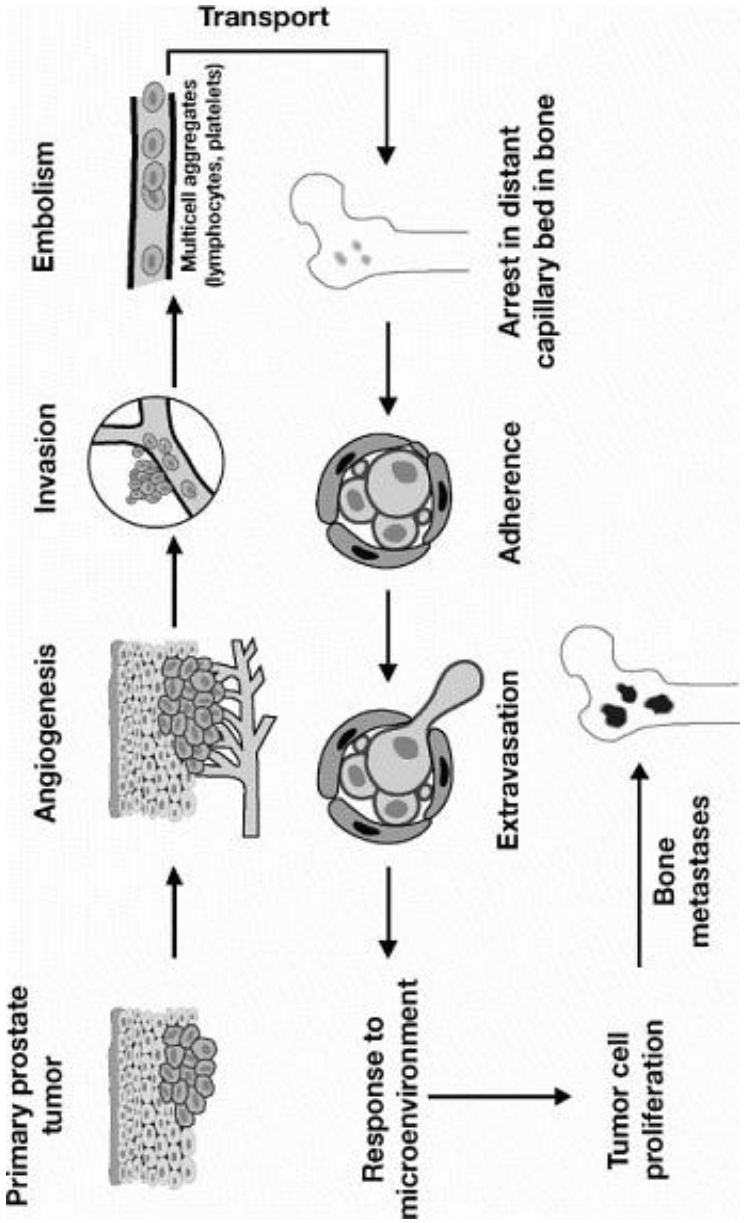

Figure 1.14 A diagram showing the processes involved in the formation of a bone metastasis. See text for details.

Adapted from Guise and Mundy Endocrine Reviews 19(1): 18–54

1.6.2 Types of Bone Metastasis

Malignant cancer cells in bone are traditionally divided into two types depending on how they disrupt bone remodelling. These are osteolytic (lytic) metastases that cause excess bone resorption and osteoblastic (sclerotic) metastases that cause excess bone formation. In reality, both processes are normally present to some extent in any skeletal site afflicted with a metastasis, but for simplicity metastases are clinically divided into 'lytic', 'sclerotic' or 'mixed' subtypes, depending on their pathologic appearance (175, 197, 198). Breast cancers commonly lead to lytic metastases, while prostate cancers typically cause sclerotic metastases (198-200). However, it should be noted that 25% of breast cancer patients with bone metastases will have sclerotic lesions in addition to their osteolytic metastases, and that many prostate cancer patients have lytic lesions (198, 201).

No matter what the type of metastasis, tumour cells disrupt the remodelling cycle and cause the release of factors that allow the tumour cells to proliferate, and so cause more disruption of the remodelling cycle. This is known as the 'vicious' cycle of bone metastasis. Four major components make up the contributors to the 'vicious cycle'; tumour cells, osteoclasts, osteoblasts and the bone matrix. Each affects one or more of the other contributors in various ways summed up in Figures 1.15 and 1.16.

1.6.2.1 Osteolytic bone metastasis

Osteolytic bone metastases are formed by malignant tumour cells colonising the bone microenvironment and secreting factors that directly or indirectly enhance osteoclastic bone resorption. These factors include cytokines and growth factors such as IGF-1, TGFβ, M-CSF, VEGF, PTHrP, MMPs and Interleukins (ILs). Some of these factors directly stimulate the maturation of osteoclast precursors to become mature osteoclasts, while others increase the activity and survival of the mature osteoclasts. Some factors instead act on osteoblasts, causing either an increase in the production of osteoclastagenic factors or a reduction in the expression of factors that inhibit osteoclast formation. PTHrP is the most studied factor and is known to induce osteolysis by increasing osteoblast expression of RANKL, while at the same time inhibiting release of its decoy receptor, OPG

(202, 203). IL-8, IL-11 and M-CSF all directly promote osteoclast differentiation and function, where as IL-6, Cyclooxygenase-2 (COX2) and TGF-β indirectly increase production of factors such as PTHrP or PGE that stimulate RANKL production by osteoblasts (204).

This cancer-induced imbalance in bone remodelling leads to an increase in osteolysis and a loss of bone. As a result bone derived growth factors trapped within the bone matrix are released into the local bone microenvironment. Some of these growth factors, including IGFs, TGFβ, and BMPs, then cause an increase in tumour cell proliferation, survival and migration (205). In addition to the factors released, other changes in the bone microenvironment caused by increased bone resorption facilitate the proliferation and survival of the tumour cells. An acidic environment provides a survival advantage to certain tumour cells, while the high levels of extracellular calcium stimulate tumour cell growth through the MAPKinase signalling pathway (205). A reduction in trabecular number and mass also gives tumour cells the space to expand and grow (205). Either stimulated by growth factors or due to the environmental changes, the result is an increase in the number of tumour cells present. This in turn results in an increase in the production of osteolytic factors from the bone metastasis, and so an increase in the amount of local bone resorption. In many tumours the release of osteolytic factors is even further increased through induction by the same growth factors and environmental conditions that cause an increase in tumour cell number. For example, high calcium levels are known to increase PTHrP production, as does TGFβ (204).

In essence, the osteolytic vicious cycle comprises tumour cells entering the bone microenvironment and causing an imbalance in bone remodelling that favours bone loss. The loss of bone then releases factors and causes the environment to change so that the proliferation of tumour cells is increased. With more tumour cells present, the imbalance in bone remodelling is worsened leading to progressively more bone loss and greater increases in tumour cell growth.

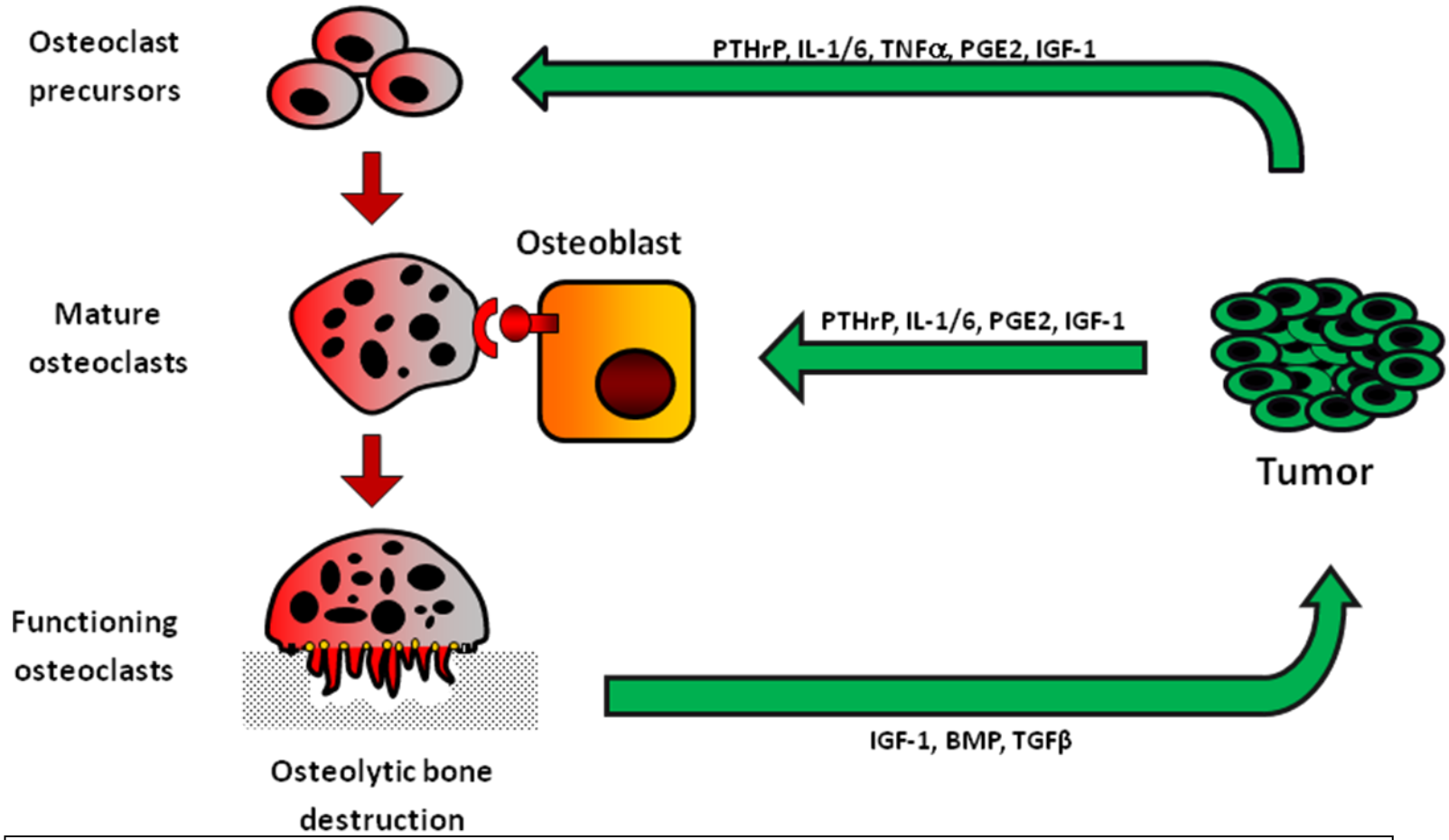

Figure 1.15A diagram showing some of the interations involved in the osteoclastic 'vicious' cycle of bone metastasis. See text for details

1.6.2.2 Osteoblastic bone metastasis

Osteoblastic bone lesions are mainly characterised by increased bone formation and have their own cycle causing bone remodelling imbalances and tumour proliferation. While purely osteoblastic metastases are possible, one of the reasons mixed metastases are most common is due to the coupling of bone formation and bone resorption. The key osteoclastic factor RANKL, and other osteclastogenic factors such as M-CSF, are produced by osteoblasts and so any significant increase in the number of mature osteoblasts is therefore likely to eventually lead to increased levels of bone resorption in addition to enhanced bone formation.

In the same way that the osteoclastic vicious cycle works, the osteoblastic cycle begins when tumour cells colonise the bone microenvironment and begin to release factors and cytokines that induce or increase bone formation. This includes IGF-1, uPA, BMPs, Wnt signalling factors and ET-1 (reviewed in (204)), some of which will be explored in more detail later. Some of these factors directly stimulate the proliferation, differentiation and function of osteoblasts, while others do so indirectly through actions that reduce the inhibition of stimulatory factors or activate other latent factors. ET-1 and IGF-1 are the most widely studied factors in osteoblastic metastases, and are both known to directly stimulate the proliferation and function of osteoblasts and in the case of ET-1 reduce apoptosis (206). The precise mechanisms that allow the vaso-constrictor ET-1 to stimulate bone formation are unknown but are likely to be related to its causing nuclear translocation of NFATc1. IGF-1 is known to stimulate both the MAPKinase and PI3K/Akt signalling pathways in osteoblasts, as well as causing an increase in the expression of Runx2 in osteoblast precursors, so stimulating osteoblast proliferation, differentiation, function and survival. IGF-2, BMPs, and TGFβ are also known to directly stimulate osteoblasts, while the proteases uPA and PSA cause the activation of TGFβ and the release of IGF-1 from IGF binding proteins (IGFBPs), and so indirectly stimulate osteoblasts (204, 205).

The overall effect of this cancer-induced induction of osteoblast function is enhanced bone formation. How this causes an increase in tumour proliferation is less well understood, but is thought to be related to the large number of growth factors present in immature bone, including IGF-1, BMPs and TGF-β. The increase in bone resorption induced

in the surrounding area will further release these factors from mature bone. In some cases factors released and/or changes in the environment such as lower pH, or higher calcium levels may cause whole tumours or parts of tumours to change from being an osteoblastic tumour to becoming an osteolytic tumour (204, 205). However, the precise mechanisms behind this are currently unknown.

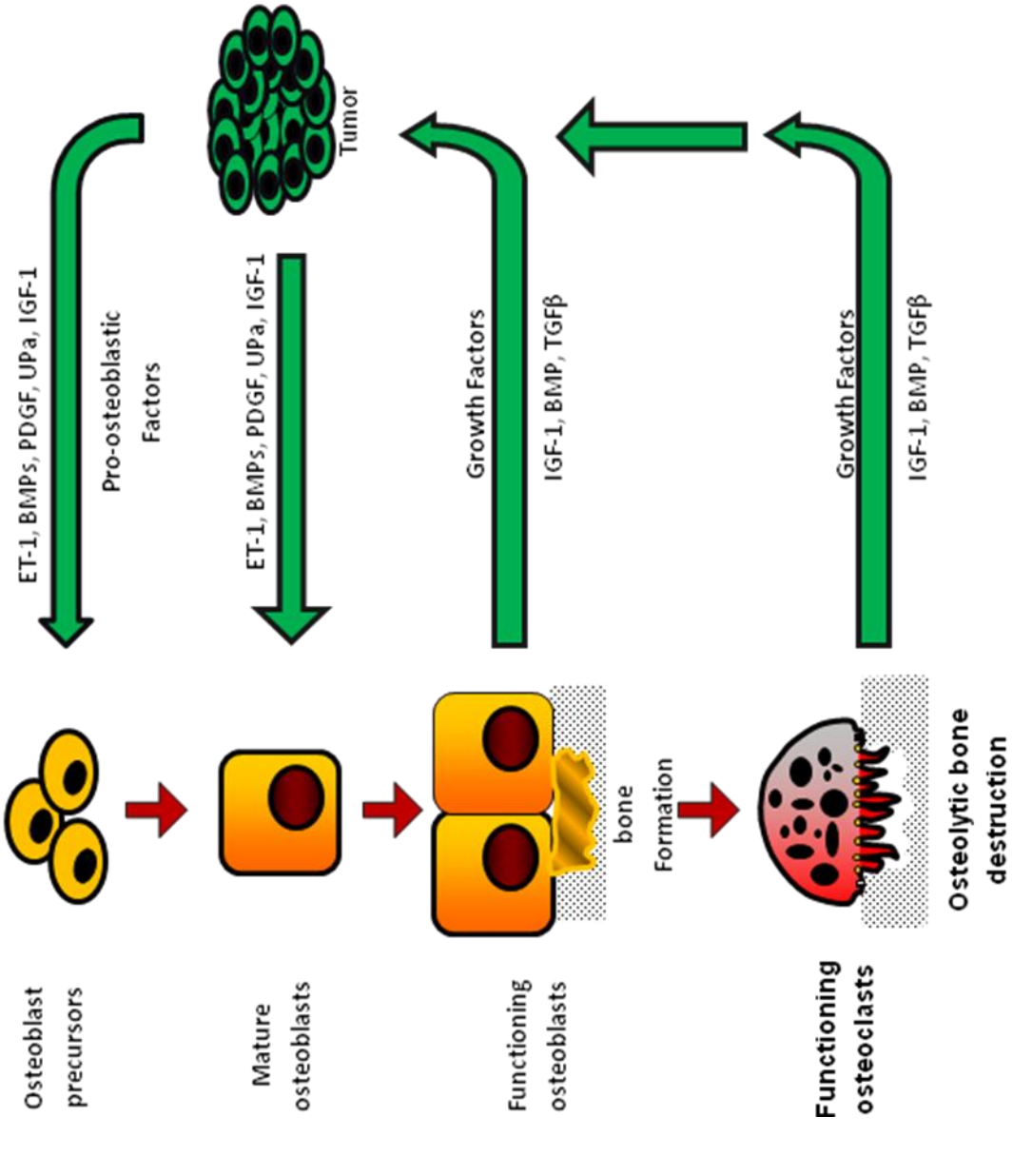

Figure 1.16 A diagram showing some of the interactions involved in the osteoblastic 'vicious' cycle of bone metastasis. See text for details.

1.6.3 Factors involved in the vicious cycle of bone metastasis

Many of the factors involved in the local molecular control of bone remodelling are the same factors that are important for bone metastasis, only the most key factors will be discussed in this section.

1.6.3.1 OPG/RANK/RANKL

The most important factors that are involved in the regulation of bone remodelling are OPG, receptor activator of NF-κB (RANK), and its ligand RANKL. These are all members of the tumour necrosis factor (TNF) superfamily of proteins and are recognised as the key factors responsible for regulation of osteoclast formation, function and survival in health and disease (1) (Figure 1.17).

RANKL is a type II homotrimeric transmembrane protein that can be found in either a membrane bound or a secreted form (207). It is expressed in tissues throughout the body, but is particularly highly synthesized in bone, bone marrow and lymphoid tissues (208, 209). In bone, RANKL is produced mainly by osteoblasts, osteoblast precursors, osteocytes and T lymphocytes. Until recently it was thought that the main source was osteoblasts but it has lately been discovered that osteocytes are capable of producing RANKL at levels 10-fold higher than osteoblasts (46). When it binds to the RANK receptor, RANKL stimulates a number of signalling cascades vital for osteoclast differentiation, survival and activity. Of particular importance is the NF-κB signalling pathway. In cells of the macrophage/monocyte lineage (osteoclast precursors), RANKL stimulates the differentiation of these cells into pre-osteoclasts and then mature osteoclasts. It has been demonstrated that RANKL is both necessary and sufficient for osteoclast formation, and experiments using knockout mice demonstrated that in its absence no osteoclasts form *in vivo* leading to an extreme osteopetrosis phenotype, with problems in both tooth eruption and B and T cell development (67). Human cases of RANKL deficiency or mutation are rare, but do occur. Patients present with osteopetrosis and while no human trials have been performed research using mouse models has suggested this could be cured by treatment

with exogenous RANKL (210). RANKL also stimulates B-cell maturation (211) and it is required during the development of both lymph nodes (212) and mammary glands (213).

The effects of RANKL-mediated signalling are initiated when RANKL binds to its receptor RANK; a type I homotrimer transmembrane protein with a large cytoplasmic C-terminal domain and an N-terminal extracellular domain (209). RANK is also widely expressed but is found at particularly high levels in macrophage/monocyte lineage cells, especially pre-osteoclasts and osteoclasts, as well as dendritic, T and B cells (119, 209, 214). RANK knockout mice have a similar phenotype to RANKL knockout mice, with severe osteopetrosis, and problems with immune cell and lymph node maturation (212, 215).

OPG is another receptor for RANKL, however instead of being membrane bound and linked to a signalling cascade it is instead a soluble secreted decoy receptor. RANKL is prevented from binding to RANK by OPG and so cannot stimulate osteoclast formation. OPG is therefore probably the most important negative regulator of bone resorption. It was the first of the RANK/RANKL/OPG axis to be identified as important in the control of osteoclast formation. OPG was simultaneously discovered by two groups in 1998 (Amgen Inc. and more bizarrely Snow Brand Milk Products Co. one of the largest dairy companies in Japan) (216, 217). It is unusual for a TNF super family member as it is normally found as a secreted protein rather than as a transmembrane protein. Like RANK and RANKL, it is widely expressed but is mainly produced in the bone microenvironment. OPG is also known to play a role in protecting blood vessels from calcification (218, 219). OPG knockout mice have an extreme osteoporosis phenotype due to increased numbers of osteoclasts (220), and humans with dysfunctional or hypo-OPG diseases may have a variety of skeletal problems including osteoporosis (221), Paget's disease (222) or idiopathic hyperphosphatasia (223).

The rate of RANKL binding to RANK is the major determining factor controlling osteoclastogenesis, and is controlled by changes in the ratio of available RANKL to OPG decoy receptor (224). RANKL to RANK binding stimulates a number of signalling pathways including recruitment of TNF receptor-associated factors (TRAFs), the activation of inhibitor of κB kinase complex (IKKα,β and γ), and the NFκB transcription factor family (Figure 1.17). Inactivation of any of TRAF6, IKKβ or the NF-κB p50 and p52 proteins in mice causes severe osteoclast defects and severe osteopetrosis (225-227).

Disruption of the RANK/RANKL/OPG axis has been linked to a number of bone diseases including bone metastasis. A number of studies have showed that invading tumour cells stimulate osteoclastogenesis either directly through the release of RANKL, or more commonly, indirectly through the release of a variety of factors that change the rates of RANKL or OPG production in bone cells (228-231). In addition RANK expression in tumours has been linked to increased rates of metastasis to bone, particularly in breast cancers, and is a marker of shorter survival times (232-234).

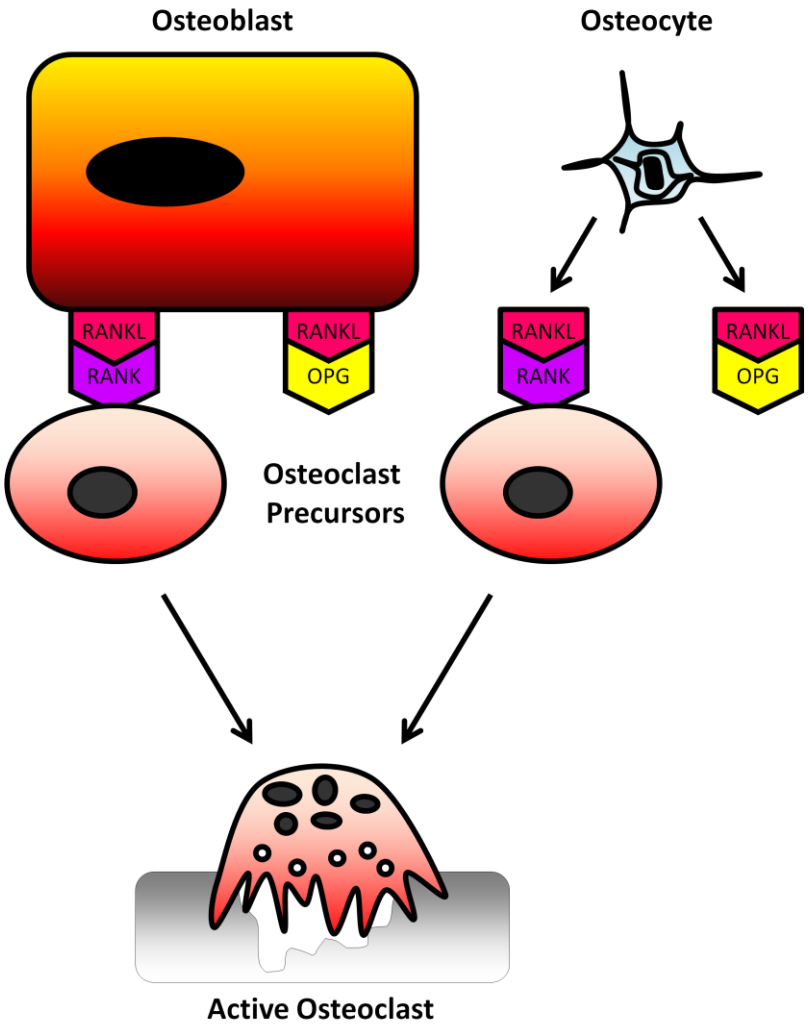

Figure 1.17 A diagram demonstrating the effects of the RANK/RANKL/OPG axis on osteoclast formation. See text for details. *Abbreviations*: RANK/L is Receptor Activator of NF-κB/Ligand, OPG is osteoprotegerin

1.6.3.2 M-CSF

The second essential factor for osteoclast formation is Macrophage Colony Stimulating Factor (M-CSF), a disulphide-linked dimeric glycoprotein found in both soluble and membrane bound forms (235, 236). It is known to be produced by osteoblasts in both forms and acts on pre-osteoclasts causing proliferation, migration and increases in levels of RANK expression, leading to osteoclast differentiation (237). It is also thought to support osteoclast survival through increasing expression of anti-apoptotic factors such as Bcl-2 (238).

In bone, M-CSF acts through the receptor encoded by the proto-oncogene c-Fms. It stimulates a large number of signalling pathways including the essential PI3K/Akt and MAPKinase pathways (239). Mice that lack either M-CSF or c-Fms have osteopetrotic phenotypes with very few mature macrophage or osteoclasts present, though they do have some TRAcP positive cells which would normally indicate osteoclast formation (120, 240-242). M-CSF and c-Fms are both thought to play a role in the pathophysiology of bone metastasis. Specifically, M-CSF has been found to be secreted by various tumour cell types (243, 244), and c-Fms is not only a proto-oncogene but has also been linked to increased rates of metastasis in various cancers, particularly breast carcinomas (233, 243).

1.6.3.3 PTHrP

One of the first factors associated with bone metastases was PTHrP. PTHrP plays a key role in osteolytic metastases and has been found to be produced in large quantities by a variety of different bone metastasising tumour cell types (245, 246). A correlation between PTHrP expression and the frequency of bone metastases in breast cancers has also been observed, suggesting a role of this protein in the homing of tumour cells to bone (247). Demonstrating how prevalent, and specific PTHrP is to osteolytic bone metastases, studies have shown that 92% of breast cancer bone metastases express PTHrP compared to only 50% of primary breast tumours and 17% of metastases in other locations (248). Neutralising antibodies to PTHrP have also been reported to inhibit the development and progression of breast cancer bone metastases in mouse models (249).

Tumour derived PTHrP acts in a paracrine fashion and leads to an increase in bone resorption. This occurs as it binds to the type 1 PTH/PTHrP receptor (PTHR1) expressed on osteoblasts and stromal cells and causes an upregulation in the production of RANKL by these cells. This then leads to localised increases in osteoclast formation and activity.

In health, PTHrP is found to be abundantly expressed in tissues that are the target of circulating PTH, namely kidney and bone. It is also expressed in particularly high concentrations in growth plate chondrocytes and is thought to play a role in promoting their proliferation and preventing their differentiation into hypertrophic chondrocytes (1, 250). As opposed to the catabolic effect seen in bone metastasis, in health PTHrP conversely has an overall osteoanabolic effect as it directly stimulates bone formation (1, 251). This action is through a shared mechanism with PTH, which it shares homology with at it's the N-terminal domain. Both PTH and PTHrP are thought to regulate bone formation through the stimulation of osteoblast differentiation and formation, and it is these that are the dominant effects of the two molecules in healthy bone. PTHrP knockout mice have severely impaired osteoblast formation, and as a result reduced bone formation resulting in an osteoporosis phenotype. It should be noted that PTHrP deficient mice also have reduced numbers of osteoclasts due to reduced levels of RANKL production (252).

Unlike PTHrP, PTH is a circulating hormone produced by the parathyroid glands and is known to be the primary regulator of calcium homeostasis in the body through actions in both bone and the kidneys. As a circulating hormone, PTH is not commonly found expressed by tumour cells, and is not generally linked to bone metastasis. Excessive and prolonged exposure to PTH can cause bone loss in a similar fashion to PTHrP (1), but intermittent treatment with PTH is a common treatment used to increase bone mass, as under this regimen its effects on bone formation are primary (253, 254).

Table 1.1 A table summarising the skeletal effects of locally acting cytokines and growth factors produced by tumour cells during bone metastasis. See text for references. ↑; Increase, ↓ decrease, ↔ unchanged.

Local cytokines and growth factors	Bone formation	Bone resorption	Tumour growth
RANKL	↔	↑	↑
OPG	↔	↓	↓
M-CSF	↔	↑	↑
TNFα	↓	↑	↑
IL-1β	↓	↑	↑
IL-6	↔	↑	↑
IL-8	↔	↑	↑
IL-11	↔	↑	↑
IL-17	↔	↑	↑
BMP-4	↑	↔	↑
BMP-6	↑	↔	↑
BMP-7	↑	↔	↑
ET-1	↑	↓	↑
IFN-γ	↔	↓	↓
TGF-β	↑	↑	↑
IGF1	↑	↑	↑
PDGF	↑	↔	↔
FGFs	↑	↑	↑
PGE2	↑	↑ or ↓	↑ or ↓
NO	↓ or ↑	↑ or ↓	↑ or ↓
PTHrP	↑	↑	↔
MMPs	↔	↑	↑
VEGF	↔ or ↑	↔ or ↑	↑

1.6.3.4 TGFβ

Transforming growth factor β (TGFβ) is the eponymous factor of the TGFβ superfamily known to be involved in the regulation of cell development, differentiation, cell cycle control and various other vital cellular functions (255-257). TGFβ was also one of the first factors to be associated with the pathophysiology of bone metastases, specifically osteolytic metastases. It has been linked to increases in tumour aggressiveness, tumour metastasis in general and cell homing to bone in particular (258-262). Expression of TGFβ has been specifically correlated to poor patient outcome (263, 264). Studies of both pharmacological inhibition and genetic inactivation demonstrate that inhibiting TGFβ signalling reduces both the number of bone metastasis that arise and size and damage caused by those that do present (260, 265-267).

Typically TGFβ derives from two locations in bone metastasis; it can be produced by the tumour cells themselves or is released from within the bone matrix during bone resorption (258). Whatever the origin, TGFβ stimulates the proliferation and growth of tumour cells, particularly in late stage tumour progression (258, 268). Perhaps more importantly it also stimulates the tumour cell production of PTHrP, and other osteoclastic factors such as IL-11 (269). Therefore, in bone metastasis the direct effect of TGFβ on bone cells is not necessarily important, it is the enhancing effect of TGFβ on tumour cells and their release of osteolytic factors that makes it important.

In health, TGFβ has a very different role in bone as it is thought to be involved in the coupling of bone formation and resorption (270). It acts on various bone cells through binding to its type II receptors and recruiting its Type I receptor to form a ternary holo-complex that initiates a signalling cascade through the SMAD proteins (257, 258). In osteoclasts and their precursors, TGFβ directly inhibits cell proliferation, differentiation and resorption (271). However, TGFβ also indirectly stimulates bone resorption by increasing the production of PTHrP by osteoblasts. In this way TGFβ is involved in recruiting osteoclast precursors to the site of resorption (270). On the other hand, it directly stimulates bone formation through increasing osteoblast proliferation and mineralised matrix deposition (272).

1.6.3.5 IGF-1

Insulin-like growth factor-1 (IGF-1) is the most abundant growth factor in the bone microenvironment (273). IGF-1, along with its receptor (IGF-1R) and binding proteins (IGF1BPs), has long been known to play an important role in bone homeostasis. More recently there has been increasing interest in the part the IGF-1 system might play in the development of cancers. Breast cancer, prostate cancer and a variety of other tumours have all been linked to elevated cellular expression of IGF-1 and its receptor (274, 275). Moreover, increased circulating levels of IGF-1 and IGF-1 binding protein 3 have been linked to increased risks of breast and prostate cancer development (276-279). Less work has been performed studying the direct role of IGF proteins in bone metastasis, but it has been shown that various tumour cells that commonly migrate to bone express and secrete IGF-1 (280), that IGF-1 and IGF-1R regulate the preferential metastasis of some tumours to bone (281-283) and can direct the migration of cells to bone (273, 284).

In health, IGF-1 is thought to regulate bone remodelling through both endocrine and paracrine mechanisms. IGF-1 is expressed by most tissues and is mainly found as circulating IGF-1 produced by the liver, allowing it to regulate growth and other functions in many different tissues. IGF-1 acts through a complex regulatory network consisting of IGF-1, its receptor and IGF-1 binding proteins. When IGF-1 binds to IGF-1R it induces various signalling cascades including the PI3K/Akt, the MAPKinase and the non-canonical Wnt signalling pathway (285, 286). This stimulates cell survival, differentiation and changes the expression of various proteins associated with cell survival and inhibition of apoptosis. IGF-1 is also produced by a variety of different bone cells including osteoblasts, osteoclasts and their precursors. It acts on both osteoblasts and osteoclasts, but is thought to be particularly important in the regulation of bone formation as it stimulates osteoblast differentiation, migration and function (287-289). IGF-1 knockout mice have severely reduced bone formation and reduced bone mass, along with various other growth abnormalities (290). However, osteoclasts are also stimulated by IGF-1 treatment, which induces both osteoclast formation and bone resorption (291-293). In fact genetic inactivation of IGF-1 has been demonstrated to protect mice from ovariectomy induced bone loss (294). As IGF-1 effects both bone resorption and bone formation, and is known to

act as a chemo-attractant for osteoblasts, it is often considered a coupling factor in bone remodeling.

In a similar way to TGFβ, IGF-1 is involved in the regulation of several aspects of the 'vicious cycle' of bone metastasis. It is both produced by tumour cells, stimulating both bone formation and bone resorption, and is released locally from the bone matrix, the largest store of IGF-1 in the body (295). Once released from the bone matrix, IGF-1 acts both as a potent stimulator of cancer cell proliferation and survival, and as a chemo-attractant recruiting further cancer cells into the local area of the lesion. This is true in both osteolytic and osteoblastic metastasis, but is thought to be particularly important for osteoblastic metastases (296).

1.6.3.6 Interleukins

The interleukins (ILs) are a group of 17 related protein types belonging to the pro-inflammatory chemokines family (288). Their name is derived from the fact that they were first seen to be expressed by leukocytes and were at first thought to mainly act on or be produced by leukocytes. In fact they have since been found to be expressed by many cells within the body, and regulate a number of different processes in various different organs. Of particular interest in bone metastases are IL-6, IL-8, and IL-11 all of which have been found to be expressed by tumour cells found in bone.

The IL-6 family comprises of 10 proteins known to be produced by various cells including bone cells such as osteoblasts, macrophage, and monocytes. IL-6 binds to a heterotrimeric membrane-associated receptor, consisting of an α subunit (gp80) and two β subunits (gp130), which is a member of the class I cytokine receptor family. This activates signalling pathways including JAK/STAT, PI3K/Akt and MAPKinase (297). Gp130 is thought to be ubiquitously expressed, while gp80 is only found in cells that respond to IL-6. In bone, gp80 is expressed by both osteoclasts and osteoblasts and IL-6 is known to have a dual effect, stimulating bone resorption through causing the differentiation of mature osteoclasts, and stimulating bone formation in conditions of high bone turnover (298-300).

In cancer, IL-6 is thought to act via autocrine/paracrine signalling to increase tumour cell proliferation, invasion and angiogenesis (301). In bone metastasis, IL-6 mainly increases bone resorption through both direct effect on osteoclasts, and indirectly through causing increases in the expression of RANKL in osteoblasts and macrophages, as well as causing increases in tumour cell production of pro-osteolytic factors such as PTHrP, PGE2, IL -8 and IL-11 (299, 300). IL-6 also affects the proliferation of tumour cells and bone formation, although its overall effect is probably determined by the balance of interactions with other bone metastasis factors (300).

IL-8 and IL-11 are both known to stimulate bone resorption in bone metastases, causing increased levels of osteolysis (302, 303). IL-8 binds to the CXCR1 receptor on osteoclasts and macrophage thereby causing RANKL independent stimulation of osteoclast activity (304), while IL-11 is known to mediate osteoclastogenesis acting via the IL-11 receptor (305). In addition, IL-8 or IL-11 expression in tumour cells has been associated with high rates of bone metastasis and both cytokines are also linked to higher levels of osteolytic damage (300, 306). During the vicious cycle, IL-8 and IL-11 are produced by tumour cells and osteoblasts in response to exposure to prostaglandins (300).

1.6.3.7 TNFα

Tumour Necrosis Factor-α (TNFα) is a member of the TNF family that comprises of type II homo- or hetero-trimeric transmembrane proteins, many of which are cleaved to generate soluble ligands, including RANKL (307). TNFα is a key, but not essential, regulator of osteoclastogenesis through its interactions with its receptors; TNF receptor 1 and 2 (TNFR1 and TNFR2) (307, 308). Binding of TNFα to TNFR1 enhances osteoclast differentiation by stimulating signalling through pathways including the NFκB, MAPKinase and PI3K/Akt signalling pathways (307, 308). When TNFα binds TNFR2 on the other hand it causes inhibition of osteoclastogenesis through unknown mechanism(s) (308, 309). One possibility is that TNFR2 induces a 'ligand passing' mechanism that causes a local increase in TNFα. This then induces apoptosis by TNFR1-mediated mechanism(s) (309).

Excessive bone resorption in various diseases is thought to be related, at least in part, to changes in TNFα expression. This has been a particularly important finding in

relation to post-menopausal osteoporosis, as oestrogen negatively regulates TNFα production (310, 311). In cancer, TNFα is thought to play a key role in the development of several tumour types including breast cancer, as it is a potent stimulator of tumour cell proliferation and a strong inducer of angiogenesis (312, 313). High serum concentrations have been linked to progression of cancers, and an increase in aggressive tumour biology. In bone metastasis, expression of TNFα has been linked to poor prognosis, increased metastasis to bone and increased osteolysis in bone. This appears to be either due to direct production of it by tumour cells, or stimulation of its production in bone cells by tumour released factors including interleukins (312, 313). In addition to its direct effects on osteoclasts it is also thought to stimulate the production of IL-6 (314). Recently it has been demonstrated that inhibiting TNFα causes a reduction in the number and severity of bone metastases from breast cancers (312).

1.6.3.8 BMPs

Bone morphogenetic proteins (BMPs) are a group of 20 highly related cytokines of the TGFβ super family. They were initially identified by their shared role in inducing endochondral bone formation (300, 315, 316). They bind to type IA, type IB or BMP type II receptors inducing signalling cascades through the SMAD and MAPKinase pathways (317). In bone, BMPs play an important role in the development of osteoblasts, stimulating cell proliferation and bone formation by an autocrine/paracrine mechanism (300, 317).

BMPs have been linked to osteoblastic tumours associated with prostate cancer, and are thought to be responsible for much of the bone formation caused by prostate cancer cells. For example, BMP-4, BMP-6, and BMP-7 have been shown to be produced by prostate tumour cells within the bone micro-environment (300, 318, 319). In fact, when prostate tumour cells that normally caused osteoblastic metastases were made to over express the BMP inhibitor noggin, they lost their osteoinductive properties. In breast cancer, current reports are contradictory, with some studies suggesting that BMPs promote bone metastasis, while others suggest they inhibit it (reviewed in (320)). BMPs are also released from the bone matrix by resorption, and like many other factors, are thought to stimulate the proliferation of tumour cells in addition to their effect on osteoblasts (300). A

further effect of BMPs is their angiogenic effect which may also contribute to the growth of tumours in bone metastasis (321).

1.6.3.9 ET-1

Endothelin-1 (ET-1) is a potent vasoconstrictor which stimulates DNA synthesis and cell proliferation of various healthy cell types, such as fibroblasts, as well as malignant epithelial cells including prostate cancers (300, 322). ET-1 is also thought to indirectly promote tumour growth by causing the release of VEGF in response to hypoxia, thereby allowing the vascularisation of tumours (300, 322). ET-1 signals through the ET_A receptor (ET_AR) and causes a signalling cascade that can interact with other signalling pathways including the PI3K/Akt and MAPKinase pathways (322).

ET-1 has two roles in bone metastasis. First, it is linked to increased rates of metastasis in tumour cells. This is thought to be due to the fact that it can both induce the expression of extra-cellular matrix degrading proteins including several MMPs, and stimulates the phosphorylation of Focal Adhesion Kinase (FAK), an action that is linked to general tumour cell migration (322, 323). Secondly, ET-1 appears to be a vital factor in the development of osteoblastic bone metastases (300, 322, 324). It stimulates bone formation by both increasing osteoblast actions and inhibiting the function and migration of osteoclasts (322, 324). In osteoblasts, ET-1 increases both proliferation and function. The exact mechanisms behind this are unclear, but it is thought to be related to increasing the levels of OPN and OCN expression and through enhancing the effects of other pro-osteoblast factors (324). Various factors have been shown to induce the production of ET-1 in tumour cells, including TGFβ, TNFα and IL-1 which are all commonly found in the bone microenvironment (322). The key role of ET-1 in osteoblastic bone metastases from prostate cancers has been demonstrated by studies showing that inhibiting the actions of ET-1 caused reductions in the number of metastases, inhibited tumour growth by inhibiting cell proliferation and angiogenesis, and reduced the excess bone formation observed reducing patients bone pain (300, 322).

1.6.3.10 VEGF

Vascular Endothelial Growth Factor (VEGF) is a critical regulator of blood vessel formation, and is involved in the development of vascularisation during bone development (325). VEGF is produced by bone cells including chondrocytes and osteoblasts (326), and has been shown to directly stimulate bone formation by increasing osteoblast proliferation and differentiation (300, 327), as well as stimulating bone resorption by increasing osteoclast survival (328).

In cancers, increased VEGF has been associated with increased metastasis and rapid growth of tumours, as it allows the vascularisation of tumour sites (329). This is probably also the major effect of VEGF in bone metastases; however it can also exert direct effects on bone as stated above. Either way VEGF is affective at supporting the development and progression of both osteolytic and osteoblastic bone metastases(300).

1.6.3.11 Prostaglandins

Prostaglandins, and Prostaglandin E_2 (PGE_2) in particular, are known to have a complex role in bone in health and disease. They are enzymatically derived metabolites of polyunsaturated fatty acids, in the case of PGE_2 the fatty acid is arachidonic acid, and are involved in a diverse range of actions in many different tissues (330, 331). PGE_2 increases both bone formation and bone resorption *in vivo*, though its overall effect is normally to increase the total quantity of bone and it has been particularly linked to fracture healing (332-335). PGE_2 acts through four G-protein coupled receptors termed E-prostanoid (EP) 1-4. Of these, EP2 and EP4 are the most widely expressed in bone. EP2 knockout mice have impaired osteoclast formation, due to a reduction in the ability of osteoblasts to stimulate osteoclastogenesis by producing RANKL (336). EP4 knockout mice have no bone phenotype during growth, but develop accelerated age-related bone loss due to a reduction in osteoblast activities. Cell cultures from the EP4 knockout mice demonstrated that bone nodule formation was impaired, as was PGE_2 stimulated osteoclast formation. In addition fracture experiments showed that bone repair was inhibited by the loss of the EP4 receptor (330, 336).

In bone metastasis, PGE_2 is not normally highly expressed by tumour cells. However, Cyclooxygenase-2 (COX-2), which is responsible for PGE_2 synthesis, is expressed by breast cancer cells, and increased COX-2 expression is induced by other factors produced by tumour cells such as TGFβ (300). High COX-2 expression has also been found to be linked to the development of several tumours and increased metastasis of cancers including metastasis to bone (337-340). Inhibitors of the PGE_2 receptors EP2 and EP4 have been shown to reduce osteolysis and tumour growth in the bone microenvironment (339, 341).

1.6.3.12 MMPs

The matrix metalloproteinases (MMPs) are a family of proteolytic enzymes that are capable of degrading components of the extracellular matrix and various secreted or membrane bound proteins including growth factors, cytokines, cell surface receptors, and adhesion molecules (342). Surprisingly, MMPs have only a limited involvement in osteoclast function and they have been shown to play a minor role in the degradation of the extracellular matrix during bone resorption, the cathepsin proteins are far more vital for this. MMP-9 and MMP-13 produced by other bone cells have been shown to be involved in the differentiation of osteoclasts, and other MMPs have been hypothesised to prime the bone surface for resorption (reviewed in (343)). MMP-13 has also been shown to bind to receptors on osteoblasts, chondrocytes and fibroblasts. The effect of this is unknown, but it has been suggested that these cells internalise and degrade MMP-13 thereby regulating the extracellular levels of metalloproteinases (343).

MMPs are particularly important in the development of cancers as they have been implicated in not only tumour migration and invasion, but also tumour development, angiogenesis and apoptosis (344). In bone metastasis, MMP-1, MMP-2, MMP-9, and MMP-13 have all been linked to metastatic disease caused by either breast or prostate cancers (344-349). This is either due to direct MMP production by tumour cells, or activation of their production in other cells by factors produced by tumour cells. In addition to their direct actions on both bone and tumour cells, they have the added effect of releasing bone derived growth factors trapped in the bone matrix, such as TGFβ and IGF-1 (300).

1.6.3.13 PDGF

Platelet derived growth factors (PDGF) are a family of growth factors composed of polypeptide dimers linked by disulphide bonds (350). PDGFs are synthesised by various cells including platelets, fibroblasts and bone cells such as macrophage and osteoblasts (351). Acting mainly on PGDFRα and PDGFRβ receptors (352), PDGF causes mitogenic effects in numerous cell types including fibroblasts, glial cells, muscle cells and osteoblasts, and is responsible for some organogenesis during development, and angiogenesis and wound healing after tissue damage (352).

In bone, PDGF is particularly important for bone repair after a fracture. Produced in high quantities by platelets at the site of a wound or fracture, PDGF stimulates the proliferation, differentiation, migration and function of osteoblasts in the area local to the wound (352, 353). It has also been found to be produced by osteoclasts, and so may act as a coupling factor between bone resorption and bone formation (353).

Inhibition of PDGF has been suggested as a treatment for bone metastases associated with both breast and prostate cancer, due to its stimulatory effects on angiogenesis (354, 355). Targeting PDGF in bone metastasis from breast cancers did not directly effect osteolysis, but reduced growth of tumour cells within bone (355). In osteoblastic prostate cancers, inhibition of PDGF activity caused not just a reduction in tumour growth, but also reduced the cancer induced bone formation observed and in some cases prevented the initial development of bone metastases (354, 356).

1.6.3.14 FGFs

Fibroblast Growth Factors (FGFs) are a family of 23 structurally related polypeptide growth factors that act through the tyrosine kinase FGF receptors (FGFR) 1-4. FGFs are known to play various vital roles in embryonic development and tissue repair (300, 357). Various FGFs, but FGF-18 in particular, are involved in endochondral ossification, while others affect both osteoblast and osteoclast differentiation in the adult bone (358). FGF-2 is thought to be one of the major regulators of adult osteoblast differentiation due to its action via the JAK/STAT signalling pathway (358).

FGFs play an important role in the development of bone metastases associated with prostate cancers. FGF-1, 2, 6, 8 and 17 have all been shown to stimulate the growth of

prostate tumours, while FGF-8 has been found to be over expressed in 76% of prostate cancer bone metastases (300, 357). In bone, FGF-8 stimulates the differentiation of both osteoclasts and osteoblasts and increases the growth of prostate tumour cells. Inhibition of FGF-8 reduced both tumour burden and osteolysis in experimental animals (357).

1.6.4 Treatment of bone metastasis

There are few cases of bone metastases that can be successfully resolved, and as such most treatments are palliative, attempting to lessen pain and slow the progress of the disease, rather than cure it. Treatments include drugs that directly relieve pain, drugs that interfere with the mechanisms of the metastasis that lead to pain, and radiotherapies and surgeries to either remove the tumour and/or relieve pain. In most cases a combination of therapies will be used to treat a patient.

1.6.4.1 Analgesics

Both osteolytic and osteoblastic metastases can be incredibly painful, and so most patients are given some form of pain relieving treatment. The form and extent of this treatment varies according to the severity of the pain, and type of metastasis. Pain is caused directly by the loss of mechanical function due to either bone loss or inappropriate bone formation, or indirectly by the release of chemical pain mediators and the compression or irritation of nerve fibres. There are two basic types of pain relieving drug used in the treatment of bone metastases, opioid analgesics, and non-opioid analgesics. Non-opioid drugs are used for milder pain, and where the patient wishes to avoid addictive opioids. These include Tramadol, and NSAIDS including COX-2 inhibitors. Opioids are more frequently used in cases of moderate to severe bone pain and include a wide range of drugs from codeine to stronger opiates such as morphine and methadone (Reviewed in (359)).

1.6.4.2 Surgery

Surgery is performed to either remove the area of bone affected by the metastasis as a therapeutic treatment, or to relieve pain in the area. In either case it is generally undertaken as a way of preventing a pathologic fracture, and allowing stabilisation of the afflicted bone region. Surgeries range from vertebroplasty or kyphloplasty stabilisation of vertebrae to complete removal of large section of the bone, or even amputation (359). Bone grafts or prosthesis are used to replace the lost bone. In most cases surgery is not considered a curative intervention, as the nature of the metastatic diseases means that recurrence, and multiple metastases in other bones and further organs are likely to occur. Instead the life expectancy and impact that surgery will have on the quality of life of a patient are considered before determining the type and extent of surgery to perform (360).

Developments in new implantable materials and biosynthetic implants have lead to the hope that in the future surgery may be able to offer more to bone metastasis patients. In particular it has been suggested that it may soon be possible to use biological techniques to create natural tissues that could allow fully reconstructed natural bones to be created, perhaps even with implants that allow the controlled localised release of anti-cancer agents. This would allow the repair and treatment from a surgery that is currently an irreparable removal of tissue, with little hope of overall curative affect (360).

1.6.4.3 Radiotherapy

Radiotherapy is the use of localised high doses of radiation to cause DNA damage in cells leading to apoptosis. Cancer cells are thought to be more susceptible to this than healthy cells due to their mutated and dysfunctional DNA damage-repair mechanisms. It has become the standard treatment for localised uncomplicated bone metastases that are considered painful. Response rates are good with between 50% and 90% of patients achieving some pain relief and 10-50% becoming free of pain (361-365). Many patients are even able to reduce or in some cases completely stop their use of analgesics. However there are many drawbacks to radiotherapy. Recurrence of bone pain is common as the metastasis regrows, or recolonizes the site, this leads to further radiotherapy treatment at the site, increasing the damage to healthy tissues and making side effects more likely. Side

effects are generally radiation related acute toxic effects such as skin reactions, or gastrointestinal problems including nausea and vomiting. Increased risk of pathologic fractures may possibly also occur after radiotherapy treatment (359, 360).

1.6.4.4 Bisphosphonates

The most common bone targeted therapies used for the treatment of bone metastases are bisphosphonates. These are a group of analogues of pyrophosphate that have had the oxygen atom replaced with a carbon atom and can have various side chains attached giving the bisphosphonate compound different potency and side effect profiles [reviewed in (366, 367)]. There are three subdivisions of the bisphosphonates defined by their side changes. The first generation bisphosphonates, Clodronate and etidronate, had simple alkyl side chains, while the second generation, pamidronate and alendronate, contained nitrogen and so were known as aminobisphosphonates. The latest generation of bisphosphonates is the third generation which contain a cyclic side chain in addition to nitrogen and include ibandronate, risedronate and zoledronate (368, 369).

Bisphosphonates basic mechanism of action is through their ability to inhibit bone resorption. This occurs as they bind strongly to bone, hydroxyapatite in particular, throughout the body and are subsequently internalised by resorbing osteoclasts (370). This disrupts various osteoclast processes in different ways depending on the type of bisphosphonate, generally resulting in cell apoptosis (369, 371)]. The effects of bisphosphonates on osteoblasts are more controversial, with some research suggesting that they stimulate osteoblast differentiation and function (372, 373), but other work showing that they inhibit bone formation and may even cause osteoblast apoptosis (374-376).

Both osteolytic and osteoblastic bone metastasis patients can achieve pain relief through treatment with bisphosphonates, though effects are far better in osteolytic metastases. The reduction in bone remodelling both reduces the risks of any pathologic fractures and also may diminish, or at least prevent the deterioration, of the release of chemical pain mediators, the irritation of nerves and the loss of mechanical function. As such various bisphosphonates are generally given from the point of diagnosis. Side effects

are a major limiting factor in bisphosphonates, and may include gastrointestinal upset, oesophagitis, renal abnormalities, and in rare cases osteonecrosis of the jaw (366, 368, 377). Most of these are related to long term use, and as such do not occur often in bone metastasis cases, however some trials of high dose zoledronate suffered from increased rates of renal abnormalities.

It has recently been suggested that some bisphosphonates may also have specific anti-tumour effects, both by reducing angiogenesis and by directly inhibiting tumour growth. In particular, nitrogen-containing bisphosphonates have been demonstrated to reduce angiogenesis *in vitro,* and *in vivo*, and to prevent tumour associated angiogenesis in various different cancer models. The mechanism behind this is thought to be related to the reduction in the recruitment of myeloid cells, specifically macrophages, to the tumour site. Since these cells produce large amounts of the pro-angiogenic factors VEGF and MMP-9 tumour vascularisation is inhibited. While more poorly understood, there is growing evidence to support bisphosphonate inhibition of tumour metastasis to soft tissues and direct *in vivo* inductions of tumour cell apoptosis in some cases. Mechanisms behind this are unclear and while these studies have raised the possibility that bisphosphonates may exert an anti-tumour effect, in patients with breast cancer (378-380) the AZURE study showed no overall benefit of Zoledronic acid on patient mortality rates.

1.6.4.5 Denusomab

Recently, denusomab, a monoclonal human anti-RANKL antibody has been developed (381). Denusomab selectively binds to the key osteoclast factor RANKL and effectively prevents the differentiation, formation and function of osteoclasts. It has been shown to be an effective treatment for the relief of pain associated with both osteolytic and osteoblastic bone metastases, and 3 recent stage 3 clinical trials have shown that it is more effective than bisphosphonates at reducing both the initial onset of a pathologic fracture, and the incidence of multiple fractures (382-384). It had similar side effect profiles to the third generation bisphosphonate zoledronate in each case. As denusomab acts on osteoclasts it is unsurprising that a direct anti-tumour effect has been demonstrated in

giant tumour cells (385). Studies to determine any effects on other tumour types are ongoing are currently ongoing (386).

1.6.4.6 Novel treatments

A variety of novel treatments for bone metastasis exist, ranging from diverse chemotherapies and radiopharmaceuticals targeting the cancer cells, to the recent development of a hyperthermia treatment for bone metastases using magnetic materials (359, 360, 387). One promising new treatment is the development of SRC inhibitors, initially trialled as anti-tumour and anti-metastasis agents, recent investigations using SRC knockout mice have shown that inhibiting SRC also reduces osteoclast formation (388). In every case the treatment generally is aimed at reducing bone pain, while also lessening tumour burden. More research is needed to increase our understanding of the mechanisms behind bone metastasis, allowing us to develop treatments that can more effectively treat both the bone and tumour components of this disease.

1.6.5 Why Study Bone Metastasis?

While our understanding of the mechanisms behind bone metastasis has evolved substantially over the past decades, much still remains unclear. The effect of current treatments on patient outcomes has been minimal and it is clear that new therapeutic targets are needed to move the aim of treatment away from being purely palliative and towards being curative. In bone metastasis a complex web of interacting cell types, growth factors and cytokines that lead to multiple possible outcomes is emerging, and better research tools are required to investigate this. Research is needed to understand exactly how all these elements interact, to identify new therapeutic targets, and to develop novel treatments that can address the major clinical problems caused by both osteolytic and osteoblastic bone metastases.

1.7 Aim of this study

The general aim of this thesis was to design, develop and test a model system to study the interaction between cancer and bone cells *in vitro*, *ex vivo* and *in vivo*.

The specific aims of the work reported in this thesis were:

- To develop a model system for the study of breast and prostate cancer cell – induced:
    - bone cell signalling, proliferation, survival and activity *in vitro*.
    - focal osteolysis in organ cultures of bone.
    - bone cell proliferation and activity *in vivo* and osteolysis in animal models of metastatic bone disease
- To test this system by using it to examine the effects of a novel potential therapeutic agent on the cancer-induced osteoclastic and osteoblast changes associated with breast cancer. For this purpose the IGF-1 receptor kinase inhibitor PQIP was chosen. This was due to the known effects of IGF-1 on bone cells and in the development of breast cancer and bone metastasis, as well as the novelty of looking at IGF-1 receptor inhibition in this context in comparison to signalling induced by other factors found to be produced by cancer cells in this model, and due to the drug being made available to us by a kind gift from OSI pharmaceuticals.

Chapter 2

Materials and Methods

2 Materials and Methods

2.1 Tissue Culture

2.1.1 Tissue culture conditions

All tissue culture work was carried out in a sterile laminar flow hood. Cultures were kept in incubators with standard conditions of 37˚C in a humidified atmosphere of 5% CO_2, 95% air. A sterilised water bath was used to warm all solutions to 37˚C prior to use and plastic-ware was either bought pre-sterilised or autoclaved prior to use. Cultures were checked regularly to assess confluence or contamination using a phase-contrast microscope.

2.1.2 Standard tissue culture medium

All cells were cultured in standard αMEM. Standard αMEM consists of α-Modified Eagle's Medium (αMEM) supplemented with 10% foetal calf serum (FCS), 2 mM L-Glutamine, 100 IU/ml Penicillin and 100IU/ml Streptomycin.

2.1.3 Cell lines

Human breast cancer cell lines MDA-MB-231 and MCF7, human prostate cancer cell line PC3, mouse breast cancer cell line 4T1, mouse MC3T3-E1 pre-osteoblasts and mouse osteosarcoma cell line MC57G cell lines were purchased from ATCC (Manassas, VA, USA). Cells were cultured in 75 cm^2 flasks and passaged every 48-72 hours at a ratio of 1:5 (MCF7), 1:10 (MDA-MB-231, MC3T3, PC3, MC57G) or 1:20 (4T1). Briefly, culture medium was removed, cells washed in PBS and detatched by treatment with trypsin. Standard αMEM was added to inactivate the trypsin and cells were then transferred to a fresh sterile 15 ml tube which was then centrifuged at 1200 rpm for 3 minutes. The supernatant was discarded and cells resuspended in 1 ml standard αMEM before a percentage of the suspension was placed into a fresh 75 cm^2 flask containing 12.5 ml standard αMEM.

2.1.4 Viability assay

The Alamar Blue assay was used to measure cell viability (389). This assay assesses cell viability using an oxidation/reduction (redox) reaction. The amount of the redox indicator that present in the AlamarBlue solution changes from oxidised (non-fluorescent, blue) to a reduced form (fluorescent, violet) is directly proportional to the number of viable and active cells. Briefly, 10% (v/v) of AlamarBlue™ reagent was added to each culture well and cultures were then incubated at 37˚C for 2-4 hours under standard tissue culture conditions. A plate reader (Bio-Tek Synergy HT) was then used to read the fluorescence of the wells (excitation wavelength 540 nm – emission wavelength 590 nm). Control wells of standard αMEM plus 10% v/v AlamarBlue solution were used to correct the data for background fluorescence.

2.1.5 Bone marrow isolation and cultures

C57B6 mice aged 8-12 weeks were sacrificed by surgical dislocation and their long bones (tibia and femur) removed and transported to a sterile laminar flow hood. Long bones were then placed into a glass petri-dish, the soft tissue removed using a scapel and the ends of each bone cut off to reveal the bone marrow. To extract bone marrow (BM) cells from the isolated bones a 5 ml syringe filled with standard αMEM and with a 25 gauge (G) needle attached was inserted into the bone marrow cavity and used to flush out the bone marrow into a fresh 60 mm petri-dish. To homogenise the cell suspension the bone marrow cells in standard αMEM were passed through a series of needles of increasing gauge (19G to 25G). This cell suspension was then placed into a 15 ml tube and centrifuged at 1200 rpm for 3 minutes. The pellet was resuspended in 10 ml standard αMEM plus 100 ng/ml M-CSF and plated into a fresh 100 mm petri-dish. Bone marrow cultures were left in standard conditions for 72 hours by which point adhered cells were considered to be M-CSF generated macrophage (referred to in this thesis as M-CSF generated osteoclast precursors).

2.1.6 Osteoclast and macrophage cultures

Adherent M-CSF generated osteoclast precursors were scraped from the surface of their petri-dish, counted using a haemocytometer, and plated into 96 well plates at an initial seeding density of 12 x 10^3 cells per well in 150 µl standard αMEM containing M-CSF (25 ng/ml) and, for osteoclast cultures, RANKL (100 ng/ml). 50% of the medium was refreshed after 24 hours with the addition of any desired test compounds. Medium and treatments were again refreshed after a further 48 hours and the cultured terminated 24-48 hours after that. Viability of macrophage was assessed using the Alamar Blue assay, while osteoclast number was assessed by manual counting following TRAcP staining.

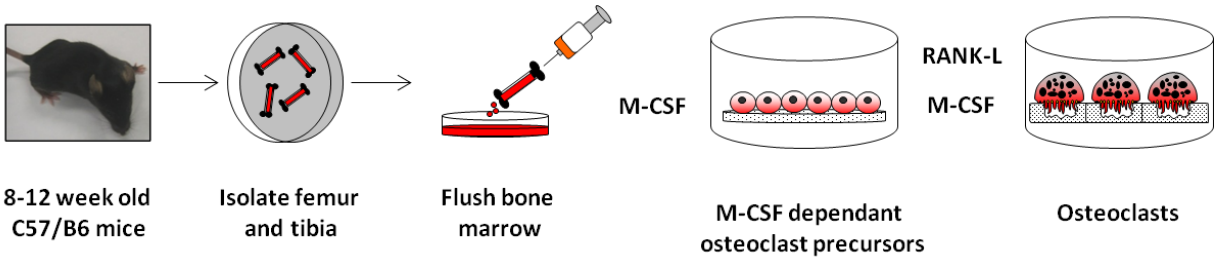

Figure 2.1 A diagram describing the method behind primary macrophage and osteoclast cultures. See text for more details.

2.1.7 TRAcP Staining

Osteoclast cultures were fixed in 4% (v/v) para-formaldehyde in PBS. Osteoclasts were then identified by TRAcP staining as described in van't Hof *et al* (390). Briefly, 100 µl of TRAcP staining solution (See Appendix 2) was added to each well and plates incubated at 37˚C for 45-60 minutes. The TRAcP staining solution was then removed and cells rinsed twice with PBS. 200 µl of 70% (v/v) ethanol was added to each well and plates wrapped in cling-film and stored at 4˚C. To assess osteoclast cell number, TRAcP positive cells with 3 or more nuclei were considered to be osteoclasts and manually counted on a Zeiss Axiovert light microscope using a 10x objective lens.

2.1.8 Resorption assay

Osteoclasts cultures were generated on Corning® Osteo Assay Surface multiple well plates (Corning, USA). Following culture period, adherent osteoclasts were incubated in 50% bleach (Clorox-Ultra, USA) for 10 minutes and plates were rinsed 4 times with PBS. 200 μl of 70% (v/v) ethanol was added to each well and plates wrapped in cling-film and stored at 4˚C. Resorption pits were visualised by phase contrast microscopy on an Olympus ScanR microscope using a 10x objective lens and area resorbed was quantified by Image Analysis using ImageJ software.

2.1.9 Calvarial osteoblast cultures

Primary osteoblasts were isolated from the calvarial bones of 2-day-old mice sacrificed by decapitation. Calvariae were dissected out, washed in Hank's Balanced Salt Solution (HBSS) and transferred to a sterile 15 ml tube containing 2 ml of collagenase type I in PBS (1 mg/ml). Calvariae were incubated at 37˚C in a shaking water-bath for 10 minutes, the supernatant discarded and a further 4 ml of collagenase in PBS (1 mg/ml) added to the 15 ml tubes. After 30 minutes, additional incubation at 37˚C in a shaking water-bath the supernatant was removed and transferred to a sterile 15 ml tube containing 4 ml standard αMEM (fraction 1). The calvaria were then decalcified by incubation with ethylenediaminetetraacetic acid (EDTA) (4 mM) in PBS at 37˚C in a shaking water-bath for 10 minutes. The supernatant was removed and transferred to a sterile 15 ml tube containing 4 ml standard αMEM (fraction 2). To obtain fraction 3 the remaining tissues were incubated in 4 ml of collagenase type I (1 mg/ml) in PBS for 30 minutes in a shaking water bath at 37˚C. The supernatant was again removed and added to 4 ml standard αMEM (fraction 3).

All three fractions were transferred into 15 ml tubes and centrifuged at 1200 rpm for 3 minutes. The supernatant was discarded and cell pellets resuspended in 1 ml standard αMEM. Two 75cm^2 flasks containing 11 ml standard αMEM had 50% of each fraction added to them. These were then cultured under standard conditions, with the medium being changed after 24 hours, to remove any non-adherent cells, and every 48 hours after that until the flasks became confluent.

Once the 75 cm^2 flasks of osteoblasts were confluent, medium was removed and the monolayer washed in PBS before being detached using trypsin treatment. Standard αMEM was added to the flask to deactivate the trypsin and the now detached cells were transferred to a fresh 15 ml tube. This was centrifuged at 1200 rpm for three minutes and the supernatant discarded. Cells were resuspended in 1 ml standard αMEM and manually counted using a haemocytometer.

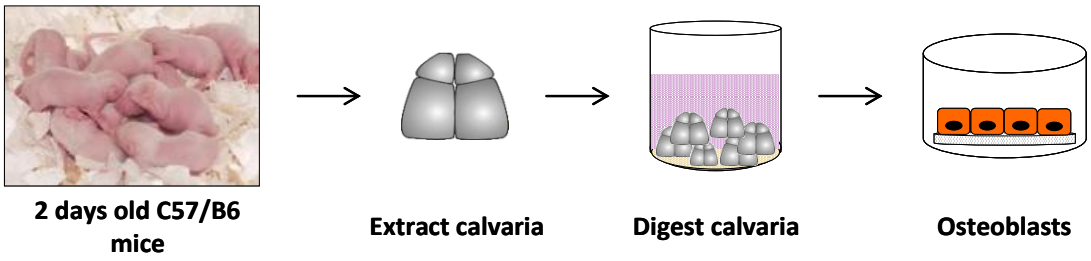

Figure 2.2 A diagram describing the method behind primary osteoblast cultures. See text for more details

2.1.10 Osteoblast viability

For studies of viability alone osteoblasts were plated in 96-well plates at a seeding density of 5 x 10^3 cells/well in 100 µl of standard αMEM. After 24 hours 50% of the medium was refreshed and desired treatments added. Cultures were left for 48 or 72 hours in standard culture conditions and cell viability at the end analysed using the Alamar Blue assay.

2.1.11 Mineralisation cultures

To study mineralisation and osteoblast differentiation osteoblasts were plated in 12 well plates at a seeding density of 100 x 10^3 cells/well in 1 ml standard αMEM and medium changed every 48 hours until the cultures were 100% confluent. The medium was then removed and replaced with standard αMEM supplemented with 50 µg/ml Vitamin C and 3 mM beta-glycerophosphate (osteogenic medium) in the presence and absence of desired treatments. Cultures were then left for 3 weeks under standard conditions with medium

and treatments refreshed every 48-72 hours. To terminate cultures cells were fixed in 70% (v/v) ethanol.

2.1.12 Alazarin red assay

At the end of mineralisation cultures, Alizarin Red S staining was used to detect any mineralised bone nodules produced by the osteoblasts. Alizarin red interacts with the calcium deposits found in mineralised tissue and bone nodules. It binds to the calcium to form a complex that causes calcium ions to precipitate and form brick red deposits.

Alizarin Red was dissolved in dH_2O at a concentration of 40 mM and the pH adjusted to 4.2 with 10% ammonium hydroxide. Fixed osteoblast cultures were washed 5 times in dH_2O before 500 µl of the alizarin red solution was added to each well and the plate incubated on a rocker for 20 minutes at room temperature. The staining solution was removed, cultures rinsed 3 times in dH_2O, and the plates left to air dry overnight.

A flatbed scanner was used to take images of the alizarin red stained cultures. In order to quantify the amount of bone nodules formed, cultures were de-stained by adding a solution of 10% (w/v) cetylpyridinium chloride in 10 mM sodium phosphate (pH 7.0) and placed on a rocker at room temperature for 30 minutes. Absorbance of the extracted stain was then measured at 562 nm using a Biotek Synergy HT plate reader and compared to an Alizarin Red standard curve. The values were normalised to cell number as determined by the AlamarBlue assay (391).

2.1.13 Alkaline phosphatase assay

To measure osteoblast differentiation the Alkaline Phosphatase assay was used. This is based on the conversion of p-nitrophenyl phosphate to p-nitrophenol by the alkaline phosphatase enzyme highly expressed in osteoblasts. This conversion changes the solution from colourless to a yellow colour, allowing the amount of alkaline phosphase present to be calculated using a plate reader.

At the end of the culture period, osteoblasts were homogenised in 500 µl alkaline phosphatase lysis buffer (Appendix 2) for 20 minutes and cell lysates collected and stored at -20˚C. To calculate the alkaline phosphate activity in each sample, cell lysates were mixed with an equal volume of paranitrophenyl-phosphate at a concentration of 20 mM in lysis buffer and absorbance measured 414 nm at 37°C in relation to a standard curve of p-Nitrophenol known concentrations. Absorbance was then measured at 562 nm using a Biotek Synergy HT plate reader and compared to p-Nitrophenol standards. Alkaline Phosphatase activity was normalised to cell number as determined by the AlamarBlue assay (391).

2.1.14 AlamarBlue assay

AlamarBlue assay was used to measure cell number (391). At the end of culture period AlamarBlue reagent (10%, v/v) was added to each well. The cells were then incubated for a further 3 hours and fluorescence measured (excitation, 530 nm, emission 590 nm) using a Biotek Synergy HT plate reader.

2.1.15 Bone cell – cancer cell co-cultures

Bone marrow cells were isolated and generated as described above. For bone marrow – cancer cell co-cultures, BM cells were plated into 96 well plates and cultured for 24 hours to allow attachment of BM cells prior to the addition of cancer cells. For osteoblast-cancer cell co-cultures osteoblasts were allowed to reach confluence before the addition of cancer cells. Cancer cells were passaged, counted and then cells added to the bone cell cultures at initial seeding densities ranging from 10 to 5000 cells depending on cell types and culture conditions. All cultures were then allowed to proceed as described for BM cell culture experiments described above. Drug treatments were added 6 hours after the addition of cancer cells in order to avoid these compounds affecting cancer cell adherence and spreading.

2.1.16 Conditioned medium assays

Conditioned medium from cancer cells was obtained by culturing cancer cells in 75 cm^2 flasks as described above. They were allowed to grow to 80% confluence in standard αMEM. Then standard αMEM was removed and replaced with serum free αMEM (αMEM supplemented with 2 mM L-Glutamine, 100 IU/ml Penicillin and 100 IU/ml Streptomycin). Cells were then cultured for a further 24 hours and the now conditioned medium was then removed and filtered through a 0.2 µm filter. Control conditioned medium was created from serum free αMEM cultured in the same way as cancer conditioned medium, but in a sterile flask with no cancer cells added.

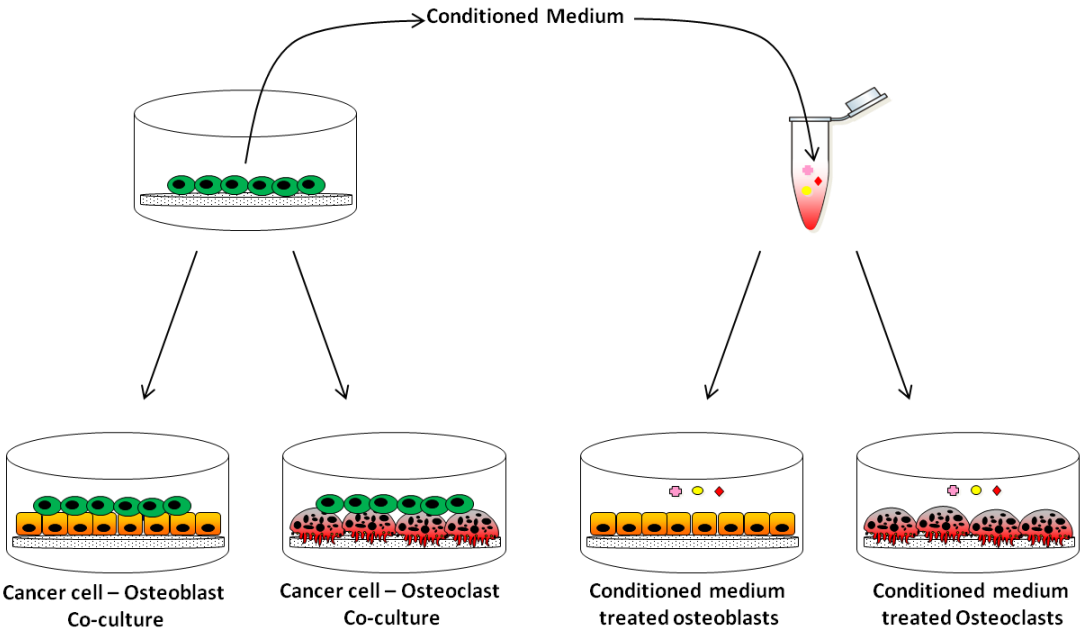

Figure 2.3 A diagram describing the method for cancer cell – bone cell co-cultures and conditioned medium treatments. See text for more details

2.1.17 Cancer cell adherence and spreading

The Xcelligence assay was used to measure cancer cell adherence and spreading. The Xcelligence system is a real-time, label free, cellular analysis system (Roche) which uses specialised culture plates with interdigitated gold-micro-electrode coated on the bottom. This allows the quantitative measurement of electrical impedance caused by the presence of cells in the well. Changes in electrical impedance in the well can then be related to

changes in cell number, viability, morphology, movement as well as various other aspects. The Xcelligence machine was placed into a incubator at 37˚C, 5% CO_2 and linked to a laptop running the RTCA Xcelligence monitoring software (Roche).

Standard αMEM containing test compounds was added to Xcelligence plates and the plate read on the Xcelligence machine to establish a base reading for normalisation. Cells were then added to the Xcelligence plate, the plate placed onto the Xcelligence machine and monitoring of electrical impedance started. For cancer cell studies readings were taken as follows:

- 1 reading per minute for 1 hour
- 1 reading every 10 minutes for 7 hours
- 1 reading every 30 minutes for 40 hours

For osteoclast studies, M-CSF generated macrophages were added to the Xcelligence plate and left in standard αMEM plus 25 ng/ml M-CSF for 24 hours prior to addition of 100 ng/ml RANKL and test compounds for a further 48 hours. Readings were taken after every medium refresh as follows:

- 1 reading per minute for 1 hour
- 1 reading every 10 minutes for 7 hours
- 1 reading every 30 minutes for 40 hours

2.1.18 Wound healing assay

The wound healing assay was used to measure the migration rate of MC3T3 cells as previously described (392). MC3T3 cells were plated at 500 x 10^3 cells per well in 12 well plates and allowed to grow until confluent. Cultures were then scored with a fine pipette tip to produce a gap in the cell layer and treated with vehicle or test compounds for 24 hours. The migration of cells into the wound was visualised and monitored using phase-contrast light microscopy on an Olympus ScanR microscope. This system was automated to take photomicrographs of three points along each wound every 10 minutes for 24 hours.

The rate of wound closure was calculated using the wound assay image analysis program Tscratch (393). These values were normalised to average starting size of the initial vehicle treated wounds. Graphs of wound size versus time were plotted for each experiment and the speed of wound closure calculated from the linear portion of the graph.

2.2 Western blot

Western blot was used to study cell signalling in bone and cancer cells as previously described (394).

2.2.1 Preparation of cell lysates

Cells were plated into 6 well plates at 250 x 10^3 cells/well in 2.5 ml of standard αMEM until they reached 80% confluence or in the case of osteoclast cultures, until a significant number of osteoclasts appeared. Medium was replaced with serum free medium and the cells incubated for 24 hours or in the case of osteoclasts for 2 hours. Test compounds were then added for appropriate lengths of time until the termination of the cultures. Cultures were terminated by removing medium, washing with PBS, and then lysing cells by gentle scraping in RIPA lysis buffer (Appendix 2), with 2% (v/v) protease inhibitor cocktail and 0.4% (v/v) phosphatase inhibitor cocktail. Plates were left on ice for 10 minutes before lysates were transferred to fresh Eppendorfs and centrifuged at 12000 g for 10 minutes at 4˚C. Supernatants were then collected and stored at -20^{o}C until further use.

2.2.2 Measuring protein concentration

The Pierce protein assay using bicinchoninic acid (BCA) was used to calculate protein concentrations. Bovine serum albumin (BSA) was used to create a standard curve of protein concentrations (0-2000 µg/µl). 10 µl of these and test protein samples were pipetted into a fresh 96-well plate in duplicate. 200 µl of copper (II) sulphate in BCA (1:50) was added to each well and plates were then incubated at 37^{o}C for 15 minutes. Absorbance was measured at 562 nm using a Biotek Synergy HT plate reader and compared to BSA standards.

2.2.3 Gel electrophoresis

Protein samples (30 - 50 µg) were mixed with appropriate volumes of 5x protein loading buffer and heated at 95˚C for 5 minutes in order to denature proteins. Samples were then loaded into wells of a Criterion^{TM} XT BioRad (12% Bis-Tris) pre-cast polyacrylamide gel in an electrophoresis tank filled with electrophoresis running buffer (Appendix 2.4, page 272). A mix of Kaleidoscope pre-stained standard and a Magic Marker XP western standard were added to a separate well to allow identification of molecular weights. Gels were then run for 40 minutes at a constant voltage of 200V.

2.2.4 Electrophoretic transfer

Proteins were transferred from the polyacrylamide gel to a polyvinylidene difluoride (PVDF) membrane (Hybond^{TM}-P membrane, Amersham). Briefly, the gel was removed from the gel cassette and placed into transfer buffer (appendix 2) for 5 minutes. The PVDF membrane was cut to the size of the polyacrylamide gel and immersed in 100% methanol for 30 seconds before being placed into transfer buffer for 5 minutes. A blotting sandwich was prepared by arranging successive layers of three pads pre-soaked in transfer buffer, nitrocellulose or PVDF membrane, SDS polyacrylamide gel, three pre-soaked pads (Figure 2.4). The sandwich was orientated so that when an electrical current was applied the negatively charged proteins would move out of the polyacrylamide gel and transferred across to the membrane. The transfer was performed at a 90 mA current for 150 minutes.

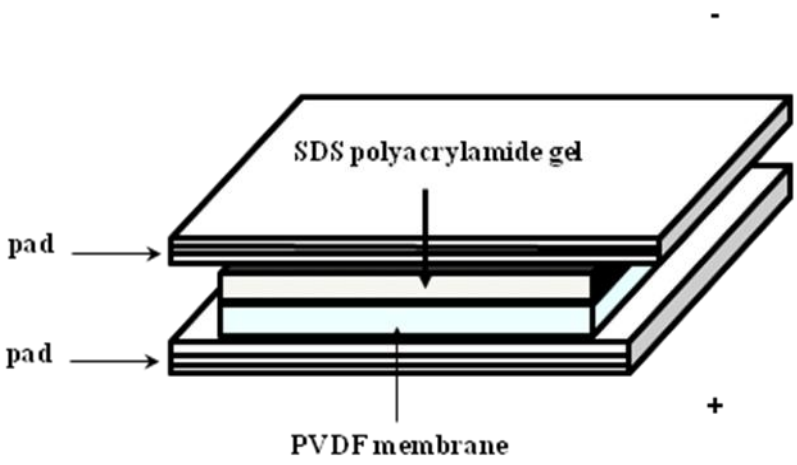

Figure 2.4 A diagram of gel transfer assembly for western blotting. Adapted from Idris AI. Methods Mol. Biol. 2012;816:223-32. See text for more details

2.2.5 Immunostaining and antibody detection

Once transfer was complete the PVDF membrane was washed three times in Tris buffer saline (TBS) supplemented with 0.1% (v/v) Tween 20 (TBST) and then placed into blocking solution (Appendix 2) for 1 hour on a rocker at room temperature. This blocks any non-specific binding sites on the membrane and so reduces false positives and background staining. The membrane was then washed 3 times in TBST, each wash lasting 10 minutes on a rocker at room temperature. Then, the membrane was incubated with the appropriate primary antibody overnight (1:2000 in 3% BSA). The next day the membrane was removed and washed a further 3 times in TBST, 10 minutes each wash, before being incubated with the appropriate secondary anti-body solution (1:5000 in blocking solution (Appendix 2)) for 1 hour at room temperature on a rocker. A final three 10 minute washes in TBST followed, before the immunoreactivity of the membrane was visualised using the Pierce SuperSignal® West Dura Extended Duration chemiluminescent detection system on a Syngene Genegnome Bio Imaging System.

To probe for other proteins on the same membrane, membranes were incubated in stripping buffer (Appendix 2) at 50˚C for 10 minutes, or until no bands were observed upon re-visualisation of the membrane. Membranes were then washed three times in TBST (5 minutes per wash) and re-blocked for 1 hour in blocking solution (Appendix 2). Three washes in TBST (10 minutes per wash) followed before membranes were left overnight at 4˚C on a rocker in 3% BSA in TBST containing the new relevant primary antibody. All steps then followed as before.

2.3 Quantitative PCR

2.3.1 RNA extraction

Cells were cultured in 6 well plates in standard αMEM under standard conditions until confluence, or in the case of osteoclasts a significant number of osteoclasts were formed. Following culture period, medium was removed and adherent cells were washed with 1 ml ice cold PBS and then lysed in 1 ml of Total RNA Isolation (Trizol®) reagent. Lysates were transferred to Pyrocarbonate (DEPC)–treated 1.5 ml Eppendorf tubes and stored at -80˚C.

To extract the RNA from Trizol, samples were defrosted and incubated at room temperature for 5-10 minutes. 200 µl of chloroform was then added to each lysate and they were mixed by shaking. Samples were incubated for a further 3 minutes at room temperature before being centrifuged at 12000 g for 15 minutes at 4^{o}C. The aqueous phase of each sample was transferred into a fresh DEPC-treated 1.5 ml Eppendorf tube containing 500 µl isopropanol. This was then mixed by inverting the Eppendorf tubes, incubated for 10 minutes at room temperature and then centrifuged at 12000 g for 10 minutes at 4^{o}C. Supernatant was discarded and 1 ml 75% (v/v) ethanol added to the RNA pellet. Samples were centrifuged at 7500 g for 5 minutes at 4^{o}C and the supernatant removed. Samples were then air-dried for 5 minutes to remove the last ethanol and 20-30 µl of DEPC treated water added to each sample. The RNA pellet was allowed to dissolve in DEPC water on ice for 10 minutes before samples were heated at 65^{o}C for 5 minutes to ensure all RNA had been resuspended. RNA samples were then stored at -80^{o}C.

2.3.2 Measuring RNA concentration

RNA concentrations were measured using a Nanodrop 1000 spectrophotometer (Thermo Scientific). 1 µl of a sample was added to the nanodrop reader and the absorbance read at 230, 260 and 280 nm. Absorbance at 260 nm was used to calculate the concentration of RNA in ng/µl, while the ratios of absorbance at 260 nm and 280 nm, and 230 nm and 260 nm were used to judge the purity of the RNA. If the 260:280 ratio was below ~2.0 or the 260:230 ratio was not between 1.8 and 2.2, then the RNA sample was considered to contain too many phenol contaminants to be of use and was not used any further.

2.3.3 Reverse Transcription

The RNA samples were reverse transcribed to produce cDNA. An equal concentration of RNA (10 pg – 5 µg) was diluted in DEPC treated water to a total volume of 13 µl and placed in a nuclease free microcentrifuge tube with the following reagents:

- 1 µl of oligo$(dT)_{20}$ (50 µM)
- 1 µl of 10 mM dNTP mix (10 mM each)

The microcentrifuge tubes were then heated to 65^{o}C for 5 minutes and then incubated on ice for at least 1 minute. The samples were briefly centrifuged and the following reagents were then added:

- 4 µl of 5X first-strand buffer
- 1 µl of 0.1M DTT
- 1 µl of RNaseOut Recombinant RNase Inhibitor (40 U/µl)
- 1µl of SuperScript III Reverse Transcriptase (200 U/µl)

The microcentrifuge tubes were mixed by gentle flicking and briefly centrifuged. Samples were then incubated at 50^{o}C for 60 minutes in a MJ Research thermocycler and the reaction terminated by heating at 70^{o}C for 15 minutes.

2.3.4 qPCR amplification

Quantative polymerase chain reactions (PCR) were performed on the cDNA produced by reverse transcription using primers and TaqMan probes specific to the genes being studied (see Appendix 3). These were designed using the Roche Universal Probe Library (UPL) Assay Design Center (http://www.roche-applied-science.com/sis/rtpcr/upl/index.jsp?id=UP030000). The TaqMan probes have two labels, one that fluoresces, and one that quenchers that fluorescence. During the extension phase of the PCR reaction the Taq polymerase cleaves the probe from its target sequence causing the fluorescent reporter label to be separated from the quencher label and thereby allowing it to fluoresce. Fluorescence was quantified using a MJ Research Chromo 4 Real Time PCR thermocycler and MJ OpticonMonitor 3.1 analysis software.

For each gene to be studied a test sample was used to create a cDNA standard of known concentration. To do this, PCR reactions were set up as follows:

Volume of Reagent		Final concentration
• 5 µl of cDNA	→	Varied
• 25 µl of 2X SensiMix(dT) Taq polymerase	→	1X
• 0.5 µl of Universal ProbeLibrary Probe (10 µM)	→	100 nM
• 0.5 µl of Forward Primer (20 µM)	→	200 nM
• 0.5 µl of Reverse Primer (20 µM)	→	200 nM
• 1 µl of $MgCl_2$ (50 mM)	→	4 mM
• 17.5 µl of RNase-free H_2O	→	N/A

Total volume = 50 µl

The thermal cycler protocol for the PCR reactions was as follows:

1. 95°C for 10 minutes
2. 95°C for 15 seconds

3. 60^{o}C for 30 seconds

4. 72^{o}C for 15 seconds

5. Repeat steps 2 to 4 for 45 cycles

qPCR products were purified using the QIAquick PCR Purification Kit and 5 µl loaded onto a 1% agarose gel containing sybersafe. The gel was run at 100V for 1 hour and visualized under UV light on Genesnap software. The concentration of these target products was quantified using the Nanodrop 1000 spectrophotometer as described above.

Standard curves were generated by serial 10-fold dilutions of the quantified cDNA standard products. qPCR was performed on both samples and standards and fluorescence was then measured using a the MJ OpticonMonitor 3.1 analysis software. The concentration of the target gene in the sample was measured by comparing fluorescence intensity of samples to those of standard curve.

2.3.5 Normalisation

To ensure all samples had equivalent amounts of starting cDNA, in addition to nanodrop measurement, the expression levels of the housekeeping genes GAPDH and 18S ribosomal RNA were calculated for each sample as described above. For GAPDH the PCR reactions were run as for every other gene, but for 18S the PCR reaction was instead set up as follows:

- 5 µl of cDNA
- 25 µl of 2X SensiMix(dT) Taq polymerase
- 2.5 µl of TaqMan® Gene Expression Assay Mix for 18S ribosomal RNA
- 1 µl of $MgCl_2$
- 16.5 µl of RNase-free H_2O

Total volume 50 µl

All other steps were run as described above. All results were then adjusted to account for 18S and GAPDH expression levels.

2.4 *Ex Vivo Cultures*

2.4.1 Adapted calvarial organ culture

A cancer cell – mouse calvaria organ culture system developed by Dr Aymen Idris was used as previously described in Frantzias *et al* 2011. 14 day old C57B6 mice were culled by surgical dislocation and the calvaria was removed as described above. Calvaria were then divided into equal halves along the median sagittal suture. The separated half-calvariae were explanted onto surfaces of stainless steel rafts in 48-well plates containing standard αMEM with either no cells or 3 x 10^3 MDA-MB-231 cells per well seeded 24 hours in advance. Medium was removed and replaced with fresh standard αMEM containing either vehicle or test compounds. Medium was at a level that partially covered the calvarial half, leaving a significant portion of the topside exposed. Cultures were maintained for 7 days with medium and treatments being refreshed every 48 hours. Calvaria were then fixed in 4% para-formaldehyde in PBS overnight and then transferred to 70% ethanol and stored at 4˚C. They were analyzed by micro-computed tomography (µCT) as described below. The viability of MDA-MB-231 cells in the calvarial organ culture were analysed using the Alamar Blue assay as described above.

2.4.2 Adapted Femoral organ culture

10 week old C57B6 mice were culled by surgical dislocation and femurs were isolated as described above. They were then either fixed in 4% para-formaldehyde in PBS overnight and then transferred to 70% ethanol, or placed into 6 well plates containing standard αMEM. Test compounds were added with standard αMEM and the volume of medium adjusted so that the femurs were approximately 80% covered. Femurs were cultured for 14 days, with medium and treatments refreshed every 48-72 hours. Following the culture period, femurs were fixed in 4% para-formaldehyde in PBS overnight and then

transferred to 70% ethanol. Femurs were then analyzed by micro computed tomography (μCT) as described below.

2.5 Animal work

All experimental protocols were approved by the Ethics Committee at the University of Edinburgh and were conducted in accordance with the UK Home Office regulations (personal licence number 60/12005, project licence number 60/3981).

2.5.1 Animals

C57BL/6, Balb/C and Balb/C Nude mice were housed in a designated animal facility. Rooms were pathogen-free and maintained at a constant temperature with 12 hours light/12 hours dark cycles. All animals had free access to water and standard commercial rodent feed pellets (SDS, Special Diets Service).

2.5.2 Intraosseous implantation

Balb/C and Balb/C nude mice were anesthetised by inhalation (isoflurane 5% in 100% oxygen in an induction chamber until anesthetised then maintained at isoflurane 2%) and their hind limbs were scanned using an *in vivo* μCT scanner (SkyScan) at a resolution of 9 microns. Human MDA-MB-231 or mouse 4T1 breast cancer cells were passaged using trypsin and manually counted using a haemocytometer. MDA-MB-231 or 4T1 cells (10×10^2, 5×10^3 or 10×10^3) were suspended in 20 μl of warm sterile PBS and transported to the animal facility. Mice were anesthetised by inhalation of isoflurane (as above) and the tibia was exposed using a sterile scalpel. It was important that the bone marrow cavity was visible before implantation was commenced as this reduced the chance of an off target injection. A 27 gauge needle with the point bent to a 45° angle was then used to drill two small holes through the cortex of the tibia and into the bone marrow cavity. These holes were located roughly 2 mm and 4 mm below the growth plate of the tibia. This location avoids damaging the majority of the trabecular bone present in the tibia. A sterile syringe filled with PBS and attached to a second 27 gauge needle with the point bent at a 45° angle

was used to flush through the lower hole, causing bone marrow to be expelled out of the upper hole. A second syringe attached to a third 27 gauge needle was then used to inject 20 µl of the PBS containing cancer cells into this newly created cavity in the bone marrow. Both openings were quickly sealed with dental wax to prevent leakage into the surrounding tissue environment. The site is then flushed with sterile water and wound was sutured. Mice are then left to recover for 7 days with analgesics added to their water supply.

After the sutures have been removed (7 days post injection) mice were anesthetised and their hind limbs were scanned using an *in vivo* µCT scanner (SkyScan) every three days for the duration of the experiment. Treatment with test compound was begun on week 2 after this second *in vivo* µCT scan. Damage to the injected tibia of mice was monitored by µCT scans and by checking the injected limbs for excessive swelling or loss of movement. Mice received an injection of calcein (10 mg/kg) 5 days and 1 day prior to culling. Experiments were terminated by cervical dislocation after 8 weeks for MDA-MB-231 cell implantations or 3 weeks for 4T1 cell implantations. The hind limbs were isolated and fixed in 4% formalin overnight followed by transfer into 70% ethanol for storage at 4°C.

2.5.3 PINP and CTX serum assays

Serum was extracted from mice to allow analysis of serum bone formation and bone resorption markers, specifically type I procollagen (PINP) (bone formation) and C-terminal telopeptide fragments of type I collagen (CTX)(bone resorption). Briefly, 400 – 1000 µl of blood was collected by cardiac puncture and transferred to fresh sterile Eppendorf tubes on ice. Serum was obtained by centrifugation of the whole blood at 3000 rpm for 10 minutes at 4^{o}C and removing the top clear layer into a fresh sterile Eppendorf tubes. Serum samples were stored at -20^{o}C until further use.

Both the PINP and CTX serum assays are enzyme immunoassays that allow quantitative determination of their respective proteins. PINP is released during collagen synthesis and so is considered to be a specific marker of bone formation (395), while CTX is released from the bone matrix and into serum during bone resorption (395). CTX is therefore considered a marker of bone resorption, although it is also used as a marker of the rate of bone remodelling in general. PINP and CTX assays were carried out according to the manufacturer's instructions (Immunodiagnostic Systems Ltd, Boldon Colliery, UK).

2.5.3 Micro computed tomography (µCT)

Micro computed tomography (µCT) was used to assess bone mass and architecture. For intratibial injection studies, the hind limbs of the mice were scanned using an *in vivo* µCT scanner (Skyscan) throughout the course of the experiment as described above, and *ex vivo* using an *ex vivo* µCT scanner (Skyscan). For *ex vivo* calvarial co-cultures, calvarial halves were fixed in 4% (v/v) parafolmadehyde in PBS and stored in 70% (v/v) ethanol. They were loosely wrapped in parafilm to prevent desiccation and placed in an *ex vivo* µCT scanner (SkyScan) in an upright position in a 2 ml syringe with both ends cut. This was placed into the *ex vivo* µCT scanner (SkyScan), fixed in an upright position on a platform within the scanner and processed in the same way as with the legs described below.

For both types of scan, SkyScan software was used to set the x-ray radiation source to 60kV and 150µA. A 0.5 mm aluminium filter was added for a 180˚ scan with a rotation step of 0.6 degrees. The pixel size was set at 9 µm for scanning mouse legs and 5 µm for scanning calvarial halves. In the *in vivo* scanner the camera is rotated around the fixed in place mouse/legs to provide pictures from all 180˚, while on the *ex vivo* scanner the samples are rotated and the camera fixed. NRecon software (Skyscan) was used to produce 3D image stacks by reconstructing the data from the rotation image projections. The top of the tibia on each leg was used as a reference line, and the 1000 frames below that were chosen for reconstruction. The entireties of calvarial halves were chosen for analysis. The parameters for reconstruction are shown in Table 2.1.

Table 2.1 Reconstruction parameters used in NRecon software

Parameter	Description	Setting
Smoothing	Smoothes image and removes noise	Width of 1 pixel
Beam Hardening Factor Correction	Corrects for the absorbance of low energy x-ray on the outside of the specimen	9%
Ring correction level	Corrects for the non-linear behaviour of pixels causing ring artefacts	3

Using CTAn software (SkyScan) the reconstructed images were analysed by selecting the region of interest. For tibias, this was from the region just below the growth plate where the calcified cartilage ridges of growth plate fuse together and extended 60 frames. This area was used for analysis as it is the most trabecular rich area. For calvaria the whole calvarial half was analysed. The region of interest was selected using a free-hand drawing tool to highlight the area required for analysis, this was repeated at intervals of 10 frames for legs and 50 frames for calvaria. The CTAn software used auto-interpolation to determine the region of interest at every other level.

The selected regions of interest were subject to a total bone analysis and analysed by 3D-reconstruction using the CTAn software. The parameters for 3D-reconstruction are shown in Table 2.2.

Table 2.2 3D Reconstruction parameters used in CTAn software

Parameter	Description	Setting
Smoothing	Smoothes images and removes noise	Medium filter; 2D space, radius 1
Threshold	Segments the foreground from background to binary images	Global; low level 100, high level 255
Despeckle	Removes speckles from binary Images	Image; remove white speckles <150 voxels
3D-Model	Creates a 3D surface from binary images	Adaptive rendering; file saved as *.p3g*
3D-Analysis	Calculates 3D parameters of binary images	Requested for basic values, trabecular thickness, number and separation

The parameters that were obtained for each scan of tibia are listed in Table 2.3. For calvarial halves only total bone volume and 3D images were analysed. SkyScan CTVol software was used to visualise the 3D models produced.

Table 2.3 3D Trabecular bone parameters calculated by µCT analysis

Parameter	Abbreviation (unit)
Trabecular bone volume	BV/TV (%)
Trabecular Thickness	Tb.Th (□m)
Trabecular Separation	Tb.Sp (□m)
Trabecular Number	Tb.N (1/mm)
Trabecular Pattern factor	Tb.Pf (1/mm)

2.5.4 Bone histomorphometric analysis

After µCT analysis of legs was complete they were processed for bone histomorphometric analysis as follows. The proximal tibia of each leg was dissected out and placed into an embedding basket in a Leica automatic tissue processor at room temperature for 28 hours. An 8 stages protocol of dehydration in ethanol dilutions and tissue clearing in xylene. The protocol used is as follows:

1. PBS 45 minutes
2. 50% Ethanol 2 hours
3. 70% Ethanol 2 hours
4. 80% Ethanol 2 Hours
5. 96% Ethanol 2 Hours
6. 100% Ethanol 3 hours
7. 100% Ethanol 3 hours
8. Xylene 1 hour
9. Xylene 12 hours

Following this processing, tibia were then placed into fresh methyl methacrylate (MMA) infiltration solution (Appendix 2) and kept in an air tight vaccum desiccator for 1 week at 4˚C. Now infiltrated, tibia were removed from vacuum and placed into individual block embedding moulds which were then filled with the same MMA solution as for infiltration, which had also been stored at 4˚C for a week. Moulds were shut and sealed airtight, placed into a 30˚C water bath and allowed to polymerise for 24-48 hours. The now

solid resin blocks were mounted on embedding rings using a fast-hardening mounting medium consisting of two thirds dibenzoylperoxide and one third N,N-dimethyl-p-toluidine.

Blocks were sectioned on a low speed microtome using a steel edge. They were trimmed until reaching the sagittal plane of the tibia, and multiple 5 µm thick sections then cut and placed onto microscope slides covered in 96% ethanol. The ethanol allowed smoothing of the sections to ensure they were flat on the slide. A removable plastic coverslip (Kisol foil) was placed onto each slide, and the slide left to dry under pressure at 37^{o}C for 24-48 hours. Then the resin was removed by immersing the slides in 2-Methoxyethyl acetate (MEA) for 60 minutes split into 3 x 20 minute washes. The slides were then rehydrated using the following program of washes.

1. Xylene 10 minutes
2. Xylene 10 minutes
3. 100% Ethanol 1 minute
4. 100% Ethanol 1 minute
5. 96% Ethanol 1 minute
6. 80% Ethanol 1 minute
7. 70% Ethanol 1 minute
8. 50% Ethanol 1 minute
9. dH_2O 1 minute

Slides were stained with Von Kossa and paragon staining for bone histomorphometric analysis. Briefly, sections were then immersed in 1.5% (v/v) aqueous silver nitrate and incubated in the dark for 5 minutes and rinsed 3 times in dH_2O before being immersed in 0.5% (w/v) aqueous hydroquinone for 2 minutes. 3 further washes in dH_2O followed. Following Von Kossa staining, the slides were counterstained using Paragon stain. This is a 1:5 mixture of Paragon solution with Borax buffer solution (Appendix 2). They were immersed in this for 1 minute and again washed three times in dH_2O. Sections were

then air dried in a fume hood, briefly dipped in xylene and covered with DPX mounting medium.

Bone histomorphometry analysis was performed on the Von Kossa stained sections, and on blank sections for calcein labelling analysis as follows. The tibial proximal metaphysis distal to the epiphysial growth plate were visualised using a Zeiss Axio Imager microscope fitted with a QImaging Retiga 4000R camera. Custom software developed by Dr. Rob J. van't Hof using the Aphelion Image Analysis tool kit (Adcis SA, Hérouville-Saint-Clair, France) was used to perform static and dynamic bone histomorphometry (396). Parameters defined by this were calculated according to the ASBMR Histomorphometry Nomenclature Committee (397) and are shown in Table 2.4.

Table 2.4 ASBMR Histomorphometry Nomenclature Committee Bone histomorphometry parameters

Parameter	Abbreviation (unit)	Calculation/Expression
Bone Volume per Total Volume	BV/TV (%)	Value x 100
Active resorption area per Bone Surface	Oc.S/BS (%)	Value x 100
Osteoclast Number per Bone Surface	Oc.N/BS (# of cells/mm)	Osteoclast number/Bone surface
Osteoblast Number per Bone Surface	Ob.N/BS (# of cells/mm)	Osteoblast number/Bone surface
Osteoclast Number per total section area	Oc.N/T.Ar (# of cells/mm^2)	Osteoclast number/Section area
Osteoblast Number per total section area	Ob.N/T.Ar (# of cells/mm^2)	Osteoblast number/Section area
Single Labelled Surface	sLS (µm)	Calculated by software
Double Labelled Surface	dLS (µm)	Calculated by software
Bone Surface	BS (µm)	sLS + dLS + unlabelled surface
Labelled Width	L.Wi (µm)	Calculated by software
Mineral Apposition Rate	MAR (µm/day)	L.Wi /# of days
Mineralising Surface per Bone Surface	MS/BS (ratio)	(dLS + sLS/2)/BS
Bone Formation Rate (at bone surface level)	BFR (μm^2/day)	MAR*(MS/BS)

Slides were stained with TRAcP and aniline blue staining for osteoclast identification. Briefly, slides were placed into the TRAcP staining solution (Appendix 2) for 2

hours at 37˚C or until the red stain had begun to develop. They were the washed 3 times in dH_2O, before being placed into aniline blue counter stain (Appendix 2) for 20 minutes. Sections were then air dried in a fume hood and then briefly dipped in xylene. Sections were then air dried in a fume hood, briefly dipped in xylene and covered with DPX mounting medium. TRAcP and Aniline blue stained slides were used for image purposes only.

2.6 Statistical Analysis

Student's t test was performed to determine the significance level of differences between two sets of results. Where appropriate comparison between groups was done by analysis of variance (ANOVA) followed by Bonferroni post-hoc test using SPSS for Windows version 11. A p-value value of 0.05 or below was considered statistically significant, and a p-value of 0.01 or below highly statistically significant.

Chapter 3

Models to study cancer-induced bone cell activity *in vitro*

3.1 Summary

Bone metastases in breast cancer patients generally cause osteolytic lesions as the invading tumour cells release a variety of factors that up regulate bone remodelling in a manner that favours bone resorption. The main aim of this chapter was to develop *in vitro* models to study this cancer-induced osteolysis. Given the limitations of cancer cell lines as models for the study of cancer, a number of mouse and human cancer cell lines were chosen for this purpose.

Human MDA-MB-231, human MCF7, mouse 4T1, and mouse MC57G breast cancer cells significantly enhanced RANKL and M-CSF-stimulated osteoclast formation, size and nuclearity in cancer cell - bone marrow (BM) co-cultures regardless of number of cancer cells seeded. In the absence of RANKL, human and mouse breast cancer cells failed to induce osteoclast formation regardless of number of cancer cells seeded. This demonstrates that breast cancer cells alone are incapable of stimulating osteoclast formation.

To study the role of breast cancer derived factors in the absence of the cancer cells themselves, conditioned medium derived from human and mouse breast cancer cells was used. Conditioned medium derived from human MDA-MB-231, human MCF7, mouse 4T1, and mouse MC57G increased osteoclast formation, size and nuclearity. Functional studies with conditioned medium showed that MDA-MB-231 stimulated osteoclast signalling and increased the RANKL/OPG ratio in osteoblasts. Treatment of M-CSF dependant osteoclast precursors with conditioned medium from human and mouse enhanced the adhesion and spreading of these cells without affecting cell viability. In contrast, conditioned medium from human and mouse reduced osteoblast differentiation without affecting cell viability.

Overall, this chapter describes an *in vitro* model to study cancer-induced bone cell differentiation, survival and activity. These models will be utilised to test the effects of novel therapeutic agents on cancer induced osteoclastic bone destruction (chapters 5 and 7).

3.2 Introduction

The bone microenvironment is the most common metastasis site for the three most common human cancers; breast, prostate and lung (182). Bone metastases are apparent in more than 80% of advanced stage breast cancer patients (181). Our understanding of the precise mechanisms behind the development and pathophysiology of bone metastases is currently limited. Research is needed to elucidate the complex interactions between bone and tumour cells, identifying new drug targets and testing novel therapeutic agents.

Bone metastases observed in breast cancer patients are generally osteolytic as the invading tumour cells release a variety of factors that up regulate bone remodelling in a manner that favours bone resorption. In this chapter I will be discussing the development of models to aid studies into the effects of tumour cells on the three key bone cell types; osteoclasts, osteoblasts and bone marrow derived osteoclast precursors. I will present studies showing the effect of co-cultures with tumour cells, as well as the effect of conditioned medium from tumour cells.

In vitro techniques for culturing a variety of cancer cell lines are well established as are cultures of primary bone cells including macrophage, osteoclasts (398) and osteoblasts (399), and various immortalised bone cell lines such as RAW 264.7 cells (400) and MC3T3 cells (401). However there are far fewer recent examples of successful direct co-cultures containing combinations of both bone and cancer cells. This is a useful and currently under-used tool for studying the interactions between cancer and bone cells *in vitro*.

One technique that has been successfully utilised by various groups is the use of conditioned medium from tumour cells as a treatment to be applied to various bone cell types. Here I will demonstrate a range of different analyses that can be applied using conditioned medium protocols.

3.3 Aim

The aim of this chapter was to design and set up co-culture and conditioned medium *in vitro* models of the interactions and cross-talk between osteolytic breast cancer cells and three bone cell types; osteoclasts, osteoclast pre-cursors and osteoblasts. The models would then be used to investigate the effect of the tumour cells on the bone cell differentiation and activity in this chapter and the modulating action various therapeutic agents could have on that effect in later chapters.

3.4 Results

3.4.1 Breast cancer cells?

The most important factor in designing any co-culture system is the cell types that will be used. In this study, osteoclasts, osteoblasts and M-CSF generated bone marrow macrophage cultures were used as these are the most important bone cell types. This leaves the vital question of which tumour cells to use. The two most common cancers to metastasise to bone in humans are breast and prostate cancers (402). These two cancers are classically thought to have distinct pathologies within the bone microenvironment; breast cancers causing osteolytic lesions and prostate cancers causing osteoblastic lesions. While this does typically hold true, in reality the situation is more complex and either cancer can cause either type of lesion, and lesions can display both osteolytic and osteoblastic characteristics. Mindful of the limitations of cancer cell lines as models for studying cancer, a number of mouse and human cancer cell lines were chosen. Table 3.1 shows the cancer cell lines used to study cancer cell-induced osteolysis.

Cell Line	Species	Cancer Type	Notes
MDA-MB-231	Human	Breast Cancer	One of the two most commonly used breast cancer cell lines. Triple negative (ER, PR and Her2/neu negative), highly metastatic, and has undergone EMT. Fast growing in culture (403-405).
MCF7	Human	Breast Cancer	One of the two most commonly used breast cancer cell lines. ER and PR positive and Her2/neu negative, non-metastatic and has not undergone EMT. Slow growing in culture (406, 407).
4T1	Mouse	Breast Cancer	Balb/c derived cell line. ER positive, highly metastatic, has not undergone EMT. Extremely fast growing in culture (408-410).
MC57G	Mouse	Fibrosarcoma	C57B6 derived cell line. Moderately quick growth in culture (411).
PC3	Human	Prostate	One of the two 'classical' prostate cancer cell lines. Highly metastatic and androgen independent. Relatively slow growing in culture (412, 413).

Table 3.1 A table describing the cancer cell lines used in this thesis to study cancer cell-induced osteolysis.

3.4.2 Cancer induced osteoclastogenesis

3.4.2.1 Breast cancer cells enhance RANKL and M-CSF-induced osteoclast formation and bone resorption

Cultures of RANKL and M-CSF stimulated mouse osteoclasts were used to study breast cancer-induced osteoclast formation and resorption. Mouse M-CSF generated osteoclast precursor cells were cultured in the presence of RANKL (100 ng/ml) and M-CSF (25 ng/ml) before the addition of human MDA-MB-231 cells (75 - 1200 cells/well) for 48 hours. Osteoclasts were visualised using TRAcP staining. Figure 3.1 panel A shows that the presence of MDA-MB-231 cells significantly increased the number of osteoclasts by 100-150% ($p<0.01$) at all initial MDA-MB-231 seeding densities. These effects were most evident in the cultures with the lowest seeding densities of MDA-MB-231 cells. This was in contrast to the cultures with higher concentrations of MDA-MB-231 cells which had smaller, less nucleated osteoclasts (Figure 3.1, panel C). The reason for this difference seems to be the human MDA-MB-231 cells expanding and competing with the mature osteoclasts and their precursors for space within the cultures. This reduces the space available for osteoclasts thereby inhibiting the fusion of osteoclast precursors and preventing the formation of the very large osteoclasts seen when MDA-MB-231 cell numbers are very limited. This effect is clearly evident in Figure 3.2, which shows that if the cultures are left for longer the MDA-MB-231 cells continue to expand and by 96 hours at the higher seeding densities they have out-competed the osteoclasts severely reducing the number seen.

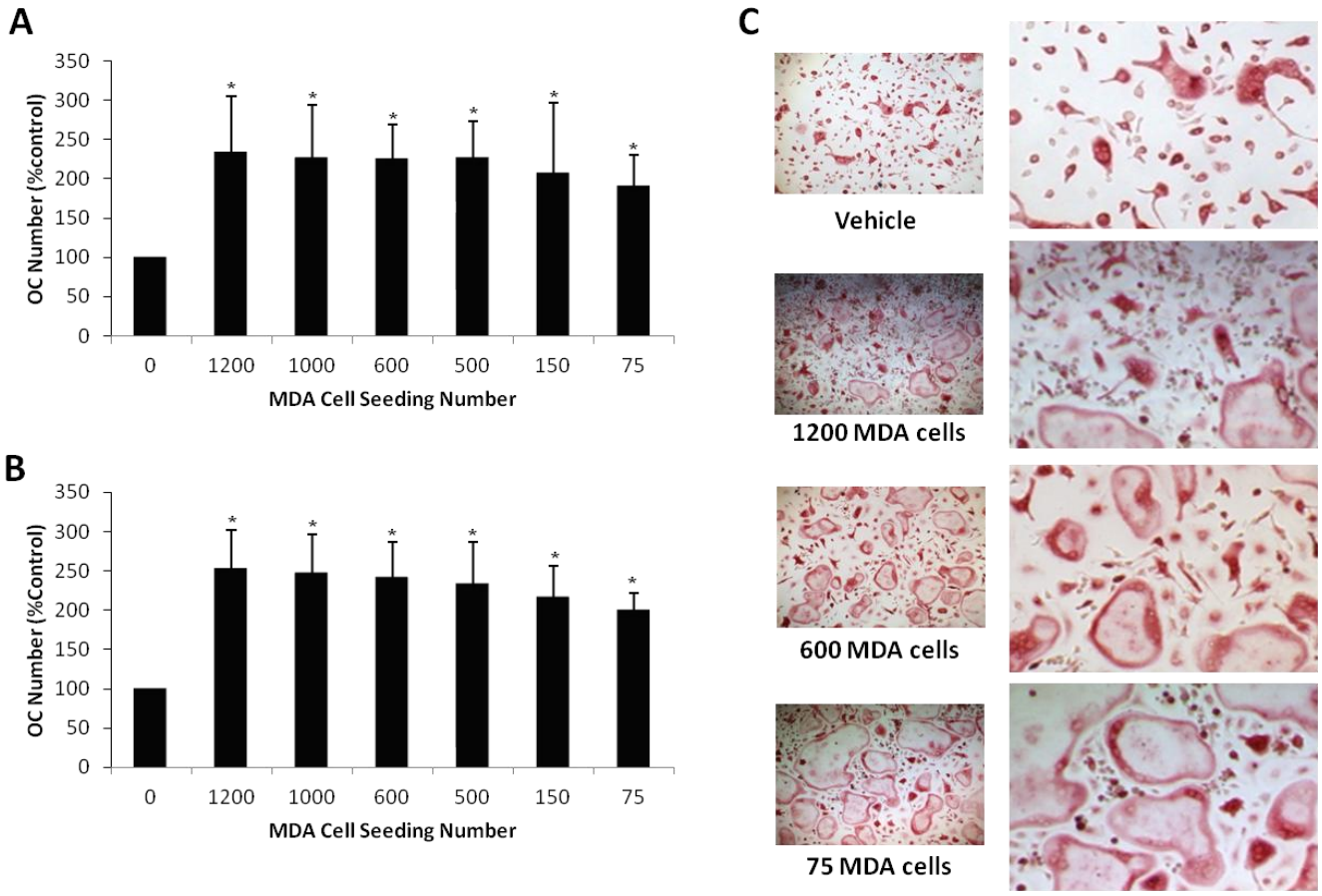

Figure 3.1. MDA-MB-231 human breast cancer cells stimulate osteoclast formation, size and nuclearity. Osteoclast precursor macrophages were seeded in the presence of M-CSF (25 ng/ml) and RANKL (100 ng/ml) and allowed to attach overnight. MDA-MB-231 cells (75-1200 initial seeding number) were then added and the co-culture allowed to proceed for 72 hrs. Multi-nucleated osteoclasts were visualised and counted following TRAcP staining. Osteoclast number is expressed as a percentage of the control well. The graphs show the number of osteoclasts when only those with 3 (A) or 10 (B) nuclei were included. C shows representative photomicrographs of the cultures. Data is from three independent experiments (N=3) performed in quintuplicate and error bars represent +/- one standard deviation. * =P<0.05 from vehicle

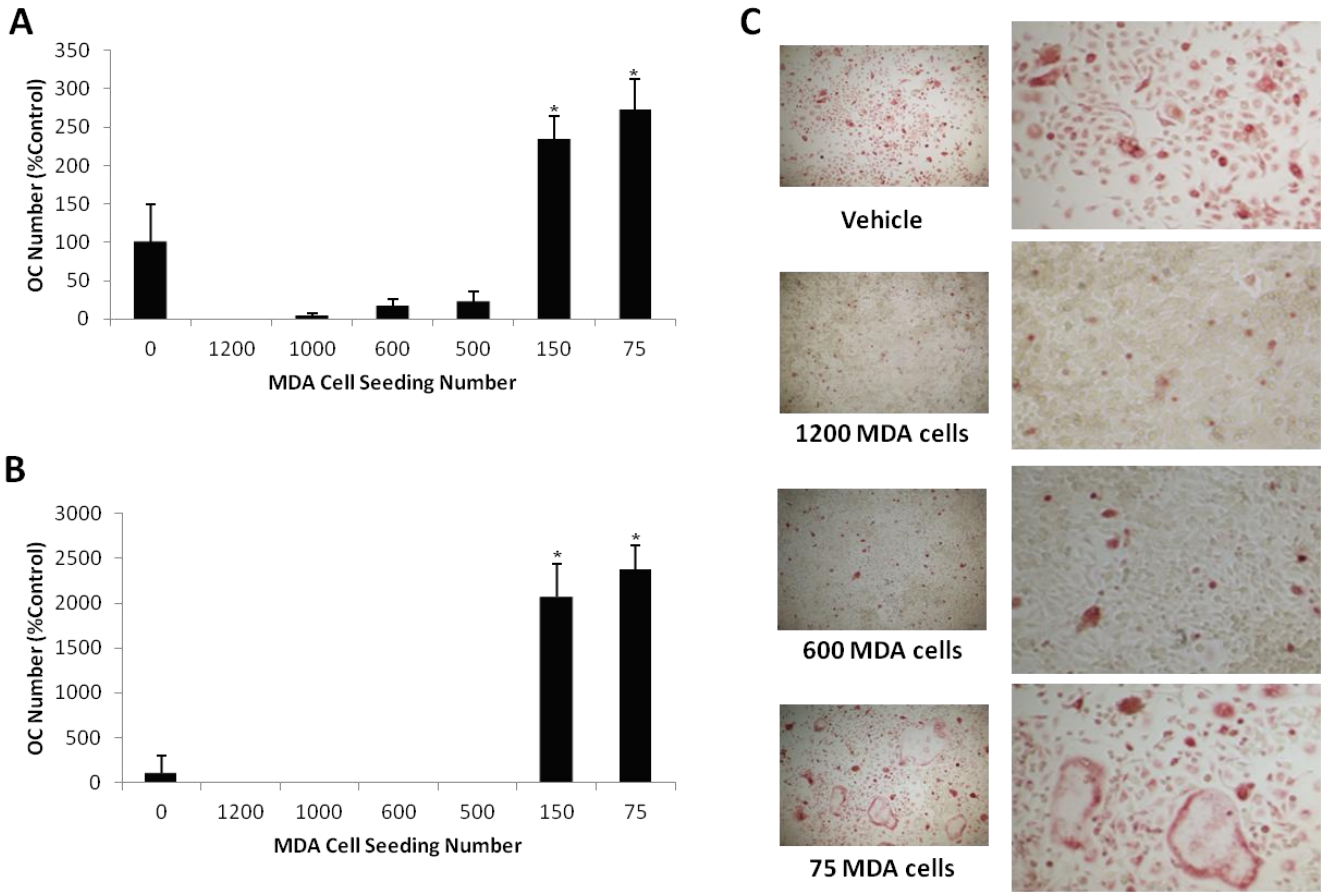

Figure 3.2. MDA-MB-231 human breast cancer cells out compete osteoclasts after 96 hours. Osteoclast precursor macrophages were seeded in the presence of M-CSF (25 ng/ml) and RANKL (100 ng/ml) and allowed to attach overnight. MDA-MB-231 cells (75-1200 initial seeding number) were then added and the co-culture allowed to proceed for 96 hrs. Multi-nucleated osteoclasts were visualised and counted following TRAcP staining. Osteoclast number is expressed as a percentage of the control well. The graphs show the number of osteoclasts when only those with 3 (A) or 10 (B) nuclei were included. C shows representative photomicrographs of the cultures. Data is from three independent experiments (N=3) performed in quintuplicate and error bars represent +/- one standard deviation. * =P<0.05 from vehicle

Cultures of RANKL and M-CSF stimulated osteoclasts were also used to study breast cancer-induced bone resorption. RANKL and M-CSF-generated osteoclasts cultures were generated as described above on Corning® Osteo Assay Surface multiple well plates (Corning, USA). Once mature osteoclasts were formed, human MDA-MB-231 breast cancer cells (300 cells / well) were added to the culture and left for 96 hours. Adherent osteoclasts were removed by adding 50% bleach (Clorox-Ultra, USA) for 10 minutes. The resorption pits were then visualised by phase contrast microscopy and the area resorbed quantified by image analysis using ImageJ. Figure 3.3 panel A shows that the presence of MDA-MB-231 cells significantly increased the area resorbed by over 700% ($p<0.01$). A small decrease (25% loss, $p<0.05$) in the number of osteoclasts was observed at the termination of the culture (Figure 3.3 panel B). This was probably due to the 96 hour length of the culture allowing MDA-MB-231 cell to out compete osteoclasts as discussed above. Alternatively, it could also be explained by the significant increase in osteoclast size resulting in a reduced total number of small osteoclasts present.

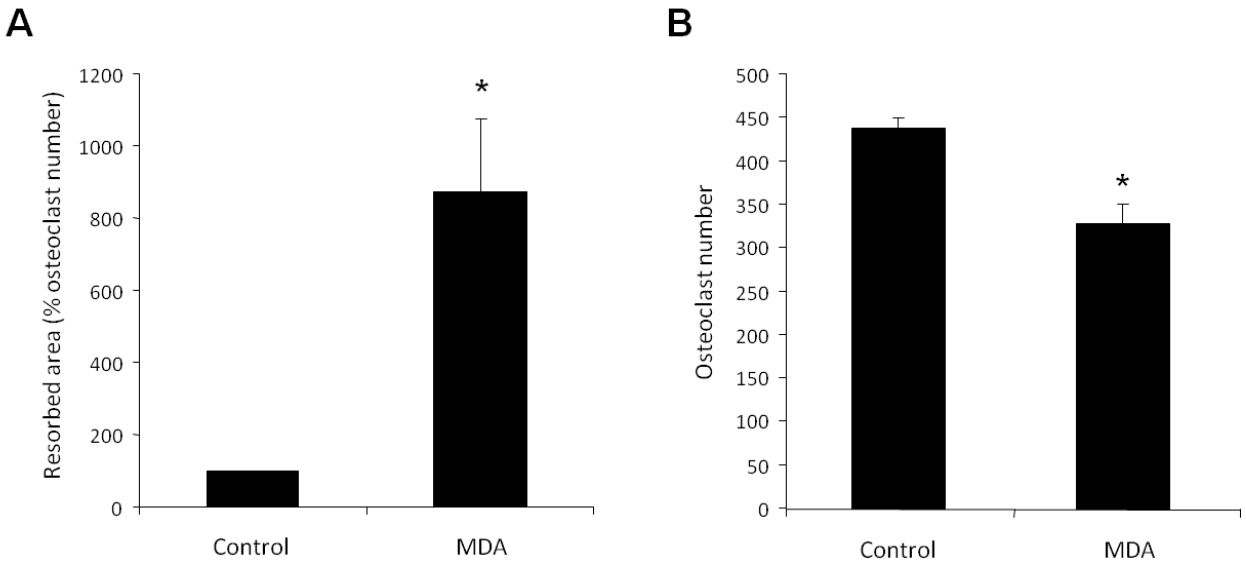

Figure 3.3. MDA-MB-231 human breast cancer cells enhance bone resorption. Osteoclast precursor macrophages were seeded onto Corning® Osteo Assay Surface multiple well plates (Corning, USA) in the presence of RANKL (100 ng/ml). Once mature osteoclasts had formed the culture was allowed to proceed for 96 hrs as before (control) or with the addition of MDA-MB-231 cells (300 initial seeding number). Multi-nucleated osteoclasts were visualised and counted following TRAcP staining. The graphs show resorbed area (A) and the number of osteoclasts when only those with 3 nuclei were included (B). Data is from three independent experiments (N=3) performed in quintuplicate and error bars represent +/- one standard deviation. * =$P<0.05$ from vehicle

Mindful of the limitations of cancer cell lines as models for studying cancer, three further cell lines were chosen to determine if the effects observed above were general or specific to the MDA-MB-231 cell line. These cell lines were human MCF7 breast cancer cells, mouse (Balb/C) 4T1 breast cancer cells and mouse (C57B6) MC57G fibrosarcoma cells (Table 3.1). All these cells have been shown to cause osteolytic bone metastases *in vivo* (414-416). M-CSF generated osteoclast pre-cursors were plated into 96 well plates with M-CSF (25ng/ml) and RANKL (100ng/ml), and left to adhere overnight. MDA-MB-231, MCF7, 4T1 or MC57G cells were then added at an initial seeding density of 300 cells per well. Photographs of these cultures are shown in Figure 3.4.

Figure 3.4 panel A shows that, in a similar fashion to MDA-MB-231 cells, the addition of MCF7, 4T1 or MC57G to RANKL and M-CSF stimulated BM cultures increased osteoclast number, size and nuclearity. MCF7, 4T1 and MC57G increased osteoclast number by 83%, 81% and 67%, respectively. However, the increase in osteoclast size and nuclearity was not consistent across all cell types. For example, smaller osteoclasts were observed in MC57G-osteoclast co-cultures. This difference was quantified when cultures were reanalysed counting only those osteoclasts with ten or more nuclei. In this count increases over control were now 375% by MDA-MB-231 cells, 294% by MCF7 cells, 319% by 4T1 cells and 166% by MC57G cells.

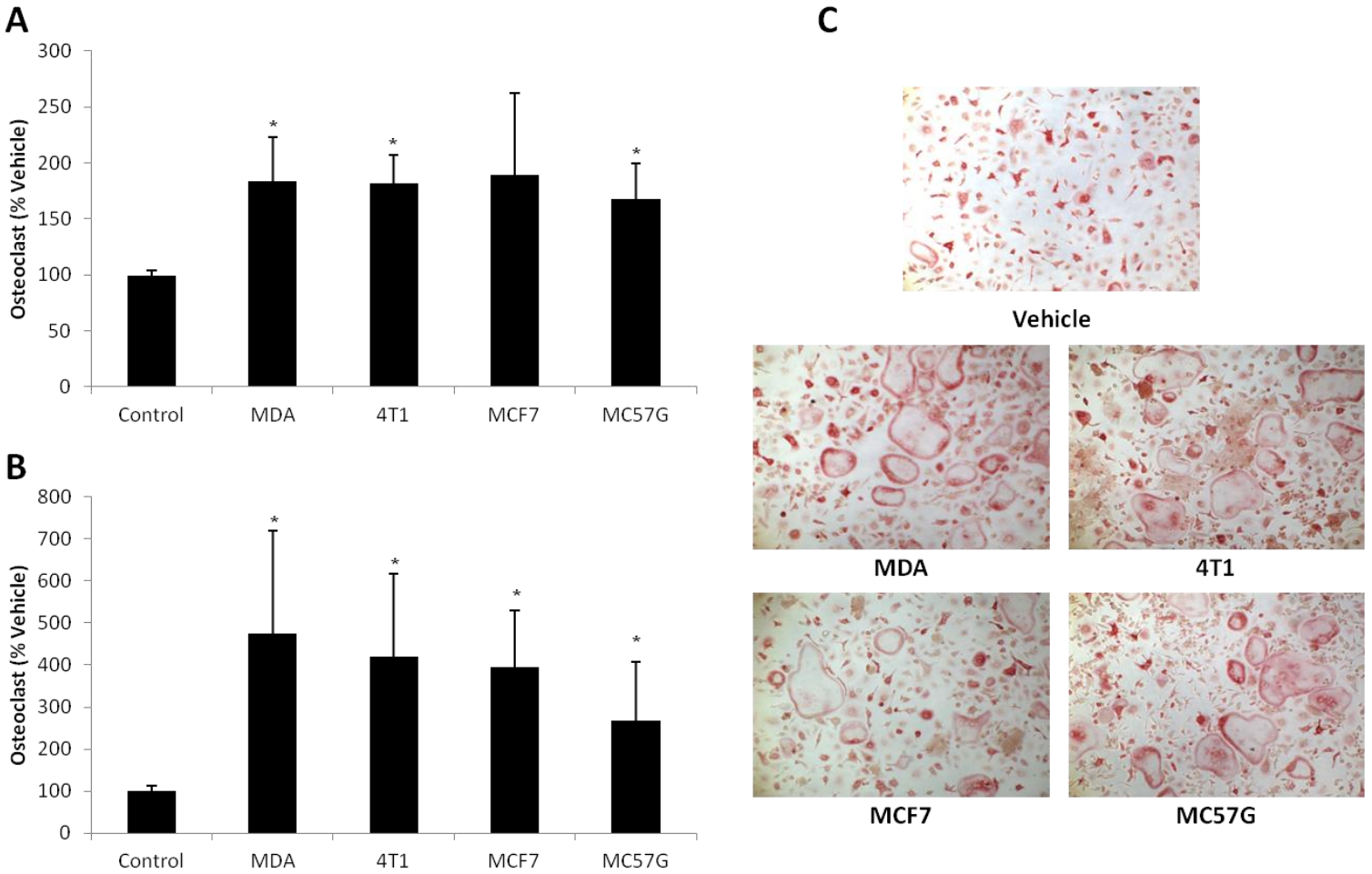

Figure 3.4 Osteolytic cancer cells stimulate osteoclast formation, size and nuclearity. Osteoclast precursor macrophages were seeded in the presence of RANKL (100 ng/ml) and allowed to attach overnight. MDA-MB-231, MCF7, 4T1 and MC57G cells were then added at an initial seeding density of 300 cells and the co-culture allowed to proceed for 72 hrs. Multi-nucleated osteoclasts were visualised and counted following TRAcP staining. Osteoclast number is expressed as a percentage of the control well which did not have any cancer cells added. The graphs show the number of osteoclasts when only those with 3 (A) or 10 (B) nuclei were included. C shows representative photomicrographs of the cultures. Data is from three independent experiments (N=3) performed in quintuplicate and error bars represent +/- one standard deviation. * =P<0.05 from vehicle

3.4.2.2 Breast cancer derived factors enhance RANKL and M-CSF-induced osteoclast formation

To study the effects of cancer-induced osteoclastogenesis in the absence of cancer cells I decided to create tumour cell conditioned medium and then use this as a treatment for our various bone cell cultures. This had the added advantage of allowing us to determine whether the effects we had already seen were determined by secreted factors or purely through cell-cell contact.

Cultures of RANKL and M-CSF generated mouse osteoclasts were used to study the effects of cancer cell derived factors on osteoclast formation. M-CSF generated BM macrophage were plated into 96 well plates and allowed to adhere overnight in the presence of RANKL (100 ng/ml). MDA-MB-231 conditioned medium and control conditioned medium were created and used to treat these osteoclast cultures at concentrations of 5, 10, 20, 50 or 100%. MDA-MB-231 cells (300 cells / well) were also added to provide a positive control for comparison. Media, and conditioned medium treatments were refreshed after 48 hours, and the culture stopped after 96 hours of treatment. Osteoclasts were identified by TRAcP staining. In initial tests when osteoclast cultures were treated with 50 or 100% (v/v) conditioned medium strong inhibition of osteoclast formation was seen and so no further work was done at these concentrations. Increases in osteoclast number were seen in all the cultures treated with MDA-MB-231 conditioned medium at 5, 10 or 20% (v/v). Figure 3.5 A shows that the increase in osteoclast number was fairly consistent between different treatments and when compared to the MDA-MB-231 cell co-culture; between 46% and 56% ($p<0.05$). However, the size of osteoclasts formed is clearly different in the photomicrographs shown in Figure 3.5 C and this observed difference is born out when only osteoclasts with 10 or more nuclei are counted (Figure 3.5 B). In this count, treatment with conditioned medium at 5% did not significantly increase osteoclast number, compared to significant increases of 73% and 110% with conditioned medium at 10 and 20% respectively ($p<0.05$). The MDA-MB-231 cell treatment shows the starkest difference with an increase in osteoclasts with 10 or more nuclei of 200% when compared to control ($p<0.05$).

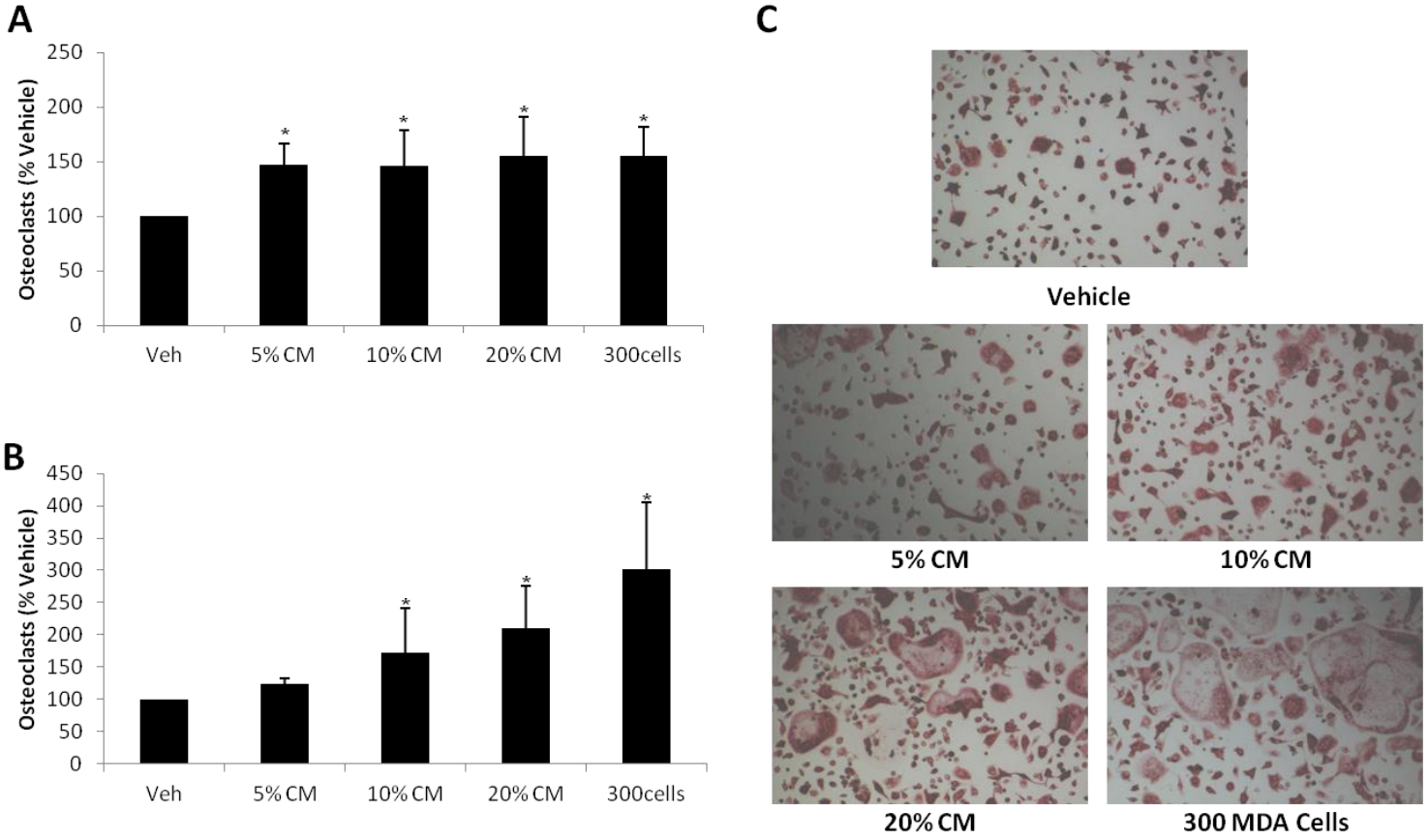

Figure 3.5 Conditioned medium from MDA-MB-231 human breast cancer cells stimulate osteoclast formation, size and nuclearity. Osteoclast precursor macrophage were seeded in the presence of RANKL (100 ng/ml) and allowed to attach overnight. MDA-MB-231 cells (300 cells) or conditioned medium (5-20%) from MDA-MB-231 flasks or from control flasks was then added and the cultures allowed to proceed for 72 hrs. Multi-nucleated osteoclasts were visualised and counted following TRAcP staining. Osteoclast number is expressed as a percentage of the control well. The graphs show the number of osteoclasts when only those with 3 (A) or 10 (B) nuclei were included. C shows representative photomicrographs of the cultures. Data is from three independent experiments (N=3) performed in quintuplicate and error bars represent +/- one standard deviation. * =P<0.05 from vehicle

As with the osteoclast co-cultures a variety of other osteolytic bone metastasis cell lines were tested to examine whether or not the effects of MDA-MB-231 conditioned medium on osteoclasts was specific to that cell line. Again, 3 further cell lines were used MCF7 human breast cancer cells, 4T1 mouse breast cancer cells and MC57G mouse fibrosarcoma cells (Table 1). M-CSF generated osteoclast precursors were allowed to attach overnight in the presence of RANKL before treatment with conditioned medium from the 4 cell types at a concentration of 10%. In each case the conditioned medium treatment increased the osteoclast number, size and number of nuclei as seen in Figure 3.6.

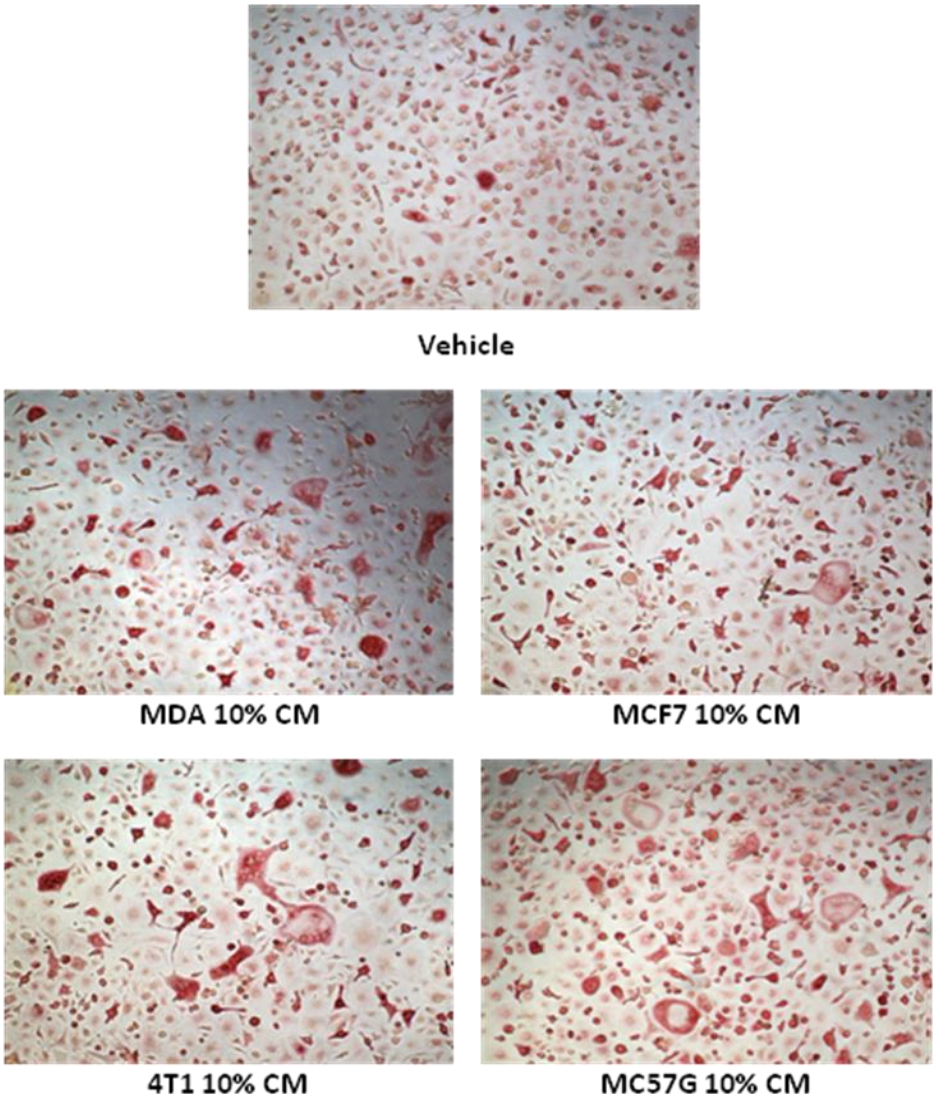

Figure 3.6 Conditioned medium from osteolytic cancer cells stimulate osteoclast formation, size and nuclearity. Osteoclast precursor macrophages were seeded in the presence of RANKL (100 ng/ml) and allowed to attach overnight. MDA-MB-231, MCF7, 4T1 and MC57G conditioned medium (10%) was then added and the co-culture allowed to proceed for 72 hrs. Multi-nucleated osteoclasts were visualised following TRAcP staining. Representative photomicrographs of the cultures are shown. Data is from three independent experiments (N=3) performed in quintuplicate.

3.4.2.3 Breast cancer cells do not produce RANK ligand in M-CSF stimulated bone marrow cultures

To establish whether breast cancer cells produce the osteoclastic factor RANKL, we studied the effect of cancer cells on osteoclast formation in M-CSF generated mouse osteoclast precursor cultures in the absence of exogenous RANKL. M-CSF generated mouse osteoclast precursors were cultured in the presence of M-CSF (25 ng/ml) for 24 hours before the addition of human MDA-MB-231 cells (75 - 1200 cells/well) for 72 hours. Osteoclasts were visualised using TRAcP staining. Figure 3.7 shows that MDA-MB-231 (75 - 1200 cells/well) failed to stimulate any osteoclast formation in the absence of RANKL (100 ng /ml). Attempts were also made using AlamarBlue to measure the effect of the MDA-MB-231 cells on the viability of the M-CSF generated bone marrow macrophages over 48 and 72 hours, however it proved impossible to separate the two cell types once they were in co-culture. This made any viability data meaningless.

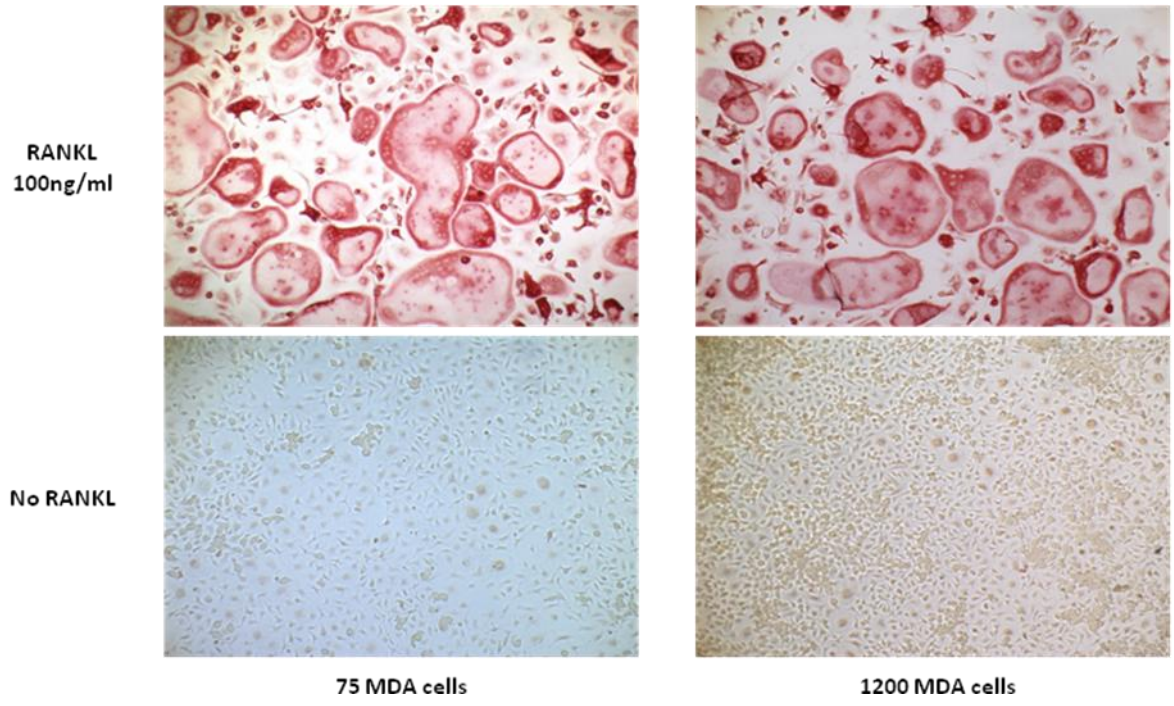

Figure 3.7 MDA-MB-231 human breast cancer cells do not induce osteoclastogenesis in the absence of RANKL Osteoclast precursor macrophages were seeded either in the presence or absence of RANKL (100 ng/ml) and allowed to attach overnight. MDA-MB-231 cells (75-1200 initial seeding number) were then added and the co-culture allowed to proceed for 96 hrs. Multi-nucleated osteoclasts were visualised following TRAcP staining. Representative photomicrographs of the cultures are shown. Data is from three independent experiments (N=3) performed in quintuplicate.

M-CSF generated BM macrophage cultures were generated and allowed to attach overnight in the absence of RANKL. They were then treated with MDA-MB-231 conditioned medium or control conditioned medium at a concentration of 10%. After 48 hours AlamarBlue was added to the cultures and they were then read in a plate reader to test the viability of the cells present. Figure 3.8 shows that both MDA-MB-231 and control conditioned medium produced a slight increase (~15%) in the number of viable cells, and while this was significantly different from the vehicle control, there was no difference between the control and MDA media.

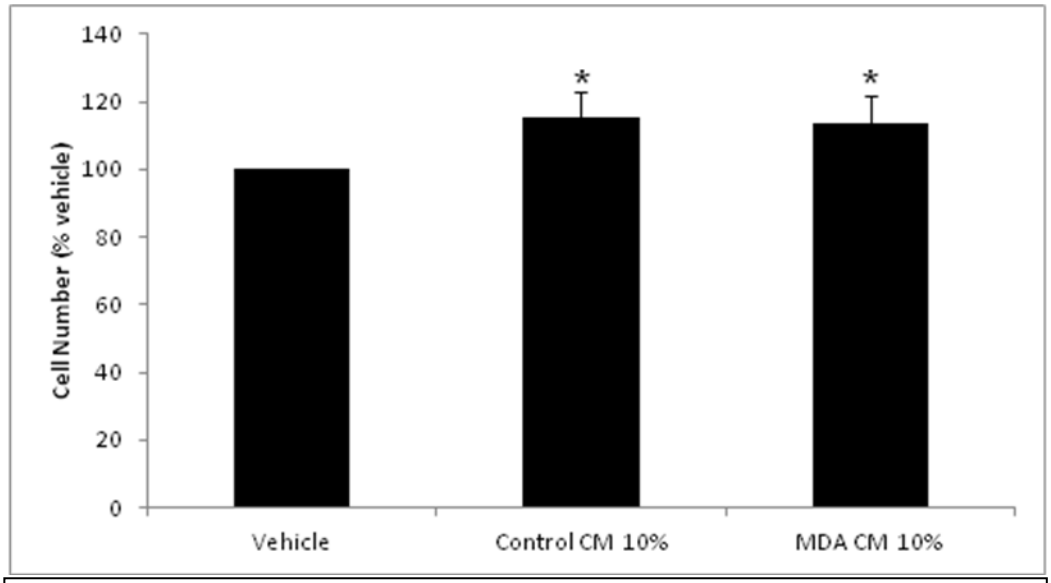

Figure 3.8 Conditioned medium from MDA-MB-231 cancer cells had no effect on macrophage viability. Osteoclast precursor macrophages were seeded and allowed to attach overnight. MDA-MB-231 or Control conditioned medium (10%) was then added and the culture allowed to proceed for 48 hrs. AlamarBlue was then added to each well at a concentration of 10% and after 4 hours the plate read in a plate reader. Data is from three independent experiments (N=3) performed in quintuplicate and error bars represent +/- one standard deviation. * =P<0.05 from vehicle

3.4.2.4 Breast cancer derived factors enhance RANKL and M-CSF-induced osteoclast motility and spreading

The motility and proliferation of osteoclast precursors was measured using the real-time Xcelligence system in the presence and absence of M-CSF, RANKL and/or MDA-MB-231 conditioned medium. M-CSF generated BM macrophages (8000 cells/well) were allowed to attach for 24 hours in the presence of 25 ng/ml M-CSF before 50% of medium was refreshed and cells treated with either M-CSF 25 ng/ml alone in 10% (v/v) control conditioned medium, or with M-CSF 25 ng/ml and RANKL 100 ng/ml in 10% (v/v) control or MDA-MB-231 conditioned medium. Impedance readings were then taken on the Xcelligence every minute for 1 hour, then every ten minutes for 8 hours, and finally every 30 minutes until treatments were refreshed after 48 hours and the reading system repeated. After treatments were refreshed, cells were left for a further 24 hours before the culture was stopped. This treatment regime was used to keep treatments and conditions as close as possible to those used for the osteoclast formation experiments described above (Section 3.4.2.2, page 109).

The Xcelligence system uses the impedance readings to produce what is known as a cell index value. Changes in this value can represent a number of different features of cells depending on the study type and time frame. In this project long-term increases in cell-index were taken to represent proliferation rates, while immediate and short-term changes represent changes in cell-shape and spreading.

In Figure 3.9 cell index values were normalised to the last time point before the first treatment and long-term changes monitored to investigate changes in cell proliferation. As expected, continuation of M-CSF treatment alone caused no change in the cell proliferation rate with an average cell doubling time of 32.5 hours observed, though this rate did increase sharply when the treatment was refreshed. Cells treated with RANKL in addition to M-CSF did not proliferate as quickly, only having a doubling time of 87.1 ($p<0.05$) hours after the addition of RANKL. The addition of MDA-MB-231 conditioned medium as well as M-CSF, and RANKL caused cells to return to proliferation rates not significantly different to those of cells treated with M-CSF alone. However, the overall cell-index values of cells treated with conditioned medium were much higher due to a rapid

increase in the first two hours after treatment that is unlikely to represent changes in proliferation; this is shown in Figure 3.10.

To investigate changes in cell shape and spreading, changes in cell index value in the first two hours after treatments were investigated in detail. Figure 3.10 shows that after the first treatment no difference between M-CSF alone and M-CSF and RANKL treated cells was observed. Both treatments caused a transient increase in cell index values, doubling times of 4.1 and 3.4 hours respectively, before settling to their long-term proliferation rates. This increase likely represents the changes in cell movement and morphology in response to fresh cytokines. In contrast, cells treated with conditioned medium in addition to RANKL and M-CSF showed a very different pattern of changes in cell index values. A short sharp increase was followed by a prolonged drop, these are likely to represent changes in cell morphology. There is then a prolonged rapid rise, likely representing a rapid increase in cell movement, with a doubling time of 0.74 hours, significantly faster than the other treatments ($p<0.01$).

Figure 3.11 shows the results after they were normalised to the last time point before the second treatment point. This shows that when the treatment was changed there was initially no difference between treatments; all increase at a doubling rate of around 1 hour. The only difference is that the conditioned medium treated cells cell index continue to increase for a prolonged period of time, as opposed to the other two treatments where the cell index began to plateau after one and a half to two hours.

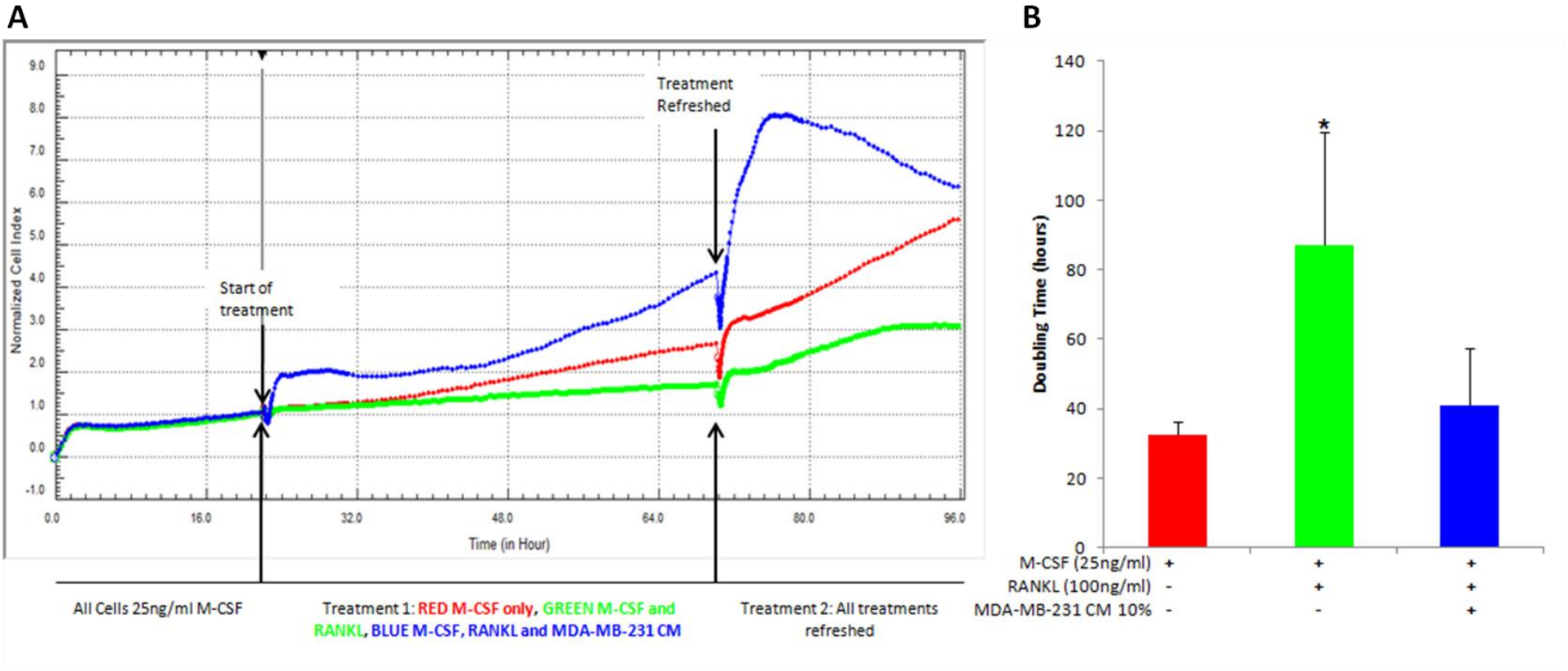

Figure 3.9 Conditioned medium from MDA-MB-231 human breast cancer cells increased osteoclast proliferation. M-CSF generated macrophages were seeded into Xcelligence plates and allowed to grow for 24 hours in M-CSF (25 ng/ml). Cells were then treated with M-CSF (25 ng/ml) alone or with the addition of RANKL (100ng/ml) plus either 10% control conditioned medium or MDA-MB-231 conditioned medium. Treatment was refreshed after 48 hours. A) shows a representative graph of the cell index values (derived from their electrical impedance) over 96 hours and normalized to the last time point before treatment. B) A graph showing the average doubling time (hours) of cells between hours 39 and 52. N=4 experiments were performed. * =P<0.05 from M-CSF alone, #=P<0.05 from RANKL alone

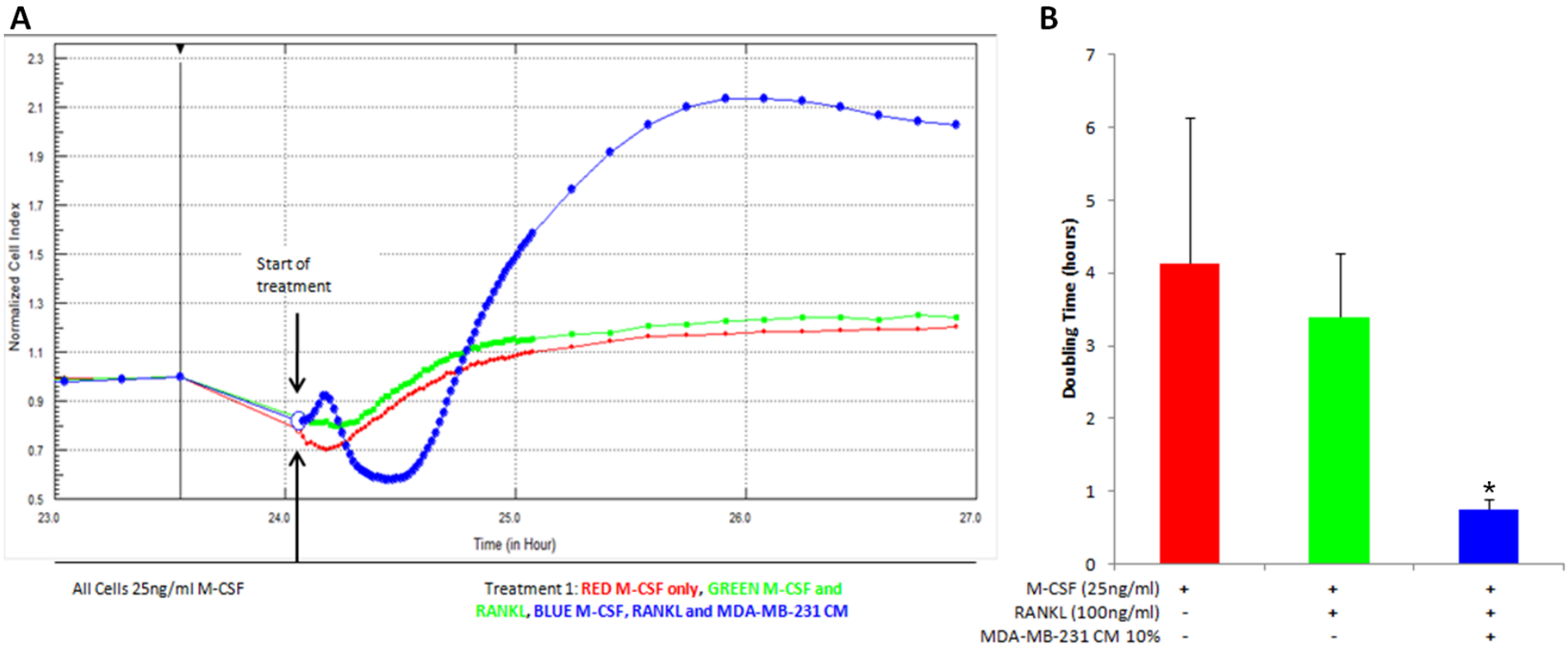

Figure 3.10 Conditioned medium from MDA-MB-231 human breast cancer cells caused a quick increase in osteoclast impedance values in Xcelligence analysis after treatment. M-CSF generated macrophages were seeded into Xcelligence plates and allowed to grow for 24 hours in M-CSF (25ng/ml). Cells were then treated with M-CSF (25 ng/ml) alone or with the addition of RANKL (100 ng/ml) plus either 10% control conditioned medium or MDA-MB-231 conditioned medium. Treatment was refreshed after 48 hours. A) shows a representative graph of the Cell index values (derived from their electrical impedance) between hours 23 and 27 of the experiment and normalized to the last time point before treatment. B) A graph showing the average doubling time (hours) of cells at the linear part of the curves between hours 24 and 25. N=4 experiments were performed. * =P<0.05 from M-CSF alone

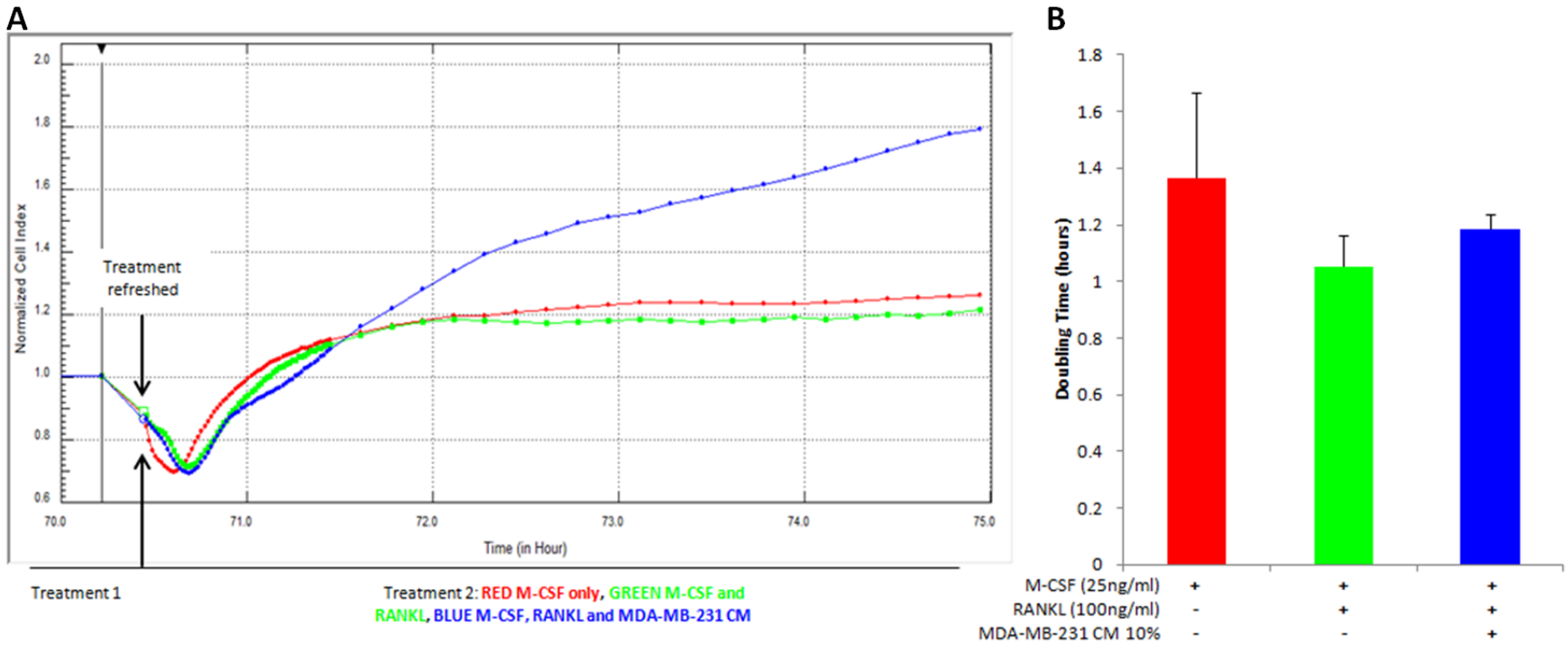

Figure 3.11 Conditioned medium from MDA-MB-231 human breast cancer cells caused a prolonged increase in osteoclast impedance values in Xcelligence analysis after treatment was refreshed. M-CSF generated macrophage were seeded into xcelligence plates and allowed to grow for 24 hours in M-CSF (25 ng/ml). Cells were then treated with M-CSF (25 ng/ml) alone or with the addition of RANKL (100 ng/ml) plus either 10% control conditioned medium or MDA-MB-231 conditioned medium. Treatment was refreshed after 48 hours. A) shows a representative graph of the cell index values (derived from their electrical impedance) between hours 70 and 75 of the experiment and normalized to the last time point before treatment was refreshed. B) A graph showing the average doubling time (hours) of cells at the linear part of the curves between hours 70 and 72. N=4 experiments were performed.

3.4.2.5 Breast cancer derived factors stimulate PI3K/Akt, MAPK and NFκB activation in osteoclasts

The effects of breast cancer derived factors on key signalling pathways in osteoclasts were investigated using western blot. As shown in Figure 3.12 – 3.14, RANKL and M-CSF generated mouse osteoclasts were treated with either standard medium or conditioned medium from human MDA-MB-231 breast cancer cells (5%, 10% or 20% v/v) for 5, 15 or 30 minutes. The PI3K/Akt signalling pathway is known to be a vital pathway for osteoclast differentiation, survival and function and is known to be stimulated by the osteoclastic factors RANKL and M-CSF (417, 418). Figure 3.12 shows that conditioned medium from human MDA-MB-231 breast cancer cells stimulated the phosphorylation of AKT at serine (Ser) 473 in a dose dependent manner. While stimulation was equally strong after 5 or 15 minutes, the difference compared to the negative control was most apparent at 15 minutes. 30 minutes after treatment phosphorylation of AKT began to decline and only at 20% was any increase over control apparent. Interestingly no stimulation of AKT phosphorylation was observed at the threonine (Thr) 308 site at any concentration or time point tested.

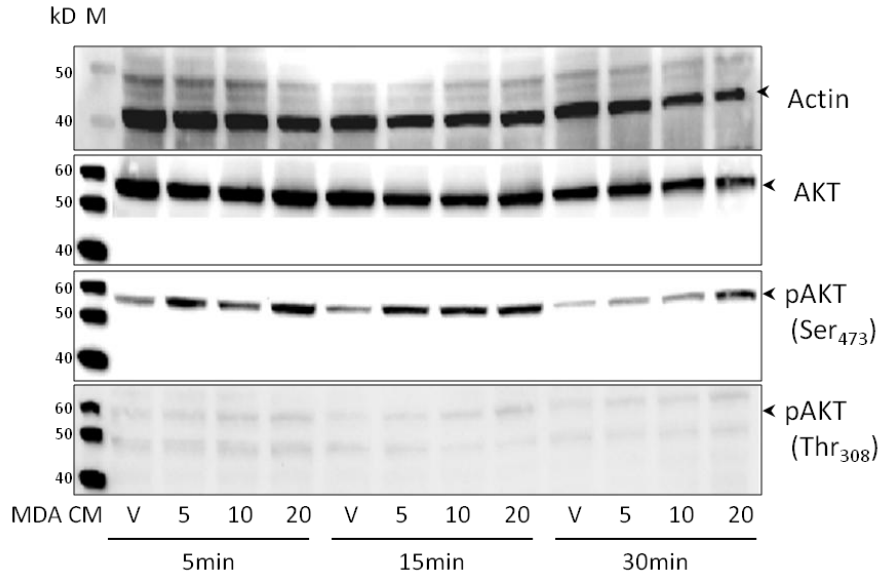

Figure 3.12 Conditioned medium from MDA-MB-231 human breast cancer cells stimulates PI3Kinase signalling in osteoclasts Osteoclast precursor macrophage were seeded in 12 well plates and treated with M-CSF (100 ng/ml) and RANKL (100 ng/ml) until a significant numbers of osteoclasts had formed. Cells were then starved for 2 hours before stimulation with MDA-MB-231 conditioned medium (5-20%) or control conditioned medium (20%) for 5, 15 or 30 minutes. Cells were then lysed, total protein extracted and 50µg run on a western blot. Blots were exposed to antibodies for A) β-Actin, Total AKT or pAKT Serine 473, pAKT Threonine 308. All antibodies are from Cell Signalling (UK) except β-Actin (Sigma-Aldrich, UK). The results shown are representative of three independent experiments.

The MAPK signalling pathway is essential for osteoclast differentiation and is known to be stimulated by the osteoclastic factors RANKL and M-CSF (419, 420). The effects of conditioned medium from human MDA-MB-231 breast cancer cells on ERK1/2 and JNK/SAPK MAP phosphorylation is shown in Figures 3.13. Strong stimulation of ERK1/2 phosphorylation was observed at all three time points, but this was strongest at 15 and 30 minutes, while only weak stimulation was seen after 5 minutes treatment. No JNK/SAPK phosphorylation was observed with any treatment at any time point.

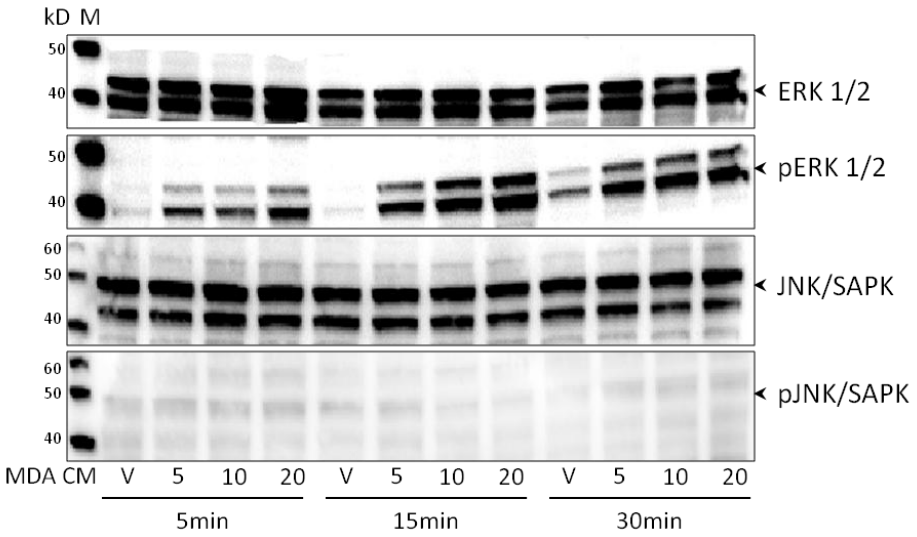

Figure 3.13 Conditioned medium from MDA-MB-231 human breast cancer cells stimulates MAPKinase signalling in osteoclasts Osteoclast precursor macrophages were seeded in 12 well plates and treated with M-CSF (100 ng/ml) and RANKL (100 ng/ml) until a significant numbers of osteoclasts had formed. Cells were then starved for 2 hours before stimulation with MDA-MB-231 conditioned medium (5-20%) or control conditioned medium (20%) for 5, 15 or 30 minutes. Cells were then lysed, total protein extracted and 50mg run on a western blot. Blots were exposed to antibodies for total ERK1/2, pERK, total JNK/SAPK and pJNK/SAPK. All antibodies are from Cell Signalling (UK) except β-Actin (Sigma-Aldrich, UK). The results shown are representative of three independent experiments.

The NFκβ signalling pathway is a vital pathway for osteoclast differentiation and is known to be stimulated by the vital osteoclastic factor RANKL. Figure 3.14 shows that MDA-MB-231 conditioned medium strongly stimulated phosphorylation of IKBα at all concentrations after 5 minutes, but only very weakly at any other time point. Weak activation of IKKα/β was observed after exposure to conditioned medium from MDA-MB-231 at all time points, and was strongest after 15 minutes.

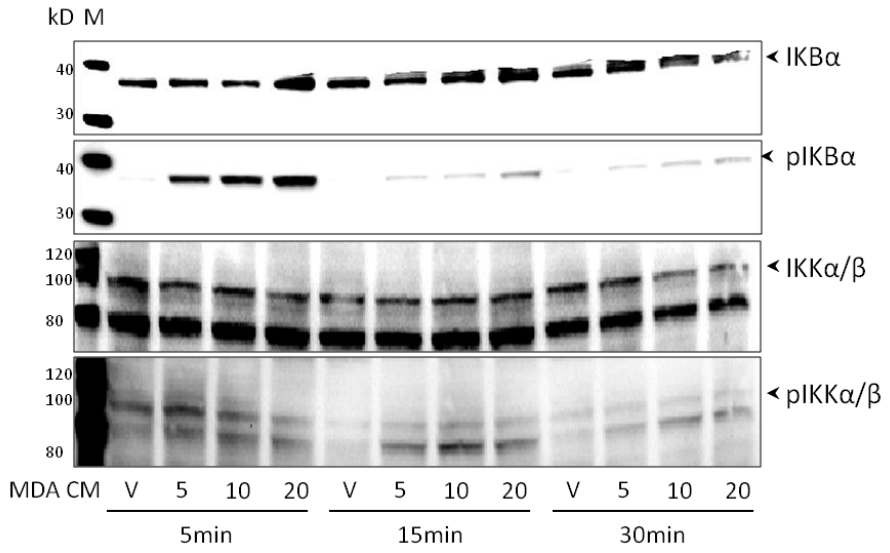

Figure 3.14 Conditioned medium from MDA-MB-231 human breast cancer cells stimulate NFκB signalling in osteoclasts Osteoclast precursor macrophages were seeded in 12 well plates and treated with M-CSF (100 ng/ml) and RANKL (100 ng/ml) until a significant numbers of osteoclasts had formed. Cells were then starved for 2 hours before stimulation with MDA-MB-231 conditioned medium (5-20%) or control conditioned medium (20%) for 5, 15 or 30 minutes. Cells were then lysed, total protein extracted and 50mg run on a western blot. Blots were exposed to antibodies total IKBα, pIKBα, total IKKα/β and pIKKα/β. All antibodies are from Cell Signalling (UK). The results shown are representative of three independent experiments.

3.4.3 Cancer induced osteoblastogenesis

3.4.3.1 Cancer derive factors inhibit osteoblast differentiation and bone nodule formation

Osteoblasts were isolated from the calvaria of 2-day old c57B6 mice and plated in 12-well plates. Once the osteoblasts had reached confluence BGP and vitamin C were added to the culture media to induce mineralisation. At this point human MDA-MB-231 breast cancer cells and human PC3 prostate cancer cells were added at initial seeding densities of 10 cells per well and the cultures were allowed to grow under standard conditions. However by the end of week 1 the MDA-MB-231 cells had grown to confluence and completely covered the osteoblast layer making any analysis of mineralisation impossible. In contrast, by the end of week 1 PC3 cells were growing in small colonies on top of the osteoblast layer, but by the end of week 3 they too had taken over the culture, see Figure 3.15.

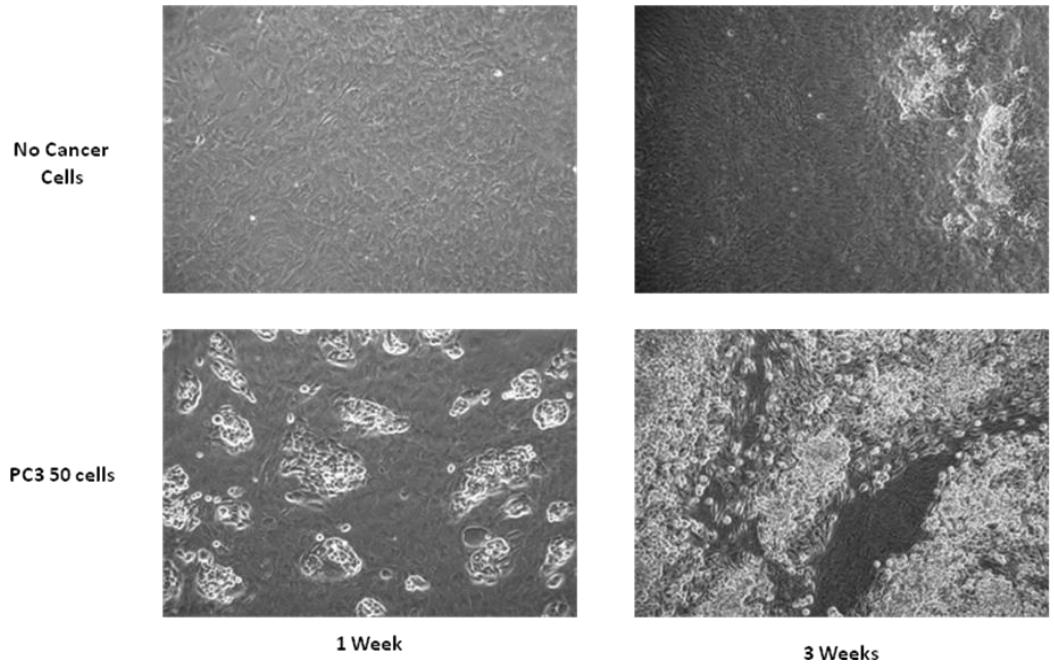

Figure 3.15 Cancer cells out compete osteoblasts *in vitro* Osteoblasts were seeded into 12 well plates and allowed to grow to confluence. Media was then supplemented with 10 mM β glycerophosphate (BGP) and 50 ug/ml L-ascorbic acid and PC3 cells were added at an initial seeding density of 10 cells. Cultures were fixed after 21 days. Representative photomicrographs of the cultures are shown. Data is from three independent experiments (N=3) performed in triplicate.

To study the effects of cancer derived factors on osteoblastogenesis, osteoblasts were cultured in osteogenic media and treated with standard or conditioned medium from MDA-MB-231 at concentrations of 1, 5, 10 or 20% (v/v). Medium and treatments were changed every 48 hours for 21 days, or until significant mineralisation had occurred in the control treated cultures. Osteoblast viability, differentiation and bone nodule formation were measured using AlamarBlue, alkaline phosphatase and alazarin red assays, respectively.

Figure 3.16 A shows that MDA-MB-231 conditioned medium had no effects on osteoblast viability at 1 and 5% (v/v). At 10% (v/v) there seems to be a modest reduction in viability of around 5% but this is not statistically significant. When treated with 20% (v/v) MDA-MB-231 conditioned medium osteoblast viability was significantly reduced by 10% ($p<0.05$).

Figure 3.16 B shows that MDA-MB-231 conditioned medium caused a dose dependent inhibition of alkaline phosphate production in osteoblast cultures, although this reduction was only statistically significant at 10 and 20%. At 5% the results were highly variable with an average reduction of 24%, while the reduction was more consistent with treatments of 10 and 20% conditioned medium resulting in reductions of 35% and 45% respectively ($p<0.05$).

Bone nodule formation was also measured in osteoblast cultures treated with 5, 10 or 20% MDA-MB-231 conditioned medium (Figure 3.16 C). All three concentrations showed a reduction in bone nodule formation when compared to standard media treatment; however at 5 and 10% the reduction was minor and not statistically significant. At 20% the conditioned medium reduced the amount of mineralisation by 30%, indicating a strong inhibition of osteoblast function ($p<0.05$).

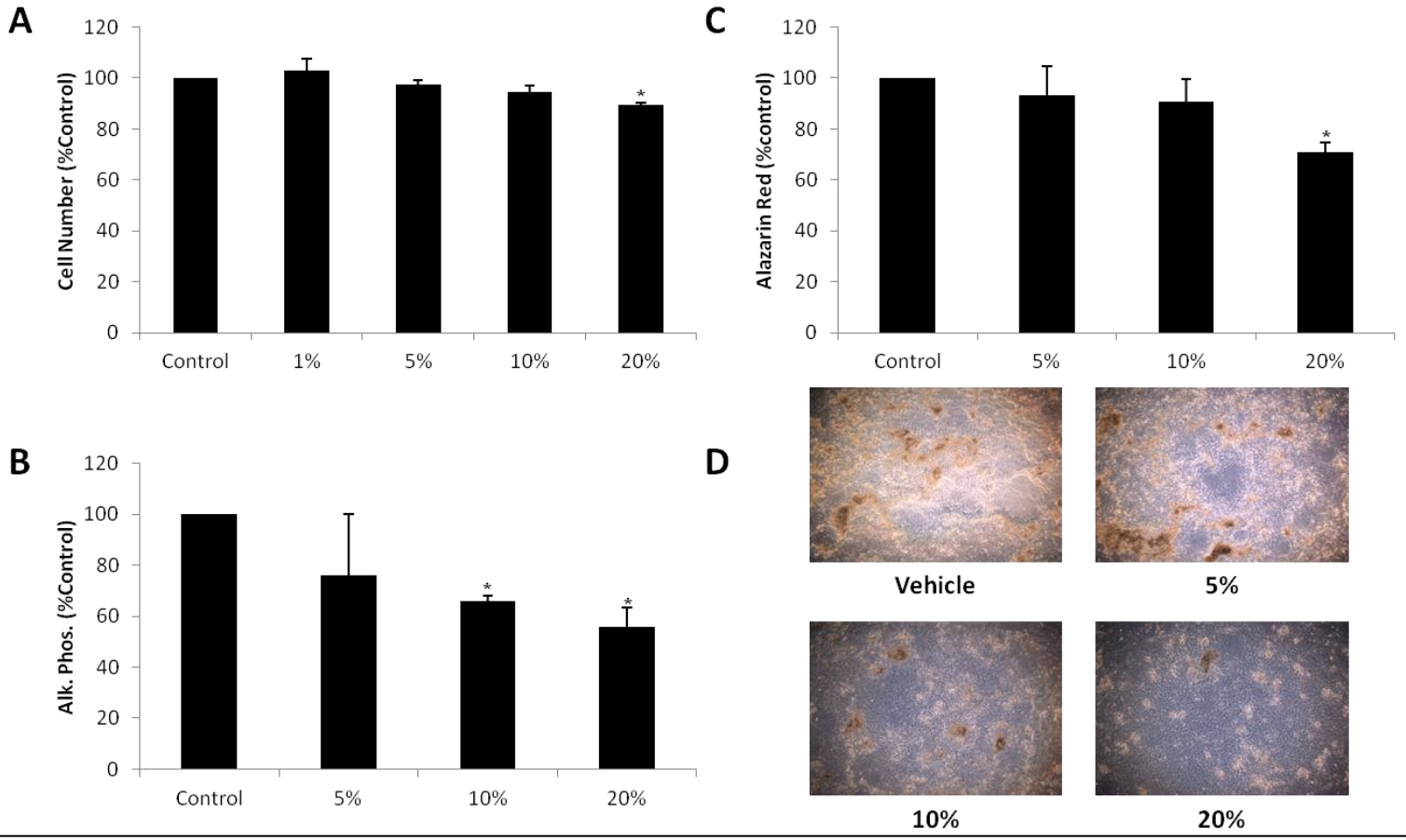

Figure 3.16 Conditioned medium from MDA-MB-231 human breast cancer cells inhibits osteoblast differentiation and mineralisation Osteoblasts were seeded into 12 well plates and allowed to grow to confluence. Media was then supplemented with 3 mM β glycerophosphate (BGP) and 50 ug/ml L-ascorbic acid. MDA-MB-231 conditioned medium (1-20%) was added and media and treatment refreshed every 48 hours. After 21 days 10% AlamarBlue was added to each well and after 4 hours the plate read on a plate reader. Each weel was washed and then either either lysed for alkaline phosphatase measurement or stained with alazarin red. Graphs show cell viability (A) as measured by alamar blue, differentiation as measured by alkaline phosphatase production (B), and mineralisation as measured by destaining of alazarin red (C). Representative photomicrographs of the cultures prior to staining are shown in D. Data is from three independent experiments (N=3) performed in triplicate and error bars represent +/- one standard deviation. * =P<0.05 from vehicle

3.4.3.2 Breast cancer derived factors stimulate PI3K/Akt and MAPK activation in osteoblasts

The effect of MDA-MB-231 conditioned medium on key signalling pathways in osteoblasts was also tested. PI3K/Akt and ERK1/2 signalling pathways play an important role in osteoblast differentiation and are known to be activated by a number of osteoblast stimulating factors including PTH, IGF1 and PGE2. As shown in Figures 3.17, MDA-MB-231 conditioned medium induced the phosphorylation of AKT at both Thr and Ser sites. Phosphorylation of ERK1/2 was also observed, however this occurred with both the MDA-MB-231 and control conditioned medium treatments and so was not considered significant.

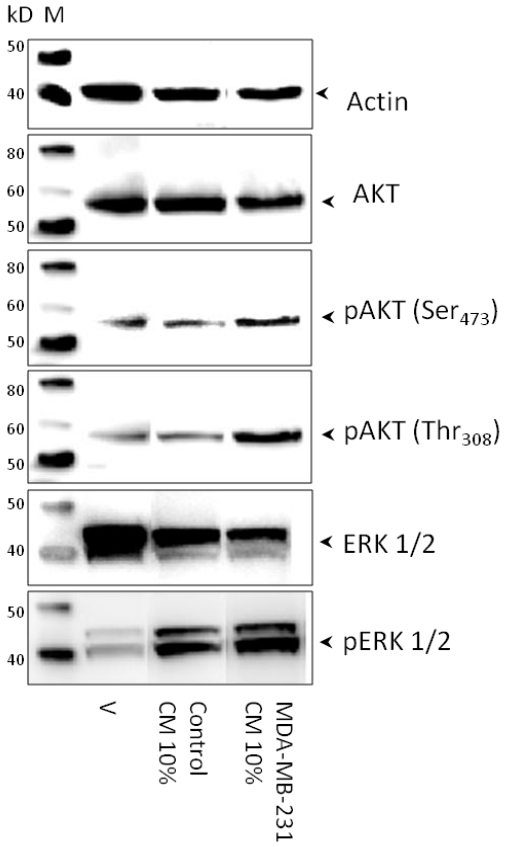

Figure 3.17 Conditioned medium from MDA-MB-231 human breast cancer cells stimulate PI3Kinase signalling in osteoblasts Osteoblasts were seeded in 12 well plates and left until confluent. Cells were then starved overnight before stimulation with nothing, MDA-MB-231 conditioned medium (10%) or control conditioned medium (10%) for 15 minutes. Cells were then lysed, total protein extracted and 50mg run on a western blot. Cells were then lysed, total protein extracted and 50mg run on a western blot. Blots were exposed to antibodies total IKBα, pIKBα, total IKKα/β and pIKKα/β. All antibodies are from Cell Signalling (UK). The results shown are representative of three independent experiments.

3.4.3.3 Breast cancer derived factors stimulate RANKL/OPG ratio in osteoblasts

The effect of osteoblast support for osteoclastogenesis was studied by measuring RANKL and OPG expression in calvarial osteoblasts in the presence and absence of breast cancer derived factors. Osteoblasts were treated with 10% (v/v) standard or MDA-MB-231 conditioned medium for 16 hours and mRNA expression of RANKL and OPG in osteoblasts was measured using qPCR. Figure 3.16 shows that MDA-MB-231 conditioned medium stimulated both OPG and RANKL expression increasing OPG production by 2.5-fold and RANKL production 13-fold. This increased the RANK/OPG ratio by almost 10 fold (992% increase ± 167, $p<0.05$

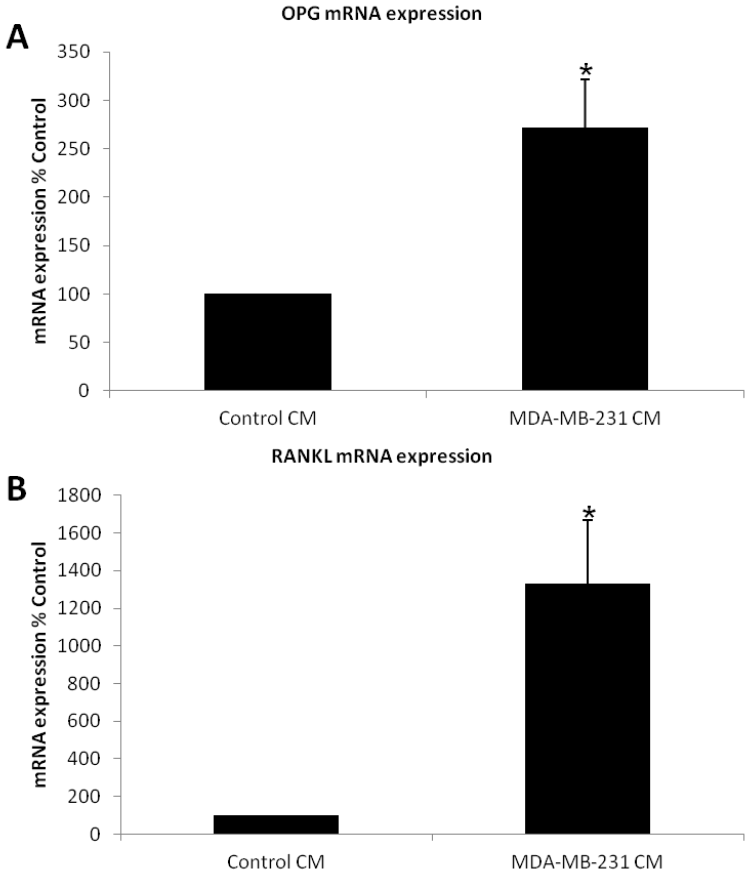

FIGURE 3.18 **Conditioned medium from MDA-MB-231 human breast cancer cells increases osteoblast RANKL and OPG expression.** Osteoblasts were seeded into 12 well plates and allowed to grow to confluence. They were then treated for 16 hours with either control or MDA-MB-231 conditioned medium (10%) before being lysed in Trizol. mRNA was then extracted and analysed using qPCR analysis. All results were adjusted to account for expression of 18S and GAPDH housekeeping genes. Graphs show the average mRNA expression levels of OPG (A) or RANKL (B) relative to control. Data is from three independent experiments (N=3) performed in triplicate and error bars represent +/- one standard deviation. * =$P<0.05$ from control CM

3.4 Discussion

It has long been known that crosstalk from the bone metastases of diverse cancers effect bone cells in various ways leading to imbalances in the bone remodelling cycle. Breast cancer metastases are known to generally cause osteolytic bone lesions. This is thought to occur via the direct and indirect stimulation of osteoclast differentiation and activity rather than through the tumour cells themselves degrading bone (421, 422), but the molecular mechanisms involved in this process are still uncertain. The aim of this chapter was to model the effect of osteolytic tumour cells, particularly breast cancer cells, on the key bone cell types osteoclasts, macrophages, and osteoblasts.

This chapter demonstrates that a general property of breast cancer cells that cause osteolytic metastases *in vivo* is that they strongly stimulate osteoclast formation, fusion and activity when co-cultured with bone marrow cells in the presence of RANKL and M-CSF *in vitro*. This occurs even when the tumour cells are seeded at very low initial seeding densities and in fact the osteoclasts formed in these cultures are larger at the lowest tumour cell seeding densities. This effect seems to be due to competition for space between the tumour cells and osteoclasts and their precursors. There have been very few co-culture experiments published since the discovery of RANKL as the key osteoclast differentiation factor and these have generally studied other facets of the tumour-bone cell interactions. Nicolin *et al* (2008) demonstrated that MCF7 human breast cancer cells induce the differentiation of RAW 264.7 murine monocyte-macrophage cells into osteoclasts when in co-culture through the direct production of RANKL (423). Ramnaraine *et al (*2006) co-cultured 4T1 cells with RAW 264.7 cells but did not look at the effect on osteoclast differentiation (424). While Ohshiba *et al* (2003) found that adding MDA-MB-231 cells to a co-culture of mouse bone marrow cells and osteoblasts greatly induced osteoclast formation and concluded that cell-cell interaction was vital for MDA-MB-231 induced osteoclast formation (425). The results of this present study confirm the hypothesis that osteolytic tumour cells directly enhance osteoclast formation and activity.

There is some disagreement in the literature over the ability of tumour cells to induce osteoclast formation in the absence of RANKL. MDA-MB-231 cells are known not to produce RANKL (203) as are the majority of osteolytic tumour cells previously tested (426, 427). The only exception to this is MCF7 cells which were found by Nicolin *et al* (2008) to

produce both soluble and membrane bound forms of RANKL (423). This result, however, contrasts with previous works that found no production of RANKL by MCF7 cells (203, 426, 427). In the present study, MDA-MB-231 failed to induce the formation of TRAcP positive cells in M-CSF generated BM macrophage cultures. A result that disagrees with Lau *et al (* 2006) who found that MDA-MB-231 cells caused osteogenesis via a RANKL independent pathway, but agrees with Thomas *et al (*1999). The reason for this may be that Lau *et al* were studying Tumour associated macrophages (TAMs) rather than the murine bone marrow used by Thomas *et al* or M-CSF generated macrophage used here. Other explanations include MDA-MB-231 cell line clonal differences, and the contamination of the cultures of Lau *et al* with RANKL-producing stromal cells.

This chapter demonstrated that factors derived from osteolytic breast cancer cells had a variety of effects on the three different bone cell types studied. In osteoclasts MDA-MB-231 conditioned medium induced dose-dependent increases in the differentiation and fusion of osteoclasts from M-CSF-generated BM macrophage in the presence of RANKL. This increase was not as effective as that seen when cells were directly co-cultured with the osteoclasts, but was still substantial. Generally there were similar increases in osteoclast number, but not similar increases in osteoclast size and nuclearity. No increase in cell viability was seen when MDA-MB-231 conditioned medium was applied to osteoclast precursors in the absence of RANKL. This result could be explained in two ways. Firstly, this could be due to the constant supply of breast cancer derived factors when the cells were present, as opposed to the discreet treatment regime used in conditioned medium treatments. The other explanation is that part of the increase observed could be due to cell-cell interactions between the cancer cells and mature osteoclasts and their precursors. The lesser effect seen when using conditioned medium is then explained as the cell-cell contact mediated effects are absent. There are conflicting reports in previous work on the effects of conditioned medium from both MDA-MB-231 and other osteolytic cell types when applied to osteoclasts and their macrophage precursors. Bendre *et al* (2005) found that MDA-MB-231 conditioned medium did not stimulate osteoclast formation in human PBMCs (304), while Tumber *et al* (2001), Grano *et al* (2000) and Guo *et* al (2008) all found that MDA-MB-231 conditioned medium stimulated osteoclast formation in bone marrow cultures, bone explants and RAW 264.7 cells respectively (428-430). An explanation for the failure of Bendre *et al* to show an increase in PBMC osteoclast number may be the 50%

concentration of conditioned medium used. Guo *et al* showed that MDA-MB-231 conditioned medium was most effective at 10% with a dose dependent drop in effect at higher concentrations leading to negligible effect at 50%. In addition, in preliminary work to the results presented here osteoclast cultures were treated with MDA-MB-231 conditioned medium at 50% and a negative effect on osteoclast formation noted. Presumably due to both the reduction in the concentration of FCS present in these cultures and the excess of toxic factors in the conditioned medium. Notably, Rucci *et al* (2004) found that conditioned medium from MCF7 cells was able to induce osteoclast formation in the absence of exogenous RANKL, suggesting a confirmation of the results reported by Nicolin *et al* (2008) mentioned above (414). However Rucci *et al* used bone marrow cultures with osteoblast and stromal cells still present, which could have provided the required RANKL.

The effect of MDA-MB-231 conditioned medium on osteoblasts was such that there was no statistically significant effect on osteoblast viability, but a slight trend towards a reduction at higher concentrations of conditioned medium. There was however a significant reduction in osteoblast differentiation as measured by alkaline phosphatase activity at all concentrations of conditioned medium except 5% and at 20% a reduction in bone nodule formation. The reason for this is likely to be factors produced by the MDA-MB-231 cells inhibiting osteoblast differentiation. This is in agreement with previous work by Mercer *et al* (2004) who showed that MDA-MB-231 conditioned medium (50% v/v) inhibited the differentiation and mineralisation of the osteoblast like cell line MC3T3-E1 by a mechanism dependant on the presence of TGFβ production (431).

The use of conditioned medium to study the effects of cancer-induced bone cell activity allowed us to explore a range of other techniques including western blot, qPCR and Xcelligence analysis. Western blot showed that factors secreted by the osteolytic breast cancer cell line MDA-MB-231 stimulated 3 key pathways involved in the differentiation, function and survival of osteoclasts. In particular, stimulation of the NFκB pathway is vital for osteoclast differentiation (432, 433). This provides a potential mechanism for the increases in osteoclast number, size and nuclearity observed in previous experiments. In osteoblasts stimulation of both the PI3K/Akt and MAPkinase signalling pathways was observed. This is again a potential mechanism behind the increases in both RANKL and OPG production seen in the qPCR results when osteoblasts were stimulated with MDA-MB-231

conditioned medium. However, as these are key survival pathways in osteoblasts it seems unlikely that this stimulation could explain the decrease in osteoblast differentiation and function noted (19, 23, 24, 322).

The increase in RANKL/OPG ratio in osteoblasts by MDA-MB-231 conditioned medium is an important finding as it suggests that tumour cells enhance osteoclastogenesis indirectly by increasing osteoblast support for osteoclast formation, survival and activity. OPG is a decoy receptor for RANKL, so any relative increase in levels of RANKL compared to OPG leads to higher amounts of RANKL free to bind RANK contribute to osteoclastagenesis. The fact that the increase in RANKL expression was a 13-fold increase compared to only a 2.5-fold increase of OPG production suggests that in the metastatic bone microenvironment this effect would lead to a sharp increase in osteoclast formation even in the absence of any direct effect of the tumour cells on the osteoclasts or their precursors.

Finally, the Xcelligence results revealed the complexity of the crosstalk between the tumour cells and osteoclasts. For example, for the moment excluding the conditioned medium effects, the Xcelligence analysis show that RANKL inhibits proliferation of M-CSF derived bone marrow cultures. This is most likely explained by changes in cell motility and spreading in M-CSF-generated BM macrophage in response to RANKL, switching from a proliferative state to one where they are migrating and searching for cells to fuse with and form osteoclasts. The overall effect of the conditioned medium was two-fold. Firstly it returned the rate of proliferation in RANKL treated cells to the same level as that seen in the M-CSF only treated cells. Secondly it caused a large and extremely rapid increase in impedance within the first two hours of treatment. I hypothesise that these two effects are caused by two different factors or sets of factors. A transit acting set of factors that causes the initial effects and a slow acting set that causes the long-term increased rate of increase in cell index value representing proliferation. However, further work using complementary techniques is needed to examine this hypothesis.

Focusing on the transit acting set of factors, upon initial treatment with breast cancer conditioned medium a small rise in cell index was observed followed by a prolonged drop and then a sharp rise. This could be explained by the transit factors in the conditioned medium causing the macrophage to change to a more elongated morphology as they search for other cells to fuse with. The small increase and sharp drop would then be

explained as the cells bunch up before elongating; this would slightly increase impedance before reducing it. This would also explain why this pattern was not repeated when the treatments were refreshed, the cells had already changed morphology and so could not do so again. The sharp increase is unlikely to be proliferation as it is far too rapid, and is more likely explained by increased spreading and fusion of the cells increasing impedance values. The long term increase in cell index values could then be explained by increased proliferation; however, no change in cell viability was noted in alamarblue studies of macrophages. This means that either the alamarblue was not sufficiently sensitive to detect any changes, or the conditioned medium only affects the viability and proliferative rate of macrophages that have been exposed to RANKL, or the increase is due to some other factor such as cell fusion. The last explanation seems most likely given the results seen in the osteoclast formation experiments. Overall, the Xcelligence analysis shows that the MDA-MB-231 conditioned medium has a wide range of effects on the developing osteoclasts and greatly changes not just their number and size but also the way in which they develop. More work is needed to elucidate exactly how this occurs. Potential candidates for the cancer produced factors causing these effects are RANKL, M-CSF, IGF-1, PTHrP, TGFβ and others which are discussed in detail in chapter 5.

In summary, the results reported in this chapter demonstrate that cancer derived factors from osteolytic human breast cancer cell lines enhance RANKL and M-CSF stimulated osteoclast formation but do not support osteoclast survival in the absence of RANKL and M-CSF. This occurs both directly, by acting on mature osteoclasts and their precursors and indirectly by increasing osteoblast support for osteoclast formation. In addition, osteoblast differentiation and bone nodule formation were also inhibited by MDA-MB-231 conditioned medium without effecting cell viability. This suggests that bone loss in osteolytic metastases may be compounded by a concurrent loss of osteoblast function. The aim of this chapter was to establish *in vitro* models of breast cancer-induced osteoclastic and osteoblastic changes that could be used for therapeutic intervention studies of osteolytic bone metastasis in later chapters (see chapter 7). This aim has been achieved as osteoclast-tumour cell co-cultures, and the use of tumour cell conditioned medium as a treatment for all bone cell types provide such techniques.

Chapter 4

Models to study cancer-induced osteolysis *ex vivo* and *in vivo*

4.1 Summary

Bone metastases observed in breast cancer patients are mainly osteolytic in nature. The aim of this chapter was to design and test established models of breast cancer-induced osteolysis *ex vivo* and *in vivo* that could be used in later chapters to test novel therapeutic agents for the treatment of osteolytic bone metastasis. With this in mind, attempts were made to set up three different models, a calvarial organ culture, a femoral organ culture and an intratibial injection model.

The *ex vivo* cancer cell – mouse calvaria organ culture used in the present study was an adaptation of the standard calvarial organ culture. Briefly, each mouse calvaria was divided into equal halves along the median sagittal suture and each half was placed into culture on stainless steel rafts in 48-well plates containing standard media or MDA-MB-231 (1×10^4 cells/well). Osteolysis was assessed using µCT. The calvaria halves co-cultured with MDA-MB-231 cells lost significant amounts of bone, confirming that this is a working model of osteolytic bone destruction. Attempts to use the same methodology to study breast cancer-induced osteolysis using MDA-MB-231 - femoral bone organ cultures were less successful. No loss of either trabecular or cortical bone was seen by µCT analysis, and there may in fact have been a slight increase in bone mass, though this was not statistically significant.

The standard model of intraosseous injection was decided as the most appropriate *in vivo* model for a study of interactions between bone and tumour cells. This method allowed the control of tumour site, and ignored the mechanisms of metastasis itself. MDA-MB-231 and a bone seeking variant failed to cause any osteolytic bone destruction when injected into the tibia of female Balb/c Nude mice despite being left for 8 weeks. This led to the use of 4T1 cells which were injected into the tibia of female Balb/c wild-type mice. After only 3 weeks experiments had to be stopped as all trabecular and most cortical bone had been destroyed in the injected legs.

Overall, this chapter was partially successful at creating usable models for *ex vivo* and *in vivo* studies of bone metastasis. The adapted calvarial organ culture and the 4T1 intratibial injection model can now be utilised in therapeutic intervention studies. Further work is needed for the adapted femoral organ culture and any other *in vivo* work.

4.2 Introduction

While Chapter 3 showed that much can be learned from investigating tumour cell-bone cell interactions *in vitro,* the overall impact of the observed effects cannot be deduced in so simplified an environment. To do this techniques that maintain the normal bone microenvironment are required. The overall effects of breast cancer cells on osteolysis can only be investigated using *ex vivo* and *in vivo* models of osteolytic bone disease. The aim of this chapter was to establish *ex vivo and in vivo* models that could later be used to test novel therapeutic agents for the treatment of osteolytic bone metastasis (see Chapter 8).

In this chapter, I will be discussing the development of several methods for investigating the influence of osteolytic tumour cells on osteolysis in both *ex vivo* and *in vivo* settings. I will demonstrate the effects of breast cancer cells on organ cultures, both calvarial and femoral, as well as what happens when these cells are placed directly into the bone microenvironment through intratibial injection.

Bone organ cultures are well established models that are routinely used to study bone turnover. This model provides a link between animal and cell culture studies while avoiding the complicating effects of systemic factors (434). Various different bones have been used including femora (435), metatarsals (436), and most commonly calvaria (434, 436, 437). The use of organ cultures to study bone metastasis has rarely been done, so here I will present a novel use of a well established technique.

Various *in vivo* models of bone metastasis exist (reviewed in (438, 439)) using a variety of different cell lines and injection sites. In this project, I am interested in the influence malignant tumour cells exert on bone cell differentiation, survival and activity once these cells are in the bone microenvironment and not the process of metastasis itself. Therefore, efforts were made to develop and adapt the existing intratibial injection based model. This allows me to standardize both the location and initial number of cells at the metastasis site.

4.3 Aim

The aim of this chapter was to use organ cultures and animal experiments to design and set up *ex vivo* and *in vivo* models to study the interactions and cross-talk between osteolytic breast cancer cells and bone. The models would then be used to investigate the effect of the tumour cells on osteolysis in this chapter and the modulating action various therapeutic agents could have on that effect in later chapters (see Chapter 8).

4.4 Results

4.4.1 Human MDA-MB-231 breast cancer cells induce osteolysis in MDA-MB-231 – mouse calvaria organ culture

To allow the investigation of crosstalk between tumour cells and bone cells *ex vivo,* the breast cancer – mouse calvaria organ culture (see Figure 4.1) was used. This method is an adaptation of the standard mouse calvarial organ culture and it was originally developed by Dr. Aymen I. Idris (440). Briefly, calvaria were removed from 7 day old mice and cut into halves along the median sagittal suture. Each half was then placed onto iron mesh platforms in 48 well plates in the presence or absence of human MDA-MB-231 breast cancer cells. Media was refreshed every 48 hours for a period of 1 week. Calvarial halves were then fixed and analysed by µCT analysis.

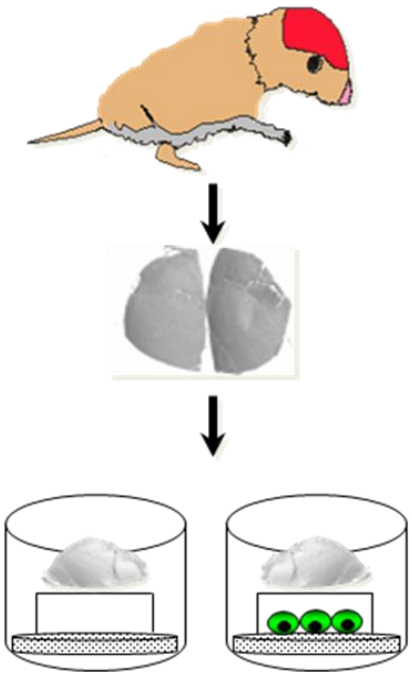

Figure 4.1 Diagram of the cancer cell – mouse calvaria organ culture
The green cells represent MDA-MB-231 human breast cancer cells

Figure 4.2 shows that factors produced by the human MDA-MB-231 breast cancer cells caused a significant loss in bone volume when co-cultured with mouse calvaria for 7 days, indicative of osteolytic bone damage (Figure 4.2 panel A). The extent of bone loss was quantified by μCT analysis (Figure 4.2 panel B), this showed that the presence of MDA In the wells significantly reduced calvaria bone volume by 46% ($p<0.01$). Wells were inspected at the end of the experient and it was found that in wells with no MDA-MB-231 cells present a number of mouse cells of mixed origin can be seen (Data not shown).

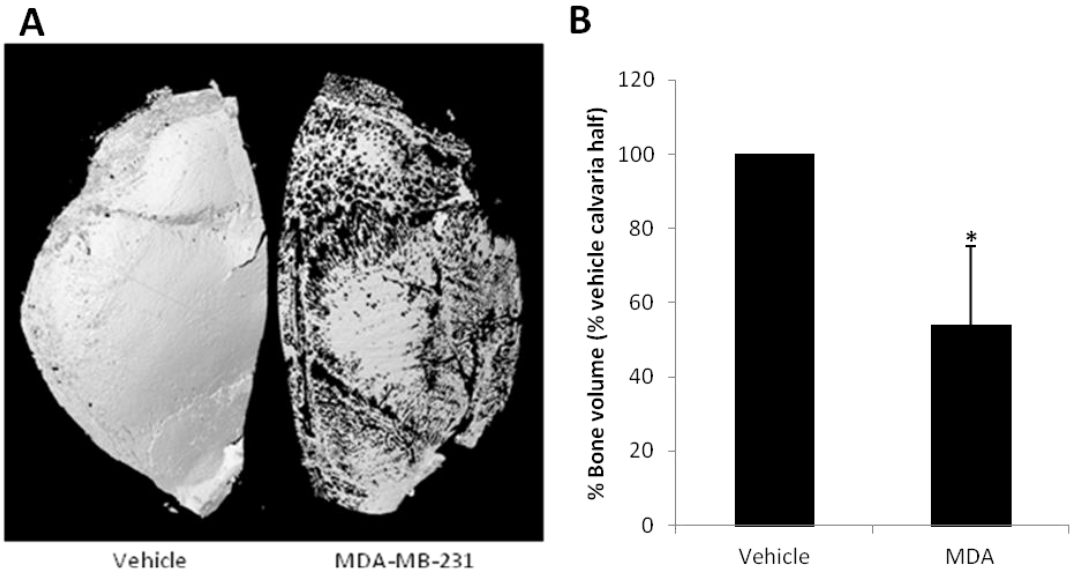

Figure 4.2. MDA-MB-231 human breast cancer cells cause osteolytic destruction of bone in human MDA-MB-231 - mouse calvaria organ culture. Panel A shows the effect of MDA-MB-231 cells on a mouse calvarial organ culture. Calvarial bones were isolated from 7 day-old mice, washed thoroughly in Hank's balanced salt solution (HBSS) and divided into equal halves along the median sagittal suture. The separated half-calvariae were explanted onto surfaces of stainless steel rafts in 48-well plates containing αMEM with either nothing or 3 x 10^3 MDA-MB-231 cells per well, seeded for 24 hours in advance. Media was refreshed every 48 hours for 7 days. Panel A shows representative microCT images of half-calvariae from the same mouse co-cultured with or without MDA-MB-231 cells. Panel B shows quantification of the bone volume in the calvaria halves by μCT analysis. Values in the graphs are means ± SD and are obtained from 4 independent experiments. * = $p<0.01$

4.4.2 Conditioned medium from MDA-MB-231 human breast cancer cells failed to induce osteolysis in femoral organ culture

Calvaria organ cultures allowed us to investigate the effect of tumour cells on flat bones; however long bones are a far more common site of metastasis. To investigate breast cancer-induced osteolysis in long bones *ex vivo*, an adaptation of the standard femoral organ culture was used. Femurs were extracted from 10 week old C57B6 mice and exposed to one of two different treatment sets. Either one femur was fixed straight away and the other left in αMEM, or both were placed into αMEM and one supplemented with 20% control conditioned medium and the other with 20% MDA-MB-231 conditioned medium. The media was refreshed every 48 hours and cultures were incubated for 2 weeks. Osteolysis was then analysed by µCT analysis.

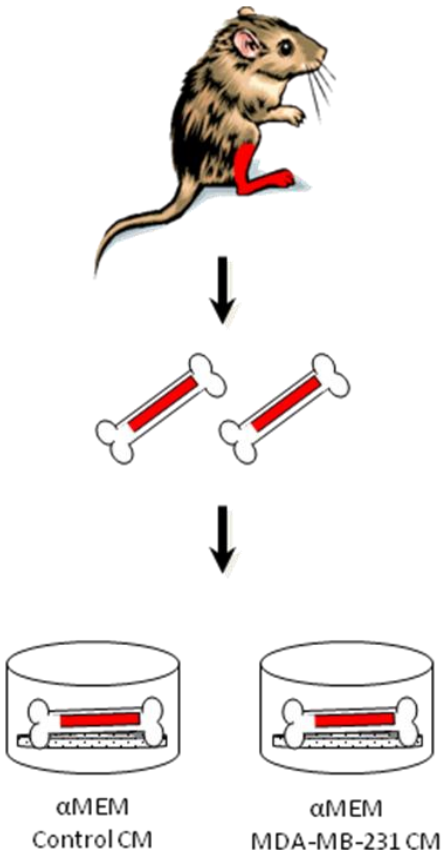

Figure 4.3 Diagram of the adapted femoral organ culture

Figure 4.4 shows that conditioned medium from MDA-MB-231 did not cause any significant change in either trabecular or cortical bone mass. Surprisingly, a minor and statistically non-significant increase in trabecular bone mass was observed in samples treated with MDA-MB-231 conditioned medium treatment. There was also no change in trabecular number, spacing, thickness or pattern factor (data not shown).

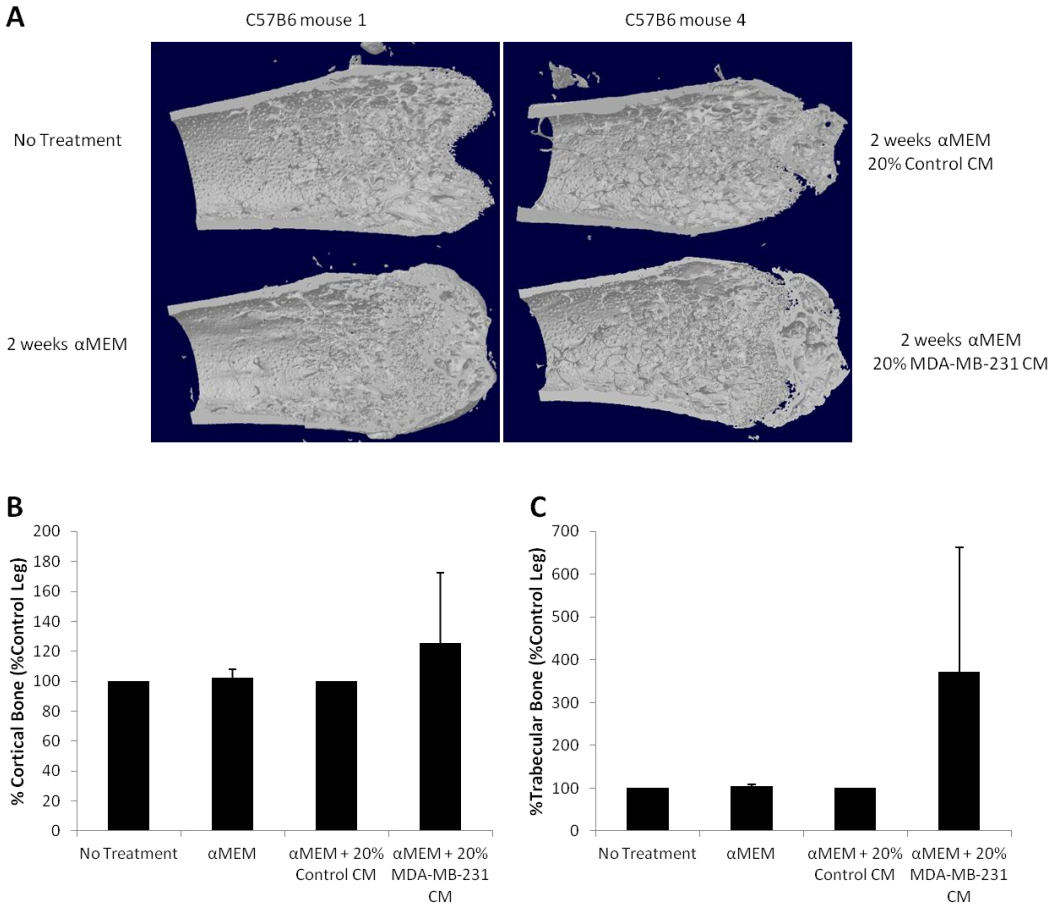

Figure 4.4 Conditioned medium from MDA-MB-231 human breast cancer cells failed to induce osteolysis in femoral organ culture. Panels A and B show the effect of MDA-MB-231 cells on a mouse femoral organ culture. Both femurs bones were isolated from 12 week-old mice, washed thoroughly in PBS and explanted to 6-well plates before being divided into two treatment regimes. In the first regime one of the two femurs was fixed straight away, and the other placed in αMEM for 2 weeks. In the second regime both femurs were placed in αMEM for 2 weeks and treated with either 20% Control or MDA-MB-231 conditioned medium. Media was refreshed every 48 hours for 14 days. Panel A shows representative microCT images of femurs from two mice, one following treatment regimen 1, and the other regimen 2. Panels B and C show percent bone volume of cortical bone (B) or trabecular bone (C) determined by µCT analysis. Values in the graphs are means ± SD and are obtained from 3 independent experiments.

4.4.3 Human MDA-MB-231 breast cancer cells failed to induce osteolysis following intratibial injection in humanised Balb/c mice

Cancer-induced osteolytic bone damage associated with human breast cancer cells was investigated in humanised mice using an intratibial injection model. Initial plans involved using the same MDA-MB-231 cells that had been used for much of the *in vitro* work. Either 10,000 or 100,000 cells were injected into the right tibia of three 6 week old female Balb/c Nude mice. These mice were monitored for any discomfort in the injected leg and analysed by *in vivo* μCT analysis once a week for 8 weeks. To avoid analysing the bone physically damaged by the act of injection only the first 30 sections below the tibial growth plate were analysed. This experiment was designed to give us an overview of how the MDA-MB-231 cells would grow in the tibia, the rough level of bone destruction they would cause and to help decide a timeframe for any therapeutic treatment in future work.

Figure 4.5 A shows that over the course of the 8 weeks of the experiment there was no obvious damage to either the cortical or trabecular bone caused by the MDA-MB-231 cells regardless of the number of cells injected. Using μCT analysis to compare the injected leg to the uninjected leg over the course of the experiment show that at no point is there any significant difference in trabecular bone volume (Figure 4.5 B and C), number, separation or trabecular pattern factor (data not shown). The only possible difference was actually a slight, and not significant, increase in bone mass when compared to the uninjected leg.

As the MDA-MB-231 cells had failed to cause any osteolytic bone destruction I decided to change the cell line used. The next cell line tested was an MDA-MB-231 variant cell line previously determined to metastasis to bone (441). Again this MDA-MB-231-BS cell line was injected into the right tibia of three 6 week old female Balb/c nude mice and two seeding densities used; 10,000 cells or 100,000 cells per mouse. Mice were again monitored and scanned by *in vivo* μCT once a week for 8 weeks; unfortunately due to a technical error data collected in week 1 was not usable. Figure 4.6 A shows that after 8 weeks there was again no obvious visual bone damage. Using detailed μCT analysis showed there was no difference between the injected or uninjected legs in bone volume (Figure 4.6 B and C), or any of the trabecular attributes measured (data not shown) and if anything a slight gain in bone mass.

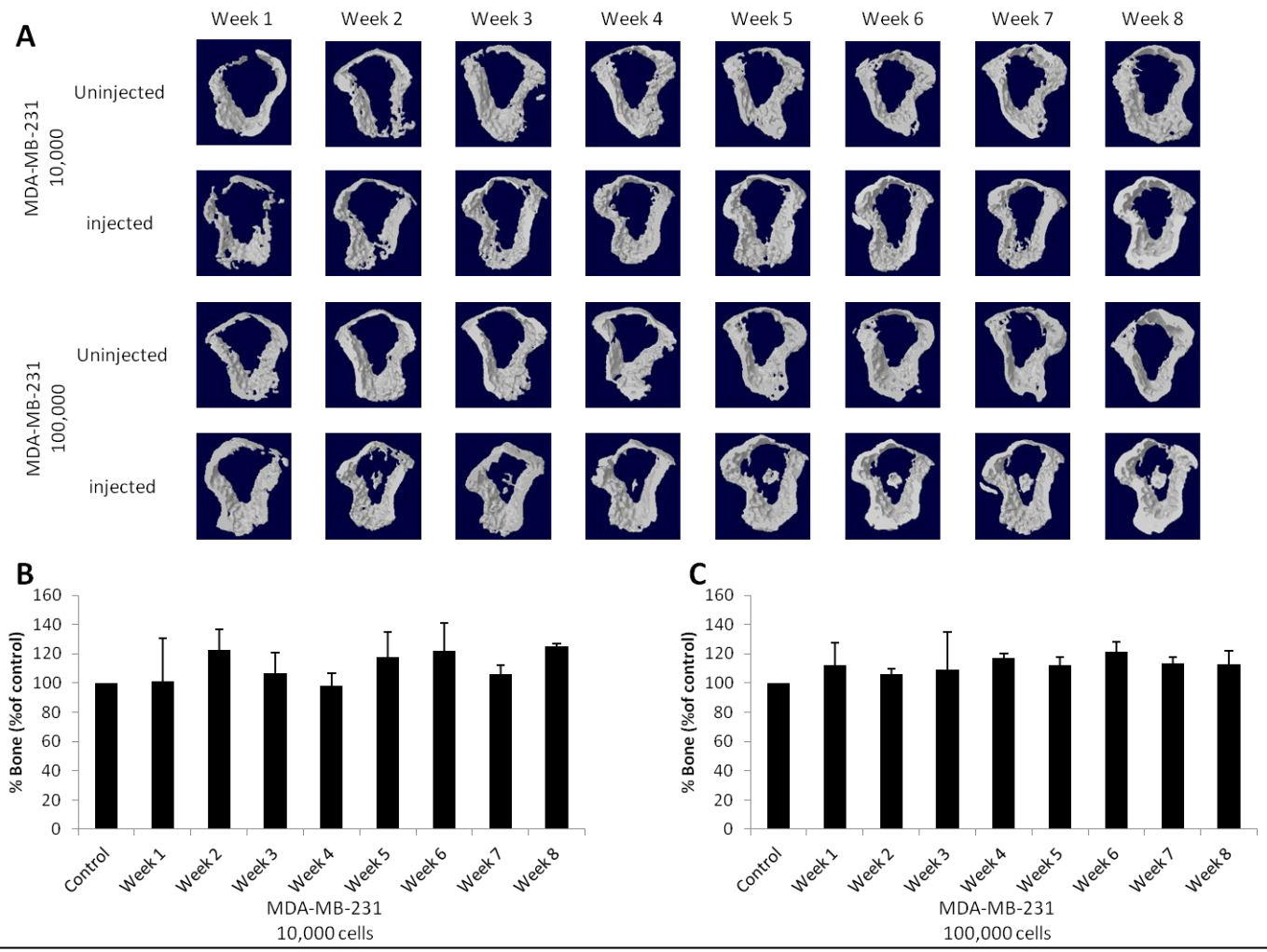

Figure 4.5 MDA-MB-231 cells did not cause osteolytic lysis when intratibially injected. 6-week old female Balb/c nude mice received intratibial injections of $1x10^4$ or $1x10^5$ MDA-MB-231 breast cancer cells into their right leg. Tibia were then analysed by *in vivo* microCT every 7 days. Animals were sacrificed at week 8. Panel A shows representative microCT images of tibia throughout the study. Panels B and C show the percent bone volume of the tibia injected with $1x10^4$ (B) or $1x10^5$ (C) MDA-MB-231 cells as a percentage of the percent bone volume of the uninjected leg through the course of the experiment. Values are means ± standard deviation. 3 mice per group.

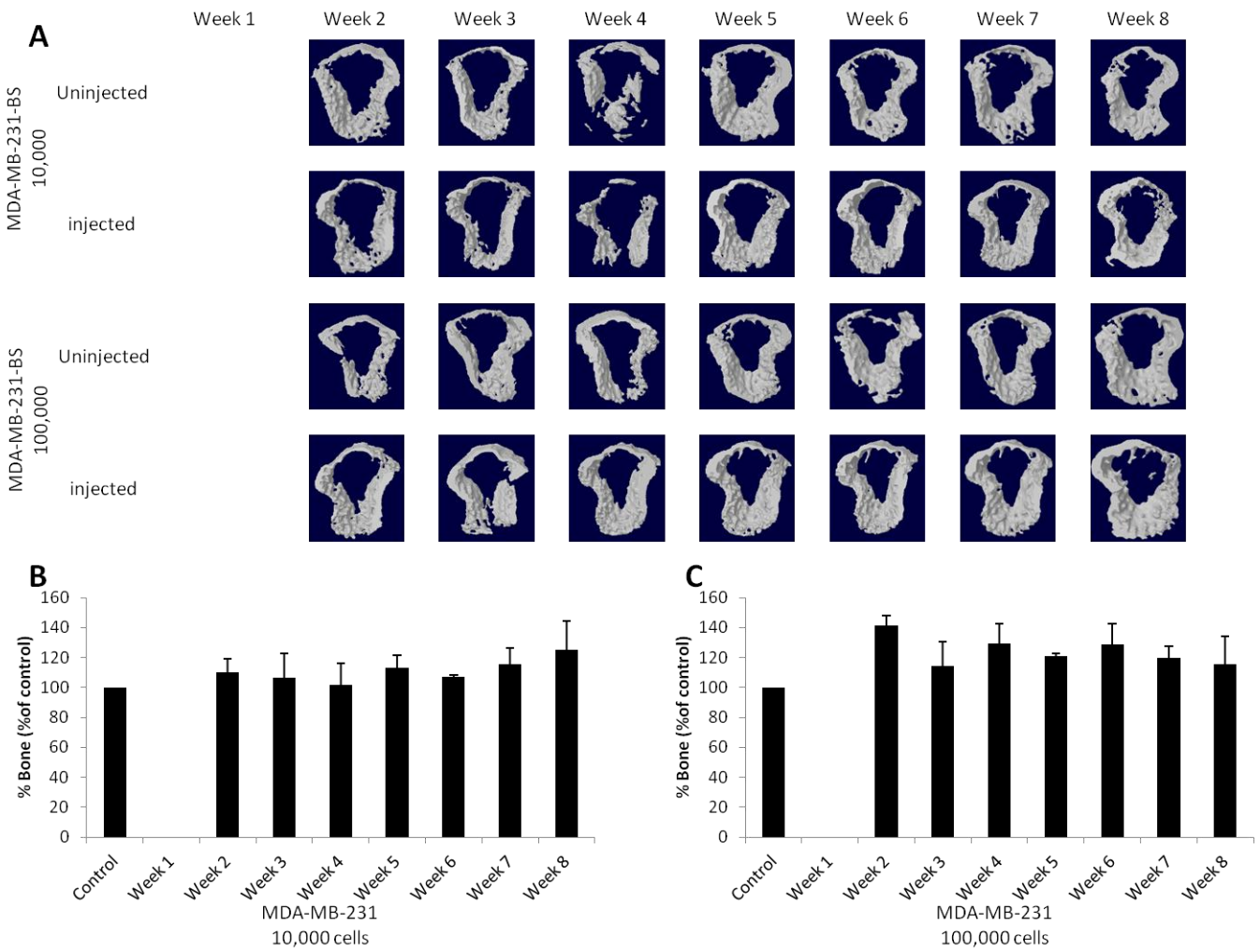

Figure 4.6 Bone seeking MDA-MB-231 cells did not cause osteolytic lysis when intratibially injected. 6-week old female Balb/c nude mice received intratibial injections of $1x10^4$ or $1x10^5$ bone seeking MDA-MB-231 breast cancer cells into their right leg. Tibia were then analysed by *in vivo* microCT every 7 days. Animals were sacrificed at week 8. Panel A shows representative microCT images of tibia throughout the study. Panels B and C show the percent bone volume of the tibia injected with $1x10^4$ (B) or $1x10^5$ (C) bone seeking MDA-MB-231 cells as a percentage of the percent bone volume of the uninjected leg through the course of the experiment. Values are means ± standard deviation. 3 mice per group.

4.4.3 Mouse 4T1 breast cancer cells caused osteolysis following intratibial injection in wild type Balb/c mice

The effect of cancer-induced osteolytic bone damage associated with breast cancer cells was investigated in wild type mice using the syngeneic mouse 4T1 cells. An initial seeding density of 5000 4T1 cells was chosen before cells were injected into the right tibia of three female 6 week old Balb/c wildtype mice. Mice were analysed by *in vivo* µCT analysis twice a week. This was planned to last 8 weeks, however after 3 weeks many of the mice were found to have lost the use of their right hind limbs and so all were culled.

Figure 4.7 shows that extensive osteolysis occurred in the injected legs over the course of the experiment. Visually, this appears to start at week 2 and leads to almost total loss of both trabecular and cortical bone in the injected legs by the end of week 3. µCT analysis showed that while no bone loss had occurred after one and half weeks, by week 2 4T1 injected legs had 43% less bone ($p<0.05$) than the uninjected control, this increased to 76% ($p<0.01$) and 80% ($p<0.01$) bone loss by weeks 2.5 and 3 respectively. As expected, trabecular number fell in line with the overall loss of bone. At week 1.5 there were 6% less trabeculi in the injected legs, falling further to 44% ($p<0.05$), 73% ($p<0.01$) and 79% ($p<0.01$) less after 2, 2.5 and 3 weeks. Trabecular thickness did not change at first remaining roughly equal in injected and uninjected legs until week 2.5 when it had decreased by 16% ($p<0.05$) in the 4T1 injected tibia, and by week 3 it had fallen by 35% ($p<0.01$). Trabecular pattern factor increased rapidly and by the end of the experiment had reached close to 500% ($p<0.01$) of the value of the pattern factor in the uninjected legs, indicative of significant loss of trabecular connectivity.

Figure 4.7 F and G show detailed *ex vivo* µCT modelling of representative injected and uninjected legs from the 4T1 experiment. The uninjected leg shows typical bone architecture for a 9 week old female Balb/c mouse. On the other hand, the leg injected with 4T1 cells shows not just a loss of bone, but also of general bone architecture, with large areas where bone seems to have been pulled or pushed away from the tibia. The sectioned view shows the normal contingent of trabeculi within the uninjected leg, while the 4T1 injected leg has none and even much of the growth plate has been destroyed.

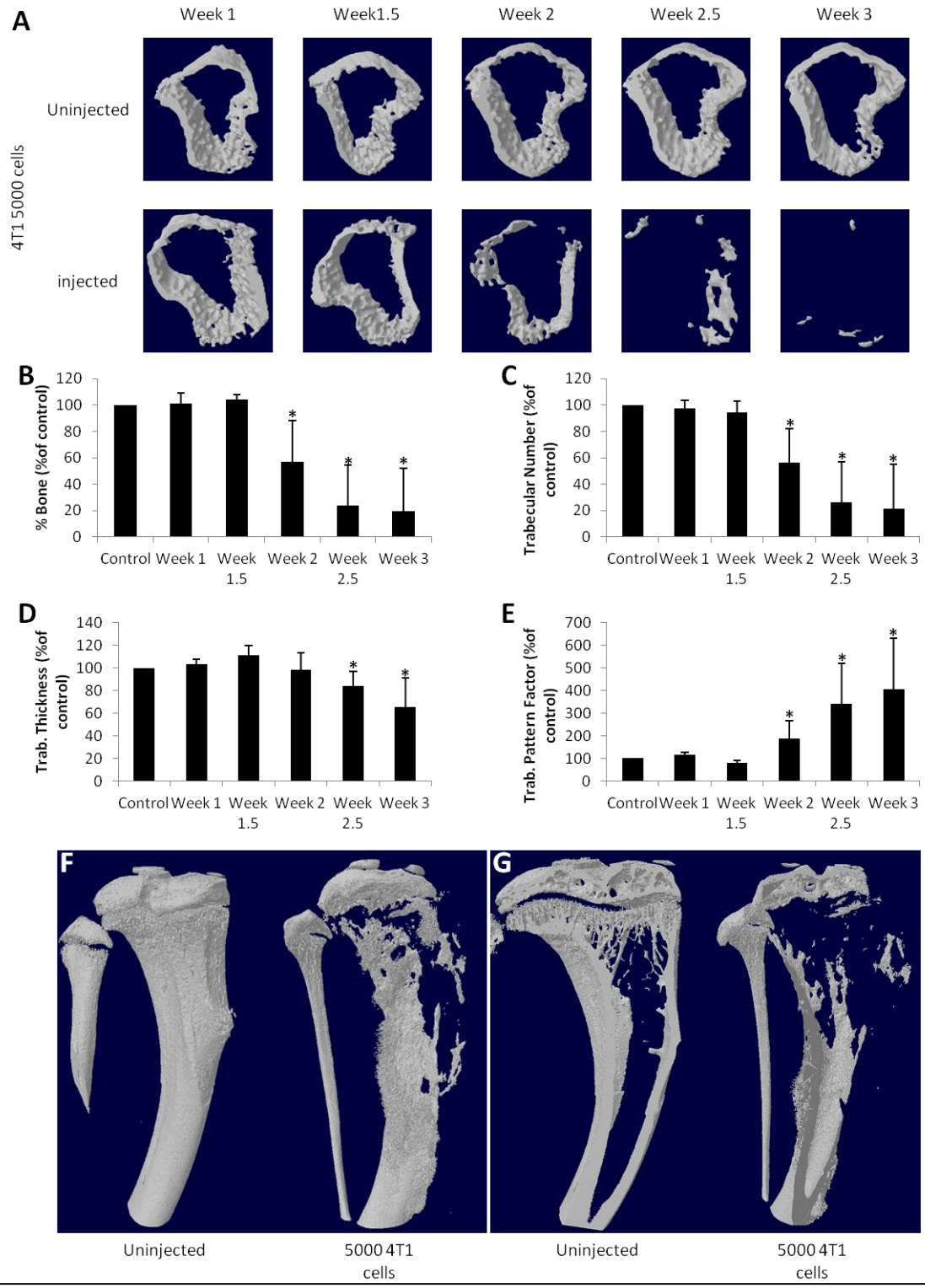

Figure 4.7 4T1 cells cause osteolytic lysis when intratibially injected. 6-week old female Balb/c mice received intratibial injections of $5x10^4$ 4T1 mouse breast cancer cells into their right leg. Tibia were then analysed by *in vivo* µCT every 7 days. Animals were sacrificed at week 3. Panel A shows representative µCT images of tibia throughout the study. Percent bone volume of the 4T1 injected tibia is shown in Panel B, trabecular number in panel C, trabecular thickness in panel D and trabecular pattern factor in panel E. All are shown as a percentage of the same feature in the uninjected tibia through the course of the experiment. Panels F and G show representative images from detailed ex vivo µCT analysis of the tibia, either whole (F) or artificially cut to reveal trabecular bone (G). Values are means ± standard deviation. 3 mice per group. * $p < 0.05$ from control.

4.4 Discussion

Osteolytic tumour cells are known to disrupt the bone remodelling cycle leading to imbalances that cause an overall loss of bone. The aim of this chapter was to create *ex vivo* and *in vivo* models to be used for the modelling of interactions between breast cancer and bone cells. Unlike chapter three, the aim was not to look at specific bone cell types, but instead to see the overall effects the tumour cells would have on bone mass, integrity and architecture.

This chapter demonstrates that while it was a general property of osteolytic tumour cells and conditioned medium to cause increases in osteoclast numbers *in vitro* (see chapter 3), this did not necessarily translate to *ex vivo* or *in vivo* settings. While adaptations to calvarial organ cultures were successful, it proved far trickier to fashion good models using either femoral organ cultures or *in vivo* intratibial models.

Bone explant cultures have been used since the 1920s (442) and in particular calvarial organ cultures and long bone organ cultures have been in use since the 1970s (443, 444) and 1980's (445), as well as more recently by Mundy *et al* at the turn of the century (446, 447). While many groups have in the past used organ cultures to study bone, very few groups have used these models to assess breast cancer-induced osteolysis or used cancer cells - organ co-culture systems combined with microCT analysis. This had made it difficult to see how our results fit with the existing literature. Some groups however have used conditioned medium to treat organ cultures. Of particular interest was Tabuenca *et al* (1995) who looked at the effect of conditioned medium from 5 breast cancer cell lines, including MDA-MB-231 and MCF7 cells, on 3 day old mouse calvaria (448). They found that the breast cancer cell conditioned medium led to an increase in bone resorption measured by release of ^{45}Ca. This is in broad agreement with our finding that culturing MDA-MB-231 cells below mouse calvaria leads to a loss of bone and osteolytic lesions.

There are two possible explanations for the bone loss observed in calvaria when they are cultured with human MDA-MB-231 breast cancer cells. The most likely is that in a similar way to that seen in the *in vitro* results of Chapter 3, the bone loss is caused by factors released by the MDA-MB-231 cells effecting bone cells. This means not only an increase in osteoclast formation and function, but as calvaria are osteoblast rich

environments in the early weeks after birth, the effects on osteoblasts may also be particularly important. MDA-MB-231 conditioned medium inhibited osteoblast differentiation and function while at the same time stimulating RANKL production. The overall effect of this is that in the co-cultured calvaria half MDA-MB-231 cells stimulate osteoclast formation, while inhibiting osteoblast differentiation and function and at the same time causing osteoblasts to further increase osteoclastogenesis through an increase in RANKL production. Future histological analysis of the calvarial bone from these experiments is needed to conclusively establish whether enhanced bone resorption or inhibition of bone formation (or both) is the mechanism behind the osteolysis observed. An alternative explanation for the bone loss seen is that changes in pH are caused by the tumour cells and this leads to a more acidic environment and it is this that causes an increase in osteoclast number. It is less likely that this could fully explain the extent of bone loss observed, and even if it does play a part this is an effect that would also occur with osteolytic bone metastases *in vivo* and so could be seen as a positive point for this model.

The fact that MDA-MB-231 conditioned medium failed to cause any bone loss in the femoral organ culture model was disappointing. This could be due to a variety of confounding factors. The most plausible explanation is the rate of turnover in the femur is significantly slower than that generally observed in the calvarial bone. Secondly, it may be that the factors in the conditioned medium were simply not reaching the bone cells either through the culture not keeping the cells in the organ alive, or through them being unable to penetrate the organ. This is countered by the fact that the legs appeared to be healthy through the course of the experiment, and that a variety of cell types were seen growing in the wells; though its possible they were from external connective tissue. Another explanation is that the concentrations of factors were simply not high enough or the lack of active production from cells meant that they did not have any great effect. It may be that using conditioned medium is not an appropriate technique for organ cultures, although both Tabuenca *et al* (1995) and Yi *et al* (2002) have successfully used it in studies of the more easily accessible calvaria (448, 449). Further work using a similar co-culture to that used with calvaria above would determine if this is true. The final explanation would be that the factors produced by the MDA-MB-231 cells used in this study have a different overall effect in long bones and particularly long-bone derived osteoblasts. Instead of inhibiting, they could slightly stimulate bone formation while failing to stimulate

osteoclastogenesis; this would then possibly explain why there is a non-significant growth in both trabecular and cortical bone mass. However, this seems unlikely given the results seen in chapter three and any increase is most likely due to variation and/or technical error.

There are many and varied *in vivo* models of bone metastasis, from autochthonous models, either naturally occurring or in GM mice (450), to mammary fat pad (451), intracardiac (452), or tail vein injections (453) and of course intraosseous injection models (454, 455). As we were not interested in the mechanisms of metastasis and wanted to ensure we had a 100% metastasis rate within a controlled location we chose to use an intraosseous model, in this case by intratibial injection. We were expecting MDA-MB-231 cells to proliferate within the bone marrow and cause osteolytic bone destruction following injection at the two injection densities chosen. This is an established effect within the literature, for example, Jones et al 2010 injected 100,000 MDA-MB-231 cells into the tibia of 6 week old female SCID mice (454). They demonstrated osteolysis noticeable on a radiograph by day 21 and severe loss of bone when mice were terminated at day 49. Gordon et al 2005 demonstrated similar results injecting 10,000 MDA-MB-231 cells into Balb/c nude mice and achieving extensive osteolytic lesions by day 28 (456), as have a variety of other groups (457-460). In many cases these groups have used identical protocols to ours and obviously it was disappointing not to be able to replicate these effects. However, Bendre et al 2005 also found that when MDA-MB-231 cells were injected into the tibia of nude mice they did not proliferate or cause bone destruction (304). Therefore it seems possible that some clones of the MDA-MB-231 cell line are unable to grow within the bone microenvironment and this may explain why our own line did not cause any bone destruction.

It was thought that using a bone seeking variant of the MDA-MB-231 cell line (441) should overcome this problem. Unfortunately that too did not cause any visible osteolysis over the course of our experiment. While it is possible that these cells could only grow in bone after intracardiac injection, as was done by Kang et al 2003, this seems unlikely. When combined with the failure of our own MDA-MB-231 intratibial injections, the most probable explanation is that something in our protocol causes the MDA-MB-231 cells, and their sub types, to undergo apoptosis either prior to or during the Intratibial injection. The most likely point is the time cells spend in PBS prior to injection or, less likely, an unforeseen

immune response in our nude mice. Another possible explanation is that the low resolution of our *in vivo* μCT analysis masked any bone loss, as it proved difficult to see trabecular bone using 18micron scans. This also seems unlikely as by the end of 8 weeks extensive cortical bone loss should also have occurred. Additionally, in a parallel experiment by another member of the group mice injected with another MDA-MB-231 variant cell line were left for 14 weeks with no visible bone destruction occurring (data not shown). Whether or not MDA-MB-231 cells proliferate in the bone could be determined by histological analysis, but it was decided that time could be used more productively. It is unfortunate that MDA-MB-231 cells proved unworkable for intratibial injection as that would have provided a more direct link between much of the *in vitro* and *ex vivo* work and our eventual *in vivo* model.

Mouse 4T1 breast cancer cells were chosen as the next best alternative. They had several advantages over other choices, firstly 4T1 enhanced RANKL and M-CSF-induced osteoclast formation in 4T1 - BM derived macrophage co-cultures (see Chapter 3). Secondly, they are also an established cell line for bone metastasis studies (415, 461) and lastly, as a mouse derived cell line they allowed the use of wild type Balb/C mice which is advantageous for several reasons. Nude mice do not have competent immune systems and as bone homeostasis is in some part regulated by immune cells (including the T-cells nude mice specifically lack) (462). This means that they do not have a normal bone remodelling cycle or bone mass. In fact in a separate study I showed that nude mice had 30-50% lower trabecular bone mass compared to their wild type counterparts (see Figure 4.8). Figure 4.7 shows that intratibial injection of 4T1 cells caused extensive bone destruction and in just 3 weeks an initial injection of only 5000 cells had removed most bone. In agreement with these findings, Thiolloy *et al* 2009 found that 10,000 4T1 cells began to breach cortical bone after 9 days (463). This is a far greater level of destruction than is practical for our use. By three weeks there was no trabecular bone left and even most of the cortical bone was absent. To remedy this lower initial cell numbers were considered for future work, but it was decided that 5000 cells was the lowest usable initial cell number before variation in counting or injecting could cause too much variability in results. It was therefore determined that the 4T1 intratibial injection model, while not perfect, could be used as it was, but with any experiments terminated by day 14. This would ensure that there would still be significant bone present for μCT and histological analysis. Unfortunately no

therapeutic treatment can be started in our animals until they have healed from the intratibial injection (day 7), which leaves only 7 days for any therapeutic intervention studies in this model (see Chapter 8).

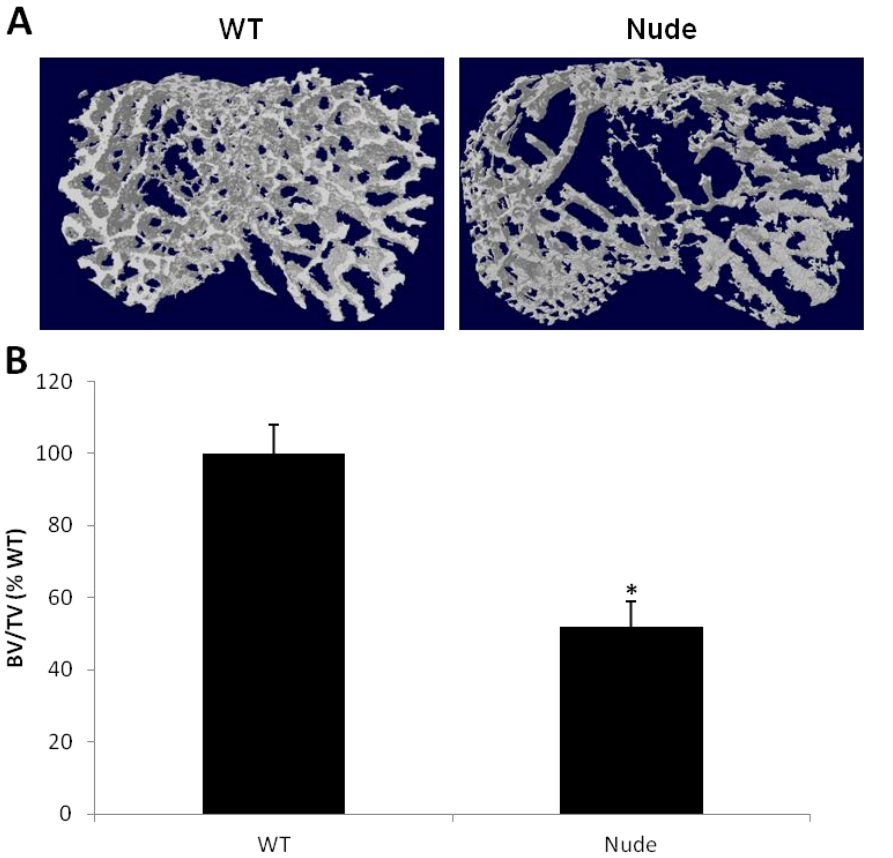

Figure 4.8 CD1 Nude mice have less trabecular bone than corresponding CD1 WT mice. Tibia were dissected out of twelve week old CD1 WT or Nude mice and submitted for µCT analysis. Panel A shows representative three-dimensional reconstructions of the trabecular bone of CD1 WT and nude tibia. Percent bone volume of the CD1 WT and CD1 nude tibia are shown in Panel B. Values are means ± standard deviation. 3 mice per group. * $p < 0.05$ from control.

In conclusion, while there is still further work needed to set up more advanced *ex vivo* and *in vivo* models for our use, in this study I successfully developed models that were usable for work presented later in this thesis. *Ex vivo* we have the fully functional adapted calvarial organ culture, where the results of any therapeutic studies can be measured both by µCT analysis of the bone, histology, and by measurement of the viability of the MDA-

MB-231 cells. *In vivo,* a 4T1 intratibial injection model is fully functional with extensive osteolytic destruction demonstrated, and a timeframe for any therapeutic intervention treatments determined. In the future, work should be done to establish both a working *ex vivo* femoral organ culture and intraosseous injection model using MDA-MB-231 or another cell type.

Chapter 5

Role of RANKL and M-CSF and in breast cancer-induced osteoclastogenesis

5.1 Summary

RANKL and M-CSF play important roles in osteoclast formation, survival and acitivity. This chapter aimed to examine the role of exogenous and breast cancer derived M-CSF and RANKL in cancer-induced osteoclastogenesis *in vitro*. First, qPCR studies in this chapter showed that human MDA-MB-231 breast cancer cells express M-CSF mRNA, but not RANKL mRNA. In contrast, mRNA expression of RANK receptor was detected, as was low expression of the M-CSF receptor C-FMS.

Co-culture and conditioned medium experiments were carried out to determine whether or not the presence of MDA-MB-231 cells was sufficient to support osteoclast formation and survival in the absence of the key osteoclastic cytokines M-CSF or RANKL. Confirming the results shown Chapter 3, these experiments showed that when RANKL was absent in MDA-MB-231 – BM derived macrophage co-cultures no osteoclasts were formed and all existing osteoclasts would undergo apoptosis. When M-CSF was absent the vast majority of cells underwent apoptosis, regardless of whether or not the experiment was investigating osteoclast formation or survival. This demonstrated that human MDA-MB-231 breast cancer cells do not produce a sufficient amount of RANKL or M-CSF to support osteoclast formation and survival in our model.

Through the use of conditioned medium it was found that treating MDA-MB-231 cells with M-CSF and/or RANKL enhanced their ability to stimulate osteoclast formation. This was particularly profound when MDA-MB-231 cells were treated with RANKL, greatly enhancing the size and nuclearity of the osteoclasts subsequently produced. This confirms our finding that the human MDA-MB-231 breast cancer cells used in this study express RANK and C-FMS. This also implies that RANK and M-CSF-mediated signalling in breast cancer cells may play an important positive feedback role in breast cancer-induced osteoclastogenesis.

MDA-MB-231 produced M-CSF and RANKL were not sufficient to explain the osteoclast stimulating effects previously observed. Therefore qPCR was used to look for other osteolytic factors produced by the tumour cells. A range of different cytokines and growth factors were produced by MDA-MB-231 cells including TGFβ, PTHrP, IL-1 and IGF-1. Overall, this chapter demonstrated that MDA-MB-231 derived RANKL and M-CSF are

unlikely to be the key factors responsible for the breast cancer-induced osteoclastogenesis observed in our models. However, signalling pathways downstream of RANK and M-CSF within tumour cells themselves merits further investigation in a future project. A range of factors known to enhance osteoclastogenesis are produced by the osteolytic cancer cells used in this study, and of these IGF-1 will be taken forward for further investigation in this thesis.

5.2 Introduction

Accumulating evidence suggests that a wide range of cytokines and growth factors are produced by tumour cells resulting in osteolytic bone metastasis (175, 180, 197, 464). These paracrine signals have a complex and multi-faceted effect on bone cells, and no one factor is likely to be the overall single cause of cancer induced osteolysis.

RANK ligand and M-CSF play important roles in osteoclast formation, survival and activity (237, 238). M-CSF is expressed by osteoblasts and binds to the transmembrane receptor c-FMS found on both osteoclast precursors and mature osteoclasts (465). This stimulates both osteoclast precursor differentiation and osteoclast survival. RANKL is a membrane bound cytokine from the TNF family expressed mainly on the surface of osteoblasts, osteocytes, mammary gland epithelial cells, T-cells and various other stromal cells (433). It is also less commonly found in a secreted soluble form (466, 467). It binds to the RANK receptor expressed by osteoclast precursors initiating their differentiation and fusion into mature multi-nucleated osteoclasts (209, 224).

As Chapters 3 and 4 demonstrated, osteolytic tumour cells strongly enhance the formation, and function of osteoclasts. The most obvious possible way in which this effect could be mediated would be through the production of either M-CSF and/or RANKL by tumour cells. While Chapter 3 showed that in the absence of RANKL MDA-MB-231 cells could not support osteoclast formation, various tumour cells have been shown to produce these factors in previous studies, and both have been linked to the osteolytic effect of bone metastases (228-231, 244). MDA-MB-231 human breast cancer cells strongly enhanced osteoclast activity both *in vitro* and *in vivo*, so here we explored RANKL and M-CSF expression by these cells, and whether this effects osteoclast formation and survival.

In addition to the ligands, the receptors themselves RANK and C-FMS, have been linked to the metastasis of breast cancer and other cancers to bone (232, 233). In particular, RANK expression has been linked to shorter survival times and accelerated metastasis to bone (234). Here we investigate whether signalling through these receptors affects the ability of MDA-MB-231 cells to enhance osteoclast formation.

5.3 Aim

The aim of this chapter was first to investigate whether MDA-MB-231 cells produce M-CSF and to determine if this could support osteoclast formation and survival in our *in vitro* model. Chapter 3 showed that MDA-MB-231 cells could not support osteoclast formation in the absence of RANKL, but RANKL expression was not investigated. So here I also aim to confirm this result, to investigate RANKL expression by MDA-MB-231 cells and wheather or not it can support osteoclast survival. The Second aim of this chapter was to determine if RANK and C-FMS receptors were expressed by MDA-MB-231 cells, and if signalling through these receptors could modulate the ability of these cancer cells to enhance osteoclast formation. Finally, this chapter aimed to determine if other candidate factors were being produced by MDA-MB-231 cells. These will then be investigated further in later chapters while testing the osteolytic bone metastasis models.

5.4 Results

5.4.1 Human MDA-MB-231 breast cancer cells express M-CSF but not RANKL

To determine if the MDA-MB-231 cells used in this study express RANKL and M-CSF we performed qPCR. Human PBMC mRNA was used as a positive control. Figure 5.1 shows human MDA-MB-231 breast cancer cells express very low RANKL mRNA (0.04% of PBMC expression). In contrast, M-CSF was detected and at the strikingly high level of 19.7% of the level seen in the PBMC positive control.

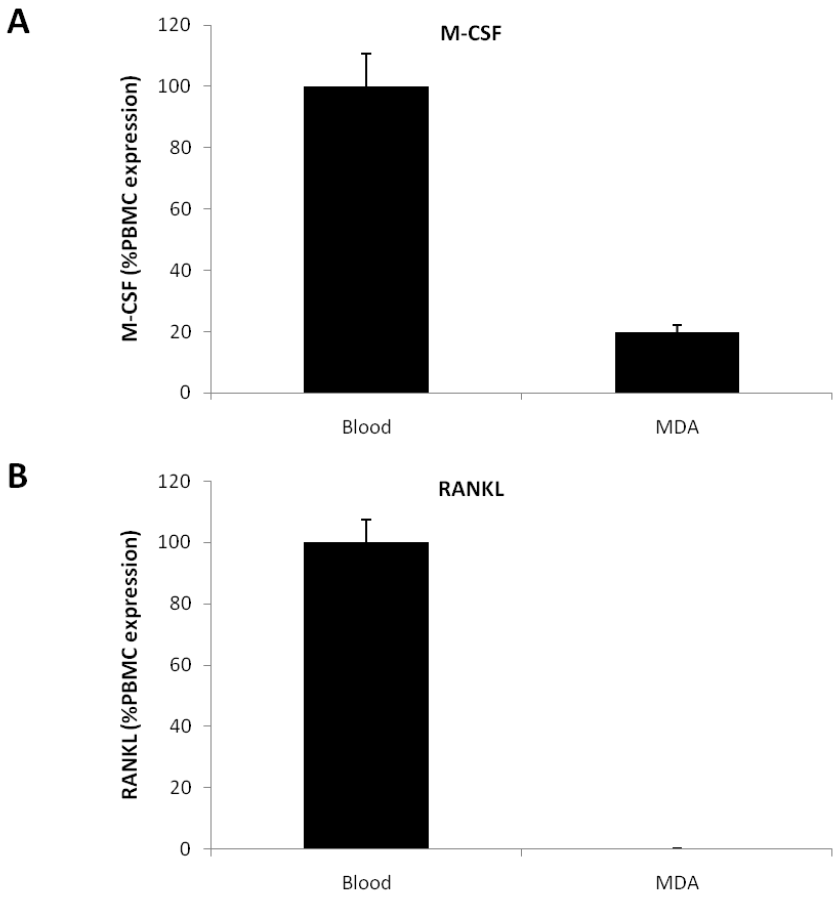

Figure 5.1 MDA-MB-231 cells express M-CSF but not RANKL. Panels A and B show the expression of M-CSF (A) and RANKL (B) in MDA-MB-231 cells and PBMCs as measured by quantitative rt-PCR followed by qPCR. Transcript numbers are corrected for expression of 18s RNA and displayed as a percentage of PBMC expression. Values in the graphs are mean ± SD and are obtained from three independent experiments.

5.4.2 Human MDA-MB-231 breast cancer cells express C-FMS and RANK receptors

To determine whether or not the MDA-MB-231 cells used in this study may themselves respond to RANKL and M-CSF treatment we performed qPCR. Human PBMC mRNA was used as a positive control. As shown in Figure 5.2, both receptors were detected in the human MDA-MB-231 breast cancer cells, but at levels far lower than those seen in the PBMC positive control. RANK was relatively high at 20.6% of the PBMC mRNA, while C-FMS was found at only 0.0001% of the PBMC mRNA. C-FMS while extremely low was however clearly above blank negative controls and so is taken to represent a positive result.

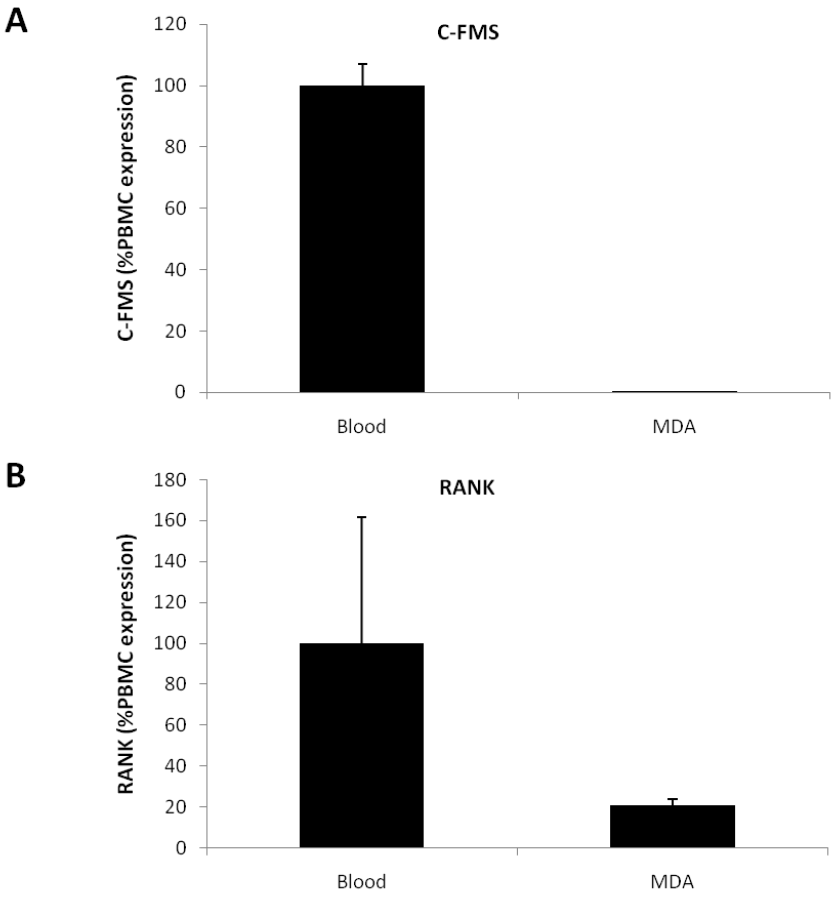

Figure 5.2 MDA-MB-231 cells express M-CSF ligand and RANK receptor Panels A and B show the expression of M-CSF receptor C-FMS (A) and RANK (B) in MDA-MB-231 cells and PBMCs as measured by quantitative rt-PCR followed by qPCR. Transcript numbers are corrected for expression of 18s RNA and displayed as a percentage of PBMC expression. Values in the graphs are mean ± SD and are obtained from three independent experiments.

5.4.3 Addition of MDA-MB-231 cells or conditioned medium to BM cultures is not sufficient to support osteoclast formation

We wished to determine if the M-CSF and/or RANKL, produced by the MDA-MB-231 cells was sufficient to support the formation of osteoclasts in cultures of BM derived macrophages. To achieve this we cultured M-CSF generated macrophages either in a co-culture with or without 300 MDA-MB-231 cells or treated with 10% control or MDA-MB-231 conditioned medium. These cultures were then exposed to RANKL (100 ng/ml) and M-CSF (25 ng/ml), RANKL alone, M-CSF alone or nothing for 72 hours. Figure 5.3 shows that when both RANKL and M-CSF are present MDA-MB-231 cells or conditioned medium increased osteoclast formation, as confirmed in Chapter 3. Also as shown in Chapter 3 figure 3.7, when RANKL was absent from the culture, only a very few mono-nucleated TRAcP positive cells and no osteoclasts were observed in the presence or absence of human MDA-MB-231 cells or conditioned medium. No change in the number of these TRAcP stained cells was present. In the absence of M-CSF, by the end of the culture the majority of cells have undergone apoptosis. Many of the remaining cells are TRAcP positive but all are mono-nucleated cells, with no mature osteoclast present. There is no difference in the number of TRAcP positive cells between the two cultures; however there does appear to be more macrophages present in the MDA-MB-231 treated cultures. Though, it is difficult to be sure due to the presence of the MDA-MB-231 cells, which cannot be distinguished from macrophages by phase contrast microscopy without the aid of specific markers. When neither RANKL nor M-CSF are present, very few macrophages and no TRAcP positive mono- or multi-nucleated cells were observed.

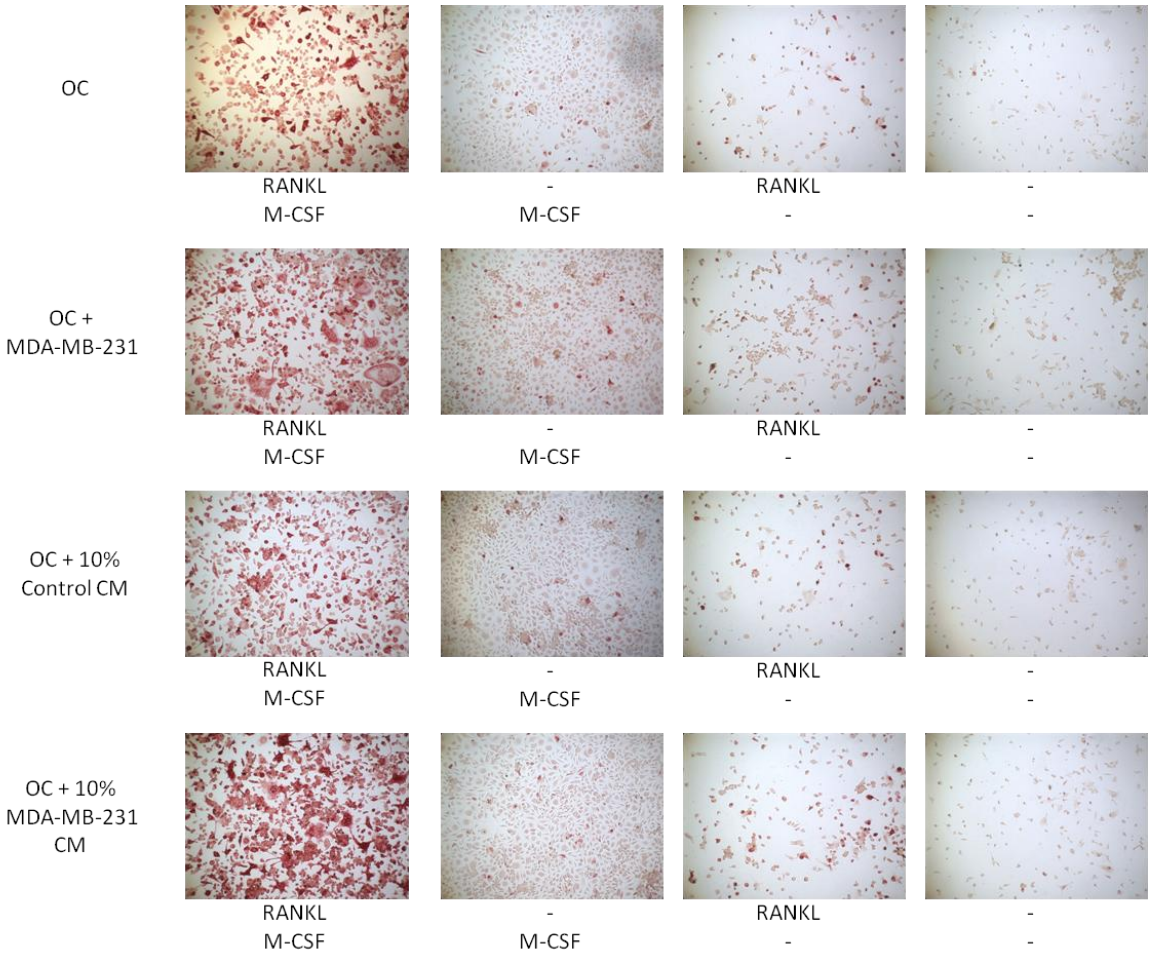

Figure 5.3 Addition of MDA-MB-231 cells or conditioned medium to BM cultures is not sufficient to support osteoclast formation. Osteoclast precursor macrophages were seeded and allowed to attach overnight. Cultures then had 300 MDA-MB-231 cells, MDA-MB-231 conditioned medium (10%), control conditioned medium 10% or nothing added. Cultures were untreated, or had M-CSF (25 ng/ml), RANKL (100 ng/ml), or both added. Media was refreshed after 48 hours and cultures fixed after 72 hours. Multi-nucleated osteoclasts were visualised following TRAcP staining. Representative photomicrographs of the cultures are shown. Data is from three independent experiments (N=3) performed in quintuplicate.

5.4.4 Addition of MDA-MB-231 cells or conditioned medium to osteoclast cultures is not sufficient to support osteoclast survival

To determine the effect of breast cancer derived factors on osteoclast survival, RANKL and M-CSF-stimulated osteoclasts were generated and then were exposed to MDA-MB-231 cells or conditioned medium from these cells in the presence and absence of RANKL or M-CSF for 48 hours. Osteoclasts were identified using TRAcP staining. Figure 5.4 shows that MDA-MB-231 cells and conditioned medium increased the number of osteoclasts in the presence of both RANKL and M-CSF. When mature osteoclasts were treated with only M-CSF the vast majority of osteoclasts underwent cell death. There are clearly many TRAcP stained cells still present but all of the large multi-nucleated osteoclasts have gone, as have most of the smaller osteoclasts, exact numbers were not counted. The MDA-MB-231 cell and conditioned medium treatments did not affect either the number of osteoclasts remaining or the number of TRAcP stained cells present. In the cultures where only RANKL treatment was present, many of the cells, osteoclast and macrophage, have undergone cell death. Numerous remaining cells were TRAcP positive but no osteoclasts were present. The presence of MDA-MB-231 cells or conditioned medium had no effects on osteoclast survival or the number of TRAcP positive cells in these cultures. Cultures where both M-CSF and RANKL were absent were identical to those where only RANKL was present.

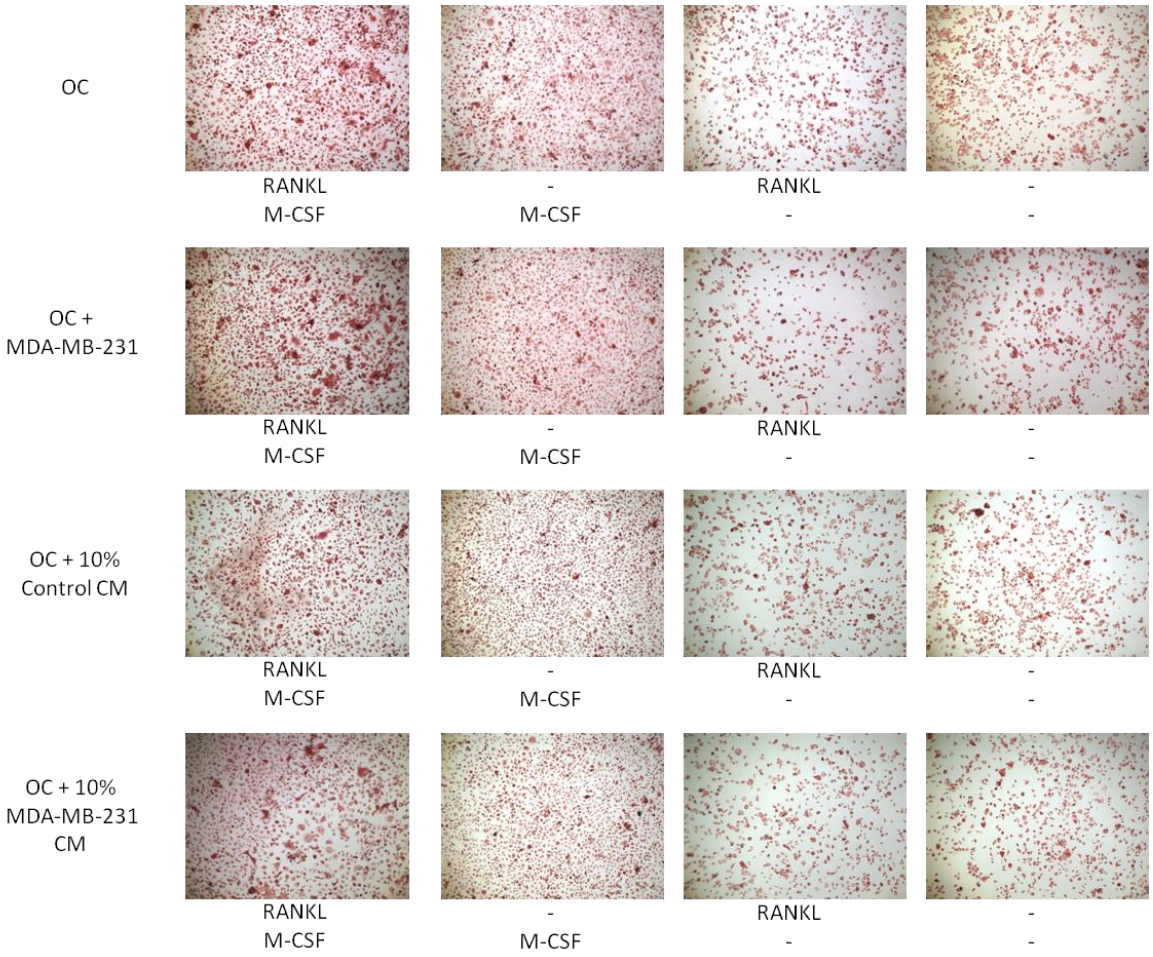

Figure 5.4 Addition of MDA-MB-231 cells or conditioned medium to BM cultures is not sufficient to support osteoclast survival. Osteoclast precursor macrophages were seeded and allowed to attach overnight in the presence of RANKL (100 ng/ml) and M-CSF (25 ng/ml). Cultures were allowed to develop for 96 hours or until a significant number of osteoclasts had formed. All media was then removed, cells washed in PBS and then 300 MDA-MB-231 cells, MDA-MB-231 conditioned medium (10%), control conditioned medium 10% or nothing added. Cultures were either left untreated, or had M-CSF (25 ng/ml), RANKL (100 ng/ml), or both added. Cultures were fixed after a further 48 hours. Multi-nucleated osteoclasts were visualised following TRAcP staining. Representative photomicrographs of the cultures are shown. Data is from three independent experiments (N=3) performed in quintuplicate.

5.4.5 Exposure to RANKL and M-CSF enhances the ability of MDA-MB-231 human breast cancer cells to stimulate osteoclast formation

As MDA-MB-231 cells expressed mRNA for both RANK and C-FMS, we wished to establish if pre-exposure of these cells to RANKL or M-CSF affected their ability to influence osteoclast formation. We treated MDA-MB-231 cells with RANKL (100 ng/ml), M-CSF (25 ng/ml) or both for 48 hours and then collected the conditioned medium. Osteoclast cultures were then treated with these various conditioned medium at a concentration of 10% for 72 hours. Osteoclasts were then identified using TRAcP staining. Figure 5.5 shows that conditioned medium from untreated MDA-MB-231 cells led to the formation of more and larger osteoclasts when compared to either the control conditioned medium treatment, or the untreated osteoclast cultures. This effect was augmented when the conditioned medium came from MDA-MB-231 cells treated with M-CSF, RANKL or both. Though an increase was also noted when control conditioned medium from an M-CSF treated flask was used. MDA-MB-231 conditioned medium from cells treated with M-CSF provided only a minor boost over that from the untreated cells, while cells treated with RANKL, or both provided a far greater increase. In fact when conditioned medium came from cells treated with both M-CSF and RANKL cultures started to look comparable to MDA-MB-231 – osteoclast co-cultures. There was a particularly marked increase in the size and nuclearity of osteoclasts.

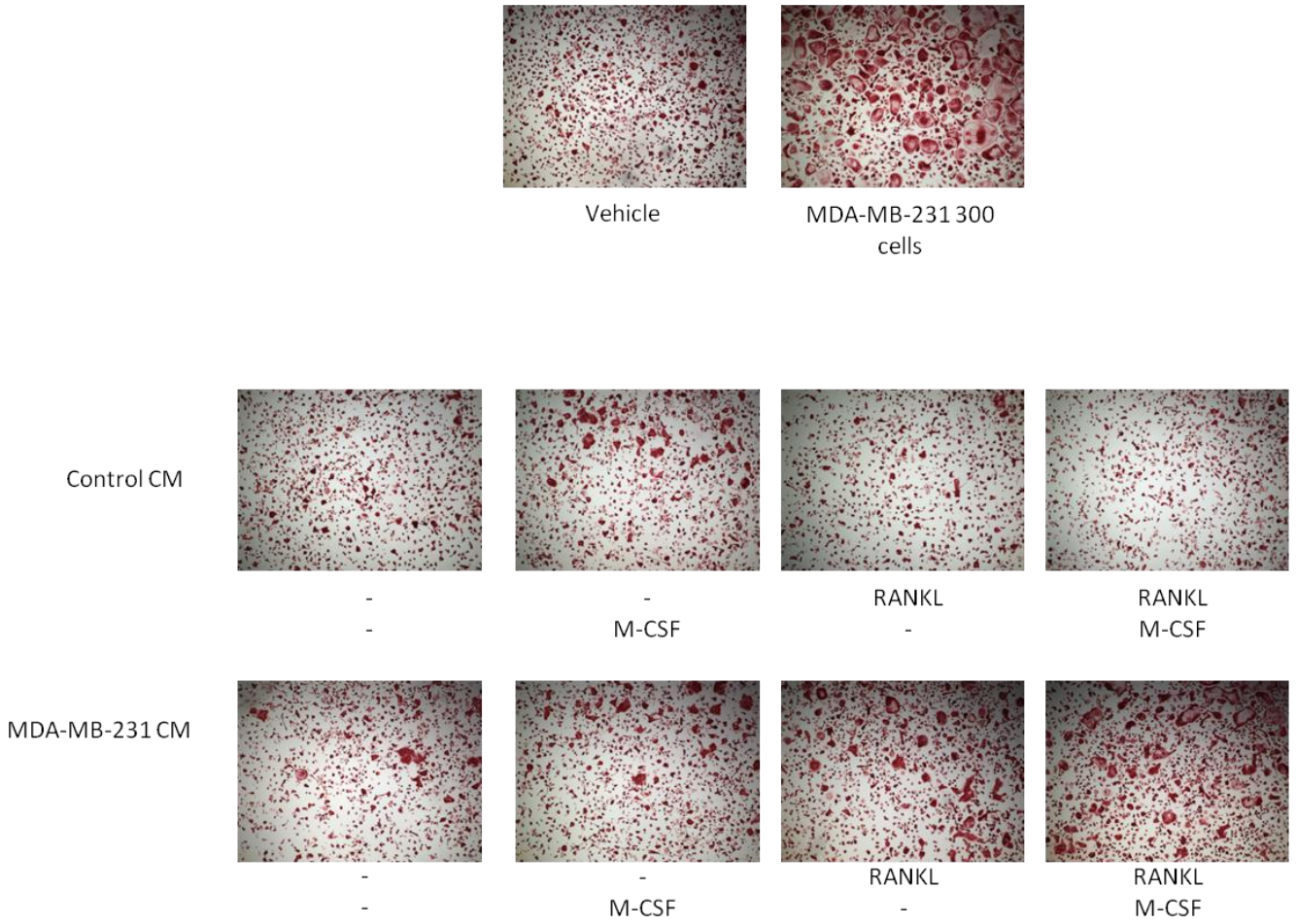

Figure 5.5 Exposure of MDA-MB-231 to RANKL and M-CSF enhanced their ability to stimulate osteoclast formation. Osteoclast precursor macrophages were seeded and allowed to attach overnight in the presence of RANKL (100 ng/ml) and M-CSF (25 ng/ml). Cultures were then untreated, had 300 MDA-MB-231 cells added, or had control or MDA-MB-231 conditioned medium (10%) added. This conditioned medium came from control or MDA-MB-231 cultures untreated or treated with M-CSF (25 ng/ml), RANKL (100 ng/ml), or both. Media was refreshed ever 48 hours and cultures fixed after 72hours. Multi-nucleated osteoclasts were visualised following TRAcP staining. Representative photomicrographs of the cultures are shown. Data is from three independent experiments (N=3) performed in quintuplicate.

5.4.6 Expression of osteolytic factors by human MDA-MB-231 breast cancer cells is unaffected by RANKL or M-CSF

To investigate other potential tumour produced factors that may be involved in MDA-MB-231 induced osteolysis I measured the mRNA expression of a number of known osteolytic factors. As shown in Figure 5.6, TGFβ, PTHrP, IL1β, uPA and IGF-1 were expressed by the MDA-MB-231 cells used in this study. No TNFα or MMP-9 mRNA expression was detected.

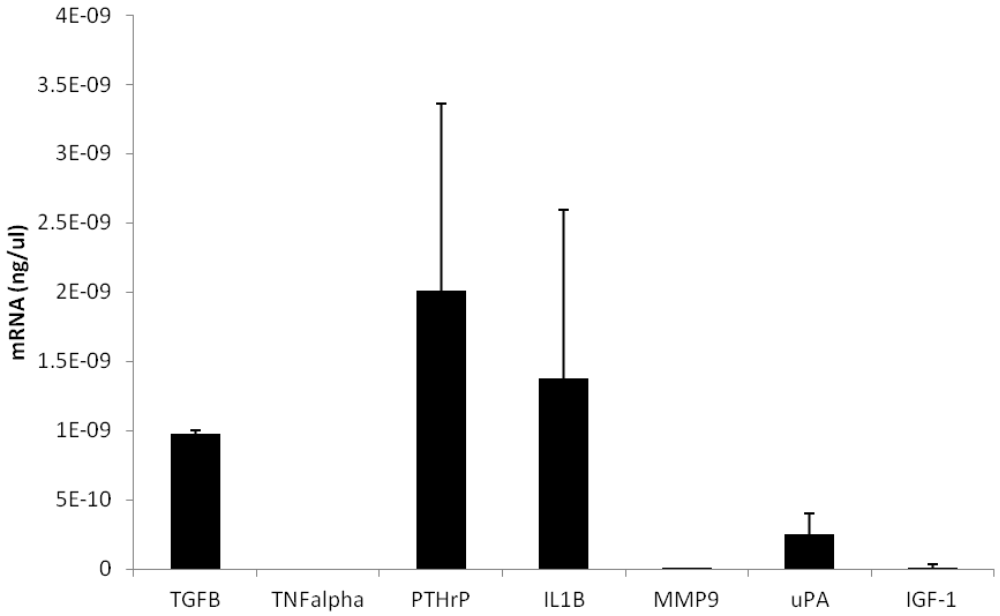

Figure 5.6 MDA-MB-231 cells express a range of pro-osteolytic factors. The expression of TGFβ, TNFα, PTHrP, IL1β, MMP9, uPA and IGF-1 in MDA-MB-231 cells as measured by quantitative rt-PCR followed by qPCR. Transcript numbers are corrected for expression of 18s RNA and displayed as ng/ul mRNA. Values in the graphs are mean ± SD and are obtained from three independent experiments.

As Figure 5.5 had suggested that RANKL and M-CSF treatment of MDA-MB-231 cell may increase their capacity to induce osteoclast formation, we studied the effect RANKL and M-CSF had on the production of tumour derived osteolytic factors. The mRNA expression of TGFβ, PTHrP, IL1β, uPA and IGF-1 was measured in the presence and absence of RANKL and M-CSF. Figure 5.7 shows that RANKL (100 ng/ml) and M-CSF (25 ng/ml) had no significant effects on the mRNA expression of these factors after 16 hours of continuous treatment.

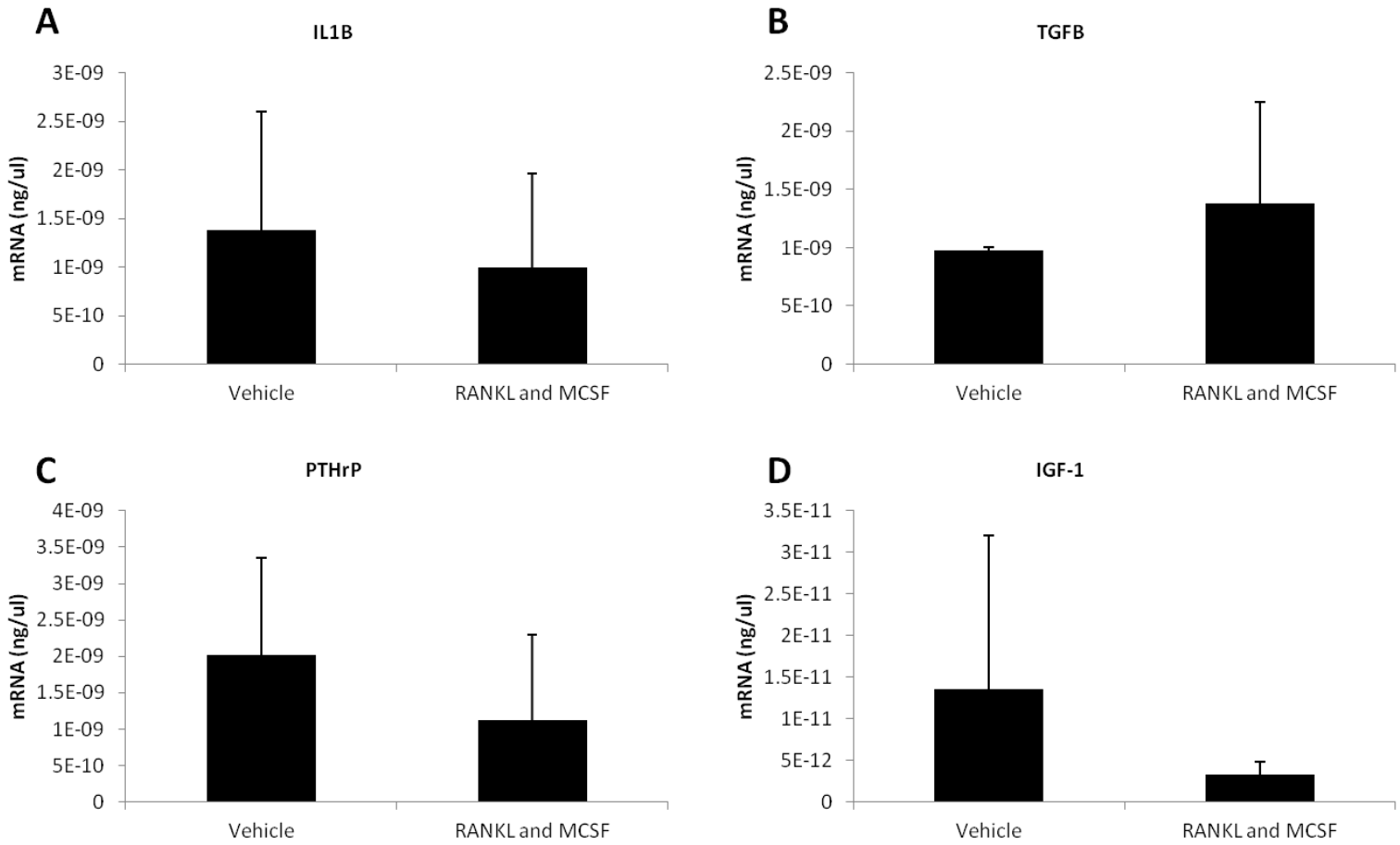

Figure 5.7 Pro-osteolytic factors produced by MDA-MB-231 cells are not affected by RANKL and M-CSF treatment. The expression of IL1β (A), TGFβ (B), PTHrP (C), and IGF-1 (D) in MDA-MB-231 cells untreated or treated with RANKL (100 ng/ml) and M-CSF(25 ng/ml) as measured by quantitative rt-PCR followed by qPCR. Transcript numbers are corrected for expression of 18s RNA and displayed as ng/ul mRNA. Values in the graphs are mean ± SD and are obtained from three independent experiments.

5.5 Discussion

RANKL and M-CSF are known to be the key factors behind the regulation of osteoclast formation and survival (433, 465). As bone metastases from a variety of tumours cause osteolysis, it was hypothesised that tumour derived RANKL and M-CSF may play an important role in cancer-induced osteoclastogenesis. The aim of this chapter was to establish whether RANKL and M-CSF were secreted by the human MDA-MB-231 breast cancer cells used in this study, and to determine if tumour derived RANKL and M-CSF play a significant role in cancer-induced osteoclastogenesis.

The data presented in this chapter demonstrates that while MDA-MB-231 express M-CSF mRNA, these cells do not produce RANKL. In osteoclast cultures, MDA-MB-231 cells were not sufficient to replace either RANKL or M-CSF and in their absence could not support osteoclast formation or survival. In contrast, the receptor RANK was highly expressed in MDA-MB-231 cells and they responded to RANKL treatment by increasing conditioned media effect on osteoclastogenesis, most likely through an increase in the production of unkown osteolytic factors.

Several groups have previously hypothesised that RANKL and/or M-CSF production from tumour cells contributes to osteolytic bone metastases. Some have even looked specifically at MDA-MB-231 cells with mixed results. Mancino *et al* (2001), Park *et al* (2003) and Ohshiba *et al* (2003) found similar results to that presented here, that MDA-MB-231 cells do not express or secrete RANKL (244, 425, 468). In contrast, Nicolin and Narducci (2010) report that they found basal levels of RANKL from MDA-MB-231 cells (469). As for M-CSF, we found a significant amount was produced, as did Mancino *et al* (2001), Gallet *et al* (2004), and Pederson *et al* (1999) (228, 244, 464). This suggests that M-CSF may play a significant role in breast cancer induced osteolysis.

While the production of M-CSF by MDA-MB-231 cells is confirmed, whether it is actively secreted by these cells in the metastatic bone environment is another matter. Work presented here shows that MDA-MB-231 cells could not replace the cytokine itself in osteoclast cultures. Neither co-culture nor conditioned medium were able to support the formation of osteoclasts in the absence of M-CSF. This is the opposite result of that found by Mancino *et al* (2001), who found MDA-MB-231 cells in co-culture with haematopoietic

cells allowed the formation of osteoclasts upon the addition of RANKL. As my work involved the use of M-CSF generated bone marrow macrophage, two possible reasons for this discrepancy are possible. Firstly, it may be that our M-CSF generated bone marrow macrophages are more sensitive to the presence of M-CSF as they have been cultured in high concentrations (100 ng/ml) for 2 -3 days, and so the relatively small amount produced by the MDA-MB-231 cells is not sufficient for their survival. The other possibility is that MDA-MB-231 cells do not secrete M-CSF, and Mancino *et al*'s results are explained by the presence of a variety of other bone cells such as bone marrow stromal cells that are known to produce M-CSF. Work by Pederson *et al* (1999) suggests that M-CSF was present in MDA-MB-231 conditioned medium and so it seems likely that the first explanation is true.

Osteoclast survival was also unaffected by the presence of MDA-MB-231 cells or conditioned medium when M-CSF was absent. Once M-CSF is removed from the cultures the vast majority of mono- and multi-nucleated cells seem to have undergone cell death, both in the MDA-MB-231 treated and untreated cultures. No difference in the number of surviving cells, let alone osteoclasts was noted. Again this suggests either that the M-CSF present in the MDA-MB-231 cells is not secreted, or is not sufficient to permit the survival of these M-CSF dependent cells. In the survival experiments, when both M-CSF and RANKL were absent cultures were identical to those where only M-CSF was absent. This supports the hypothesis that M-CSF is vital for these cells survival, as the absence of the key osteoclast survival factor (RANKL) made no further difference to the cultures.

When RANKL alone is absent from either the osteoclast formation or survival experiments there was again no difference between the MDA-MB-231 treated and untreated cultures. This was expected since no expression of RANKL was detected in MDA-MB-231 cells. However Lau *et al* (2006) have suggested that MDA-MB-231 cells are capable of inducing RANKL independent osteoclast formation (426), we observed no evidence to support this. As for survival, while there were a very few small osteoclasts apparent in the MDA-MB-231 treated cultures, this was also true for the untreated cultures with no differences noticed. This shows that MDA-MB-231 cells do not support osteoclast formation or survival either through RANKL dependent or independent mechanisms.

We next explored the possibility that RANKL and M-CSF in the bone microenvironment may act on tumour cells and enhance their osteolytic potential. Recently

studies have shown that RANK expression is associated with bone metastasis development, tumour migration and poor survival rate in breast cancer patients (232, 234). Here we show that exposure of MDA-MB-231 cells to RANKL prior to addition to BM cultures enhances the ability of these cells to increase osteoclast formation and size. This RANKL stimulated conditioned medium also leads to larger and more nucleated osteoclasts, in a similar fashion to osteoclast–MDA-MB-231 co-cultures; this was also, to a lesser extent, true for M-CSF. This suggests that one reason cells are more efficient than conditioned medium treatment at increasing osteoclast formation is that the MDA-MB-231 cells are also exposed to RANKL and M-CSF. However as MDA-MB-231 cells only produce trace levels of C-FMS and control conditioned medium also appeared to respond to M-CSF, this may be a false positive. The most successful conditioned medium when it comes to increasing osteoclast formation was from cells treated with both RANKL and M-CSF, and there was no response to control conditioned medium in this case. It therefore seems possible that MDA-MB-231 cells may contain an alternative M-CSF receptor such as V-FMS, and M-CSF signalling can enhance the production of osteolytic factors.

While M-CSF and RANKL signalling in MDA-MB-231 cells is important and will be thoroughly investigated in another project, other factors produced by the MDA-MB-231 cells are of more interest to this thesis. qPCR was used to determine the expression levels of a range of potential candidate genes, as well as whether or not any of them were enhanced if they came from cells treated with RANKL and M-CSF. Expression was found for 5 of the 7 genes, with no TNFα or MMP-9 found, but none were affected by RANKL and M-CSF treatment. The genes with the highest expression levels were TGFβ, PTHrP and IL-1β. IGF-1 and uPA showed far lower but still significant expression levels. This suggests that multiple growth factors and cytokines produced by MDA-MB-231 cells are likely to cause the effects seen in this chapter as well as Chapters 3 and 4. This is in broad agreement with Pedersen *et al* (1999) who found that a number of different factors produced by MDA-MB-231 cells could enhance osteoclast activity, and that the complex nature of their interactions with osteoclasts meant that it was difficult to single out any specific factors as being the most important (464). The three most highly expressed genes have been extensively studied in both bone, and bone metastasis, and as I had access to a novel specific IGF-1 receptor inhibitor, I will test our osteolytic bone metastasis models by investigating the effect of MDA-MB-231 produced IGF-1 further in Chapters 6 and 7.

In conclusion, I found that MDA-MB-231 cells express M-CSF but not RANKL. However, MDA-MB-231 cells were unable to support osteclast formation or survival in the absence of M-CSF and/or RANKL in BM derived macrophage cultures. This suggests that tumour derived M-CSF is not sufficient to support osteoclast formation and survival in my model. On the other hand, both RANK and C-FMS were expressed by the MDA-MB-231 cells. Moreover, MDA-MB-231 cells were found to produce conditioned medium that significantly further enhanced osteoclast formation when pre-incubated with RANKL and M-CSF. Finally, a range of osteoclastic factors were shown to be produced by MDA-MB-231 cells, suggesting any effects are likely to be due to a combination of effects from multiple factors, and of these IGF-1 and its receptor was chosen for further investigation to test our models.

Chapter 6

The effects of the novel kinase inhibitor of IGF-1 receptor PQIP on bone cell differentiation and activity *in vitro*

6.1 Summary

IGF-1 is the most abundant growth factor in the bone microenvironment and is known to be involved in the regulation of both bone formation and resorption. In Chapter 5 it was shown that the MDA-MB-231 tumour cells that enhanced osteoclast formation and function expressed IGF-1. Due to this and the fact that I had access to a novel inhibitor of IGF-1 receptor, called PQIP, I decided to test the effect of IGF-1 receptor inhibition on bone cell differentiation and activity *in vitro* prior to studying its effects on tumour cell – bone cell cross talk.

The relative expression levels of IGF-1 and its receptor in the different bone cell types was investigated using qPCR. It was found that osteoblasts expressed the highest levels of IGF-1 receptor while osteoclasts and macrophages produced more of the IGF-1 ligand. This is in agreement with the hypothesis that IGF-1 can act as an autocrine/paracrine regulator in the bone microenvironment. Western blot analysis established that IGF-1 induced signalling through the PI3K/Akt pathway in osteoblasts and osteoclasts but not in BM osteoclast precursors. PQIP treatment prevented this IGF-1 induced effect in all cell types studied.

In osteoblasts, IGF-1 treatment increased cell function, migration and RANKL production. No effects on either cell viability or differentiation were observed. Pre-treatment with PQIP reduced both IGF-1 induced and basal levels of bone nodule formation, osteoblast differentiation, cell migration and RANKL production, again without affecting cell viability.

Studies in osteoclasts and BM osteoclast precursor cells showed that PQIP inhibited basal and IGF-1 induced increases in early osteoclast formation, but that neither IGF-1 nor PQIP treatment effected mature osteoclast survival until micromolar concentration caused toxic effects. Potential direct effects of PQIP on RANKL or M-CSF signalling were eliminated as western blot analysis showed that it failed to inhibit signalling induced by either ligand.

Overall, this chapter showed that IGF-1 signalling plays an important role in the regulation of both osteoblasts and osteoclasts, as well as the interactions between the two cell types through the regulation of RANKL production. PQIP treatment was effective at

suppressing both osteoblast and osteoclast activity, suggesting it may be of use as a treatment for the excess bone turnover associated with diseases such as bone metastasis.

6.2 Introduction

IGF-1 is a polypeptide systemic hormone with 40-50% sequence homology to insulin (470-472). It binds to a tetrameric transmembrane receptor tyrosine kinase, IGF-1R, which has high homology to insulin receptor (IR) particularly in the β subunit (473). IGF-1R is widely expressed in human tissues including bone and various common tumours including breast sarcoma (471, 474). It is activated by IGF-1, IGF-2, and to a lesser extent by insulin (474). The binding of these ligands to the IGF-1R results in activation of its kinase domain leading to the initiation of various intracellular signalling pathways including the PI3K/Akt, JAK/STAT and MAPKinase pathways (474, 475).

IGF-1 is known to play a vital role in the regulation of bone remodelling in health and in disease (Reviewed in (287)). It is the most abundant growth factor in the bone microenvironment (273) and has been shown to regulate various aspects of both osteoblast (287-290) and osteoclast (291-293) growth, differentiation and function *in vitro* and *in vivo*. Specifically, IGF-1 is known to induce Osx expression in osteoblasts, enhancing osteoblast differentiation, migration and function *in vitro* (287-289, 476), while genetic inactivation of IGF-1 receptors in osteoblasts *in vivo* leads to suppressed bone formation and reduced bone mass. This was due not to a reduced number of osteoblasts, but due to a lack of mineralisation as the osteoblasts are unable to properly mineralise the bone matrix (290, 477), suggesting that IGF-1 plays an important role in osteoblast differentiation and function (290). Other studies show that IGF-1 also stimulates osteoclast formation and bone resorption (291-293). IGF-1 null mice have increased trabecular bone density and connectivity. This is partly due to a direct inhibition of osteoclastagenesis in the absence of IGF-1 and partly an indirect effect due to severely reduced RANKL expression in osteoblasts (293, 478, 479). In addition, genetic inactivation of IGF-1 or its receptor prevents ovariectomy induced bone loss through the inhibition of osteoclast formation and function (294).

In recent years there has also been increasing interest in the role of IGF-1 in tumour development and metastases (277, 471, 475, 480, 481). These findings have encouraged the development of therapeutic agents for the treatment of various cancers based on targeting the IGF-1R. One such agent is PQIP (cis-3-[3-(4-methyl-piperazin-l-yl)-cyclobutyl]-1-(2-phenyl-quinolin-7-yl)-imidazol[1,5-a]pyrazin-8-ylamine), a selective novel small

molecule inhibitor of the human IGF-1R, and to a far lesser extent the insulin receptor, which shows minimal activity against a wide panel of other protein kinases (482, 483). PQIP inhibits tumour proliferation and induces apoptosis in a variety of colon, breast and pancreatic tumour cells *in vitro*, and showed significant *in vivo* efficacy in tumour xenografts, in particular against tumours whose progression is dependent on an IGF/IGF-1R autocrine loop (483).

6.3 Aim

The aim of this chapter was to test the effects of the IGF-1 receptor kinase inhibitor PQIP on bone cell differentiation, survival and activity *in vitro*.

6.4 Results

6.4.1 IGF-1 receptors are highly expressed in osteoblasts

Quantitative PCR was used to determine the relative IGF-1R mRNA expression in macrophages, osteoclasts, and osteoblasts. As shown in Figure 6.1 A, osteoblasts express the highest level of IGF-1R, 10-fold higher than both osteoclasts and M-CSF dependent osteoclast precursors ($p < 0.05$). Expression of IGF-1 itself was also detected in all three bone cell types; with the highest mRNA level observed in M-CSF dependent osteoclast precursor cells (Figure 6.1 B). Osteoclasts expressed IGF-1 at a level 2-fold lower than M-CSF dependent osteoclast precursors and osteoblasts at a level 3-fold lower than those of osteoclasts (Figure 6.1 B).

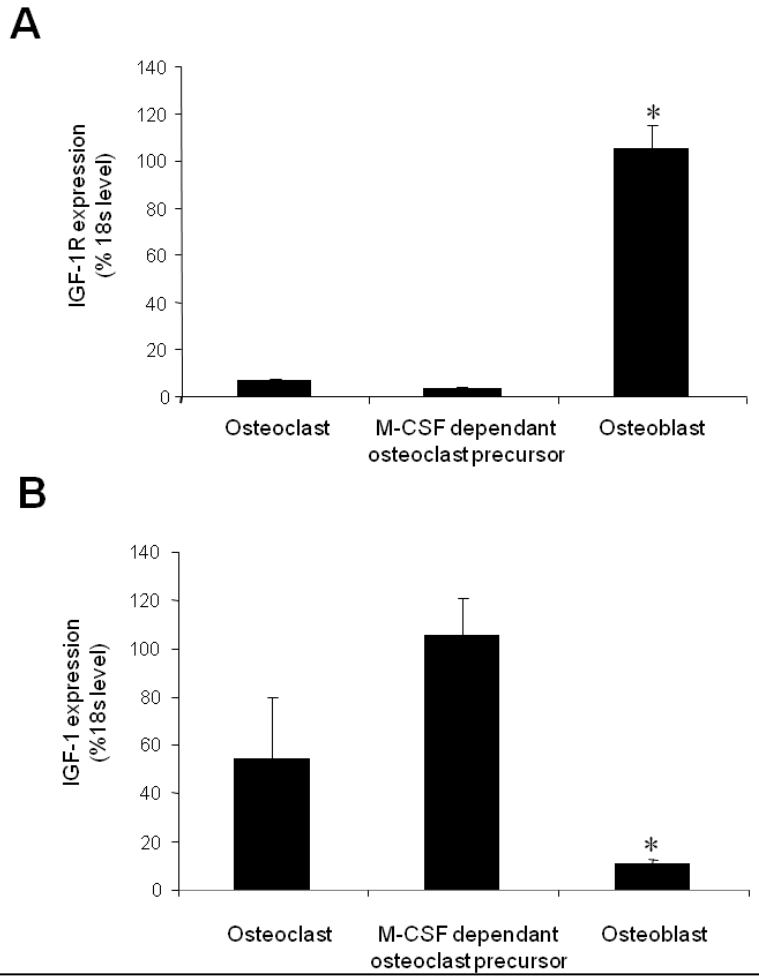

Figure 6.1 IGF-1 receptor is highly expressed in osteoblasts Panels A and B show the expression of IGF-1 (panel B) and its receptor IGF-1R (panel A) in bone cells as measured by quantitative rt-PCR followed by qPCR. Transcript numbers are corrected for expression of 18s RNA. Values in the graphs are mean ± SD and are obtained from three independent experiments. * $p < 0.05$ from M-CSF dependent osteoclast pre-cursors and osteoclasts.

6.4.2 Effects of pharmacological inhibition of IGF-1R kinase activity on osteoblastogenesis *in vitro*

6.4.2.1 The IGF-1 receptor kinase inhibitor PQIP inhibits osteoblast differentiation and bone nodule formation without affecting cell viability

As osteoblasts expressed the highest amount of IGF-1R mRNA we first investigated the effects of IGF-1 and the IGF-1R specific inhibitor PQIP on various properties of primary calvarial osteoblasts. Osteoblast viability, differentiation and bone nodule formation were assessed by AlamarBlue, alkaline phosphatase and alazarin red assays, respectively. Figure 6.2 shows that after 21 days of continuous treatment neither IGF-1 nor PQIP had any significant effect on primary calvarial osteoblast viability. The images in Figure 6.2A and C clearly demonstrate that both IGF-1 and PQIP effected bone nodule formation in a dose-dependent manner; IGF-1 increasing mineralisation and PQIP significantly reducing it. Unfortunately mistakes in the destaining and alkaline phosphatase assays mean quantative data on osteoblast formation and differentiation was not obtained from this experiment.

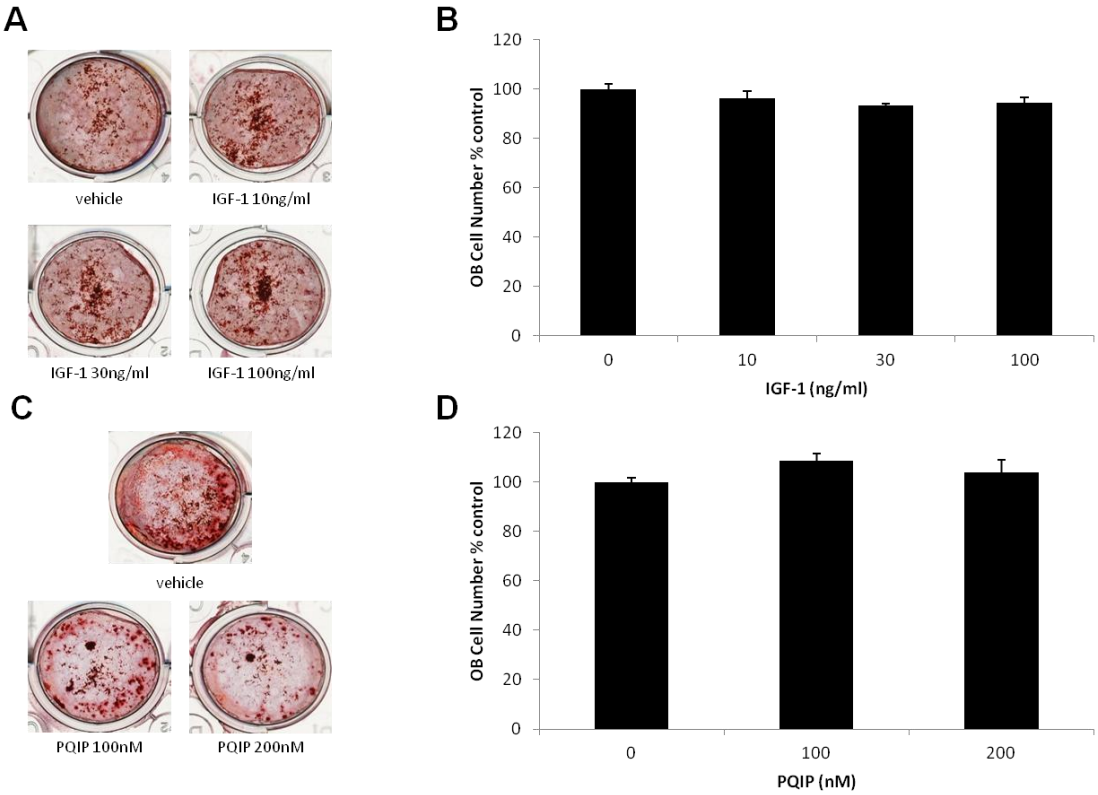

Figure 6.2 The IGF-1 receptor kinase inhibitor PQIP inhibits osteoblast function without affecting long-term cell viability in calvarial osteoblast cultures. Mouse calvarial osteoblasts were cultured in osteogenic medium containing 3 mM β-glycerol phosphate and 50 ng/ml L-ascorbic acid for 21 days in the presence and absence of IGF-1 (0-100 ng/ml) or PQIP (0-200 nM). Representative photomicrographs from cultures are shown in panels A and C. Cell number was measured by AlamarBlue assay and is shown in graphs B (IGF-1) and D (PQIP). Values in the graphs are mean ± SD and are obtained from three independent experiments.

To measure the effects of PQIP on IGF-1 induced osteoblast differentiation and bone nodule formation, bone nodule cultures were repeated. In these experiments osteoblasts were either untreated, or treated with IGF-1 100 ng/ml, PQIP 200 nM or both. Figure 6.3B shows that again after 21 days there was no significant change in osteoblast viability with any treatment. Destaining of the alazarin red demonstrated that IGF-1 caused a 25% increase in bone nodule formation ($p < 0.05$) after 21 days of continuous treatment. PQIP reduced mineralisation to 60% of vehicle in both the presence and absence of IGF-1 treatment ($p < 0.05$). As a measure of osteoblast differentiation, alkaline phosphatase activity was measured in all cultures. PQIP reduced alkaline phosphatase activity by 55% in both IGF-1 treated and untreated cultures ($p < 0.05$), while IGF-1 itself had no significant effect at the concentration found to be stimulatory to osteoblast function.

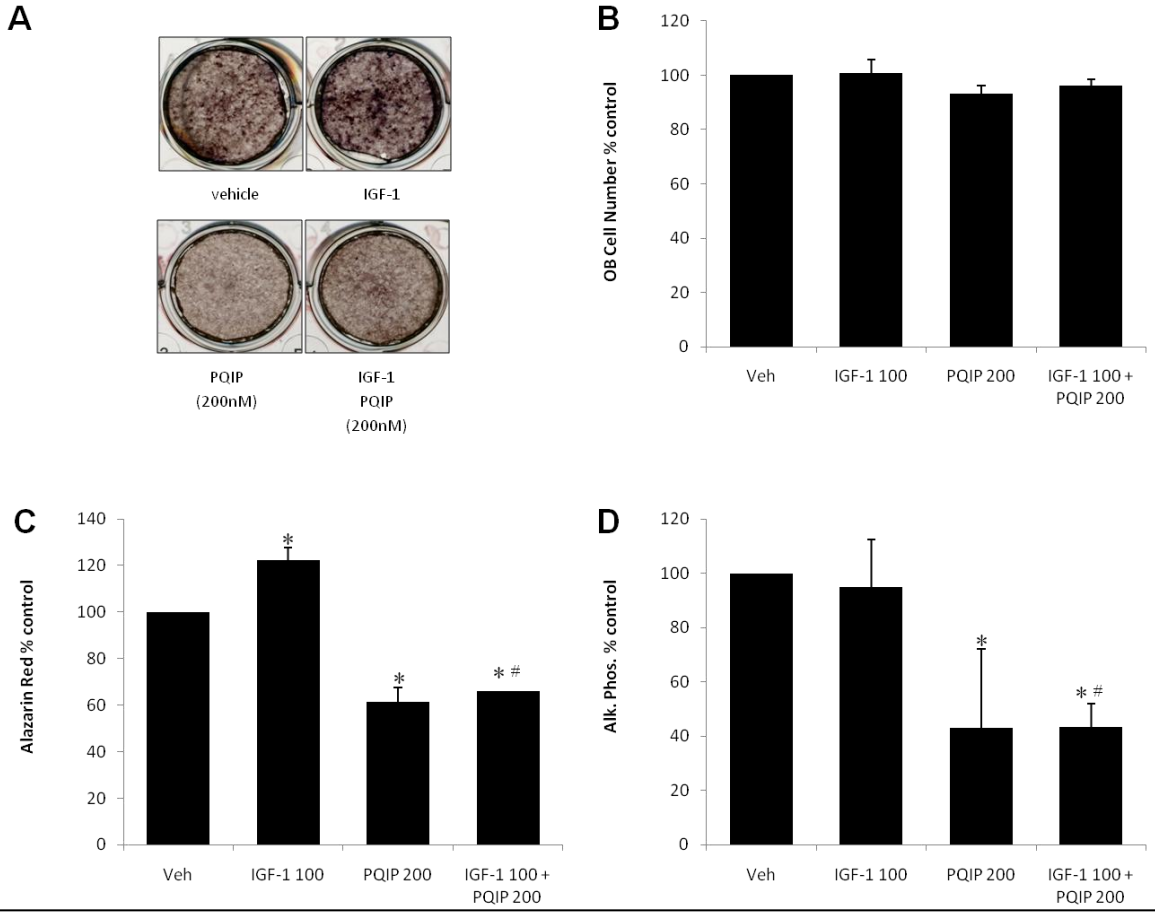

Figure 6.3 The IGF-1 receptor kinase inhibitor PQIP inhibits IGF-1 induced osteoblast differentiation and function without affecting long-term cell viability in calvarial osteoblast cultures. Mouse calvarial osteoblasts were cultured in osteogenic medium containing 3mM b-glycerol phosphate and 50ng/ml L-ascorbic acid for 21 days in vehicle (0.1% DMSO) or IGF-1 (100ng/ml) in the presence or absence of PQIP (100-200nM). Quantitation of nodule formation and osteoblast differentiation were carried out using Alazarin red (C) and alkaline phosphatase (D) assays respectively, and corrected for cell number as measured by AlamarBlue assay (B). Representative photomicrographs from cultures are shown in panels A. Values in the graphs are mean ± SD and are obtained from three independent experiments. * $p < 0.05$ from vehicle treated cultures, # $p < 0.05$ from IGF-1 treated cultures.

6.4.2.2 The IGF-1 receptor kinase inhibitor PQIP suppresses IGF-1 induced AKT activation in primary osteoblasts

IGF-1 is known to activate PI3K/Akt signalling in a variety of cell types including osteoblasts (484). Here, the effect of IGF-1 and PQIP treatment on the phosphorylation state of AKT was investigated by western blot. Figure 6.4 shows that IGF-1 (100 ng/ml) strongly induced AKT phosphorylation at serine 437 (Ser_{437}) and threonine 308 (Thr_{308}), indicative of PI3K/AKT activation. Treatment of osteoblasts with PQIP (50 – 500 nM) for 1 hour prior to stimulation with IGF-1 (100 ng/ml) caused a significant and dose-dependent inhibition of AKT phosphorylation at both phosphorylation sites, abolishing all AKT activation at 200 nM.

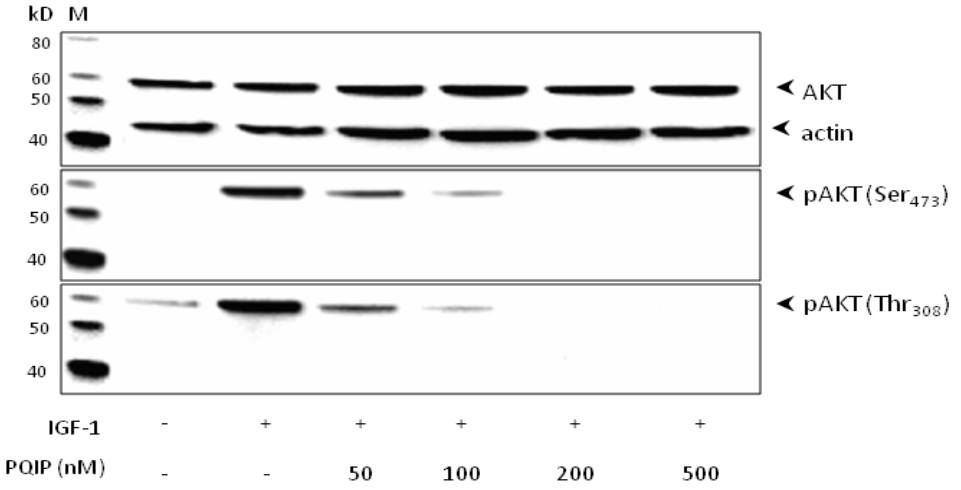

Figure 6.4 IGF-1 receptor kinase inhibitor PQIP prevents AKT activation in osteoblasts. Mouse calvarial osteoblasts were exposed to vehicle (0.1% DMSO) or PQIP (50 – 500 nM) prepared in serum free αMEM media for 1 hour prior stimulation with IGF-1 (100 ng/ml) for 15 minutes. Total cellular protein was subjected to western blot analysis (50µg/lane) using rabbit anti-phospho-AKT (Ser473), anti-phospho-AKT (Thr308), anti-AKT (Cell Signalling Biotechnology, USA) or anti-actin antibodies (Sigma-Aldrich, UK). Identical experiments have been repeated three times. Abbreviations: M – molecular weight marker; kD - kilo Dalton; p – phosphorylated.

6.4.2.3 The IGF-1 receptor kinase inhibitor PQIP suppresses IGF-1 induced osteoblast migration

Recent studies have shown that IGF-1 acts as a chemotactic agent for osteoblasts and so stimulating osteoblast migration, which is essential for their recruitment to sites of bone formation (289). Here I used wound assays to study the effects of IGF-1 and PQIP on the migration of the osteoblast-like mouse cell line MC3T3-E1. Figure 6.5 shows that treatment with IGF-1 (100 ng/ml) resulted in a modest yet significant increase in the speed of wound closure when compared to vehicle (15%; $p < 0.01$). In contrast, PQIP (200 nM) significantly inhibited both basal and IGF-1 induced migration of MC3T3-E1 cells by 11% ($p < 0.05$) and 14% ($p < 0.05$), respectively. Interestingly, though wound healing progressed faster in IGF-1 treated cultures, gaps were left in their healed wounds and cells appeared to lack the organisation of the vehicle and PQIP treated cultures. Instead cells continued to move rapidly in a disorganised fashion after the wound had healed; PQIP inhibited this effect. Figure 6.5 C shows that neither IGF-1 nor PQIP had a significant effect on MC3T3-E1 viability after 20 hours at concentrations inhibitory to cell migration.

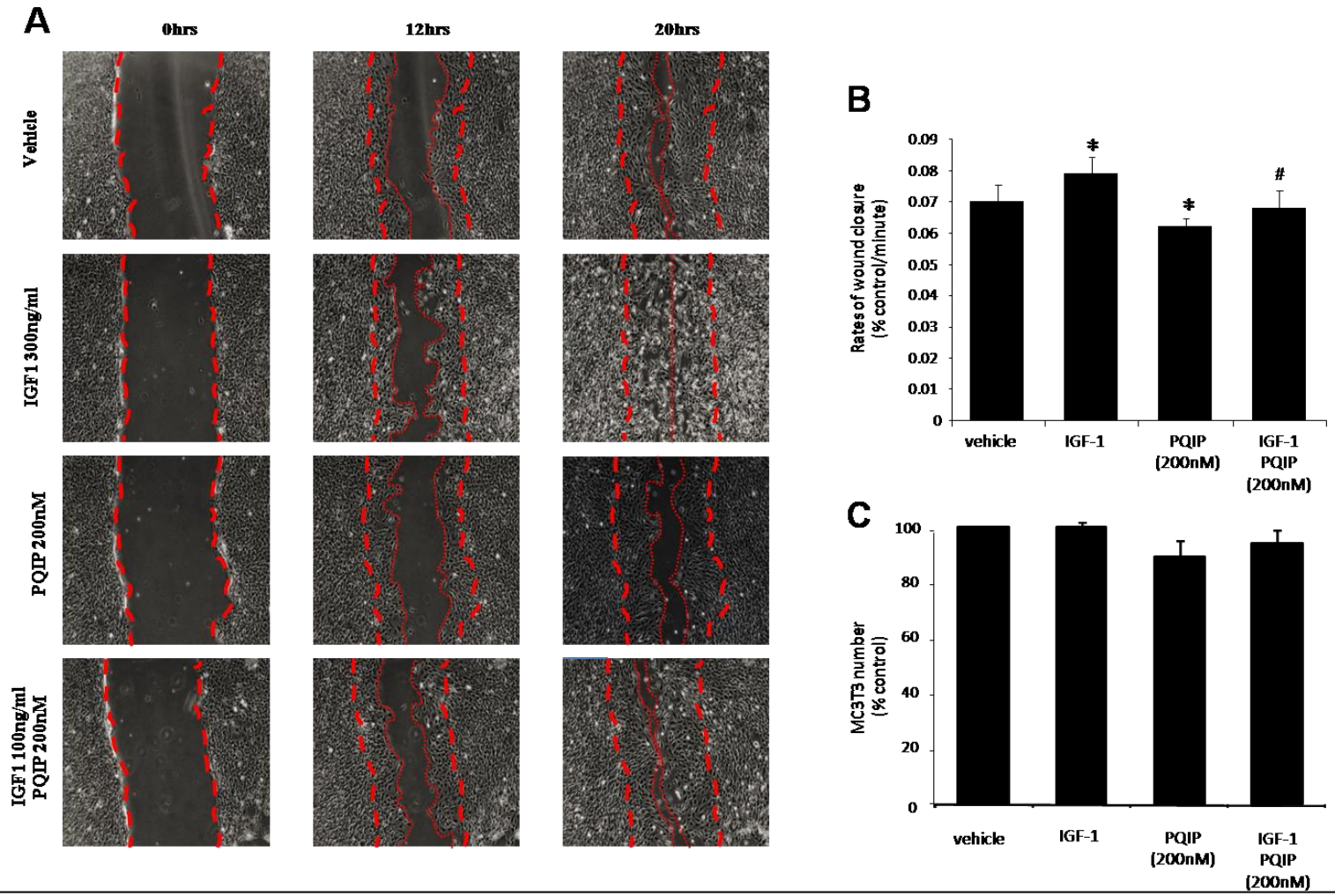

Figure 6.5 The IGF-1 receptor kinase inhibitor PQIP inhibits IGF-1 induced MC3T3 migration without affecting long-term cell viability in calvarial osteoblast cultures. Panels A and B show the effect of PQIP on basal and IGF-1 induced migration of the osteoblast-like cells MC3T3-E1. MC3T3-E1 were exposed to vehicle (0.1% DMSO) or PQIP (200 nM) prepared in standard αMEM media for 1 hour prior stimulation with vehicle (0.1% BSA) or IGF-1 (100 ng/ml) for 20 hours. Representative photomicrographs from cultures are shown in panel A. MC3T3-E1 migration was assessed by wound healing assay and rates of wound closure were calculated using ScanR microscope and Tscratch image analysis program as described in materials and methods, the results are shown in panel B. Cell number was measured by AlamarBlue assay (C). Values in the graphs are mean ± SD and are obtained from three independent experiments. *= $p < 0.05$ from vehicle treated cultures, #= $p < 0.05$ from IGF-1 treated cultures.

6.4.2.4 The IGF-1 receptor kinase inhibitor PQIP inhibits IGF-1-induced RANKL production in osteoblasts

Chapter 3 demonstrated that MDA-MB-231 conditioned medium increased the osteoblast production of the key osteoclastic factor RANKL. qPCR was used to determine the effect of IGF-1 and PQIP on this process. Figure 6.6 shows that IGF-1 (100 ng/ml) caused a significant increase in RANKL mRNA expression (19%), whereas PQIP strongly inhibited both basal and IGF-1 induced RANKL expression in osteoblasts, reducing it to less than 20% of the expression seen in untreated cells ($p < 0.05$). This suggests that IGF-1R kinase inhibition inhibits osteoblast support for osteoclast formation.

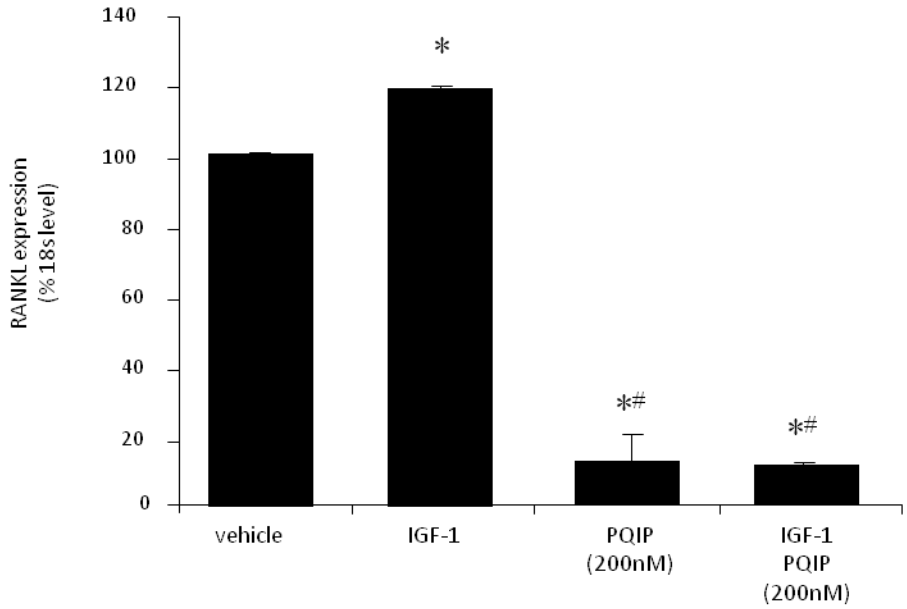

Figure 6.6 IGF-1 receptor kinase inhibitor PQIP prevents basal and IGF-1 induced RANKL expression in osteoblasts. Calvarial osteoblast cultures treated with vehicle (0.1% DMSO) or PQIP (200 nM) for 1 hour prior to stimulation with vehicle (0.1% BSA) or IGF-1 (100 ng/ml) for 16 hours. The mRNA expression of RANKL was measured by quantitative rt-PCR followed by qPCR and is displayed in the graph. Transcript numbers are corrected for expression of 18s RNA. Values in the graphs are mean ± SD and are obtained from three independent experiments. *= $p < 0.05$ from vehicle treated cultures, #= $p < 0.05$ from IGF-1 treated cultures.

6.4.3 Effects of pharmacological inhibition of IGF-1R kinase activity on osteoclastogenesis *in vitro*

6.4.3.1 The IGF-1 receptor kinase inhibitor PQIP inhibits IGF-1 induced osteoclast formation

As mature osteoclasts and their precursors were found to express IGF-1 receptors, we studied the effects of the IGF-1 receptor kinase inhibitor PQIP on IGF-1-induced osteoclast formation in RANKL and M-CSF generated osteoclast cultures. M-CSF generated macrophages were cultured in 96 well plates in the presence of M-CSF and RANKL and allowed them to grow for 24 hours. Cells were then treated with IGF-1 (50-100 ng/ml), PQIP (100-200 nM), or both for 72 hours. Figure 6.7 shows that IGF-1 increased osteoclast number in a dose dependent manner but only at 100 ng/ml was this significant (31% increase, $p<0.01$). Similarly, PQIP dose dependently inhibited osteoclast formation, but only at 200 nM was it statistically significant (40% reduction, $p<0.01$). The increase in osteoclast number caused by IGF-1 was completely prevented by PQIP, reducing the osteoclast number to similar values to those seen with PQIP treatment alone, 85% and 65% of vehicle for 100 nM and 200 nM respectively.

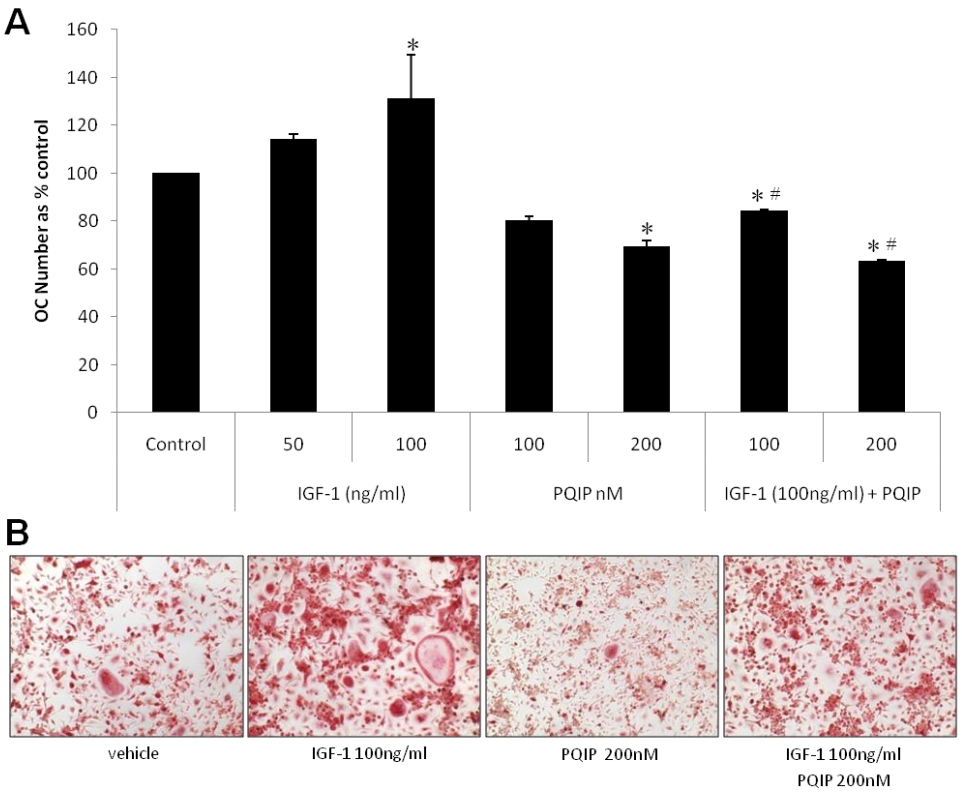

Figure 6.7 The IGF-1 receptor kinase inhibitor PQIP inhibits IGF-1 induced osteoclast formation. Mouse bone marrow cells were cultured in the presence of M-CSF (100 ng/ml) for 3 days and then exposed to RANKL (100 ng/ml) and M-CSF (25 ng/ml) for 72 hours in the presence or absence vehicle (0.1% DMSO), IGF-1 (100 ng/ml) and/or PQIP (200 nM). Osteoclast numbers were assessed by counting multinucleated TRAcP positive cells with three or more nuclei. Osteoclast numbers are shown in panels A and representative photomicrographs from the cultures in panels B. Values in the graph are mean ± SD and are obtained from three independent experiments. *=$p < 0.05$ from vehicle treated cultures, #=p<0.05 from IGF-1 100 ng/ml treatment.

6.4.3.2 The IGF-1 receptor kinase inhibitor PQIP inhibits osteoclast survival at micromolar concentrations

Here, we studied the effects of IGF-1 and the IGF-1 receptor kinase inhibitor PQIP on osteoclast survival in RANKL and M-CSF generated osteoclast cultures. This was achieved by treating cultures of M-CSF generated macrophage with M-CSF (25 ng/ml) and RANKL (100 ng/ml) for 96 hours prior to a further 48 hours treatment with the addition of IGF-1 (0-300 ng/ml) or PQIP (0-5000 nM). Figure 6.8 shows that treatment with IGF-1 had no significant effect on osteoclast survival, though there was a dose dependent trend peaking at 100 ng/ml IGF-1 treatment (22% increase). Interestedly, the IGF-1 receptor kinase inhibitor PQIP did inhibit osteoclast survival but only at a concentration of 5000 nM (27% reduction, $p < 0.05$).

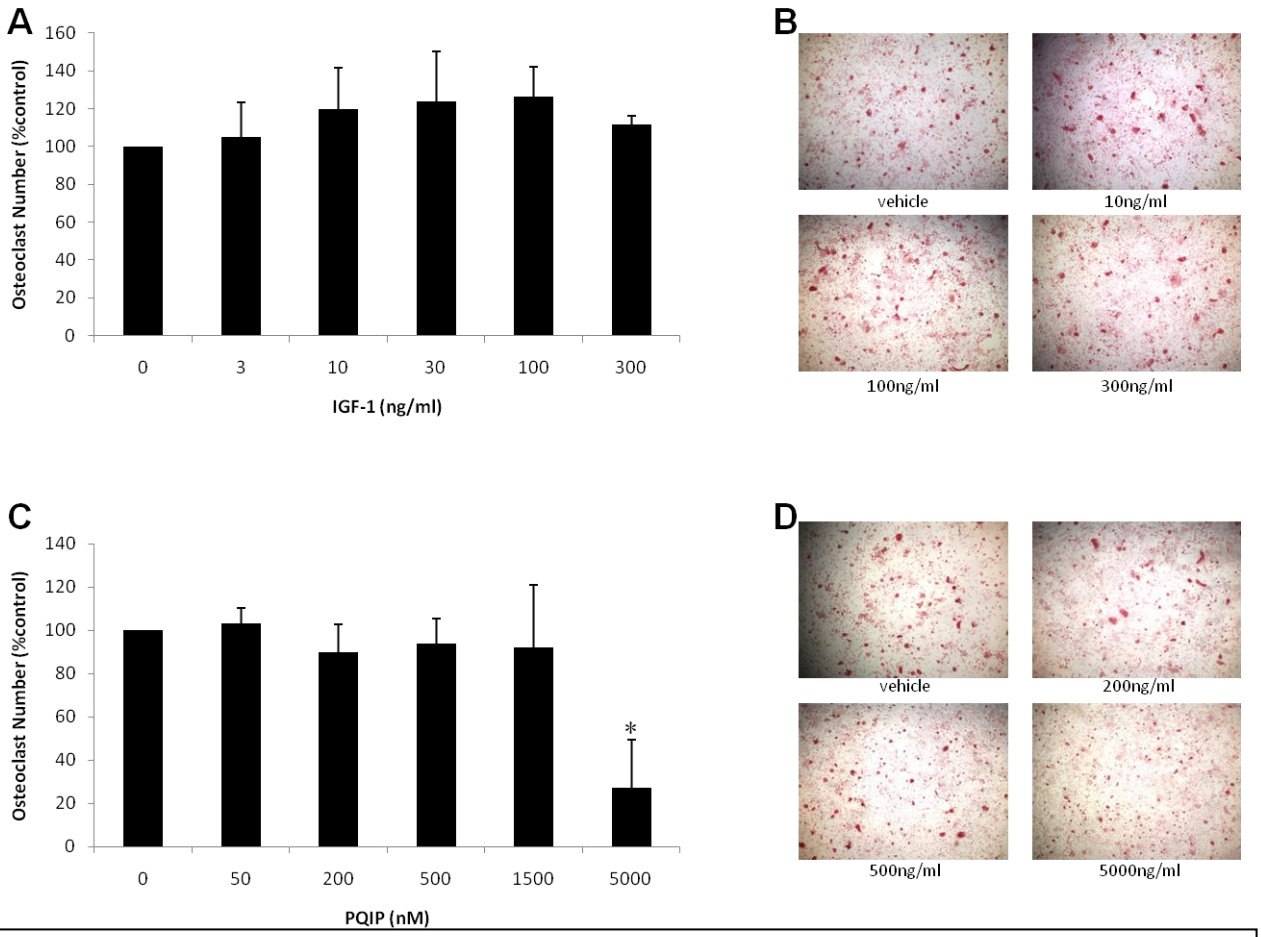

Figure 6.8 The IGF-1 receptor kinase inhibitor PQIP inhibits IGF-1 induced osteoclast survival. Mouse bone marrow cells were cultured in the presence of M-CSF (100 ng/ml) for 3 days and then exposed to RANKL (100 ng/ml) and M-CSF (25 ng/ml) for 96 hours prior to 48 hours additional treatment with RANKL (100 ng/ml) and M-CSF (25 ng/ml) in the presence or absence of IGF-1 (0-300 ng/ml) or PQIP (0-5000 nM). Osteoclast numbers were assessed by counting multinucleated TRAcP positive cells with three or more nuclei. Osteoclast numbers are shown in panels A and C and representative photomicrographs from the cultures are shown in panels B and D. Values in the graphs are mean ± SD and are obtained from three independent experiments. *=$p < 0.05$ from vehicle treated cultures

6.4.3.3 The IGF-1 receptor kinase inhibitor PQIP prevents PI3K/AKT activation in osteoclasts

Western blot was used to investigate the signaling mechanisms by which the IGF-1 receptor kinase inhibitor PQIP repressed IGF-1-induced osteoclast formation. The effect of PQIP on PI3K/AKT activation in osteoclasts was investigated. As shown in Figure 6.9, PQIP (50 – 500 nM) caused a significant and dose-dependent inhibition of both basal and IGF-1 induced AKT phosphorylation in osteoclast cultures at the serine site. No activation of the threonine site by IGF-1 was found.

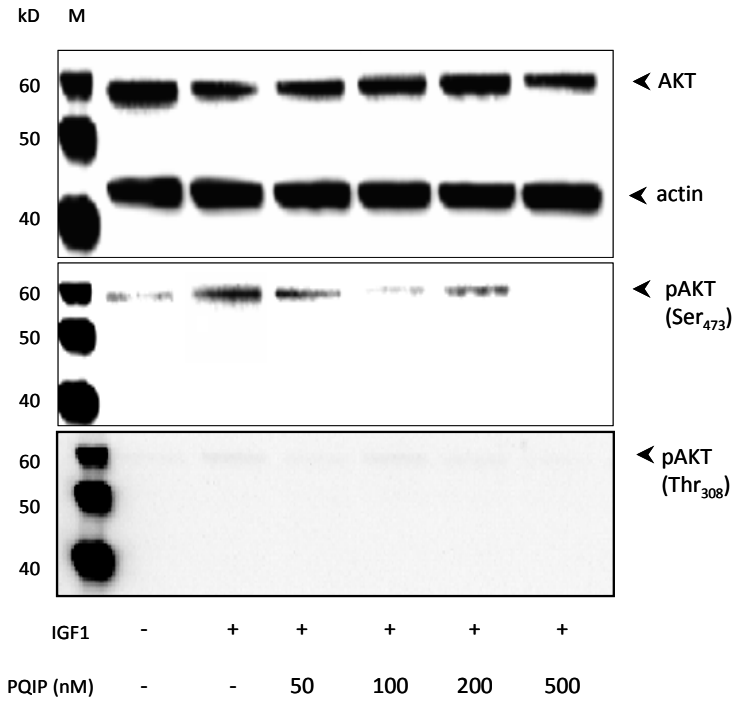

Figure 6.9 The IGF-1 receptor kinase inhibitor PQIP prevents IGF-1 induced AKT activation in osteoclasts. Mouse osteoclasts were treated with a range of PQIP concentrations (50 – 500 nM) for 1 hour prior to stimulation with IGF-1 (100 ng/ml) for 15 minutes. Total cellular protein was subjected to western blot analysis using anti-phospho-AKT (Thr_{308}), anti-phospho-AKT (Ser_{473}), anti-AKT antibodies or anti-actin antibodies. Abbreviations: M – molecular weight marker; kD - kilo Dalton; p – phosphorylated. Identical experiments were repeated on three separate occasions.

6.4.3.3 The IGF-1 receptor kinase inhibitor PQIP had no effects on RANKL and M-CSF-induced signalling in osteoclasts

Western blot was used to eliminate the possibility that the IGF-1 receptor kinase inhibitor PQIP might have direct inhibitory effects on RANKL and M-CSF signalling in osteoclasts. As shown in Figure 6.10, PQIP did not inhibit RANKL induced IκB phosphorylation or M-CSF induced ERK1/2 phosphorylation in osteoclasts even at concentrations up to 500 nM. This indicates that at the concentrations that PQIP inhibited osteoclast formation, this compound did not interfere with signalling induced by the two key osteogenic factors.

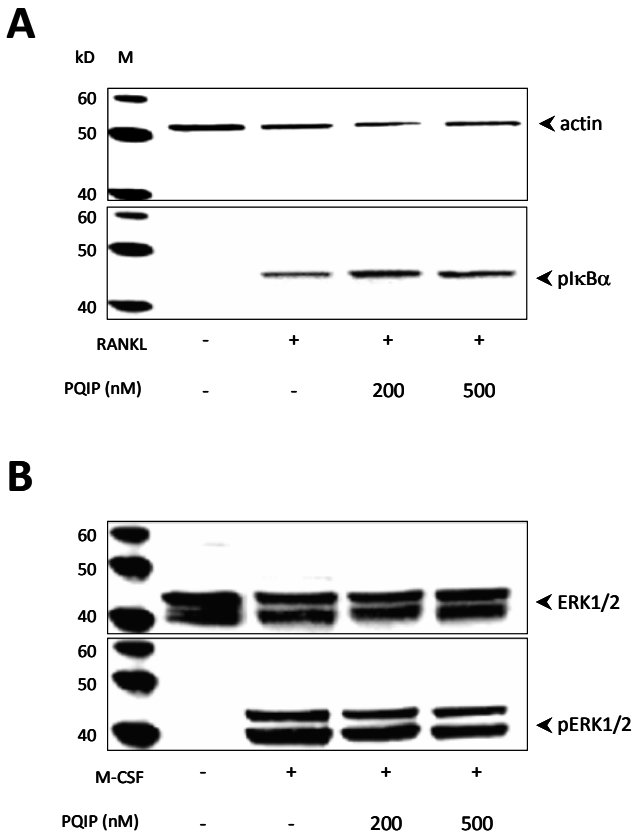

Figure 6.10 The IGF-1 receptor kinase inhibitor PQIP does not affect M-CSF induce ERK activation or RANKL induced IκB activation. Mouse osteoclasts were treated with a range of PQIP concentrations (200 and 500 nM) for 1 hour prior to stimulation with either RANKL (100 ng/ml; top panel) or M-CSF (25 ng/ml; bottom panel) for 5 minutes. Total cellular protein was subjected to western blot analysis using anti-phospho-IκBα and and anti-actin antibodies (A) or anti-phospho-ERK1/2 and anti-ERK1/2 antibodies (B). Abbreviations: M – molecular weight marker; kD - kilo Dalton; p – phosphorylated. Identical experiments were repeated on three separate occasions.

6.4.4 Effects of pharmacological inhibition of IGF-1R kinase activity on osteoclast precursor viability and growth *in vitro*

6.4.4.1 The IGF-1 receptor kinase inhibitor PQIP had no effects on the viability of M-CSF-generated BM macrophages

To determine if the inhibitory effect of PQIP on osteoclastogenesis were due to a non-specific toxic effect of the compound on the viability of precursor cells, we examined the effects of IGF-1 and PQIP on the growth of M-CSF-dependent osteoclast precursors using the AlamarBlue assay. As shown in Figure 6.11 neither IGF-1 (100 ng/ml) nor PQIP (200 nM) showed any significant effects on macrophage cell viability, though IGF-1 treatment did cause a modest (5%) but non-significant increase in cell number (Figure 6.11).

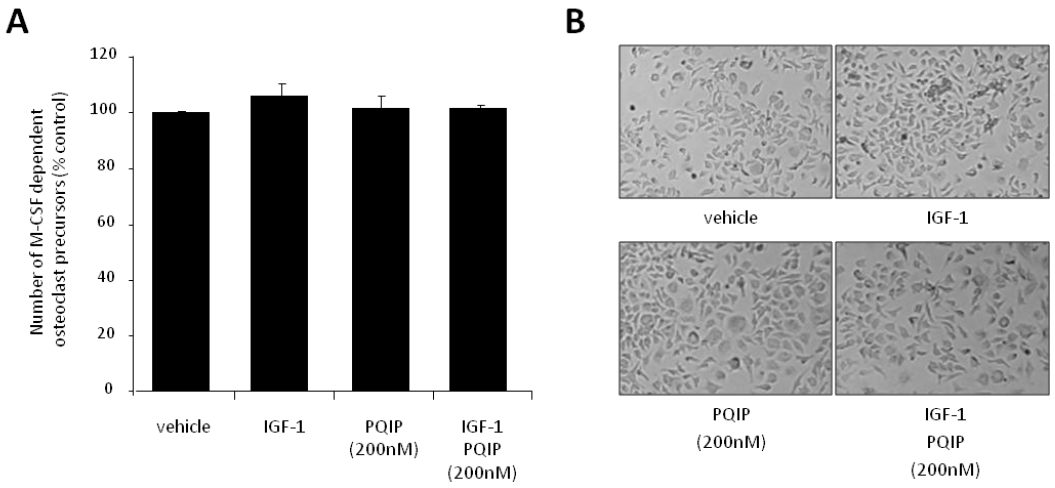

Figure 6.11 PQIP has no significant effect on M-CSF dependent osteoclast precursor viability at concentrations inhibitory to osteoclast formation. A, B, mouse bone marrow cells were cultured in the presence of M-CSF (25 ng/ml) for 3 days and then exposed to vehicle (0.1% DMSO) or IGF-1 (100 ng/ml) in the presence and absence of PQIP (200 nM). The number of M-CSF dependent osteoclast precursors was assessed by AlamarBlue assay (A). Values are mean ± S.D. and are obtained from three independent experiments. Representative photomicrographs from the cultures are shown (B).

6.4.4.2 The IGF-1 receptor kinase inhibitor PQIP prevents PI3K/AKT activation in M-CSF-generated BM macrophages

Western blot was used to investigate whether the IGF-1 receptor kinase inhibitor PQIP affect IGF-1-induced signaling in M-CSF-generated BM macrophages. As shown in Figure 6.12, IGF-1 caused only minimal, if any, activation of AKT at the serine phosphorylation site. PQIP (50 – 500 nM) caused a significant and dose-dependent inhibition of both basal and IGF-1 induced AKT phosphorylation in M-CSF-generated BM macrophage cultures at the serine site. No activation of the threonine site by IGF-1 was found.

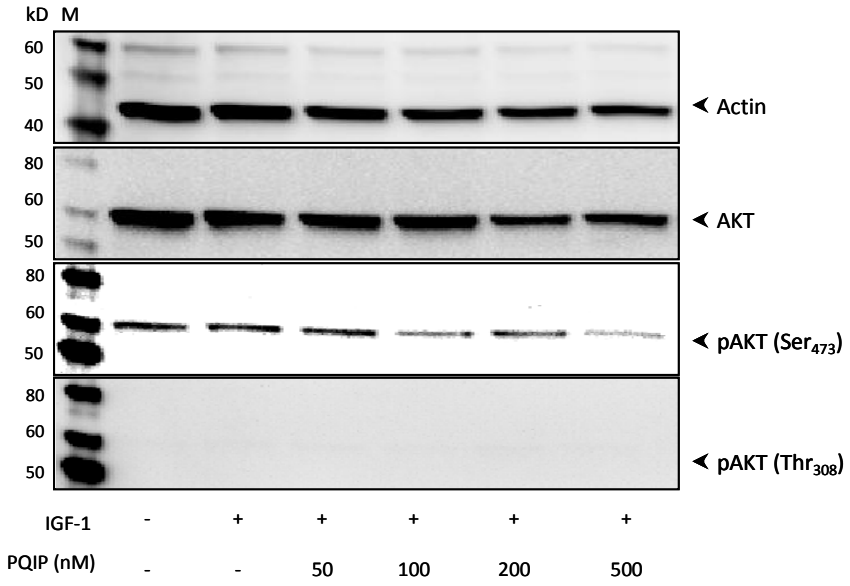

Figure 6.12 The IGF-1 receptor kinase inhibitor PQIP prevents PI3K/AKT activation in M-CSF-generated BM macrophages. M-CSF dependent osteoclast precursors treated with a range of PQIP concentrations (50 - 500 nM) for 1 hour prior to stimulation with IGF-1 (100ng/ml) for 15 minutes. Total cellular protein was subjected to western blot analysis using anti-phospho-AKT (Ser_{473}), anti-phospho-AKT (Thr_{308}) anti-AKT, and anti-Actin antibodies. Abbreviations: M – molecular weight marker; kD - kilo Dalton; p – phosphorylated. Identical experiments have been repeated three times.

6.4.4.3 The IGF-1 receptor kinase inhibitor PQIP has no effects on M-CSF-induced signalling in M-CSF-generated BM macrophages

Western blot was used to determine if the IGF-1 receptor kinase inhibitor PQIP would directly affect M-CSF-induced signaling in M-CSF-generated BM macrophages. As shown in Figure 6.13, M-CSF activated both PI3K/AKT and ERK1/2 MAPkinase in M-CSF-generated BM macrophage and these effects were unaffected by PQIP at all concentrations tested.

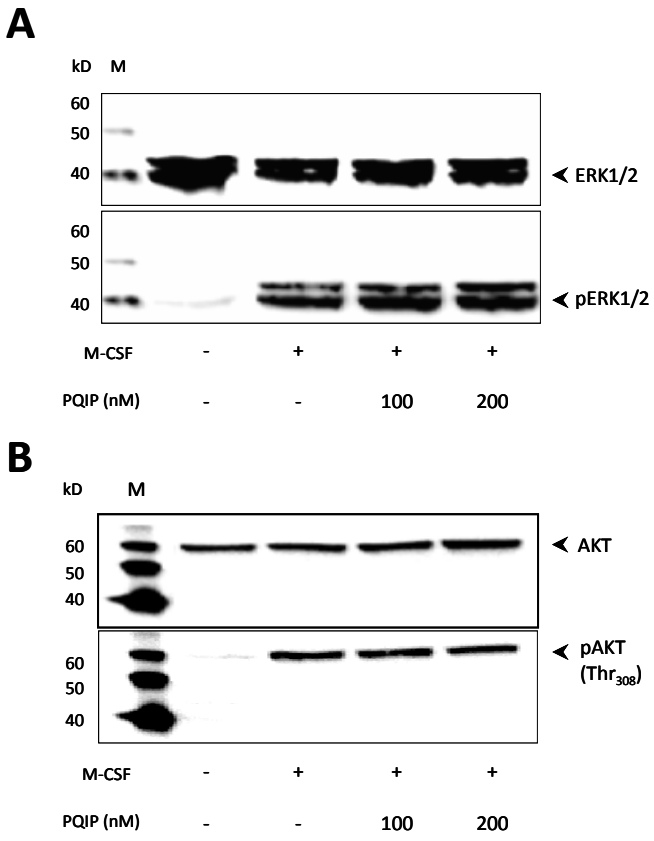

Figure 6.13 The IGF-1 receptor inhibitor PQIP does not inhibit M-CSF induced signalling in M-CSF dependent osteoclast precursors. Panel A and B show M-CSF dependent osteoclast precursors treated with a range of PQIP concentrations (100 and 200 nM) for 1 hour prior to stimulation with M-CSF (25 ng/ml) for 5 minutes. Total cellular protein was subjected to western blot analysis using anti-phospho-ERK1/2, anti-phospho-AKT (Ser_{473}), anti-phospho-AKT (Thr_{308}) anti-ERK1/2, anti-AKT, and anti-Actin antibodies. Abbreviations: M – molecular weight marker; kD - kilo Dalton; p – phosphorylated. Identical experiments have been repeated three times.

6.5 Discussion

The Insulin-like growth factor/insulin system of receptors and ligands are known to play a role in bone homeostasis. In particular, IGF-1 is the most abundant growth factor in the bone microenvironment (273) and is important for the differentiation and function of bone cells (287, 485). The balance between bone formation and resorption is tightly regulated and IGF-1 is thought to play an autocrine / paracrine role in these processes thereby affecting the actions of all bone cell types particularly cells of the osteoblast lineage (486, 487). In broad agreement with these findings, we found that IGF-1R mRNA expression was significantly higher in mature osteoblasts than in either osteoclasts or their M-CSF dependent precursors, while the reverse was true for IGF-1 mRNA expression. This is consistent with the notion that IGF-1 and its receptor play a role in osteoblast–osteoclast coupling. In particular IGF-1 is thought to regulate the expression of RANKL and OPG in osteoblasts which are key factors responsible for osteoclast formation, survival and function (488). In support of this, we demonstrated that the novel kinase inhibitor of IGF-1 receptor PQIP inhibits both basal and IGF-1 induced mRNA expression of RANKL by osteoblasts indicating that IGF-1R blockage is likely to affect osteoblast support for osteoclastogenesis.

IGF-1 is known to play a key role in osteoblast survival, differentiation and function and in particular is known to enhance the expression of Osx in osteoblasts (288, 290, 476). Here, we showed that PQIP was also able to directly inhibit both IGF-1 induced osteoblast differentiation and bone nodule formation. Interestingly, IGF-1 treatment had no effect on osteoblast differentiation in our cultures. This may have been due to the long term nature of the assay saturating osteoblast differentiation and that in reality, as previously shown, IGF-1 does have a direct stimulatory effect on osteoblast differentiation and function. Recent reports have showed that IGF-1 also stimulates osteoblast migration which is required for the recruitment of osteoblasts to sites of bone formation. Here we showed that treatment with PQIP suppressed basal and IGF-1 induced migration of MC3T3-E1 osteoblast like cells at concentrations inhibitory to bone nodule formation. Thus PQIP can directly affect osteoblast differentiation, migration and function. This raises the possibility that inhibition of IGF-1 signalling may also be effective in the prevention of enhanced osteoblast activity associated with bone metastases.

IGF-1 regulates PI3K/AKT signalling and in this study treatment with IGF-1 stimulated the phosphorylation of AKT in both osteoblasts and osteoclasts. In osteoblast cultures, IGF-1 induced signalling was completely abolished following PQIP treatment at concentrations that also inhibited bone nodule formation. Interestingly, PQIP had no effect on PTH induced ERK phosphorylation or BMP-2 induced SMAD-2 activation in osteoblasts (data not shown), indicating a specific effect on IGF-1 signalling.

Early treatment with PQIP at the start of osteoclast formation inhibited both IGF-1-induced and basal osteoclast formation in RANKL and M-CSF stimulated BM cultures. However, late treatment with either IGF-1 or PQIP had no effect on osteoclast number, with the exception of 5000 nM PQIP which reduced numbers but was most likely due to a non-specific toxic effect. This implies that inhibition of IGF-1R by PQIP directly inhibits osteoclast formation but probably does not affect survival. However, as the effect of IGF-1R inhibition on osteoclast survival was not directly studied here this cannot be stated as certain. Notably, early PQIP treatment also resulted in a significant reduction in osteoclast size, raising the possibility that IGF-1R inhibition also affects the fusion of osteoclast precursors but further work is required to confirm this. Inhibition of basal levels is likely to be due to the presence of IGF-1 in FCS media serum. Unfortunately all attempts to remove or replace serum in experiments resulted in the failure of osteoclast formation (data not shown).

As stated above, IGF-1 is known to regulate PI3K/AKT signalling. In this study IGF-1 stimulated the phosphorylation of AKT in all cell types studied with the exception of macrophages. In osteoblast cultures, IGF-1 induced signalling was completely reduced by PQIP in a dose-dependent manner and abolished following PQIP treatment at concentrations that also inhibited bone nodule formation. This provides a potential mechanism for these effects. PQIP also inhibited IGF-1 induced AKT phosphorylation in osteoclasts and importantly these effects were observed at concentrations similar to those that inhibited osteoclast formation and size. Recently it has been shown that TRAF6, the key adaptor molecule of RANK (489), is essential for AKT ubiquitination, membrane recruitment and phosphorylation (490). Activation of TRAF6 in osteoclasts plays an essential role in RANKL-mediated osteoclastogenesis (491). This suggests that AKT activation may be directly linked to the initiation of osteoclast differentiation through

RANK. Therefore the inhibition of AKT phosphorylation observed may provide a potential mechanism for the inhibition of osteoclast formation found following PQIP treatment. To exclude the involvement of RANKL and M-CSF signalling, we investigated the effects of PQIP on RANKL induced IκB phosphorylation and M-CSF induced ERK1/2 activation in osteoclasts. Our studies clearly showed that PQIP had no direct effect on either of these two key osteoclast signalling pathways. In keeping with this, PQIP also had no significant effect on cell viability of M-CSF generated osteoclast precursors, thereby excluding the possibility that PQIP's inhibitory effect was mediated by a decreased number of precursor cells. In these cells PQIP did not inhibit activation of either the PI3K/AKT or MAPkinase pathways by M-CSF, again demonstrating the specificity of its action. Taken together, our current findings are consistent with a model whereby PQIP inhibits osteoblast differentiation, function and migration, and can inhibit osteoclast formation directly by suppressing PI3K/AKT activity or indirectly by inhibiting IGF-1 induced RANKL expression by osteoblasts.

In conclusion, the studies performed here demonstrate that preventing IGF-1 signalling using the novel selective IGF-1R kinase inhibitor PQIP directly suppresses osteoblast and osteoclast differentiation, function and migration, and for the first time we have established that pharmacological inhibition of IGF-1R inhibits osteoblast support for osteoclastogenesis *in vitro*. Therefore, selective small molecule kinase inhibitors of IGF-1R such as PQIP and its analogue OSI-906, which is currently in advanced clinical development, may have clinical value in the reduction of excessive bone turnover associated with a number of bone diseases such as bone metastasis.

Chapter 7

The effects of the novel kinase inhibitor of IGF-1 receptor PQIP on breast cancer-induced bone cell activity *in vitro*

7.1 Summary

IGF-1 is the most abundant growth factor in the bone microenvironment and is known to be involved in both bone homeostasis and the development and progression of bone metastases associated with various cancers, particularly breast cancers. IGF-1 was expressed in MDA-MB-231 tumour cells in Chapter 5. Due to this and the fact that we had access to the novel inhibitor of IGF-1 receptor PQIP, we decided to test the effect of IGF-1R kinase inhibition on bone - tumour cell crosstalk using the various *in vitro* techniques developed in Chapter 3.

PQIP prevented IGF-1 induced AKT phosphorylation in human MDA-MB-231 breast cancer cells in a dose dependant manner, indicating a consistent inhibition of PI3K/AKT signalling. In contrast, effects of PQIP on breast cancer cell viability was varied; human MCF7 cells were sensitive to PQIP treatment, while MDA-MB-231 and 4T1 cell viability was unaffected.

PQIP treatment significantly exacerbated the inhibitory effect of MDA-MB-231 conditioned medium treatment on osteoblasts, leading to a marked reduction in osteoblast viability as well as differentiation and function. PQIP did however inhibit MDA-MB-231 induced increases in RANKL production in osteoblast cultures, indicating a significant inhibition of osteoblast support for osteoclastogenesis. In co-cultures and conditioned medium treatments of RANKL and M-CSF-stimulated BM cultures, PQIP was able to successfully inhibit tumour induced increases in osteoclast number, and particularly size. This was true for all tumour cell lines studied. Xcelligence analysis demonstrated that IGF-1 treatment of osteoclasts caused a similar change in cell index values to MDA-MB-231 conditioned medium, albeit with a lower increase in values. This suggests that IGF-1 plays a role in tumour cell induced effects on osteoclasts. PQIP inhibited both the IGF-1 and conditioned medium effects. Interestingly, PQIP inhibited MDA-MB-231 induced PI3K/AKT signalling in osteoblasts and osteoclasts, without affecting MDA-MB-231-induced ERK1/2 activation. This suggests that inhibition of tumour induced PI3K/AKT pathways downstream of IGF-1 may be responsible for the effects seen.

Overall, this chapter successfully demonstrated the effectiveness of the techniques devised in Chapter 3 for investigating the effects of therapeutic interventions on tumour

cell – bone cell cross-talk *in vitro*. Preventing IGF-1 signalling using the novel selective IGF-1R kinase inhibitor PQIP was found to suppress a variety of bone cell facets as well as interfering with tumour cell induced increases in osteoclast number and size. It is therefore, possible that PQIP, or more likely its analogue OSI-906, which is currently in advanced clinical development, may have clinical value in the treatment of osteolytic bone metastasis, though its effects on osteoblasts may make it more suitable for use in osteoblastic metastases.

7.2 Introduction

In addition to its role in bone remodelling, in recent years there has also been increasing interest in the role of IGF-1 in both tumour development and metastasis (277, 471, 475, 480, 481). Numerous studies have shown that IGF-1 stimulates proliferation, survival, transformation and invasiveness of tumour cells *in vitro* and *in vivo* (276, 277, 471, 475). The elevated expression of IGF-1 and its receptor has been detected in a variety of tumours (275) and the increased circulating levels of IGF-1 and IGF-1 binding protein 3 have been linked to increased risks of breast and prostate cancer development (276-279).

IGF-1 appears to be of particular importance in bone metastasis and subsequent osteolysis associated with breast cancer. Many studies have reported that a variety of breast cancer cell lines express IGF-1 and IGF-1R, and elevated activity of IGF-1 and its receptor has been detected in a variety of primary breast cancer cells, breast cancer cell lines and the plasma of breast cancer patients (492-494). Moreover IGF-1 has been linked to breast cancer metastasis and resistance to chemotherapy (495), and importantly cells with mutant IGF-1 receptors have reduced metastasis to and proliferation within the bone microenvironment (273, 496). Importantly, a bone seeking variant of MDA-MB-231 cells was shown to specifically migrate and proliferate in response to IGF-1 whilst MDA-MB-231 cells that metastasised to other locations did not, suggesting that IGF-1 signalling may be of particular importance in the development of bone metastases from breast cancers (497).

As stated in Chapter 6, the linking of IGF-1 and its receptor to the progression of various cancers, including breast cancer, has led to the development of several novel drugs that target IGF-1 or the IGF-1 receptor. One of these is the selective novel small molecule inhibitor of IGF-1R called PQIP (cis-3-[3-(4-methyl-piperazin-l-yl)-cyclobutyl]-1-(2-phenyl-quinolin-7-yl)-imidazol[1,5-a]pyrazin-8-ylamine) (482, 483). The inhibition of IGF-1R by PQIP has previously been shown to induces apoptosis and inhibit tumour growth and in a variety of breast, colon and pancreatic tumour cells *in vitro*, and *in vivo* (483). It is most effective in cells reliant on IGF/IGF-1R signaling for survival, and has proven effective enough for the analogue of PQIP called OSI-906 to reach stage 3 clinical trial for the treatment of adrenocortical carcinoma (498). The chapter presented here investigates the effect of PQIP on the cancer cells used previously in this thesis, and on their interactions with bone cells observed in Chapter 3.

7.3 Aim

The aim of this chapter was to test the effect of the novel IGF-1 receptor kinase inhibitor PQIP on breast cancer cell behaviour and cancer induced bone cell activity *in vitro*.

7.4 Results

7.4.1 Effects of pharmacological inhibition of IGF-1R kinase activity on breast cancer cell behaviour *in vitro*

7.4.1.1 The IGF-1 receptor kinase inhibitor PQIP suppresses adhesion and spreading of human and mouse breast cancer cells *in vitro*

The adhesion and spreading of human and mouse breast cancer cells were assessed by using the real-time cell analyser Xcelligence (Roche Applied Science, UK). Mouse and human breast cancer cells were plated into specialised 16-well plates (Roche Applied Science, UK) containing standard αMEM supplemented with IGF-1 (100 ng/ml) in the presence and absence of PQIP (200 nM). Figure 7.1 shows the graphs of cell impedance over the first 4 hours and analysis of the slopes of the graphs during the linear part of the initial increase in cell index. Changes in cell index during this period are thought to represent changes in cell adhesion and spreading. IGF-1 treatment did not significantly alter cell adhesion or spreading in any cell type studied. In contrast, PQIP treatment caused significant changes to the initial adhesion and spreading of both 4T1 and MCF7 cells. In 4T1 cells this change was not obvious in the cell-index graphs (Figure 7.1C), but analysis of the rate of change in cell index value shows that PQIP treatment significantly reduced the rate of cell index increase by 28% ($p<0.01$). This effect was particularly prominent at the earliest time-point, so likely represents a reduction in the initial adhesion of 4T1 cells. MCF7 cell adhesion and spreading was clearly inhibited by PQIP treatment. Figure 7.1F shows that while PQIP treatment alone did not significantly change the rate of increase in cell index values compared to vehicle treated cells, when cells were treated with both IGF-1 and PQIP the rate of increase was reduced to only 23% ($p<0.05$) of that observed in the vehicle treated cells. This was also significantly lower than in cultures treated with IGF-1 alone. PQIP treatment had no significant effects on the adhesion or spreading of MDA-MB-231 cells.

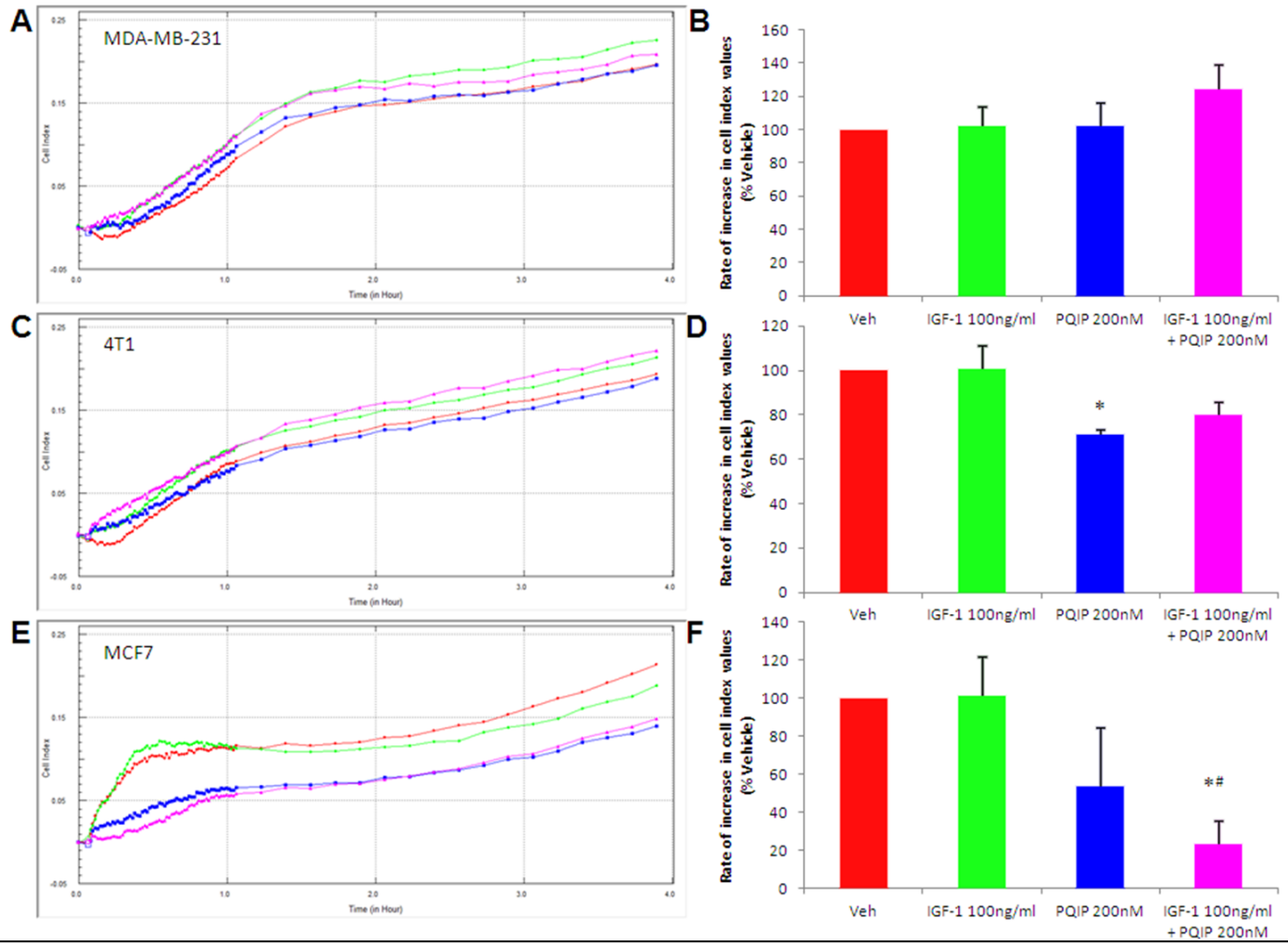

Figure 7.1 Xcelligence analysis demonstrates the short-term effects of IGF-1 and the IGF-1 receptor inhibitor on the adherence and spreading of various cancer cell lines. MDA-MB-231 (A,B), 4T1 (C,D), and MCF7 (E,F)) cells were seeded into xcelligence plates in the presence of vehicle (0.1% DMSO) or IGF-1 (100 ng/ml) in the presence or absence of PQIP (200 nM). A, C, and E shows a representative graph of the Cell index values (derived from their electrical impedance) over 4 hours. The treatments are represented as follows; Vehicle (RED), IGF-1 (GREEN), PQIP (BLUE), and IGF-1 and PQIP (PINK) B, D, and F show the average slope of the graphs at the initial linear portion of the graphs. N=4 experiments were performed. Values are mean ± S.D. and are obtained from three independent experiments. * $p < 0.05$ from vehicle treated cultures, # p<0.05 from IGF-1 100 ng/ml treated cultures

7.4.1.2 The IGF-1 receptor kinase inhibitor PQIP had no effects on the viability of human and mouse breast cancer cells

To determine if the inhibitory effect of PQIP on osteoclast formation in MDA-MB-231 – BM co-cultures was due to inhibition of the growth of breast cancer cells in these cultures, we examined the effects of IGF-1 and PQIP on the viability of MDA-MB-231. MDA-MB-231 cells were treated with IGF-1 (0-300 ng/ml) or PQIP (0-500 nM) for 48 or 72 hours, and cell viability measured by the AlamarBlue assay. Figure 7.2 shows that neither treatment had any significant effect on cell number, though following treatment with 100 ng/ml IGF-1 for 72 hours there was a modest but not significant increase in MDA-MB-231 growth.

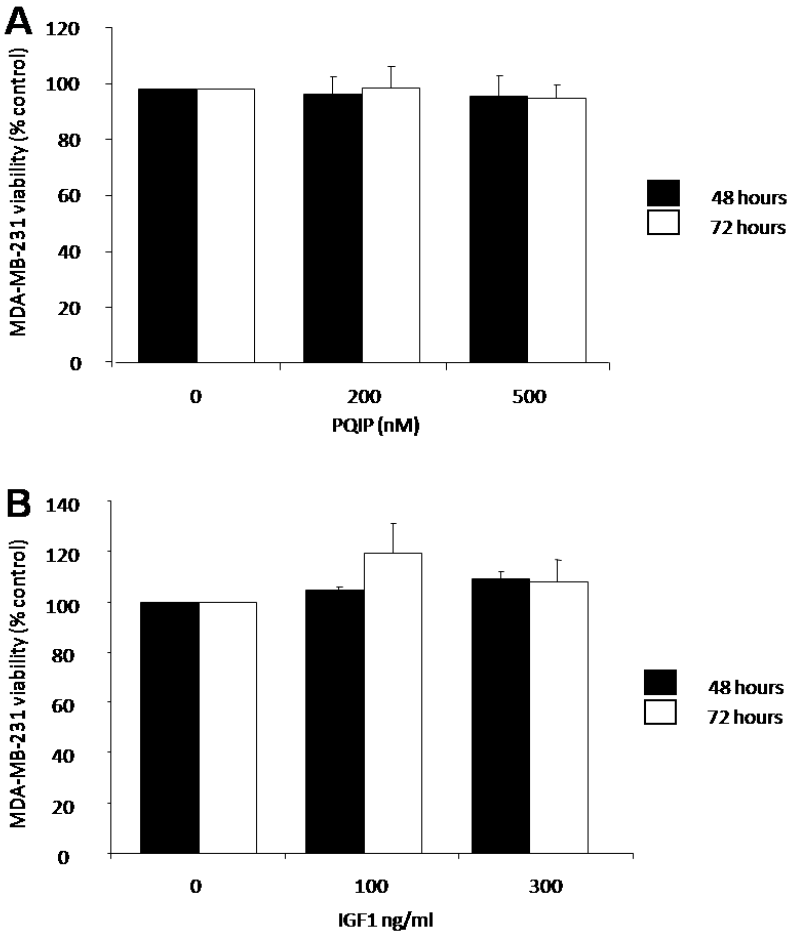

Figure 7.2 IGF-1 and the IGF-1 receptor inhibitor PQIP do not affect MDA-MB-231 human breast cancer cell viability. MDA-MB-231 cells were seeded and allowed to attach over night prior to treatment with a range of PQIP concentrations (200 and 500 nM)(A) or IGF-1 (100 and 300 ng/ml) (B) and cell number assessed by AlamarBlue after 48 and 72 hours. Values are mean ± S.D. and are obtained from three independent experiments.

The effect of PQIP on the viability of other osteolytic tumour cells used for co-culture experiments in Chapter 3 was tested. Mouse 4T1, mouse MC57G and human MCF7 cells were cultured in the presence or absence of PQIP (0-1500 nM) for 72 hours and cell viability measured by the AlamarBlue assay. Figure 7.3 shows that PQIP had no effect on the growth of mouse 4T1 and MC57G at concentrations up to 1500 nM. In contrast, treatment of MCF7 with PQIP reduced cell viability in a dose dependant manner. Even at the lowest concentrations of PQIP (200 nM) we observed a significant drop in viability of 33%. The highest concentration of 1500 nM caused reduction in cell numbers to increase to 45%.

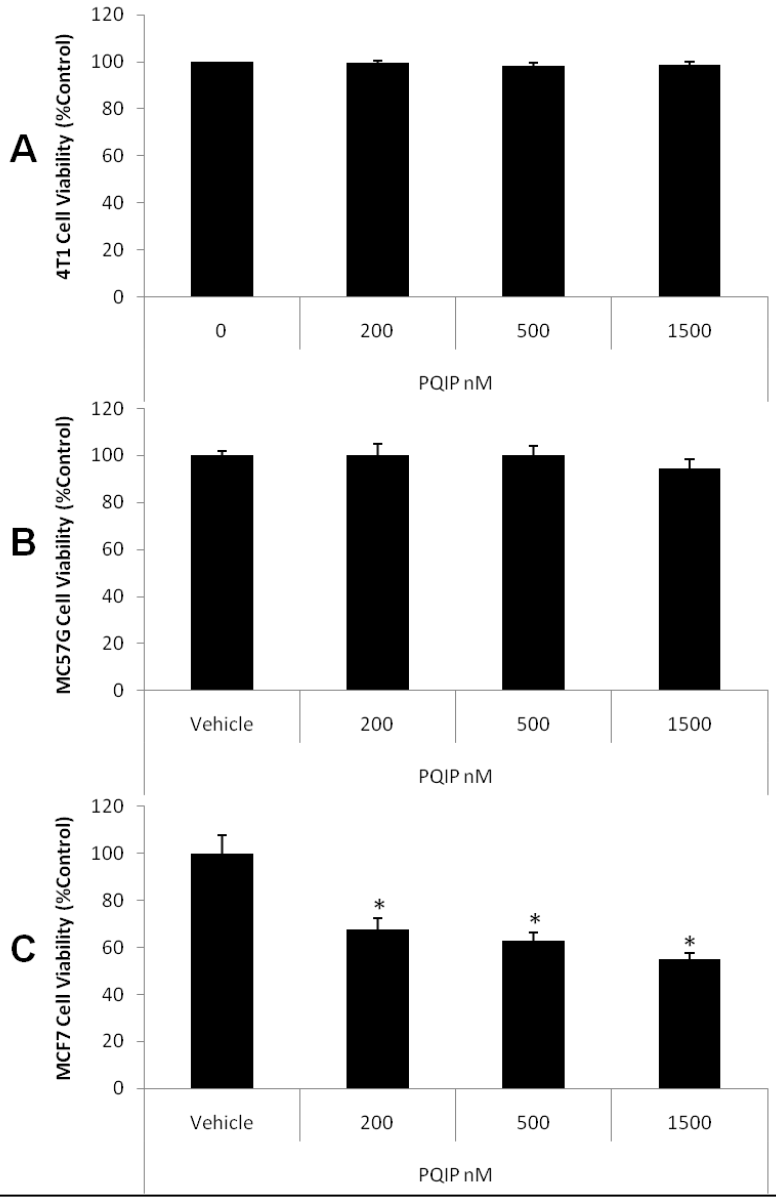

Figure 7.3 The IGF-1 receptor inhibitor PQIP did not affect 4T1 or MC57G mouse cancer cell viability, but does inhibit MCF7 human breast cancer cell viability. 4T1 (A), MC57G (B), or MCF7 (C) cells were seeded and allowed to attach over night prior to treatment with a range of PQIP concentrations (200 -1500 nM). Cell number was assessed by AlamarBlue after 72 hours. Values are mean ± S.D. and are obtained from three independent experiments. * $p < 0.05$ from vehicle treated cultures

The long term effects of PQIP on the proliferation of human and mouse breast cancer cells was also assessed by using the real-time cell analyser Xcelligence (Roche Applied Science, UK). Figure 7.4 shows graphs of the cell index values from cultures of human MDA-MB-231 and MCF7 cells or mouse 4T1 cells treated with IGF-1 (100 ng/ml), PQIP (200 nM) or both over a period of 48 hours. In this case the increases in cell index values represent the rates of cell proliferation. No significant effect on MDA-MB-231 or 4T1 cell proliferation was observed in these cultures, however both these cell types did have a trend of increased proliferation with IGF-1 treatment, and inhibition of this trend by PQIP treatment. Quantitive measurements of the graph slopes shown in Figure 7.4 B and D demonstrate that, in both MDA-MB-231 and 4T1 cell IGF-1 treatment had only minimal effect on proliferation and that this was not a statistically significant. In contrast, the proliferation rate of MCF7 cells was clearly affected by both IGF-1 and PQIP treatment. Measurement of the slopes shown in Figure 7.4E shows that IGF-1 treatment significantly increased cell proliferation by an average of 33% ($p<0.05$), while PQIP reduced proliferation rates of both vehicle and IGF-1 treated cultures respectively to 41% ($p<0.05$) and 29% ($p<0.01$) of vehicle only treated cells (Figure 7.4F).

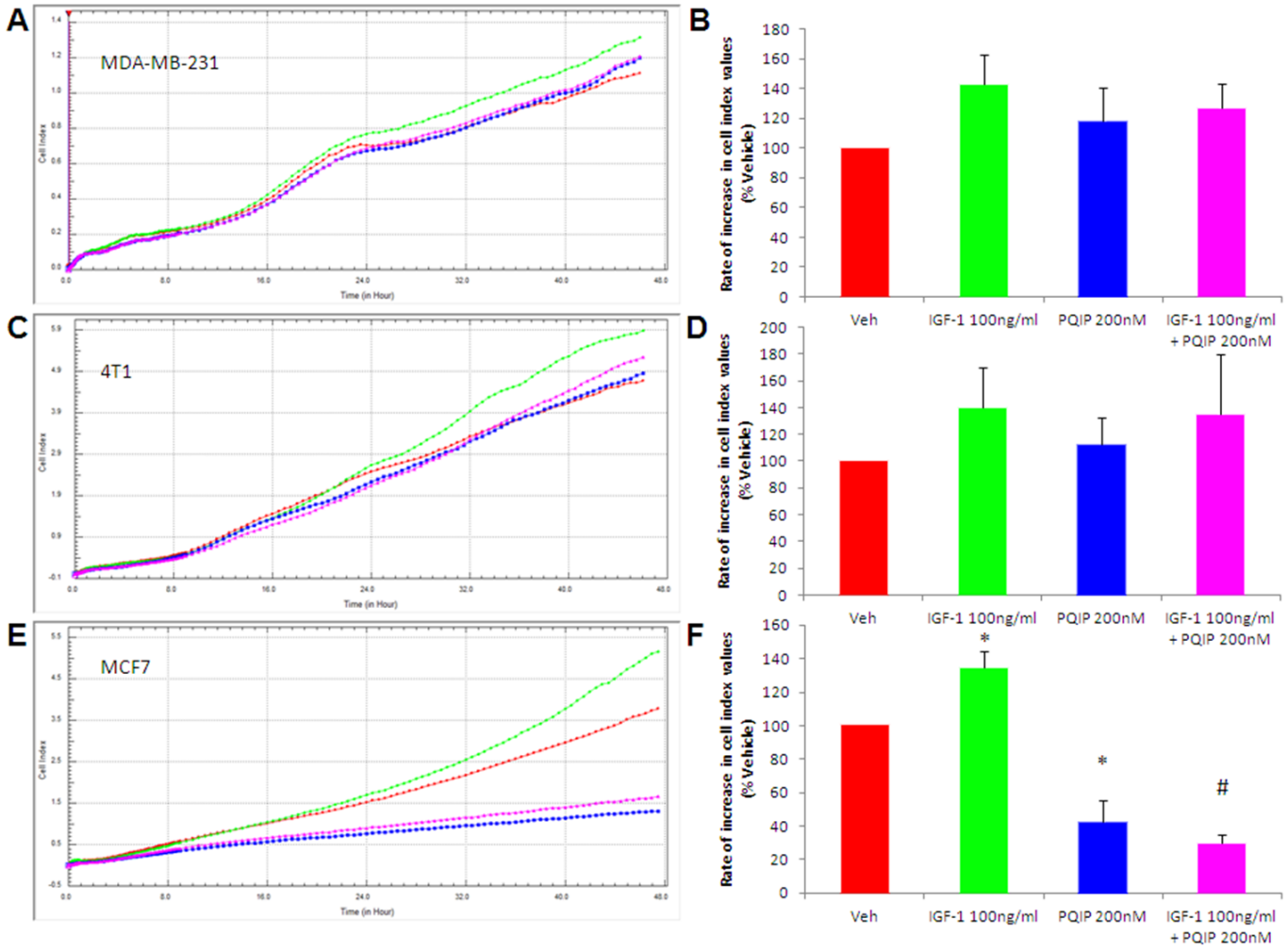

Figure 7.4 Xcelligence analysis demonstrates the long-term effects of IGF-1 and the IGF-1 receptor inhibitor on various cancer cell viabilities. MDA-MB-231 (A,B), 4T1 (C,D), MCF7 (E,F)), and MC3T3 (G,H)) cells were seeded into xcelligence plates in the presence of vehicle (0.1% DMSO) or IGF-1 (100ng/ml) in the presence or absence of PQIP (200nM). A, C, E and G shows a representative graph of the Cell index values (derived from their electrical impedance) over 48 hours. The treatments are represented as follows; Vehicle (**RED**), IGF-1 (**GREEN**), PQIP (**BLUE**), and IGF-1 and PQIP (**PINK**) B, D, F, and H are show the average slope of the graphs between hours 16 and 24. N=4 experiments were performed. Values are mean ± S.D. and are obtained from three independent experiments. * $p < 0.05$ from vehicle treated cultures, # $p<0.05$ from IGF-1 100ng/ml treated cultures

7.4.1.3 The IGF-1 receptor kinase inhibitor PQIP inhibits PI3K/AKT activation in human MDA-MB-231 breast cancer cells

Western blot was used to investigate whether the IGF-1 receptor kinase inhibitor PQIP affects IGF-1-induced signaling in human breast cancer cells. As shown in Figure 7.5, PQIP (50 – 500 nM) caused a significant and dose-dependent inhibition of both basal and IGF-1-induced AKT phosphorylation in human MDA-MB-231 breast cancer cells at both serine and threonine sites.

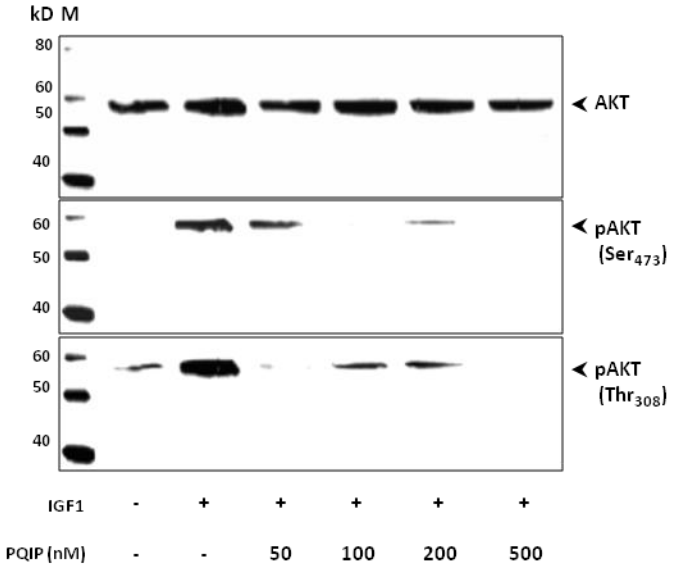

Figure 7.5 The IGF-1 receptor inhibitor PQIP inhibits IGF-1 induced AKT signalling in MDA-MB-231 human breast cancer cells. MDA-MB-231 cells were treated with a range of PQIP concentrations (50 – 500 nM) for 1 hour prior to stimulation with vehicle (0.1% BSA) or IGF-1 (100 ng/ml) for 15 minutes. Total cellular protein was subjected to western blot analysis using anti-phospho-AKT (Ser_{473}), anti-phospho-AKT (Thr_{308}) and anti-AKT antibodies. Abbreviations: M – molecular weight marker; kD - kilo Dalton; p – phosphorylated.

7.4.2 Effects of pharmacological inhibition of IGF-1R kinase activity on breast cancer-induced osteoblastogenesis *in vitro*

7.4.2.1 The IGF-1 receptor kinase inhibitor PQIP exacerbates the inhibitory effects of breast cancer cells on osteoblast differentiation and bone nodule formation *in vitro*

Chapter 3 demonstrated that MDA-MB-231 conditioned medium caused a reduction in osteoblast differentiation and function without affecting viability. Here we treated osteoblast bone nodule assays with 10% MDA-MB-231 conditioned medium in the presence or absence of the IGF-1 receptor inhibitor PQIP (200-500 nM). Figure 7.6 shows that MDA-MB-231 conditioned medium alone did not cause a significant reduction in viability, however when in combination with PQIP (200 nM), osteoblast numbers significantly fell by 15%. Treatment of calvarial osteoblast with MDA-MB-231 conditioned medium caused a significant reduction in bone nodule formation (42%, $p < 0.05$) and this effect appears to be significantly worse in the presence of PQIP (200 nM) (Figures 7.6A and D). However, while 200 nM PQIP treatment did cause a further drop in mineralisation, after alizarin red levels were adjusted for number of viable cells this was not significantly different from cultures treated with conditioned medium alone. Osteoblast differentiation levels were again assayed by measuring alkaline phosphatase activity in all cultures. PQIP treatment (200 nM) further increased the MDA-MB-231 induced reduction in differentiation from 37% to 53%, however after adjusting for cell viability these differences were not statistically significant.

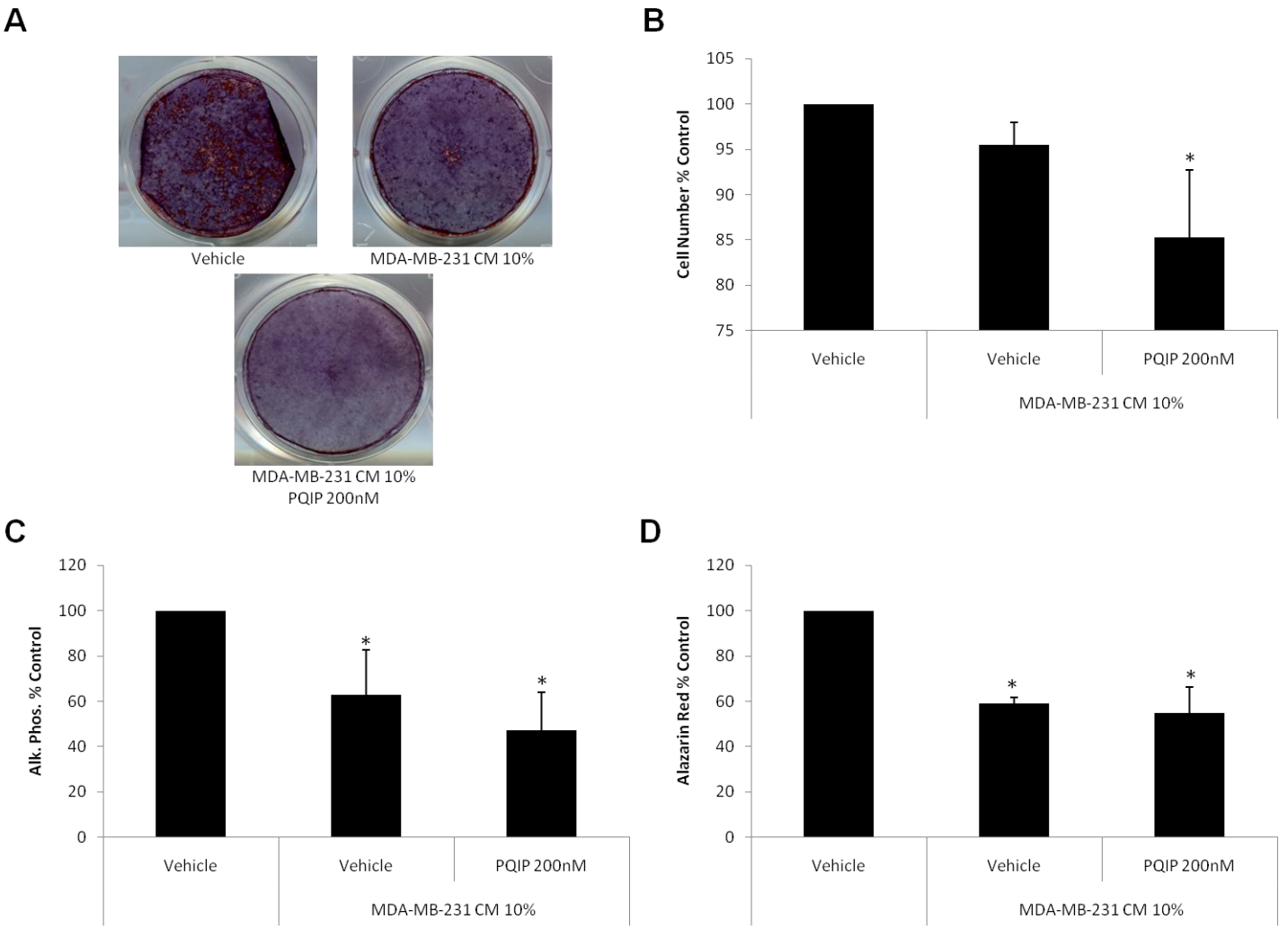

Figure 7.6 The IGF-1 receptor kinase inhibitor PQIP inhibits osteoblast viability, differentiation and function in the presence of MDA-MB-231 derived factors. Mouse calvarial osteoblasts were cultured in osteogenic medium containing 3 mM β-glycerol phosphate and 50 ng/ml L-ascorbic acid for 21 days in 10% control or MDA-MB-231 conditioned medium in the presence or absence of PQIP (100-200 nM). Quantitation of nodule formation and osteoblast differentiation were carried out using Alazarin red (D) and alkaline phosphatase (C) assays respectively, and corrected for cell number as measured by AlamarBlue assay (B). Representative photomicrographs from cultures are shown in panels A. Values in the graphs are mean ± SD and are obtained from three independent experiments. * $p < 0.05$ from vehicle treated cultures

7.4.2.2 The IGF-1 receptor kinase inhibitor PQIP prevents PI3K/AKT activation in mouse calvarial osteoblasts

Western blot was used to investigate whether the IGF-1 receptor kinase inhibitor PQIP affected MDA-MB-231-induced PI3K/AKT activation in osteoblasts. To allow comparison, IGF-1 induced activation was used as a positive control. Figure 7.7 shows that both IGF-1 (100 ng/ml) and MDA-MB-231 conditioned medium (10%) induced the phosphorylation of AKT. This activation was stronger following IGF-1 treatment, but both were clearly above the basal level seen in untreated cells. Pre-incubation with PQIP (200-500 nM) significantly inhibited IGF-1 induced activation. More importantly, PQIP prevented MDA-MB-231-induced AKT activation at both serine and threonine sites in osteoblasts. Pre-incubation with the specific PI3K inhibitor LY294002 (1µM) inhibited the activation of AKT by MDA-MB-231 conditioned medium, however this effect was not as strong as that observed with PQIP treatment.

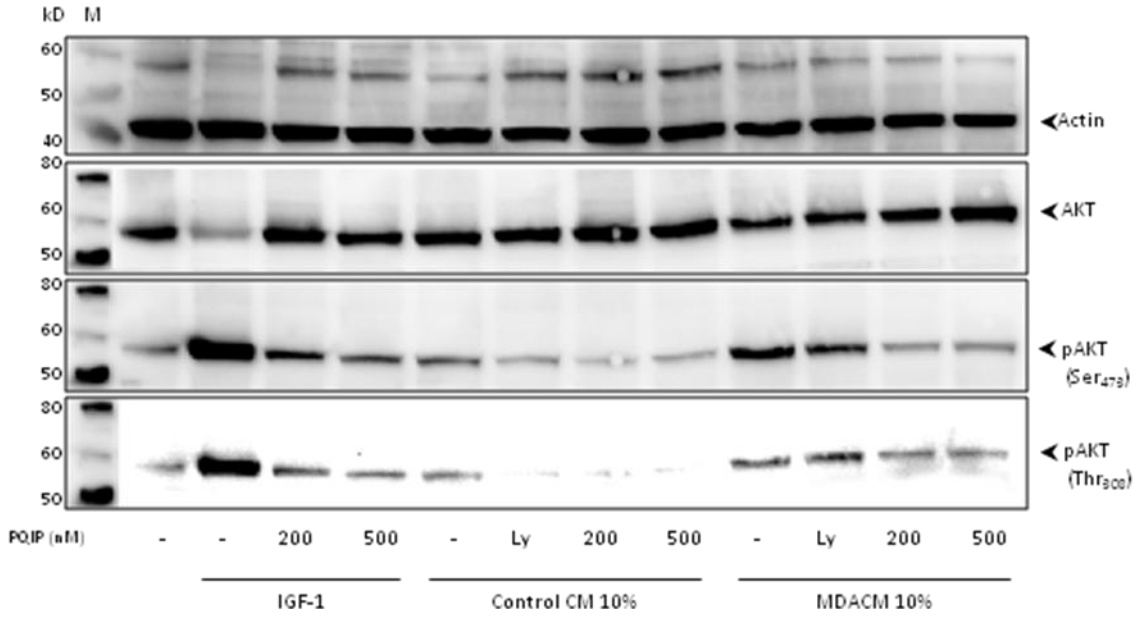

Figure 7.7 The IGF-1 receptor kinase inhibitor PQIP inhibits IGF-1 and MDA-MB-231 conditioned medium induced activation of AKT in calvarial osteoblasts. Mouse osteoblasts were treated with Ly294002 (1uM) or a range of PQIP concentrations (200 and 500 nM) for 1 hour prior stimulation with IGF-1 (100 ng/ml) for 15 minutes or MDA-MB-231 conditioned medium (10%) for 30 minutes. Total cellular protein was subjected to western blot analysis using anti-phospho-AKT ($Thr_{308,}$), anti-phospho-AKT (Ser_{473}), anti-AKT antibodies. Actin was used as a loading control. Abbreviations: M – molecular weight marker; kD - kilo Dalton; p – phosphorylated. Identical experiments were performed on 3 occasions

7.4.2.3 The IGF-1 receptor kinase inhibitor PQIP prevents upregulation of RANKL and OPG expression in mouse calvarial osteoblasts

Chapter 3 demonstrated that MDA-MB-231 conditioned medium increased osteoblast production of both RANKL and OPG. Here I performed qPCR to determine the effect of PQIP treatment (200-500 nM) on MDA-MB-231-induced RANKL/OPG ratio in osteoblasts. Figure 7.8 shows that as shown in Chapter 3, MDA-MB-231 conditioned medium increased the RANKL/OPG ratio (64.7% increase ±39%, $p<0.05$). PQIP treatment at 500 nM significantly reduced the MDA-MB-231 conditioned medium induced increase in RANKL/OPG ratio (28% reduction, $p<0.05$).

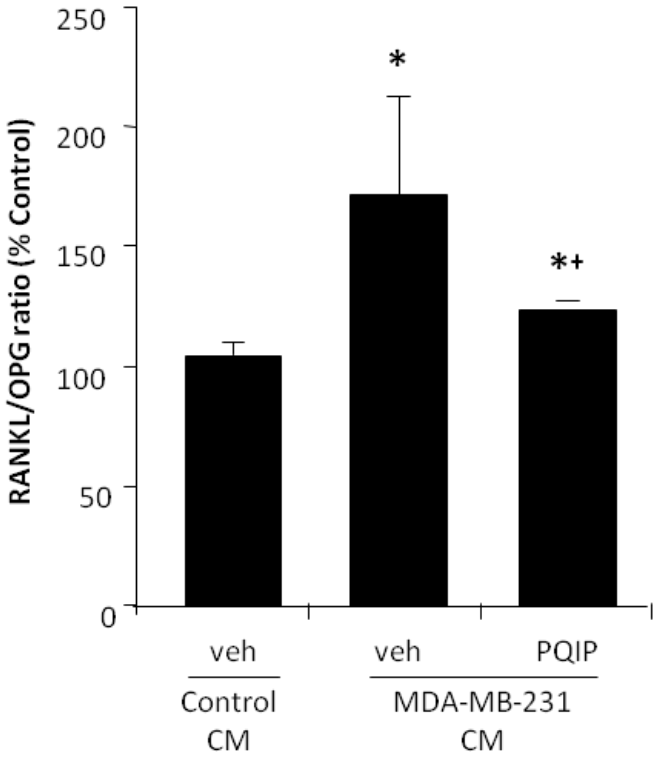

Figure 7.8 The IGF-1 receptor inhibitor PQIP inhibits MDA-MB-231-induced RANKL mRNA expression in osteoblasts. Osteoblasts were seeded into 12 well plates and allowed to grow to confluence. They were then pre-treated with vehicle (0.1% DMSO) or PQIP (200-500 nM) for 2 hours prior to 16 hours in the presence of either control or MDA-MB-231 conditioned medium (10%) before being lysed in Trizol. mRNA was then extracted and analysed for OPG and RANKL expression using qPCR analysis. All results were adjusted to account for expression of 18S and GAPDH housekeeping genes. This graph shows the average mRNA RANKL/OPG expression ratio relative to control. Data is from three independent experiments (N=3) performed in triplicate and error bars represent +/- one standard deviation. * =$P<0.05$ from vehicle, + $p<0.05$ from MDA-MB-231 conditioned medium treatment

7.4.3 Effects of pharmacological inhibition of IGF-1R kinase activity on breast cancer-induced osteoclastogenesis *in vitro*

7.4.3.1 The IGF-1 receptor kinase inhibitor PQIP suppresses breast cancer – induced osteoclast formation without affecting mature osteoclast survival and resorption *in vitro*

Chapter 3 demonstrated that MDA-MB-231 cells and conditioned medium strongly increased the number and size of osteoclasts formed in M-CSF and RANKL generated cultures. The techniques devised there were now used to study the effect of the IGF-1 receptor kinase inhibitor PQIP on tumour cell-bone cell crosstalk. First, we tested the effects of PQIP on osteoclast formation in breast cancer – BM co-cultures. Figure 7.9 demonstrates that, as before, MDA-MB-231, 4T1, and MCF7 cells all increased osteoclast number, size and nuclearity. 300 cells of each type were used and they increased osteoclast number as follows MDA-MB-231 by 83% ($p<0.05$), 4T1 by 81% ($p<0.05$), MCF7 by 89% ($p<0.58$) when compared to vehicle. Figure 7.9B demonstrates that this change was due to increases in osteoclast size and nuclearity, as when only osteoclasts with ten or more nuclei were counted this increase changed to 375% with MDA-MB-231 ($p<0.05$), 319% with 4T1 ($p<0.01$) and 294% with MCF7 ($p<0.05$). For every cell type PQIP (200-1500 nM) significantly reduced breast cancer-induced osteoclast formation and size in a dose dependant manner.

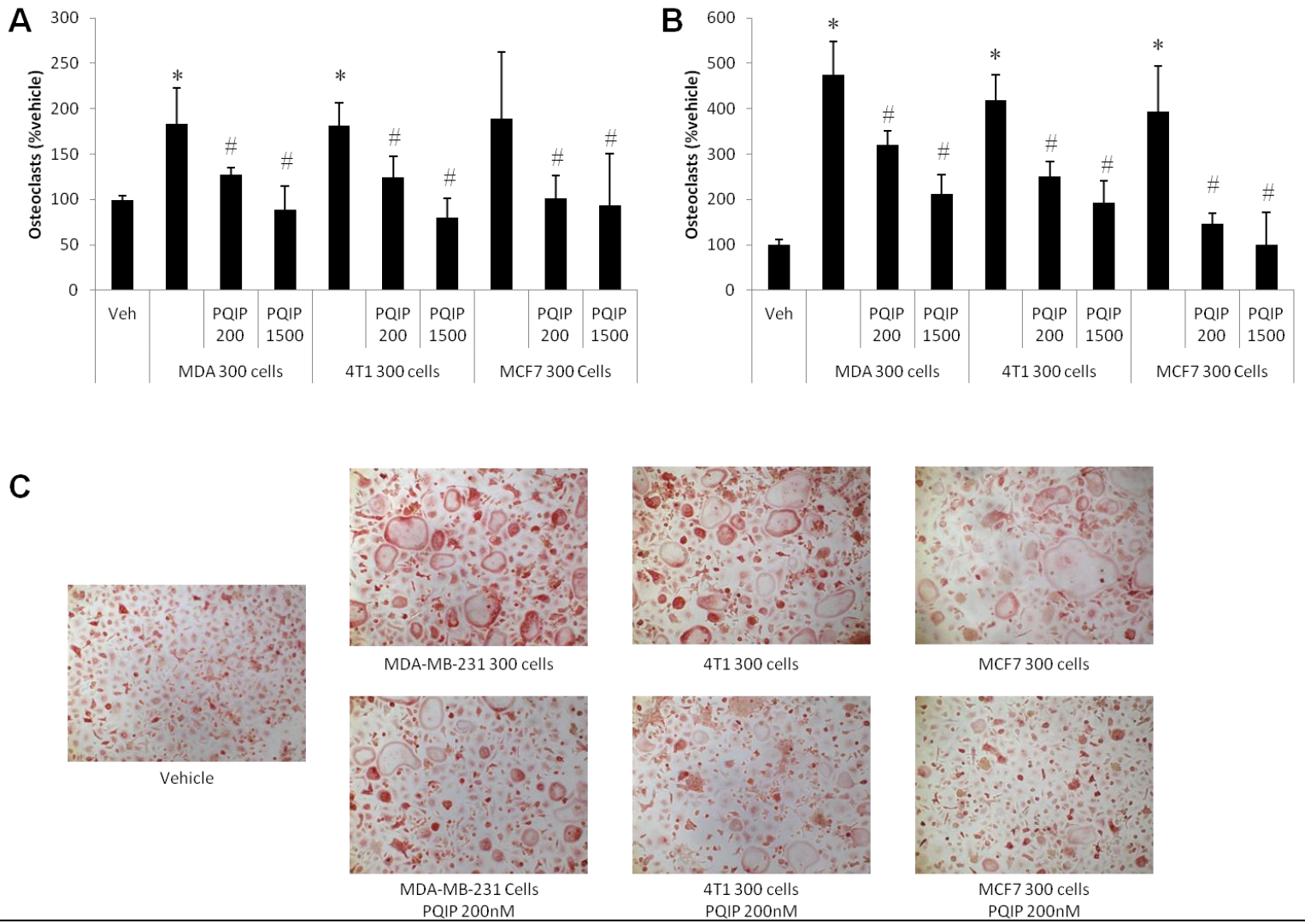

Figure 7.9 The IGF-1 receptor kinase inhibitor PQIP inhibits osteolytic tumour cell enhanced osteoclast formation. Mouse bone marrow cells were cultured in the presence of M-CSF (100ng/ml) for 3 days and then exposed to RANKL (100 ng/ml) and M-CSF (25 ng/ml) for 24 hours, prior to the addition of 300 MDA-MB-231, 4T1, or MCF7 cells in the presence of vehicle (0.1% DMSO) or PQIP (200-1500 nM). Osteoclast numbers were assessed by counting multinucleated TRAcP positive cells with three or more nuclei (A), or 10 or more nuclei (B). Osteoclast numbers are shown in panels A and B, representative photomicrographs from the cultures in panel C. Values in the graph are mean ± SD and are obtained from three independent experiments. * $p < 0.05$ from vehicle treated cultures, # $p<0.05$ from cancer cell treatment.

Figure 7.10 shows that again MDA-MB-231 conditioned medium significantly enhanced osteoclast number at all concentrations tested (43-55% increase, $p < 0.05$) and at 10% and 20% conditioned medium increased osteoclast size (79-110% increase, $p < 0.01$). The effect on osteoclast number was not suppressed following treatment with PQIP (200 nM), with the exception of the 5% MDA-MB-231 conditioned medium where it was reduced from 146% of vehicle to 60% ($p < 0.05$). It was noted that osteoclasts that were present in cultures treated with PQIP appeared to be smaller and with less nuclei. Figure 7.10B demonstrates that PQIP significantly suppressed the MDA-MB-231 conditioned medium induced increase in the number of osteoclasts with 10 or more nuclei at all concentrations tested. This also demonstrated the lesser effect 5% conditioned medium had, as in this count it failed to increase osteoclast numbers. This suggests that IGF-1R kinase inhibition is capable – at least in part - of suppressing MDA-MB-231 tumour cell support for osteoclast formation.

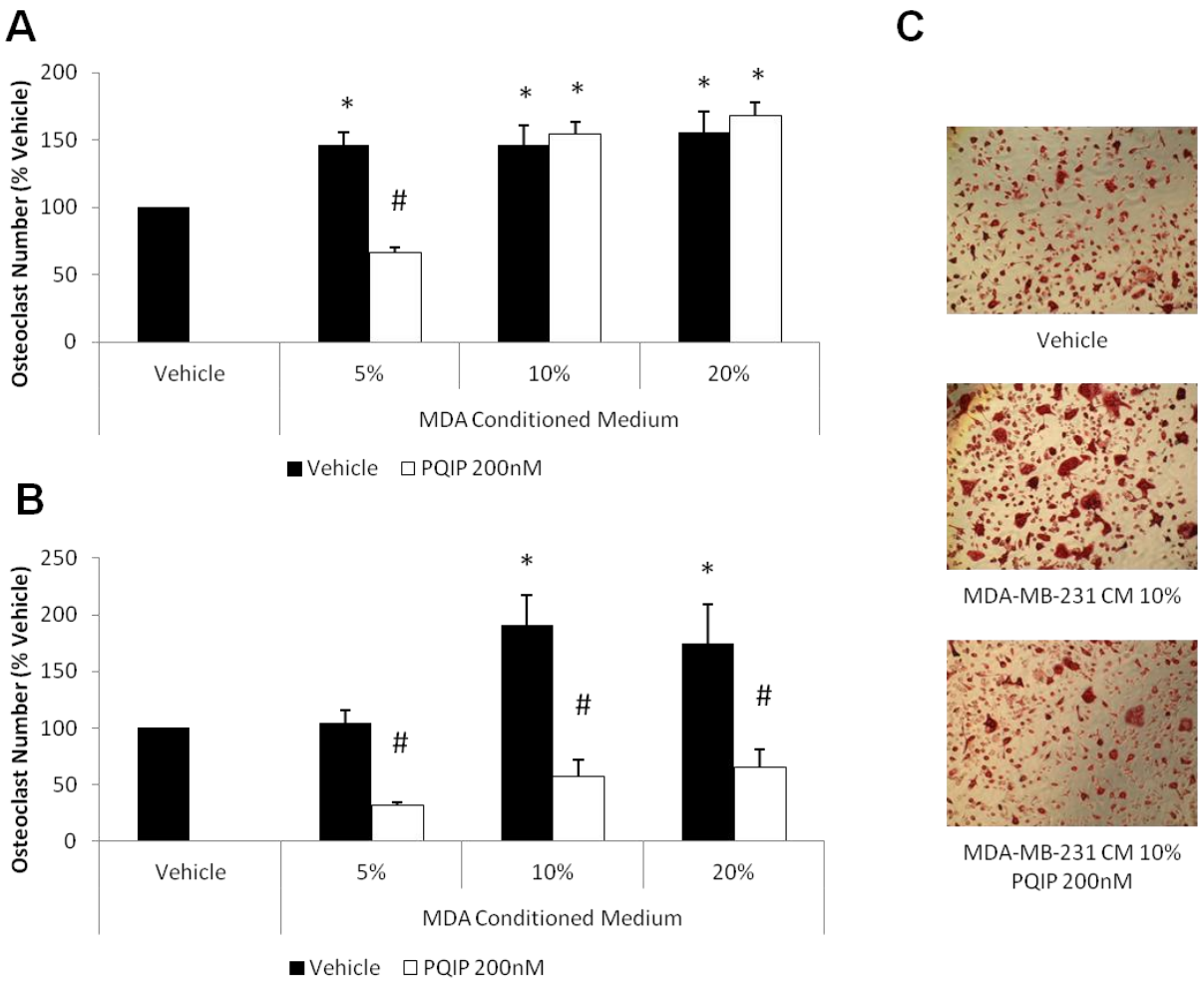

Figure 7.10 The IGF-1 receptor kinase inhibitor PQIP inhibits MDA-MB-231 conditioned medium enhanced osteoclast formation. Mouse bone marrow cells were cultured in the presence of M-CSF (100 ng/ml) for 3 days and then exposed to RANKL (100 ng/ml) and M-CSF (25 ng/ml) for 24 hours, prior to the addition of 300 MDA-MB-231 cells or treatment with control (20%) or MDA-MB-231 (5-20%) conditioned medium in the presence of vehicle (0.1% DMSO) or PQIP (200 nM). Osteoclast numbers were assessed by counting multinucleated TRAcP positive cells with three or more nuclei (A), or 10 or more nuclei (B). Osteoclast numbers are shown in panels A and B, representative photomicrographs from the cultures in panel C. Values in the graph are mean ± SD and are obtained from three independent experiments. * $p < 0.05$ from vehicle treated cultures, # $p<0.05$ from MDA-MB-231 C treatment.

To determine whether PQIP exerted inhibitory effects on mature osteoclast survival and activity, I conducted further studies in mature osteoclast cultures that were treated with PQIP in the presence and absence of MDA-MB-231 conditioned medium. I found that PQIP had no inhibitory effects on osteoclast survival (Figure 7.11A) or bone resorption (Figure 7.11B and C) at a concentration that inhibited osteoclast formation.

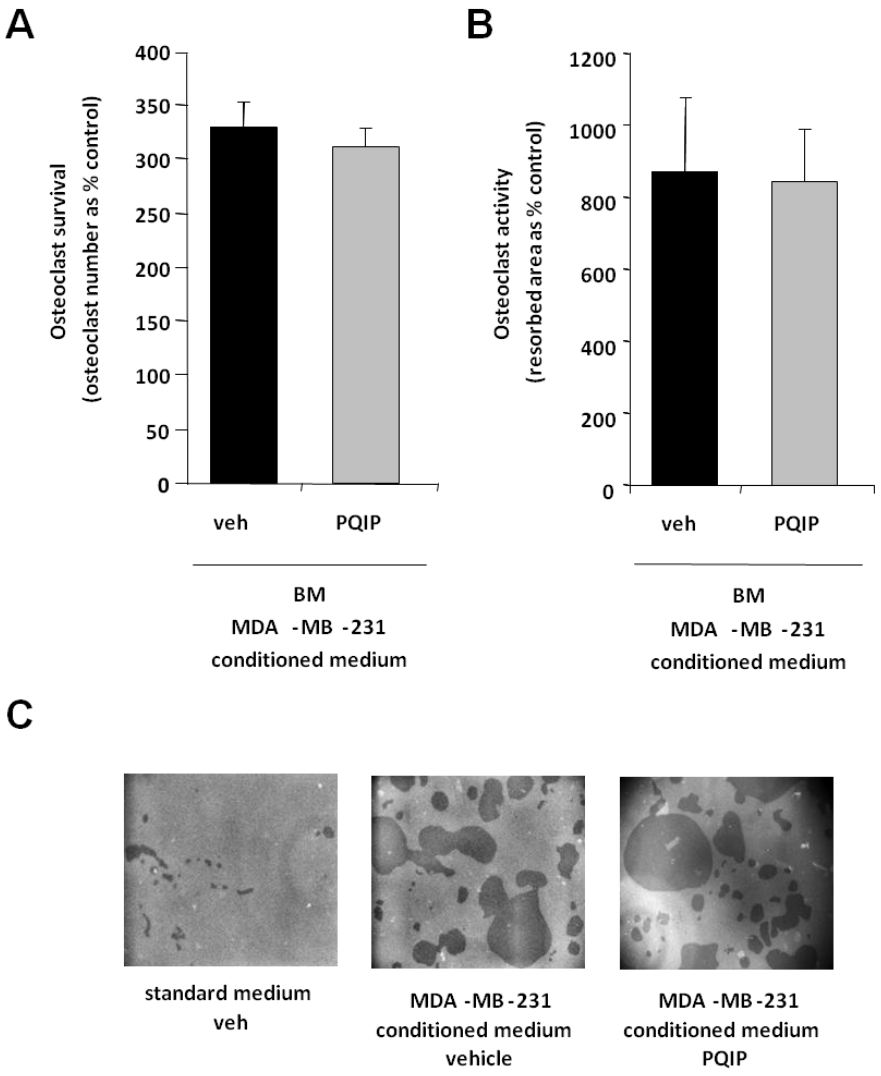

Figure 7.11 The IGF-1 receptor kinase inhibitor PQIP does not effect MDA-MB-231 conditioned medium enhanced osteoclast survival or function. Mouse bone marrow cells were cultured in the presence of M-CSF (100 ng/ml) for 3 days and then transferred to Osteo Assay Surface plates and exposed to RANKL (100 ng/ml) and M-CSF (25 ng/ml) for 24 hours, prior to the addition of MDA-MB-231 or control conditioned medium (10%) in the presence of vehicle (0.1% DMSO) or PQIP (200 nM). After 96 hours osteoclast numbers were assessed by counting multinucleated TRAcP positive cells with three or more nuclei (A). 50% bleach was used to remove adherent osteoclasts and resorption assessed by image analysis using ImageJ. Osteoclast numbers are shown in panel A and resorbed area in panel B, representative photomicrographs of the resorption pits are shown in panel C. Values in the graph are mean ± SD and are obtained from three independent experiments.

7.4.3.2 The IGF-1 receptor kinase inhibitor PQIP prevents PI3K/AKT activation in mouse osteoclasts

Western blot was used to investigate whether the IGF-1 receptor kinase inhibitor PQIP affect IGF-1- and MDA-MB-231-induced PI3K/AKT activation in osteoclasts. Figure 7.12 shows that both IGF-1 (100 ng/ml) and MDA-MB-231 CM (10%) treatments induced the phosphorylation of AKT. This activation was stronger with IGF-1 treatment, but both were clearly above the basal level seen in untreated cells. Pre-incubation with PQIP (200-500 nM) significantly inhibited IGF-1 and MDA-MB-231-induced AKT activation at both serine and threonine sites in osteoclasts.

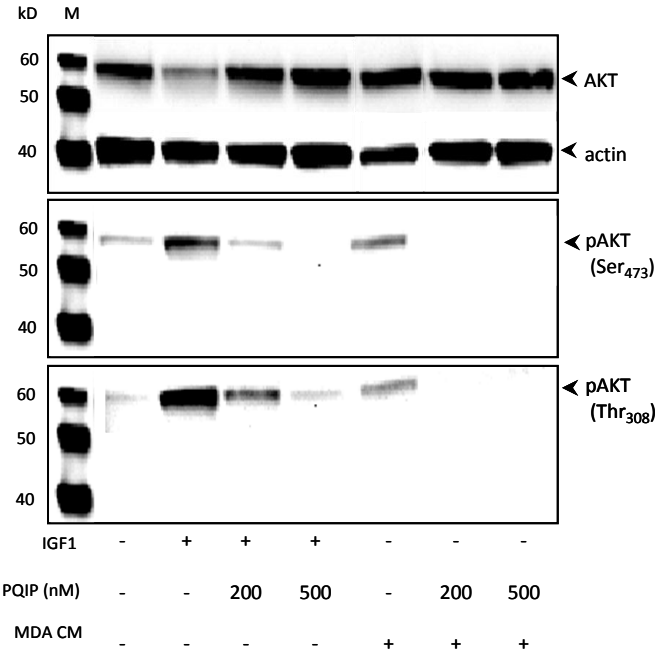

Figure 7.12 The IGF-1 receptor kinase inhibitor PQIP inhibits IGF-1 and MDA-MB-231 induced activation of AKT in osteoclasts. Mouse osteoclasts were treated with a range of PQIP concentrations (200 and 500 nM) for 1 hour prior stimulation with IGF-1 (100 ng/ml) for 15 minutes or MDA-MB-231 conditioned medium (10%) for 30 minutes. Total cellular protein was subjected to western blot analysis using anti-phospho-AKT ($Thr_{308,}$), anti-phospho-AKT (Ser_{473}), anti-AKT antibodies. Actin was used as a loading control. Abbreviations: M – molecular weight marker; kD - kilo Dalton; p – phosphorylated. Identical experiments were performed on 3 occasions

7.4.3.3 The IGF-1 receptor kinase inhibitor PQIP inhibits IGF-1 but not ERK1/2 activation in mouse osteoclasts

Western blot was used to investigate whether the IGF-1 receptor kinase inhibitor PQIP affected MDA-MB-231 conditioned medium induced the activation of ERK1/2, a key signalling pathway downstream of IGF-1 receptor (285). To allow comparison IGF-1 treatment was used as a positive control. Figure 7.13 shows that both IGF-1 (100 ng/ml) and MDA-MB-231 CM (10%) treatments induced the phosphorylation of ERK1/2. Interestingly, pre-incubation with PQIP (200-500 nM) significantly inhibited IGF-1 but not MDA-MB-231 CM-induced ERK1/2 activation in osteoclasts.

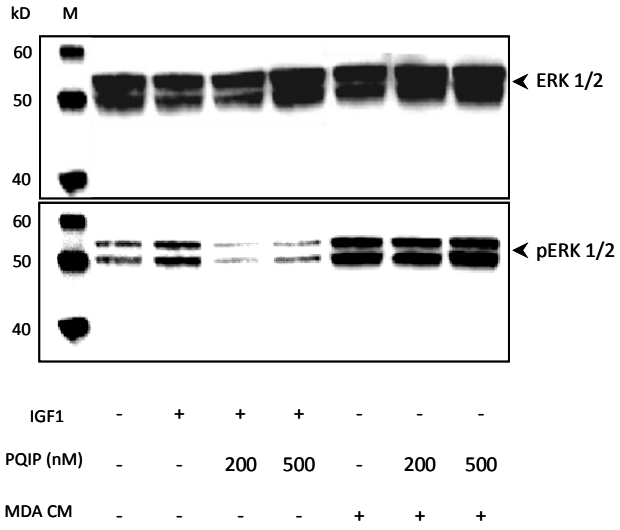

Figure 7.13 The IGF-1 receptor kinase inhibitor PQIP inhibits IGF-1 but not MDA-MB-231 induced ERK1/2 activation in osteoclasts. Mouse osteoclasts were treated with a range of PQIP concentrations (200 and 500 nM) for 1 hour prior stimulation with IGF-1 (100 ng/ml) for 15 minutes or MDA-MB-231 conditioned medium (10%) for 30 minutes. Total cellular protein was subjected to western blot analysis using anti-phospho-ERK1/2, anti-ERK1/2 antibodies (B). Abbreviations: M – molecular weight marker; kD - kilo Dalton; p – phosphorylated. Identical experiments were performed on 3 occasions

7.4.3.4 The IGF-1 receptor kinase inhibitor PQIP inhibits IGF-1 and cancer-induced spreading and motility of osteoclasts and their precursors

Xcelligence analysis was used to further elucidate the impact of IGF-1 receptor inhibition on the crosstalk between MDA-MB-231 cells and osteoclasts and their precursors. M-CSF generated macrophages were plated on Xcelligence plates and allowed to grow for 24 hours. In the presence and absence of PQIP, they were then treated with M-CSF (25 ng/ml), RANKL (100 ng/ml), and either control conditioned medium (10%), IGF-1 (100 ng/ml) or MDA-MB-231 conditioned medium (10%).

Figure 7.14 shows a representative graph of the complete changes in cell index over the 96 hours of the experiment. Long term changes in cell index value are normally thought to represent changes in proliferation rate. As seen in Chapter 3, MDA-MB-231 conditioned medium causes an immediate, rapid increase in cell index unlikely to represent proliferation, but also causes a change in the long term rate of increase in cell index that does represent cell proliferation. Here, between 24 and 72 hours, the proliferation rate of MDA-MB-231 conditioned medium treated cells was significantly higher (283% increase $p<0.05$). This was not inhibited by the IGF-1 receptor kinase inhibitor PQIP. Neither IGF-1 nor PQIP treatment alone significantly altered the long-term proliferation rate of RANKL and M-CSF stimulated BM cells.

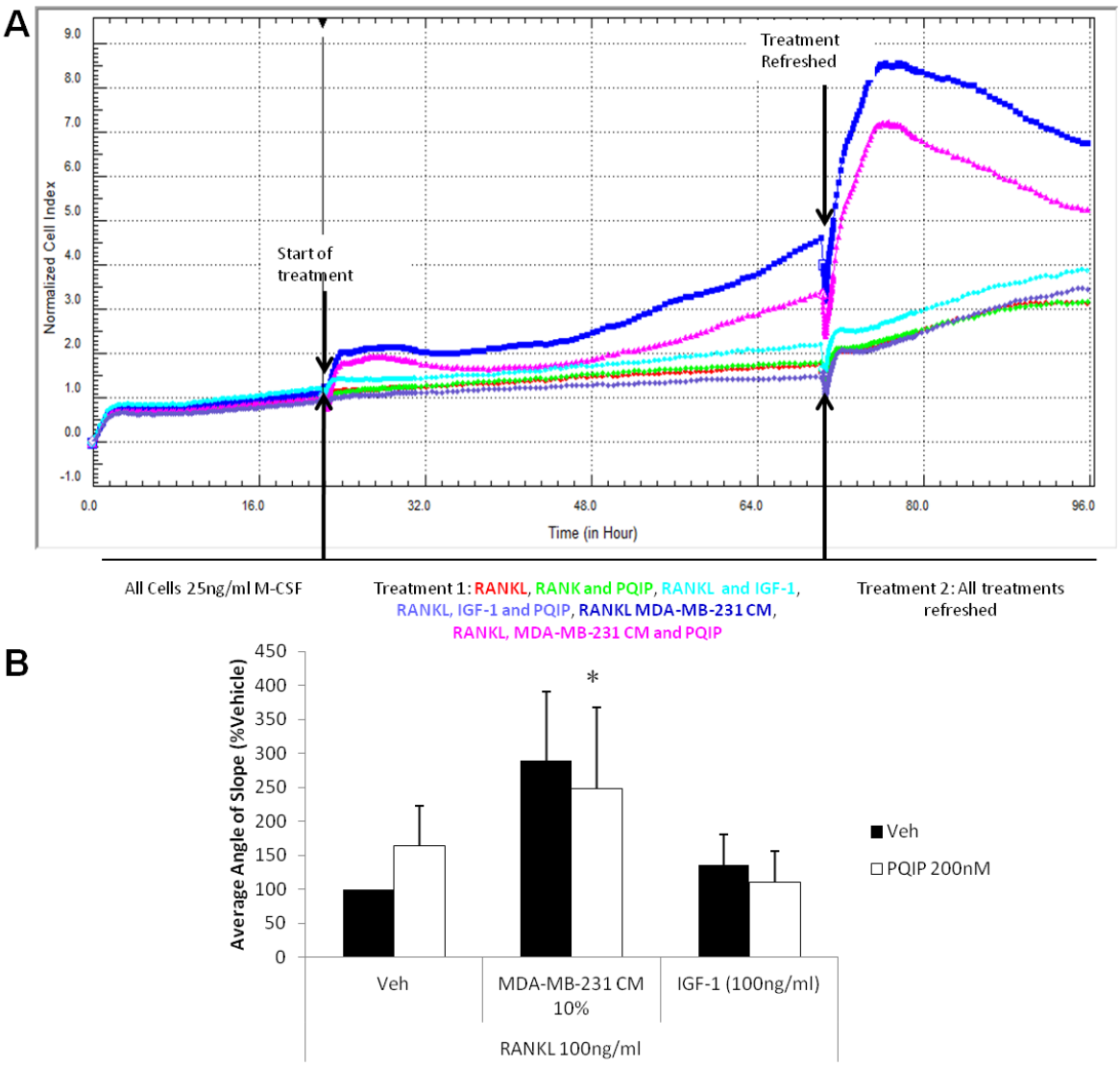

Figure 7.14 The IGF-1 receptor inhibitor PQIP inhibits long-term IGF-1 and MDA-MB-231 conditioned medium induced increases in osteoclast impedance values in Xcelligence analysis. M-CSF generated macrophages were seeded onto xcelligence plates and allowed to grow for 24 hours with M-CSF (25 ng/ml). Cells were then treated with M-CSF (25 ng/ml) and RANKL (100 ng/ml) plus vehicle, IGF-1 (100 ng/ml), or 10% MDA-MB-231 conditioned medium, in the presence or absence of PQIP (200 nM). Treatment was refreshed after 48 hours. A) shows a representative graph of the cell index values (derived from their electrical impedance) over the full 96 hours of the experiment and normalized to the last time point before the first treatment. B) A graph showing the average slope of the graph between hours 39 and 52. N=4 experiments were performed. *=p<0.05 from Vehicle

To investigate the effect of the IGF-1 receptor inhibitor PQIP on IGF-1 and breast cancer induced changes in osteoclast spreading and motility, changes in cell index value in the first three hours after treatments were investigated in detail. These changes are taken to represent different aspects of treatment effects between different time points. The first 30 minutes after treatment represent changes in cell morphology or spreading, the next two hours represent changes in cell motility or migration measured by the rate of change in cell index value. After two and a half hours cell index values are taken to represent long term proliferation. Figure 7.15 shows that MDA-MB-231 conditioned medium causes both changes in cell morphology and a large and significant increase in cell motility (442% increase $p<0.01$). PQIP treatment does not inhibit either the cancer conditioned medium induced changes in cell morphology, or the rate of increase in cell motility. However, PQIP does seem to reduce the final cell index value reached during this period, suggesting an inhibition of the overall migration of these cells. IGF-1 treatment does not cause the complex changes in cell morphology observed with MDA-MB-231 conditioned medium treatment. However, IGF-1 does cause a modest but significant increase in the motility of the cells (46% increase $p<0.05$). This was significantly inhibited by PQIP.

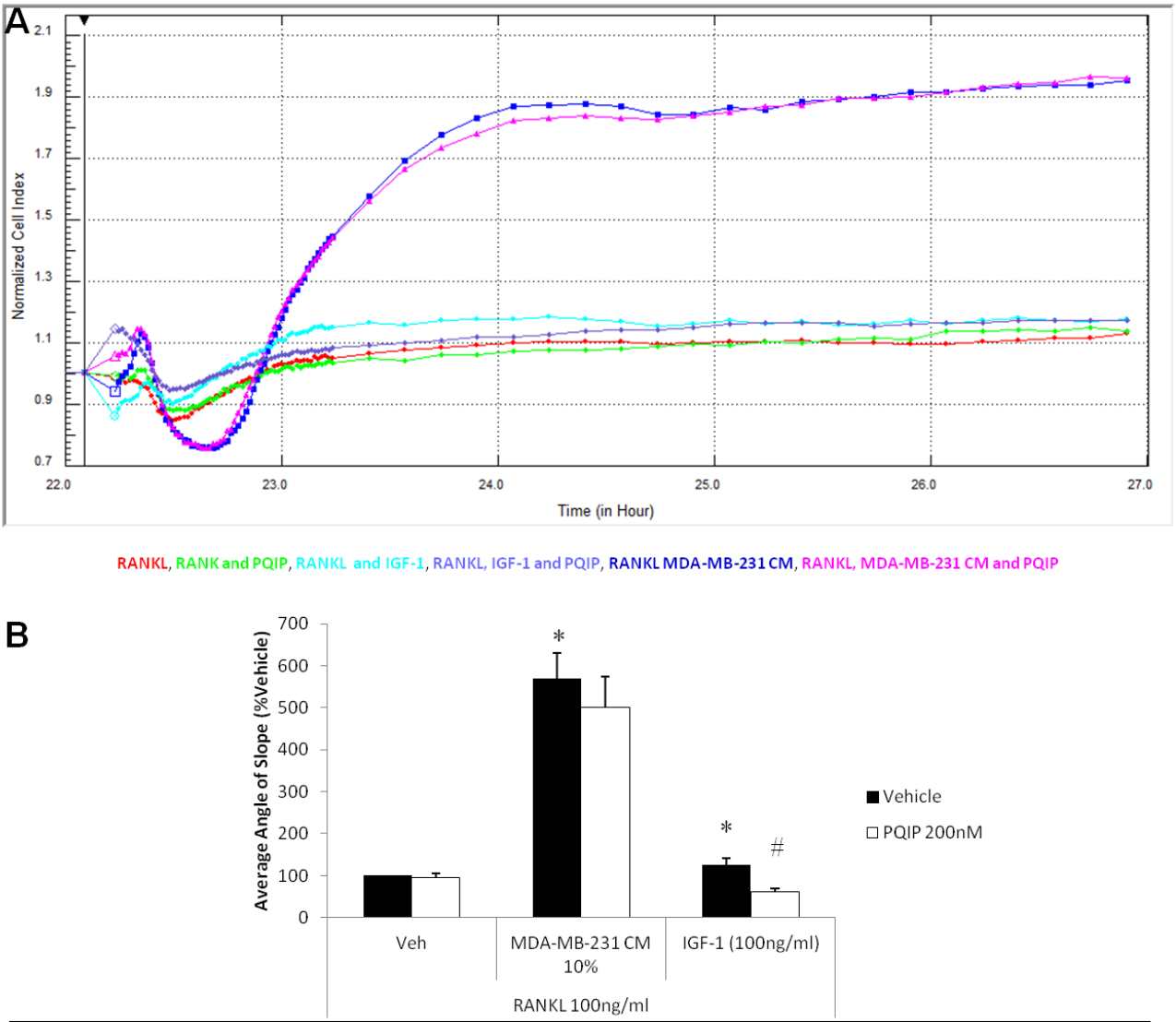

Figure 7.15 The IGF-1 receptor inhibitor PQIP inhibits initial IGF-1 and MDA-MB-231 conditioned medium induced increases in osteoclast impedance values in Xcelligence analysis. M-CSF generated macrophages were seeded into xcelligence plates and allowed to grow for 24 hours in M-CSF (25 ng/ml). Cells were then treated with M-CSF (25 ng/ml) and RANKL (100 ng/ml) plus vehicle, IGF-1 (100 ng/ml), or 10% MDA-MB-231 conditioned medium, in the presence or absence of PQIP (200 nM). Treatment was refreshed after 48 hours. A) shows a representative graph of the cell index values (derived from their electrical impedance) for the first 3 hours after the start of treatments and normalized to the last time point before the treatment. B) A graph showing the average slope of the linear portion of the graph between hours 24 and 25. N=4 experiments were performed. * $p < 0.05$ from vehicle treated cultures, # $p<0.05$ from IGF-1 (100 ng/ml) treatment.

7.5 Discussion

The insulin-like growth factor/insulin system of receptors and ligands are thought to play a major role in the proliferation and migration of various tumour types, and are likely to be involved in the development of bone metastases (277, 471). Evidence from a number of pharmacological, clinical and epidemiological studies demonstrates that high levels of circulating IGF-1 and lower levels of its binding proteins are associated with increased risk of various cancers including breast cancer (493, 499). In view of this, recent studies have focused on IGF-1 receptor as a possible therapeutic target for the treatment of tumour cell growth and metastases (277, 287, 471, 500, 501).

IGF-1 receptor inhibition has previously been shown to inhibit the viability of a variety of tumour cells (483). In this study we looked at the possibility that it may directly reduce the number of cancer cells in a bone metastasis. MDA-MB-231 cell viability was not affected by either IGF-1 or PQIP treatment after 72 hours, though IGF-1 did induce AKT phosphorylation which was inhibited by PQIP; indicating that IGF-1 signalling is active in these cells. Other osteolytic tumour cells showed a variable response, while neither 4T1 nor MC57G cells were affected by PQIP treatment, the growth of MCF7 cells was strongly inhibited. Xcelligence analysis of MDA-MB-231 cells and 4T1 cells showed no long-term effects of either IGF-1 or PQIP, though 4T1 cells did show reduced initial spreading in response to PQIP. The viability, adherence and spreading of MCF-7 cells on the other hand were strongly induced by IGF-1 and inhibited by PQIP. This finding is in agreement with previous studies which have shown that inhibition of IGF-1 signalling by PQIP inhibits tumour proliferation in a variety of human breast cancer cells including MCF7, while other cell lines were unaffected by PQIP (483). This selective inhibition of tumour cell proliferation by PQIP correlates with the co-expression of ligand-receptor pairs within the IGF axis (502).

Next, I investigated the effect of the novel IGF-1 receptor kinase inhibitor PQIP on breast cancer-induced bone cell activity *in vitro*. While not effecting MDA-MB-231 viability, PQIP was capable of suppressing osteoclast formation stimulated by the addition of conditioned medium from MDA-MB-231 cells. When all osteoclasts were counted this reduction was only apparent using the weakest conditioned medium treatment. However, when only those osteoclasts with 10 or more nuclei were counted any MDA-MB-231

conditioned medium induced increase in osteoclast number was abolished. This suggests that this effect is mainly on osteoclast size and therefore may be in response to an inhibition of osteoclast fusion, rather than their initial genesis. Testing using other osteolytic tumour cells showed that this inhibitory effect was true in each case, and was particularly strong for MCF7 cells where tumour cell viability was also affected. MDA-MB-231 cells were previously shown to induce increases in osteoblast production of RANKL (Chapter3). In this chapter we show that PQIP inhibits MDA-MB-231-induced increases in the RANKL/OPG ratio in osteoblasts. These results, together with the finding that PQIP inhibited RANKL production by osteoblasts (Chapter 6), show for the first time that IGF-1R inhibition is sufficient to disrupt both osteoblast and tumour cell support for osteoclastogenesis. The fact that PQIP inhibited AKT phosphorylation but not ERK1/2 activation by conditioned medium from MDA-MB-231 cells suggests that inhibition of PI3K/AKT pathways downstream of IGF-1 may be responsible for these effects.

In osteoblast cultures, treatment with PQIP exacerbated the inhibitory effects of MDA-MB-231 derived factors on osteoblastogenesis. Not only was inhibition of osteoblast differentiation and function significantly worsened, but while individually PQIP and MDA-MB-231 conditioned medium had little effect on cell viability, together they drastically reduced cell number. This may be a non-specific toxic effect, or may result from the removal of the positive effect of IGF-1-receptor mediated signals from the conditioned medium treatment. Regardless, these results indicate that PQIP treatment is likely to inhibit osteoblast survival, differentiation and activity in bone metastatic environment.

In both osteoblasts and osteoclasts the PI3K/AKT signalling pathway was stimulated by MDA-MB-231 conditioned medium. Importantly in both cases PQIP inhibited this tumour induced effect. However PQIP failed to inhibit ERK1/2 activation by conditioned medium from MDA-MB-231 cells, suggesting that inhibition of tumour induced PI3K/AKT pathways downstream of IGF-1 may be responsible for the effects seen, while ERK1/2 is activated by other tumour cell produced factors. Although our studies clearly indicate that PQIP exerts a direct inhibitory effect on IGF-1 induced PI3K/AKT signalling, we cannot exclude the possibility that the tumour cells may produce other factors that can act through IGF-1 receptor, or indeed through the insulin receptor, and may also contribute to signalling via these pathways, and so play a role in the effects observed.

Xcelligence analysis seems to confirm the hypothesis that inhibition of IGF-1 signalling induced by cancer cell conditioned medium by PQIP is responsible for the effects seen. IGF-1 treatment caused a similar pattern of effects to that seen with MDA-MB-231 conditioned medium treatment, albeit at a far lower efficiency and with less complexity at the initial treatment. In both cases PQIP significantly reduced the cell index values seen, and with IGF-1 treatment abolishing the increases seen. At the initial treatment point IGF-1 caused an increase in the rate of cell index increase, and this was the only early aspect of the MDA-MB-231 conditioned medium treatment inhibited by PQIP. This period is likely to represent induced increase in cell migration and spreading, fitting with the hypothesis that PQIP inhibits tumour cell induced osteoclast fusion by inhibiting IGF-1 signalling, though further work using complementary techniques is needed to confirm this. Altogether, the findings presented here imply that targeting IGF-1R signalling may be useful in the treatment of osteolytic bone disease, even if tumour growth is not directly affected.

In conclusion, the studies performed here demonstrate that preventing IGF-1 signalling using the novel selective human IGF-1R kinase inhibitor PQIP directly suppresses tumour cell support for osteoclastogenesis *in vitro*. Moreover, the results presented in this chapter have successfully shown the usefulness of the techniques developed in the preceding chapters for studies investigating tumour cell-bone cell crosstalk. Therefore, selective small molecule tyrosine kinase inhibitors of IGF-1R such as PQIP and its analogue OSI-906 (503), which is currently in advanced clinical development, may have clinical value in the treatment of bone metastasis.

Chapter 8

The effects of the novel IGF-1 receptor kinase inhibitor PQIP on breast cancer-induced osteolysis *ex vivo* and *in vivo*

8.1 Summary

In previous chapters, IGF-1 signalling was found to regulate normal bone cell function, tumour cell-bone cell cross-talk and it is known to influence tumour cell migration *in vitro*. It was therefore hypothesised that inhibiting the IGF-1R may prevent high bone turnover and osteolysis associated with breast cancer *in vivo* by inhibiting cancer-induced osteoclastic and osteoblastic changes and perhaps also indirectly reduce the proliferation of tumour cells. In view of this, the effect of PQIP on bone turnover and osteolysis associated with breast cancer was studied *ex vivo* and *in vivo*.

Ex vivo, the effects of PQIP on osteolysis were studied using the human MDA-MB-231 - mouse calvarial co-culture system. Treatment with PQIP (500 nM) prevented osteolysis and caused a significant gain in bone volume in comparison to vehicle treated cultures. This effect was likely mediated through direct effects on bone cells and tumour cell-bone cell cross-talk as PQIP had no effect on MDA-MB-231 viability and growth.

To investigate the effects of oral PQIP treatment on the development of osteolytic bone metastases *in vivo*, the mouse 4T1 breast cancer cell model was used. Oral daily administration of PQIP (100 mg/kg) inhibited osteolysis and caused a significant gain in bone volume when compared to sham mice. A detailed bone histomorphometric analysis showed that osteoclast numbers and active resorption surfaces were increased following 4T1 cell inoculation in vehicle treated mice, whereas these effects were totally prevented following treatment with PQIP. Treatment with PQIP (100 mg/kg) also reduced osteoblast number, osteoid surface, mineral apposition rate and bone formation rate, indicative of a significant reduction in osteoblast activity and bone formation. Analysis of tumour size in histological sections showed that PQIP had no effect on tumour volume within osteolytic lesions.

Overall, this chapter succeeded in demonstrating the effectiveness of the *ex vivo* and *in vivo* bone metastasis model techniques developed in Chapter 4 for examining breast cancer-induced osteolysis; though the *in vivo* model is in need of refinement. IGF-1 receptor inhibition by PQIP treatment was found to reduce osteolytic bone destruction in both *ex vivo* and *in vivo* studies. Therefore, PQIP, or its analogue OSI-906, may be a useful clinical tool in the treatment of osteolytic bone metastasis, though its effects on reducing bone formation may make it more suitable for use in osteoblastic metastases.

8.2 Introduction

As discussed in Chapters 6 and 7, IGF-1 and its receptor have been shown to be involved in the regulation of both bone and cancer. Previous *in vivo* experiments using knockout mice demonstrated that IGF-1 receptor deficiency causes a unique and complex skeletal phenotype with 24% less cortical bone and shortened femurs, but increased trabecular bone density and connectivity (293, 478, 479). Without IGF-1 signalling present both osteoblast and osteoclast function are severely reduced (290, 294, 477). Until this thesis no *in vivo* work had been performed studying the effect of IGF-1 receptor inhibition on osteolytic bone metastasis.

In Chapter 6 of this thesis the effects of IGF-1 receptor inhibition by PQIP on bone cell cultures *in vitro* was demonstrated. In all cell types IGF-1 induced PI3K/AKT signalling was inhibited by pre-treatment with PQIP and it was found that PQIP inhibited IGF-1 induced increases in various bone cell attributes. These included osteoblast differentiation, function, migration and RANKL production, as well as osteoclast formation and survival. No effects on cell viability were observed in all cultures tested.

IGF-1 and its receptor are known to be involved in the development of various cancers as well as the stimulation of both cancer cell proliferation and migration (275, 495). It appears to be particularly important for the development and progression of bone metastases from breast cancer. (273, 496, 497). In Chapter 7 of this thesis we investigated the effects of PQIP on cancer cell behaviour and cross-talk with bone cells *in vitro*. These studies showed that the IGF-1 receptor inhibitor PQIP inhibited breast cancer induced increases in osteoclast formation, resorption and fusion, as well as osteoblast support for osteoclastogenesis. Breast cancer cell conditioned medium caused a signalling cascade through the PI3K/AKT pathway and PQIP treatment was able to prevent this. However, in two of the three cell lines studied PQIP did not cause any direct inhibition of cancer cell viability.

While oral treatment with PQIP has been previously been shown to regress tumour cell growth *in vivo* in certain cell lines (483), no previous work has studied its effects on bone metastases and related bone abnormalities. Here, the *ex vivo* and *in vivo* techniques

explored in Chapter 4 were used to investigate the effects of PQIP on breast cancer-induced osteolysis *ex vivo* and *in vivo*.

8.3 Aim

The aim of this chapter was to test the use of PQIP as a potential therapeutic agent for the treatment of bone metastasis. This was achieved using the adapted calvarial organ culture and intratibial injection models of bone metastasis devised in Chapter 4. The effect of IGF-1 receptor inhibition on overall osteolysis levels and the activity of bone cells in the presence and absence of tumour cells was investigated.

8.4 Results

8.4.1 PQIP protects against breast cancer-induced osteolysis in human MDA-MB-231-calvaria organ culture

To determine the effect of IGF-1 receptor inhibition on breast cancer-induced osteolysis *ex vivo* the adapted calvarial organ cultures were used. Calvaria were divided down the median sagital suture into two equal halves. These halves were then separately placed onto mesh platforms above pre-seeded MDA-MB-231 cells in 48 well plates. Halves were treated with either vehicle (DMSO 0.1%) or PQIP (500 nM) for one week and bone mass then quantified by µCT analysis. Figure 8.1 shows representative µCT images of the calvaria halves. In the vehicle treated cultures bone loss is clearly visible throughout the calvarial tissue, indicating osteolysis. In contrast, treatment with PQIP (500 nM) can visually be seen to have prevented osteolysis in the three dimensional images and when quantified percent bone volume is 75% higher ($p<0.01$) than that found in the vehicle treated calvaria. AlamarBlue was used to determine if the effects seen may be due to a loss of MDA-MB-231 cell viability. PQIP had no significant effect on MDA-MB-231 viability and growth thereby excluding toxic effects (Figure 5C).

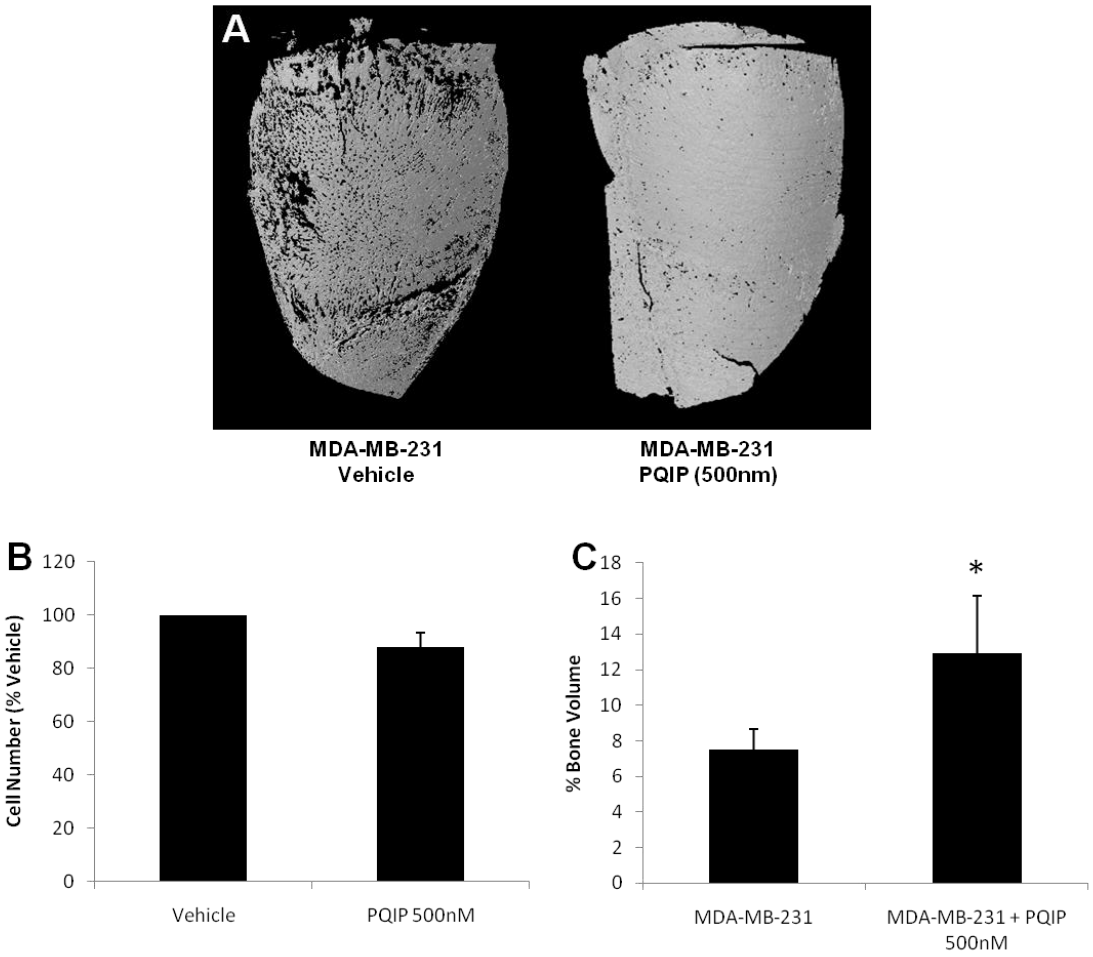

Figure 8.1 The IGF1 receptor kinase inhibitor PQIP prevents MDA-MB-231-induced osteolysis in mouse calvaria organ cultures. Panel A shows representative photomicrographs of mouse calvarias. Panel B shows the relative number of viable MDA-MB-231 cells in the wells below the calvaria as measured by the AlamarBlue assay. These were exposed to vehicle or PQIP (500 nM) through out the experiment. Panel C shows bone volume in neonatal mouse calvarias isolated from 7 day-old mice and then co-cultured with human MDA-MB-231 breast cancer cells prior exposure to vehicle (veh; 0.1% DMSO) or PQIP (200 nM) for 7 days. *=p<0.01 from MDA-MB-231 co-culture alone.

8.4.2 PQIP protects against breast cancer-induced osteolysis in mice

To determine the effects of IGF-1 receptor inhibition on osteolytic bone metastasis *in vivo* an intratibial injection experiment using 4T1 cells was performed. 12 six-week old Balb/c wild type mice were randomly divided into two groups of six, one group received once daily oral treatment with vehicle (tartaric acid 25 mM) and the other with 100 mg/kg PQIP. After the injection of 4T1 cells, 7 days were allowed for recovery and establishment of metastases before oral treatment began. The effects of PQIP on 4T1 intratibial injection induced bone loss were then monitored by examining trabecular bone loss at the proximal tibiae metaphysis using *in vivo* μCT analysis. All results were compared to data derived from *in vivo* μCT of the tibiae prior to intratibial injection.

Figure 8.2B shows that by day 7 after intratibial injection the presence of 4T1 cells had caused significant osteolysis. Before the start of oral treatment (day 7) there was no difference between the mice to be treated with vehicle (24.41% bone loss±1.67) and those to be treated with PQIP (23.38% bone loss ±4.83). In both groups bone loss was significantly higher than that seen in the sham injected legs ($p<0.01$). After treatment (Figure 8.2C) in the mice treated with vehicle the percentage of bone lost continued to increase through the treatment period (43.5% bone loss ±3.85). In contrast, in the mice treated with PQIP trabecular volume did not significantly differ from the start of the treatment period and was significantly lower than in the vehicle treated mice (17.84% bone loss ±2.84, $p<0.01$). It should be noted that sham injections alone also caused significant bone loss (17.86± 6.09, $p<0.01$).

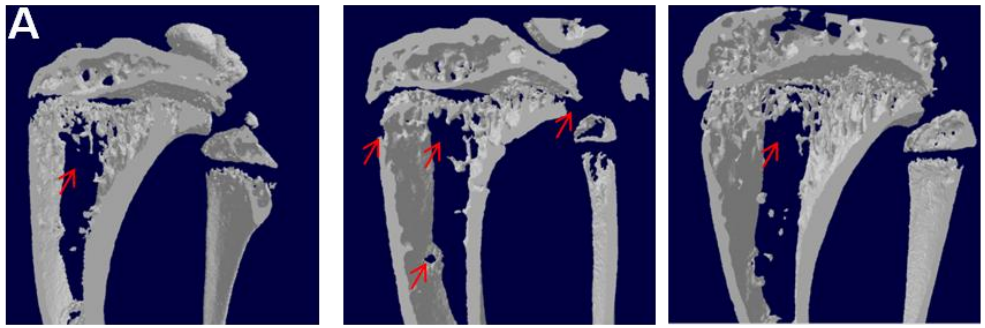

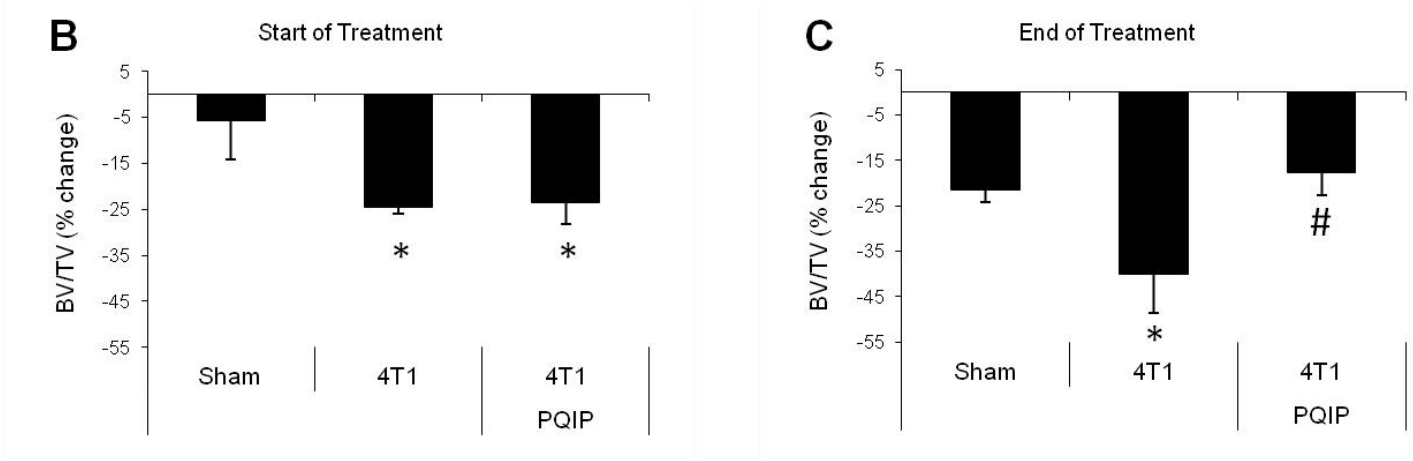

Figure 8.2 The IGF1 receptor kinase inhibitor PQIP prevents 4T1-induced osteolysis *in vivo*. 6-week old female Balb/c WT mice received intratibial injections of $5x10^3$ 4T1 breast cancer cells into their right leg and a sham injection of PBS into their left leg. After 7 days once daily oral treatment with either vehicle or PQIP (100 mg/kg) was begun and continued for one week. Tibia were analysed by *in vivo* microCT analysis. Animals were sacrificed 14 days after intratibial injection. Panel A shows representative microCT images of the proximal tibia metaphysis at the conclusion of the study. Panels B and C show the percent change in the trabecular bone volume of the tibia from the beginning of the study to when treatment was started (B) after 7 days and the conclusion of the experiment (C). Values are means ± standard deviation. 6 mice per group. *=p<0.05 from Sham, #=p<0.05 from 4T1 injected, vehicle treated.

Detailed μCT analysis of several features of the trabecular bone in the proximal tibial metaphysis was performed. The results seen complement the pattern of bone loss shown above. Figure 8.3 shows that 7 days after inoculation with 4T1 cells there was a significant reduction in trabecular thickness when compared to sham (loss of 6.47% ±1.78 or 9.51% ±2.26, $p<0.05$). While the presence of 4T1 cells appeared to cause a reduction in trabecular number and an increase in trabecular pattern factor, at the start of treatment this was not significantly different from sham. Prior to the start of PQIP treatment there was no difference between the two sets of 4T1 injected tibiae. By the end of the treatment period the trabecular bone of vehicle treated, 4T1 inoculated tibia had significantly lost both trabecular thickness (11.97% ± 1.53 loss, $p<0.05$) and number (35.70% ± 3.20 loss, $p<0.01$) when compared to sham. Trabecular pattern factor was increased but was not significantly different from sham. In mice treated with PQIP, by the end of the experiment 4T1 injected tibiae were no longer significantly different from sham injected tibia. In comparison to the 4T1 injected tibia of vehicle treated mice, PQIP treatment had significantly reduced the loss of trabecular thickness, number and increases pattern factor ($p<0.01$ in each case).

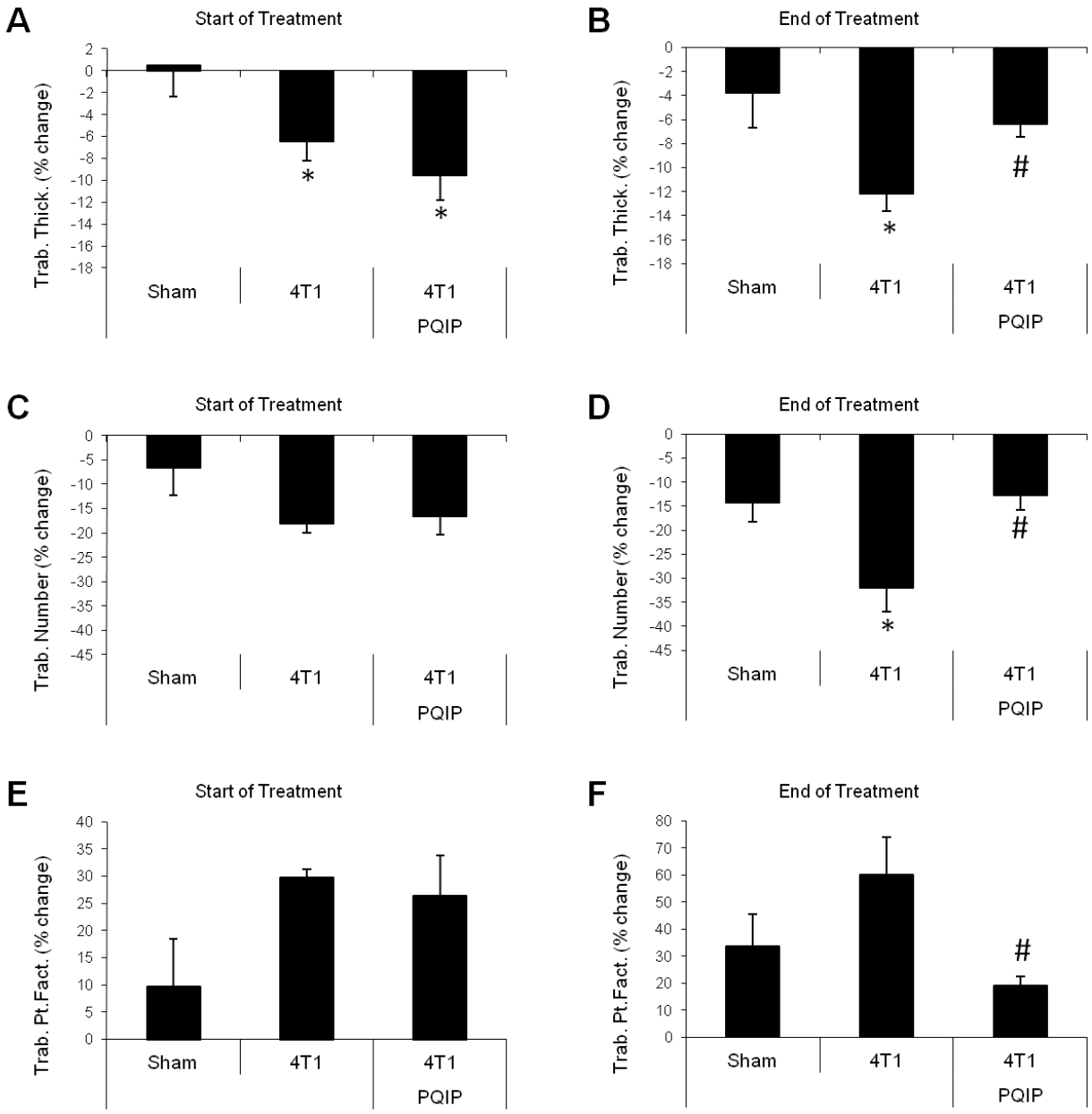

Figure 8.3 The IGF1 receptor kinase inhibitor PQIP prevents 4T1-induced changes to trabecular thickness, number and pattern factor. 6-week old female Balb/c WT mice received intratibial injections of $5x10^3$ 4T1 breast cancer cells into their right leg and a sham injection of PBS into their left leg. After 7 days once daily oral treatment with either vehicle or PQIP (100 mg/kg) was begun and continued for one week. Tibia were analysed by *in vivo* microCT analysis. Animals were sacrificed 14 days after intratibial injection. Trabeculae were analysed at day 7, the start of treatment (A, C and E), and at the conclusion of the experiment (B, D, and F) Trabecular aspects analysed were trabecular thickness (A, B), number (C, D) and pattern factor (E, F). Values are means ± standard deviation. 6 mice per group. *=p<0.05 from Sham, #=p<0.05 from 4T1 injected, vehicle treated.

8.4.3 PQIP inhibits breast cancer-induced osteoclast formation and resorption in mice

Detailed histomorphometry analysis was carried out to determine the cellular mechanisms behind the effects of PQIP on trabecular bone volume and attributes observed in Figures 8.2 and 8.3. Figure 8.4 shows that both osteoclast number (68% increase, $p<0.01$) and active resorption surfaces (88% increase, $p<0.01$) increased following 4T1 cell inoculation in vehicle treated mice, indicating a significant increase in osteoclast formation and function *in vivo*. Treatment with PQIP (100 mg/kg) totally prevented the increase in osteoclast number (31.8% reduction, $p<0.05$) and significantly reduced the 4T1-induced stimulation of active resorption surfaces (38.5% reduction, $p<0.05$). Serum was analysed for concentrations of C-terminal telopeptide of type I collagen (CTX) to allow conformation of the reduction in bone metabolism uncovered by histomorphometry. Figure 8.4B shows that both vehicle and PQIP treated mice demonstrated an increased concentration of CTX in serum, indicating increased bone resorption (56% increase, $p<0.05$). No reduction in serum CTX was observed in response to PQIP treatment.

A Parameter	Sham		5000 4T1 Cells	
	Vehicle	PQIP	Vehicle	PQIP
Oc.N/BS (mm-1)	1.61±0.15	1.65±0.15	2.71±0.23 *	1.85±0.11 #
ES (%)	3.69±0.29	3.44±0.31	6.94±0.7 *	4.27±0.24 #

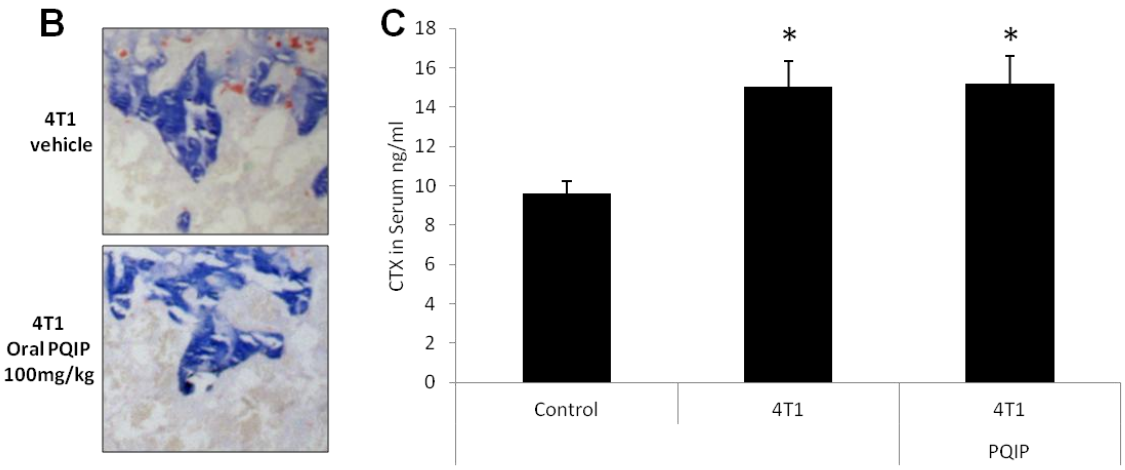

Figure 8.4 The IGF1 receptor kinase inhibitor PQIP prevents 4T1-induced increases in osteoclast number and activity *in vivo*. 6-week old female Balb/c WT mice received intratibial injections of $5x10^3$ 4T1 breast cancer cells into their right leg and a sham injection of PBS into their left leg. After 7 days once daily oral treatment with either vehicle or PQIP (100 mg/kg) was begun and continued for one week. At the conclusion of the experiment serum was collected and tibia were analysed by histomorphometry. Panel A is a table displaying the number of osteoclasts per bone surface (Oc.N/BS) and the percentage of bone surface undergoing resorption (ES%) in each group studied. Panel B displays representative images of histological sections from 4T1 injected tibia of mice treated with vehicle or oral PQIP (100 mg/kg). These are stained with Aniline blue (collagen) and TRAcP stain (Red) for the osteoclasts. Panel C shows a graph of the serum concentrations of C-terminal telopeptide of type I collagen (CTX) in the mice used in this study and control mice. Values are means ± standard deviation. 6 mice per group. *=p<0.05 from Sham, #=p<0.05 from 4T1 injected, vehicle treated.

8.4.4 PQIP inhibits basal and breast cancer-induced bone formation in mice

Detailed histomorphometry and calcein double labelling analysis was performed to examine the effect of 4T1 intratibial injection and oral PQIP treatment on osteoblasts and bone formation *in vivo*. Figure 8.5A shows that inoculation with 4T1 cells did not cause any significant change in osteoblast number, bone formation rate or osteoid surface or width. Mineral apposition rate however was moderately but significantly increased (13% increase, $p<0.05$) in the presence of the cancer cells. During the 7 days of treatment, inhibition of the IGF-1 receptor by PQIP in the absence of tumour cells did not cause a reduction in the number of osteoblasts or the area where they were producing osteoid. It did however significantly reduce the width of the osteoid (15% less, $p<0.05$), the mineral apposition rates (19% less, $p<0.01$) and most strikingly the bone formation rate (31% less, $p<0.01$). In tibiae where 4T1 cells were present, the effect of PQIP was enhanced. The 4T1 induced increase in mineral apposition rate was abolished (35% less, $p<0.01$), and bone formation rate was more than halved (53% less, $p<0.01$). In addition to the significant loss of osteoid width also observed with PQIP treatment alone, when 4T1 cells were also present PQIP decreased the percentage of bone surface covered with osteoid (29% less, $p<0.01$). Overall, PQIP treatment inhibited bone formation in the absence of cancer cells, inhibited any positive effects on bone formation observed in response to intratibial injection of 4T1 cells, and caused further negative changes to osteoblasts when in combination with cancer cells.

Serum was analysed for concentrations of procollagen type 1 amino-terminal propeptide (P1NP) to allow conformation of the reduction in bone formation observed in response to PQIP treatment. Figure 8.5B shows that the presence of 4T1 cells caused a significant increase in serum P1NP (52% increase, $p<0.05$), this effect was abolished in mice treated with PQIP ($p<0.01$).

A Parameter	Sham		5000 4T1 Cells	
	Vehicle	PQIP	Vehicle	PQIP
Ob.N/BS (mm-1)	19.2±1.4	20.12±0.61	18.2±0.7	17.8±0.54
Os.S (%)	24.4±1.7	25.0±2.17	26.2±1.1	18.7±1.2 #
Os.W	1.66±0.09	1.42±0.07	1.7±0.08	1.35±0.06 #
MAR (um/day)	3.48±0.15	2.84±0.1 *	3.92±0.11 $	2.56±0.14 *
BFR (um/day)	2.10±0.1	1.45±0.08 *	2.20±0.08	1.03±0.09 *

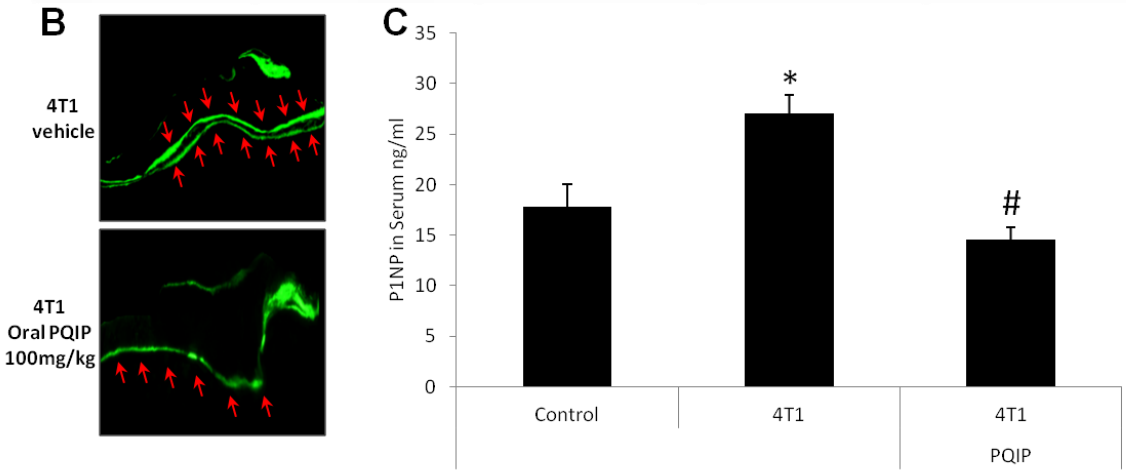

Figure 8.5 The IGF1 receptor kinase inhibitor PQIP inhibits basal and 4T1-induced increases in bone formation. 6-week old female Balb/c WT mice received intratibial injections of $5x10^3$ 4T1 breast cancer cells into their right leg and a sham injection of PBS into their left leg. After 7 days once daily oral treatment with either vehicle or PQIP (100 mg/kg) was begun and continued for one week. At the conclusion of the experiment serum was collected and tibia were analysed by histomorphometry and calcein double labelling analysis. Panel A is a table displaying the number of osteoblasts per bone surface (Ob.N/BS), the percentage of bone surface covered with osteoid (Os.S), Osteoid width (Os.W), Mineral Apposition rate (MAR) and Bone Formation Rate (BFR) in each group studied. Panel B shows representative images of calcein double labelling from 4T1 injected legs of mice treated with vehicle or oral PQIP (100 mg/kg). Panel C shows a graph of the serum concentrations of C procollagen type 1 amino-terminal propeptide (P1NP) in the mice used in this study and control mice. Values are means ± standard deviation. 6 mice per group. *=p<0.05 reduction from vehicle treated, #=p<0.05 reduction from 4T1 injected, vehicle treated, $=p<0.05 increase from sham.

8.4.5 PQIP has no effects on tumour growth and size in mice

The effect of oral PQIP treatment (100 mg/kg qd) on the growth of 4T1 breast cancer cells within the proximal tibial metaphysis was analysed through measurement of tumour volume in histological sections. Figure 8.6 shows that no significant change in tumour volume was observed.

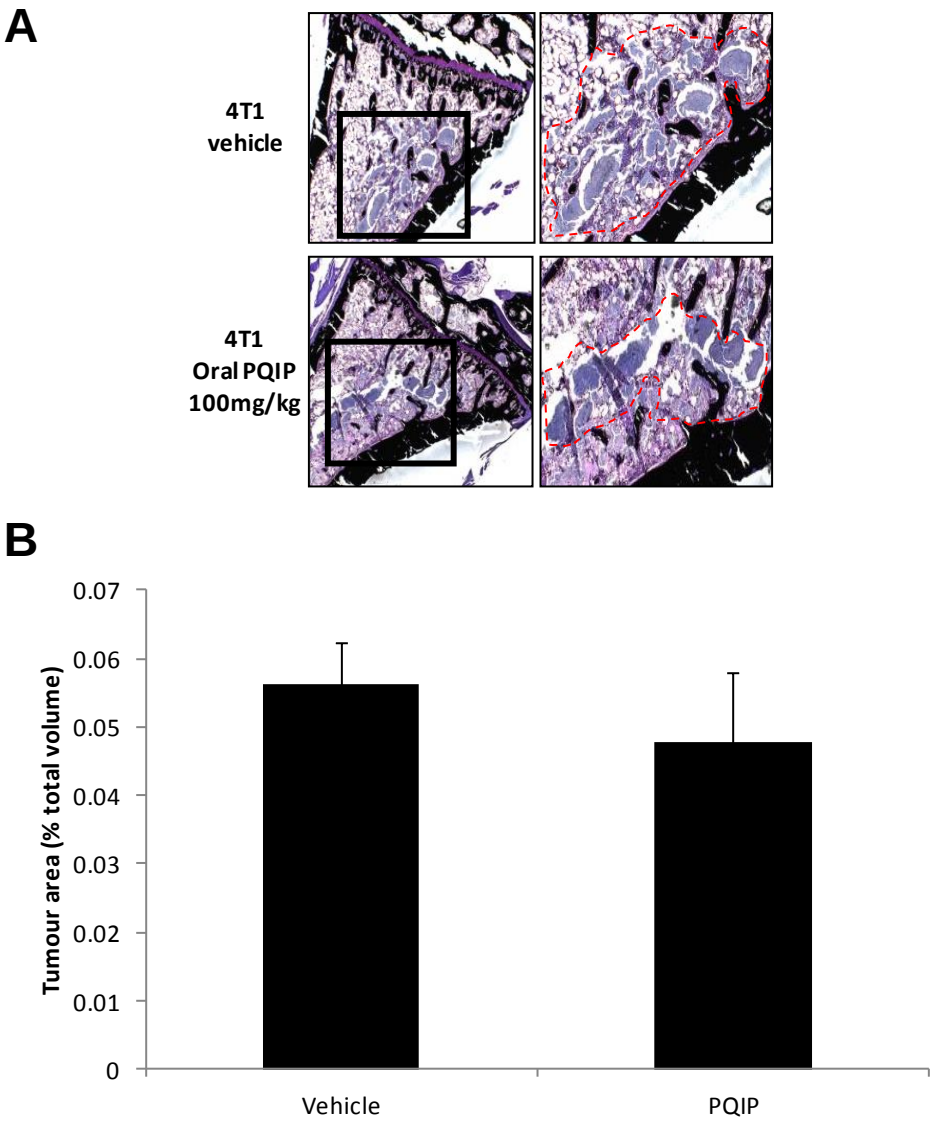

Figure 8.6 The IGF1 receptor kinase inhibitor PQIP did not inhibit 4T1 tumour growth *in vivo*. 6-week old female Balb/c WT mice received intratibial injections of $5x10^3$ 4T1 breast cancer cells into their right leg and a sham injection of PBS into their left leg. After 7 days once daily oral treatment with either vehicle or PQIP (100 mg/kg) was begun and continued for one week. At the conclusion of the experiment tumour size was analysed by histological analysis. Representative images of the histological sections stained with Von Kossa and paragon staining are shown in A. A graph of the tumour area as a percentage of total volume is displayed in B. Values are means ± standard deviation. 6 mice per group.

8.4.6 PQIP reduced body weight in mice

IGF-1 is known to play an important role in the regulation of development and growth (504-506). As shown in Figure 8.7, treatment with PQIP (100 mg/kg, qd) caused a significant reduction in body weight (13% reduction, $p < 0.05$) in mice after 7 days of continuous treatment.

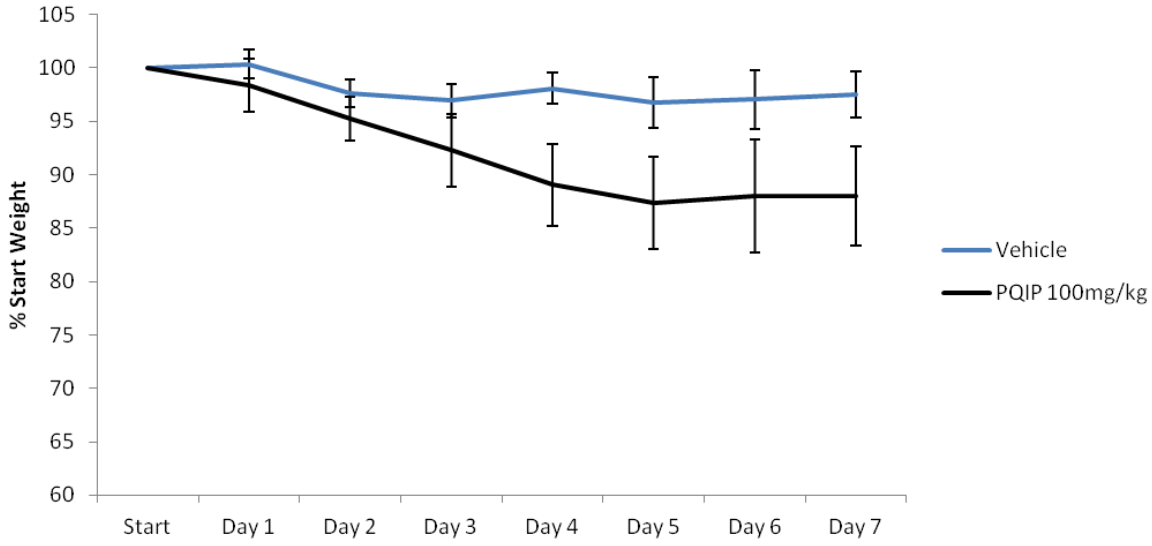

Figure 8.7 The IGF1 receptor kinase inhibitor PQIP caused a significant reduction in body weight. 6-week old female Balb/c WT mice received intratibial injections of $5x10^3$ 4T1 breast cancer cells into their right leg and a sham injection of PBS into their left leg. After 7 days once daily oral treatment with either vehicle or PQIP (100 mg/kg) was begun and continued for one week. The weights of mice were recorded every day and are displayed above. Values are means ± standard deviation. 6 mice per group.

8.4.7 PQIP has no effects on mortality in mice

No animals associated with this study died before or during the experimental period.

8.5 Discussion

IGF-1 signalling is known to be important for both bone homeostasis and in the development and metastasis of tumour cells to bone. A number of recent studies have reported that tyrosine kinase inhibitors and monoclonal antibodies that inhibit the IGF-1 receptor, alone or in combination with inhibition of other receptors, exert anti-tumour effects in animal models of cancer (507). A derivative of PQIP, OSI-906, that inhibits both IGF-1R and IR is currently in clinical trials for this very purpose (503). Here, instead of focusing on the possible effect on tumourgenesis and viability, we investigated the potential synergistic effects of IGF-1 receptor kinase inhibition on osteolytic bone disease. IGF-1 is known to be produced by tumour cells, as well as being the most abundant growth factor in the bone microenvironment, in particular being released from the bone matrix by resorption. We therefore hypothesised that inhibiting IGF-1 signalling would lead to reduced tumour induced osteolytic damage, and may also reduce the proliferation of tumour cells supported by bone and tumour derived IGF-1 production.

First, we investigated the effects of PQIP on the osteolysis associated with human breast cancer using the human MDA-MB-231 - mouse calvarial organ culture developed in chapter 4. In this culture system treatment with PQIP completely prevented MDA-MB-231-induced osteolysis leading to the observation of significantly higher calvarial bone volumes both visually in 3 dimensional μCT reconstructions, and quantifiably through μCT analysis. At concentrations that prevented osteolysis, PQIP had no effects on the survival of MDA-MB-231 breast cancer cells. This implies that IGF-1R signalling in or from breast cancer and/or bone cells may contribute to breast cancer-induced osteoclast formation and osteolysis. In this study, PQIP has been shown to reduce osteoclast number and size as well as the production of the key osteogenic factor RANKL by osteoblasts (Chapter 6). Based on these findings, it seems likely that a combination of direct inhibition of basal and tumour induced osteoclast formation, and indirect inhibition through reduction in RANKL production is responsible for the reduction in osteolysis observed.

The *in vivo* intratibial experiment presented here suffered from a variety of problems. The most obvious of which is the strong induction of trabecular bone loss observed in the sham injected legs. This was probably to be expected. Whilst every effort was made to avoid analysis of the sites of injection, it is likely that some of the observed

bone loss is due to physical destruction caused by the needle during intratibial injection, or by the pressure of the PBS fluid pushing out bone marrow as it was injected into the bone cavity. Even once the process of injection was finished, inflammatory and immune responses within the injection site are likely to have led to further loss of bone mass. In addition to this, the highly proliferative nature of the 4T1 cells and low initial seeding density meant that there was a high degree of variability between 4T1 injected legs and that only a small therapeutic window of PQIP treatment (one week) was possible.

Despite these problems the experiment was a success. 4T1 cells caused the significant reduction in trabecular bone mass indicative of osteolysis, without causing the extensive cortical damage seen in long term experiments (Chapter 4). This 4T1-induced osteolysis was characterised by a significant reduction in both trabecular number and thickness, as well as an increase in trabecular pattern factor, indicating a reduction in bone connectivity. This suggests a loss of bone caused by an increase in bone resorption, which was confirmed as histological analysis demonstrated a significant increase in both osteoclast number and resorption. Oral PQIP treatment resulted in a significant reduction but not complete prevention of these changes at the experiments conclusion. Analysis of serum from the mice at the end of the experiment showed an increase in CTX levels in mice inoculated with 4T1 cells; another indication of increased bone resorption. However in this case PQIP treatment failed to reduce the cancer induced increase. This failure is disappointing but may be explained by the high levels of variability associated with serum CTX. While every effort was made to maintain similar conditions between grouping of mice relatively minor differences in diet and time of sampling are known to cause serum CTX values to vary by up to 60% (508).

Analysis of tumour size in histological sections showed that PQIP (100 mg/kg, qd) had no effect on tumour volume within osteolytic lesions in the metaphysis of the proximal tibia. While this is disappointing, it is consistent with the results shown in Chapter 7. There it was shown that while PQIP treatment does cause apoptosis in some cancer cells (483), it had no effect on 4T1 cell viability or proliferation *in vitro*. The direct effect of PQIP on cancer cell viability has been demonstrated to be related to co-expression of ligand-receptor pairs within the IGF axis (502). It was hypothesised that preventing osteolytic destruction may also indirectly inhibit the *in vivo* growth of tumour cells by disrupting the

'vicious cycle' signalling inducing the proliferation of tumour cells. This may still be true but was not observed in this short-term study. Either the fact that 4T1 cells proliferate rapidly or the short period of treatment time could explain why this effect was not seen.

Osteoblasts were the most affected cells when PQIP was analysed *in vitro* (Chapter 6), and so osteoblast cell number and function were here analysed by histomorphometry and calcein labelling analysis. In both sham and 4T1 injected legs PQIP caused a significant reduction in both mineral apposition rates and bone formation rates. This reflects work by Zhang *et al* (2002) who showed that an osteoblast conditional knockout of IGF-1 receptor resulted in reduced mineralisation (290). Interestingly this reduction was stronger in the 4T1 injected tibia, and this could not be fully explained by the modest increase in mineral apposition rate induced by the presence of 4T1 cells. Tellingly, when osteoblast cells and osteoid were analysed by histomorphometry, only in 4T1 injected tibia did PQIP treatment cause a significant reduction in osteoblast cell number and the percentage of trabecular bone covered by osteoid. This finding is consistent with the effects of PQIP on bone nodule formation *in vitro* (Chapter 6), where only in combination did MDA-MB-231 conditioned medium and PQIP cause a reduction in osteoblast viability. Analysis of serum from the mice at the end of the experiment showed that PINP levels were significantly reduced by PQIP, thereby indicating a significant reduction in bone turnover and to some extent confirming the inhibition of bone formation and mineral apposition observed in the PQIP treated mice.

Overall, the results of the present study show that inhibition of IGF-1 receptor kinase activity in bone and tumour cells caused a significant reduction in cancer-induced osteoclastic and osteoblastic changes thereby leading to a significant reduction in bone turnover and the osteolysis associated with breast cancer. Despite this, more work is needed and there are several questions that must be answered by future research. Firstly, is the inhibition of bone loss observed significant enough to prevent further skeletal complications such as bone pain and fractures? Secondly, does the inhibition of IGF-1 receptor signalling cause a reduction in tumour cell proliferation induced by the vicious cycle? And lastly is the positive effect of the inhibition of bone loss out-weighed by the negative effects of reduced bone formation and severe side effects including dramatic weight loss? Might not PQIP treatment be of more use in the treatment of osteoblastic bone metastasis? To answer these questions different *in vivo* models and long term

experiments need to be carried out in the future. These should be models of osteoblastic bone metastases. Or if osteolytic metastases are to be studied, models should allow a greater therapeutic treatment period, should allow measurement of tumour cell numbers, and should causes less inherent damage to the bone microenvironment. Preferably they should do this whilst retaining the control of metastasis site seen in this model. To achieve this, a number of different models may have to be used including a refined intraossious injection model, and either/or an intracardiac or mammary fat pad injection model. To allow tracking and quantative observation of the tumour cells, a luminous or fluorescently tagged cell line should be used.

The aim of this chapter was not simply to evaluate the therapeutic value of PQIP, but also to test the value of the *in vivo* models of bone metastasis designed in Chapter 4. It succeeded in this, showing that while the *ex vivo* adapted calvarial organ culture is fully functional, the intratibial injection model, while still usable, has several problems. Future work should refine, expand or replace this *in vivo* model.

In conclusion, oral treatment with PQIP was demonstrated to successfully inhibit tumour cell induced osteolytic bone destruction *ex vivo* and *in vivo*. IGF-1 receptor inhibition may therefore be of use as a therapeutic treatment for osteolytic bone metastases; though the results presented here suggest it may be associated with a significant loss in both bone formation and body weight. The usefulness of the *ex vivo* adapted calvarial organ culture for bone metastases studies was successfully demonstrated, and while the *in vivo* intratibial injections provided usable results, more work is clearly needed to improve this bone metastasis model.

Chapter 9

Discussions, Conclusions and Future Work

9.1 Discussions and Conclusions

Bone metastasis is a common, painful, and often fatal occurrence associated with a number of the most common human cancers. Current treatments are insufficient and our understanding of the mechanisms underlying the interactions between bone and cancer cells is incomplete. The presence of malignant cancer cells in the bone microenvironment disrupts the bone remodelling cycle leading to imbalances in the relative amounts of bone formation and bone resorption; this then causes either excess bone formation, excess bone resorption or both. The origins of the cancer cells strongly correlate with the overall effect the malignant tumour cells have on the bone microenvironment. This clearly indicates that cancers of the same type likely interact with bone cells through crosstalk involving similar factors and signalling pathways. While some of the molecular mechanisms behind these interactions are known, most are incompletely understood, or are entirely unknown. This thesis set out with the aim to use existing and novel techniques to set up *in vitro, ex vivo* and *in vivo* models to study the interactions between osteolytic breast cancer cells and the main bone cell types. These models were then used to identify a novel therapeutic target for the treatment of osteolytic bone metastasis, and this target used to test the effectiveness of the models in a study demonstrating the effects of this novel therapeutic intervention on bone metastasis.

In Chapter 3, the initial steps of this study broke the 'vicious' cycle of bone metastasis down into three basic cellular components to allow the development of *in vitro* techniques. These components were the bone forming osteoblast cells, the bone resorbing osteoclast cells, and the osteolytic tumour cells themselves. Basic primary cell cultures and cell lines of all of these are individually frequently used and various assays are possible to look at different aspects of these cell types. To model the interactions between the cancer cells and the two bone cell types in isolation from any other influences two techniques were used; co-cultures of the cell types, and cancer conditioned medium treatments of bone cells. This allowed the development of a comprehensive *in vitro* model of these interactions involving studies using cell cultures, western blot, quantitative RT-PCR, Xcelligence analysis, and assays for cell viability, formation, differentiation, and function. Prior to this study few groups had used the simple technique of co-culturing cells to look at the interactions between these cell types. And while various groups had used conditioned

medium, few of these groups had studied the effects on bone cells using these techniques in as much depth as is presented in this study.

In Chapter 4, two separate models were used to study the overall effects of the osteolytic tumour cells on the bone microenvironment. An *ex vivo* model was used that studied tumour cells separated from the bone microenvironment in the form of organ cultures. While using an intratibial injection model allowed studies of the overall effects of interventions in an environment where all cell types and other local or global factors influencing bone turnover were present. In contrast to the success of the *in vitro* models both of these attempts to model the tumour cell-bone cell interactions had flaws, both minor and serious. In the *ex vivo* model, while the adapted calvarial organ culture was highly successful at modelling interaction in a flat bone formed by intramembraneous ossification, the adapted femoral organ cultures were a failure and clearly need further work before a *ex vivo* model of the more common long bone – bone metastasis is usable. As for the intratibial injection model, despite several flaws associated both with the technique itself and the circumstances of this study, it was shown to be a usable model of *in vivo* bone metastasis focusing purely on the effects of interactions between the bone cells and the tumour cells and ignoring the process of metastasis itself.

Chapters 3 and 4 established that osteolytic cell lines cause osteolysis through a number of different mechanisms. The human MDA-MB-231 – mouse calvaria organ cultures and 4T1 intratibial injections showed that the presence of these tumour cells leads to severe osteolysis. While the *in vitro* studies provided various mechanisms to explain this; osteolytic tumour cells caused direct stimulation of osteoclast formation, fusion, and function, indirect stimulation of bone resorption through the stimulation of RANKL production by osteoblasts, and reduction of bone formation through the inhibition of osteoblast differentiation and function. The mechanism behind this was not investigated in detail, but it was demonstrated that conditioned medium from tumour cells induced signalling through the PI3K/AKT and MAPKinase signalling pathways in both osteoclasts and osteoblasts.

As M-CSF and RANKL are the two key factors in the formation and survival of osteoclasts, the possibility of these factors being produced by osteolytic breast cancer cells was studied in detail (Chapter 5). In agreement with Ohshiba *et al*, Mancino *et al*, and Park

et al (244, 425, 468), but not Nicolin *et al* (469), I found no evidence of any expression, let alone secretion of RANKL by MDA-MB-231 cells. However, as previously noted by Mancino *et al*, Gallet *et al* and Pederson *et al* (228, 244, 464) MDA-MB-231 cells express and possibly even secrete M-CSF. While it was felt that this was notable and M-CSF is likely to be an important factor involved in cell-cell interaction, further studies on the impact of MDA-MB-231 produced M-CSF showed that either they were negligible, or that due to the dependence on exogenous M-CSF in the specific cultures used in this thesis this was not an appropriate protein to study. In light of this, it was decided to investigate other factors produced by the MDA-MB-231 cells. PTHrP, TGFβ, IL-1β and IGF-1 were identified and IGF-1 receptor was chosen for further investigation.

The IGF system has long been known to affect both bone and cancer cells in a variety of ways, but little is known about its importance in bone metastasis. Following the pattern set down by the *in vitro* models designed in Chapter 3, the effect of treatment with both IGF-1 and the novel inhibitor of IGF-1 receptor kinase, PQIP, on the individual cell types was established in Chapter 6. This was followed by looking at PQIP's effect on osteolysis and the interactions between the osteolytic cancer cells and the bone cells in Chapters 7 and 8.

The mRNA levels of IGF-1 and its receptor were measured in bone cells and it was found that IGF-1 was more highly expressed by osteoclasts while the IGF-1 receptor was found in all cell types with the highest levels being in osteoblasts. This agrees with the hypothesis that IGF-1 acts as a local autocrine/paracrine agent in the bone microenvironment, and can act as a linking agent between bone resorption and bone formation. PQIP has been previously shown to inhibit the viability of tumour cells *in vitro* and prevent their growth *in vivo* (483). In this study, except at extremely high doses, PQIP treatment did not affect the viability of any of the cell types with the exception of the MCF7 human breast cancer cell previously shown to be susceptible to IGF-1 receptor inhibition (483). Buck *et al* 2010 demonstrated that in many cell types inhibiting only IGF-1 receptor led to the upregulation of other signalling pathways including through the insulin receptor (509). This may explain the lack of any effect on viability with PQIP treatment in the cancer cells observed in this study.

In the individual cell types PQIP was found to inhibit various IGF-1 induced aspects. This included in osteoblasts, differentiation, function, migration and RANKL production, in osteoclasts, formation and fusion, and in cancer cells cell adhesion and spreading in some cell types. More importantly PQIP was found to modulate the effects cancer cells have on bone cells with opposing effects depending on the bone cell type being treated with osteolytic cancer cell conditioned medium.

In osteoblasts, PQIP increased the effect of the cancer conditioned medium, causing a further reduction in osteoblast differentiation and bone nodule formation. In addition, when in combination with the conditioned medium PQIP caused a loss of cell viability that was not seen when either treatment was given in isolation. It seems likely that the observed effects are due to separate pathways being influenced by the two treatments. The loss of IGF-1 signalling, known to be important in osteoblast differentiation and function, is compounding the overall negative effect on osteoblasts of the large number of factors produced by the cancer cells. This includes TGFβ, which is known to inhibit osteoblast differentiation and function. PQIP had two other important modulating effects in conditioned medium treated osteoblasts. First, it completely inhibited conditioned medium induced increases in the RANKL/OPG ratio, implying that *in vivo* it may prevent any indirect stimulation of osteoclast formation due to cancer cells acting on osteoblasts. Secondly, western blot experiments demonstrated that PQIP inhibited PI3K/AKT signalling induced by the osteolytic cancer conditioned medium. This provides a possible mechanism for the cancer cell induced effects on osteoblasts described above and the modulation of them by PQIP.

In contrast to osteoblasts, in osteoclasts PQIP reduced the impact the cancer cell and their derived factors had. In both co-cultures and conditioned medium studies PQIP reduced the cancer induced increase in osteoclast size and formation. These effects were focused on early formation and fusion of osteoclasts as PQIP had no effect on mature osteoclasts or cancer induced bone resorption.

The mechanisms behind the effects of PQIP at inhibiting both IGF-1 and cancer induced effects on bone cells were investigated. IGF-1 is known to stimulate signalling through the PI3K/AKT and MAPkinase signalling pathways and western blot analysis demonstrated that this occurred in the cell types used here. These pathways are known to

play roles in cell survival and proliferation in general, and osteoclast formation in particular through RANKL and M-CSF signalling. Western blot analysis excluded any indirect effect of PQIP on RANKL or M-CSF actions in osteoclasts. In each cell type IGF-1 induced phosphorylation of AKT or ERK, and pre-treatment with PQIP totally ablated this effect at concentrations as low as 200-500 nM. In osteoclasts and osteoblasts, MDA-MB-231 cancer conditioned medium was shown to stimulate PI3K/AKT and MAPKinase signaling pathways. PQIP treatment prevented any cancer conditioned medium induced stimulation of the PI3K/AKT pathway, but had no effect on activation of the MAPKinase pathway. This suggests that the inhibition of tumour-derived factors signalling through the IGF-1 receptor may have been responsible for the effects of PQIP observed in this model. IGF-1 is the factor produced by tumour cells most likely to be signalling through the IGF-1 receptor but I cannot rule out other factors acting on the receptor including IGF-2 and insulin.

I therefore hypothesised that PQIP inhibits cancer induced osteoclast formation by inhibiting the actions of tumour derived IGF-1 and other factors that act through the IGF-1 receptor as well as the autocrine/paracrine actions of bone cell derived IGF-1. This would explain the partial inhibition observed as PQIP would not inhibit the effects of the other factors produced. Further support of this hypothesis was provided by Xcelligence studies, which showed that IGF-1 treatment had a lesser but similar effect on osteoclast spreading and fusion to MDA-MB-231 conditioned medium treatment. PQIP completely abolished the IGF-1 effects in this study, but only partially reduced the impact of the conditioned medium treatment, suggesting inhibition of only the IGF-1 component of the conditioned medium.

The *ex vivo* and *in vivo* results (Chapter 8) confirmed what was seen *in vitro*, as in both cases PQIP treatment was able to inhibit cancer induced osteolysis. In particular the *in vivo* results mirrored much of the *in vitro* work, as cancer induced increases in osteoclast number were significantly reduced but not totally ablated *in vivo*, and osteoblast numbers were only significantly reduced when both cancer cells and PQIP were present. It can be assumed that the reduction in osteoclast numbers was due to multiple effects PQIP had on different cell types. It directly inhibited IGF-1 enhanced osteoclast formation both from the basal IGF-1 found in the bone microenvironment and osteoclast formation induced by the cancer cells, and also indirectly inhibited osteoclast formation and survival by inhibiting the production of RANKL by osteoblasts. The results of this *in vivo* study are encouraging,

however it should be noted that this was by necessity only a short term study of the effects of PQIP and the reduction in bone loss observed may have only been a temporary effect. In addition PQIP, as expected, strongly inhibited osteoblast function *in vivo* in sham injected legs, and even more strongly in the legs where cancer cells were present. This along with the 13% loss of weight observed in PQIP treated mice suggests that PQIP is probably not suitable as a long term treatment for osteolysis, but could be of use as a short term treatment for severe acute bone metastasis where long term effects are not a consideration. Alternatively PQIP may be of more use in the treatment of osteoblastic bone metastases such as those typified by prostate tumours. There it may both inhibit the overall bone gain, and reduce any excess osteoclast activity also stimulated by the presence of the tumour cells.

Overall, while much could be improved upon, the results reported in this thesis clearly demonstrate that the overall aims at the outset have been met. A system for specifically exploring each component part of the crosstalk between osteolytic tumour cells and bone has been designed using existing and novel techniques. The utility of this system has then been demonstrated using the example of IGF-1 receptor kinase inhibition by PQIP, and its possibilities as a novel therapeutic in this area successfully explored. Future work should complete and improve upon these model systems by developing the *ex vivo* femoral organ culture and improving upon or replacing the existing intratibial injection model of bone metastasis. Investigations into the utility of PQIP should be continued, focusing on inhibition of IGF-2 signaling, and the long term effects of PQIP treatment *in vivo*. In conclusion, this bone metastasis investigation system has been successfully implemented and makes it possible to screen targeted novel therapeutics for their effects on bone cell to cancer-cell interactions. Components of it could even be used as a high throughput screening mechanism allowing the identification of further novel targets for bone metastasis therapy. Finally, this study has highlighted the intricate nature of the molecular mechanisms and cellular cross-talk involved in bone metastasis. This reinforces the need for future investigations of potential therapeutic agents to use a combination of complex *in vivo* models and simplified *in vitro* and *ex vivo* models of bone metastasis.

9.2 On going and future work

Much of this thesis has involved the setting up and testing of existing and novel models of the interactions between bone cells and cancer cells. These models should now be utilised and expanded upon in a number of different projects. In fact several projects in the Edinburgh Bone and Cancer group are already doing this.

The first project to continue this work should, as dicussed above, complete investigations into the potential theraputic use of PQIP or indeed its analogue OSI-906 using expanded *in vivo* models of bone metastasis. These should include models of osteoblastic metastases such as those from prostate cancers, as well as models of osteolytic disease that either allow a longer treatment period for study, or also model the process of metastasis itself.

Work is ongoing to complete and expand the models described in this thesis. New MDA-MB-231 cells have been obtained that have been shown to grow in the bone microenvironment. These are being used both for intraossious implantation and intracardiac injection models of bone metastasis. They have also had bioluminescent or flourescent reporter genes incorporated into them that allow the *in vivo* monitoring and tracking of the progress of metastases. Efforts are also underway to complete the *ex vivo* model with tests of variations of the femoral organ culture in progress to determine a working version. Conditioned media experiments have also been expanded, with ongoing work demonstrating that the *in vivo* injection of MDA-MB-231 CM above the calvaria causes osteolytic bone destruction.

Another ongoing line of inquiry that arose in this thesis is the role that RANK expression in breast cancer cells may play in both the targeting of metastasising cancer cells to bone and the osteolytic damage caused by them once they are there. This has formed the basis of a new PhD project which is using the models described here to compare the metastatic potential and osteolytic effects of cancer cells with or without RANK expression knocked down using RNAi techniques. Both the RANK signalling pathway in these cells and their responses of to RANKL are also being studied in depth.

A second major project that has sprung from this thesis is an effort to identify the osteolytic factors in the conditioned medium using both ELIZAs to measure concentrations

of specific candidate factors and fractional analysis of the conditioned media followed by mass spectrometry to identify new candidates. This is then followed by similar efforts using the models to compare the effects of cancer cell with or without the candidate factors knocked down by RNAi.

In addition to these larger projects several candidate therapeutic agents have already been tested or are being tested using the models described here. These include hydrogen sulphide releasing NSAIDs (440), canabanoid agonists and antagonists, IKK inhibitors and TGFβ inhibitors.

Finally, I would propose two further projects based on this thesis. Firstly, a high throughput screen of a small molecule library could be performed using the conditioned media-osteoclast *in vitro* models. This could help to identify candidate therapeutic agents for the treatment of bone metastasis. Secondly, I would propose a reversal of the work presented here and look instead at the effect of factors produced by bone cells on cancer cells using the same conditioned media techniques presented here. This could help to identify the reasons why bone metastasis is so common, and may aid in the identification of anti-metastasis drugs to prevent the spread of cancer to bone in the first place.

Bibliography

Reference List

(1) Primer on the Metabolic Bone Diseases and Disorders of Mineral Metabolism. 5th ed. The American Society for Bone and Mineral Research.; 2006.

(2) Mescher AL. Bone. In: Mescher AL, editor. Junqueira's Basic Histology Text and Atlas. 12th ed. McGraw-Hill Medical; 2012. p. 121-39.

(3) Young B, Lowe JS, Stevens A, Heath JW. Organ Systems:Skeletal Tissues. In: Young B, Lowe JS, Stevens A, Heath JW, editors. Wheater's Functional Histology: A Text and Colour Atlas. 5th ed. Churchill Livingstone (Elsevier); 2012. p. 186-206.

(4) Eriksen EF. Cellular mechanisms of bone remodeling. Rev Endocr Metab Disord 2010;11:219-27.

(5) Ducy P. Cbfa1: a molecular switch in osteoblast biology. Dev Dyn 2000;219:461-71.

(6) Komori T, Yagi H, Nomura S, Yamaguchi A, Sasaki K, Deguchi K, et al. Targeted disruption of Cbfa1 results in a complete lack of bone formation owing to maturational arrest of osteoblasts. Cell 1997;89:755-64.

(7) Otto F, Thornell AP, Crompton T, Denzel A, Gilmour KC, Rosewell IR, et al. Cbfa1, a candidate gene for cleidocranial dysplasia syndrome, is essential for osteoblast differentiation and bone development. Cell 1997;89:765-71.

(8) Lecka-Czernik B, Gubrij I, Moerman EJ, Kajkenova O, Lipschitz DA, Manolagas SC, et al. Inhibition of Osf2/Cbfa1 expression and terminal osteoblast differentiation by PPARgamma2. J Cell Biochem 1999;74:357-71.

(9) Oyajobi BO, Lomri A, Hott M, Marie PJ. Isolation and characterization of human clonogenic osteoblast progenitors immunoselected from fetal bone marrow stroma using STRO-1 monoclonal antibody. J Bone Miner Res 1999;14:351-61.

(10) Reinhold MI, Naski MC. Direct interactions of Runx2 and canonical Wnt signaling induce FGF18. J Biol Chem 2007;282:3653-63.

(11) Zhang C, Cho K, Huang Y, Lyons JP, Zhou X, Sinha K, et al. Inhibition of Wnt signaling by the osteoblast-specific transcription factor Osterix. Proc Natl Acad Sci U S A 2008;105:6936-41.

(12) Marie PJ. Transcription factors controlling osteoblastogenesis. Arch Biochem Biophys 2008;473:98-105.

(13) Krishnan V, Moore TL, Ma YL, Helvering LM, Frolik CA, Valasek KM, et al. Parathyroid hormone bone anabolic action requires Cbfa1/Runx2-dependent signaling. Mol Endocrinol 2003;17:423-35.

(14) Wang BL, Dai CL, Quan JX, Zhu ZF, Zheng F, Zhang HX, et al. Parathyroid hormone regulates osterix and Runx2 mRNA expression predominantly through protein kinase A signaling in osteoblast-like cells. J Endocrinol Invest 2006;29:101-8.

(15) Tobimatsu T, Kaji H, Sowa H, Naito J, Canaff L, Hendy GN, et al. Parathyroid hormone increases beta-catenin levels through Smad3 in mouse osteoblastic cells. Endocrinology 2006;147:2583-90.

(16) McCarthy TL, Chang WZ, Liu Y, Centrella M. Runx2 integrates estrogen activity in osteoblasts. J Biol Chem 2003;278:43121-9.

(17) Paredes R, Arriagada G, Cruzat F, Olate J, Van Wijnen A, Lian J, et al. The Runx2 transcription factor plays a key role in the 1alpha,25-dihydroxy Vitamin D3-dependent upregulation of the rat osteocalcin (OC) gene expression in osteoblastic cells. J Steroid Biochem Mol Biol 2004;89-90:269-71.

(18) Duque G, Macoritto M, Kremer R. 1,25(OH)2D3 inhibits bone marrow adipogenesis in senescence accelerated mice (SAM-P/6) by decreasing the expression of peroxisome proliferator-activated receptor gamma 2 (PPARgamma2). Exp Gerontol 2004;39:333-8.

(19) Celil AB, Campbell PG. BMP-2 and insulin-like growth factor-I mediate Osterix (Osx) expression in human mesenchymal stem cells via the MAPK and protein kinase D signaling pathways. J Biol Chem 2005;280:31353-9.

(20) Lee MH, Kwon TG, Park HS, Wozney JM, Ryoo HM. BMP-2-induced Osterix expression is mediated by Dlx5 but is independent of Runx2. Biochem Biophys Res Commun 2003;309:689-94.

(21) Lee KS, Kim HJ, Li QL, Chi XZ, Ueta C, Komori T, et al. Runx2 is a common target of transforming growth factor beta1 and bone morphogenetic protein 2, and cooperation between Runx2 and Smad5 induces osteoblast-specific gene expression in the pluripotent mesenchymal precursor cell line C2C12. Mol Cell Biol 2000;20:8783-92.

(22) Lee MH, Kim YJ, Kim HJ, Park HD, Kang AR, Kyung HM, et al. BMP-2-induced Runx2 expression is mediated by Dlx5, and TGF-beta 1 opposes the BMP-2-induced osteoblast differentiation by suppression of Dlx5 expression. J Biol Chem 2003;278:34387-94.

(23) Ahdjoudj S, Lasmoles F, Holy X, Zerath E, Marie PJ. Transforming growth factor beta2 inhibits adipocyte differentiation induced by skeletal unloading in rat bone marrow stroma. J Bone Miner Res 2002;17:668-77.

(24) Valta MP, Hentunen T, Qu Q, Valve EM, Harjula A, Seppanen JA, et al. Regulation of osteoblast differentiation: a novel function for fibroblast growth factor 8. Endocrinology 2006;147:2171-82.

(25) Shimoyama A, Wada M, Ikeda F, Hata K, Matsubara T, Nifuji A, et al. Ihh/Gli2 signaling promotes osteoblast differentiation by regulating Runx2 expression and function. Mol Biol Cell 2007;18:2411-8.

(26) Gilbert L, He X, Farmer P, Rubin J, Drissi H, van Wijnen AJ, et al. Expression of the osteoblast differentiation factor RUNX2 (Cbfa1/AML3/Pebp2alpha A) is inhibited by tumor necrosis factor-alpha. J Biol Chem 2002;277:2695-701.

(27) Li Y, Li A, Strait K, Zhang H, Nanes MS, Weitzmann MN. Endogenous TNFalpha lowers maximum peak bone mass and inhibits osteoblastic Smad activation through NF-kappaB. J Bone Miner Res 2007;22:646-55.

(28) Katagiri T, Takahashi N. Regulatory mechanisms of osteoblast and osteoclast differentiation. Oral Dis 2002;8:147-59.

(29) Troen BR. Molecular mechanisms underlying osteoclast formation and activation. Exp Gerontol 2003;38:605-14.

(30) Manolagas SC. Birth and death of bone cells: basic regulatory mechanisms and implications for the pathogenesis and treatment of osteoporosis. Endocr Rev 2000;21:115-37.

(31) Miller SC, Bowman BM, Smith JM, Jee WS. Characterization of endosteal bone-lining cells from fatty marrow bone sites in adult beagles. Anat Rec 1980;198:163-73.

(32) Parfitt AM. Osteonal and hemi-osteonal remodeling: the spatial and temporal framework for signal traffic in adult human bone. J Cell Biochem 1994;55:273-86.

(33) Bonewald LF. The Amazing Osteocyte. J Bone Miner Res 2010;26:229-38.

(34) Mullender MG, van der Meer DD, Huiskes R, Lips P. Osteocyte density changes in aging and osteoporosis. Bone 1996;18:109-13.

(35) Mikuni-Takagaki Y, Kakai Y, Satoyoshi M, Kawano E, Suzuki Y, Kawase T, et al. Matrix mineralization and the differentiation of osteocyte-like cells in culture. J Bone Miner Res 1995;10:231-42.

(36) Franz-Odendaal TA, Hall BK, Witten PE. Buried alive: how osteoblasts become osteocytes. Dev Dyn 2006;235:176-90.

(37) Marotti G. The structure of bone tissues and the cellular control of their deposition. Ital J Anat Embryol 1996;101:25-79.

(38) Noble BS. The osteocyte lineage. Arch Biochem Biophys 2008;473:106-11.

(39) Palumbo C, Palazzini S, Marotti G. Morphological study of intercellular junctions during osteocyte differentiation. Bone 1990;11:401-6.

(40) Su M, Jiang H, Zhang P, Liu Y, Wang E, Hsu A, et al. Knee-loading modality drives molecular transport in mouse femur. Ann Biomed Eng 2006;34:1600-6.

(41) Zhao S, Zhang YK, Harris S, Ahuja SS, Bonewald LF. MLO-Y4 osteocyte-like cells support osteoclast formation and activation. J Bone Miner Res 2002;17:2068-79.

(42) Kogianni G, Mann V, Noble BS. Apoptotic bodies convey activity capable of initiating osteoclastogenesis and localized bone destruction. J Bone Miner Res 2008;23:915-27.

(43) Verborgt O, Tatton NA, Majeska RJ, Schaffler MB. Spatial distribution of Bax and Bcl-2 in osteocytes after bone fatigue: complementary roles in bone remodeling regulation? J Bone Miner Res 2002;17:907-14.

(44) Heino TJ, Hentunen TA, Vaananen HK. Osteocytes inhibit osteoclastic bone resorption through transforming growth factor-beta: enhancement by estrogen. J Cell Biochem 2002;85:185-97.

(45) Kramer I, Halleux C, Keller H, Pegurri M, Gooi JH, Weber PB, et al. Osteocyte Wnt/beta-catenin signaling is required for normal bone homeostasis. Mol Cell Biol 2010;30:3071-85.

(46) Nakashima T, Hayashi M, Fukunaga T, Kurata K, Oh-Hora M, Feng JQ, et al. Evidence for osteocyte regulation of bone homeostasis through RANKL expression. Nat Med 2011;17:1231-4.

(47) Robling AG, Bellido T, Turner CH. Mechanical stimulation in vivo reduces osteocyte expression of sclerostin. J Musculoskelet Neuronal Interact 2006;6:354.

(48) Keller H, Kneissel M. SOST is a target gene for PTH in bone. Bone 2005;37:148-58.

(49) Robling AG, Niziolek PJ, Baldridge LA, Condon KW, Allen MR, Alam I, et al. Mechanical stimulation of bone in vivo reduces osteocyte expression of Sost/sclerostin. J Biol Chem 2008;283:5866-75.

(50) Strom TM, Juppner H. PHEX, FGF23, DMP1 and beyond. Curr Opin Nephrol Hypertens 2008;17:357-62.

(51) Thompson DL, Sabbagh Y, Tenenhouse HS, Roche PC, Drezner MK, Salisbury JL, et al. Ontogeny of Phex/PHEX protein expression in mouse embryo and subcellular localization in osteoblasts. J Bone Miner Res 2002;17:311-20.

(52) Feng JQ, Ward LM, Liu S, Lu Y, Xie Y, Yuan B, et al. Loss of DMP1 causes rickets and osteomalacia and identifies a role for osteocytes in mineral metabolism. Nat Genet 2006;38:1310-5.

(53) Nampei A, Hashimoto J, Hayashida K, Tsuboi H, Shi K, Tsuji I, et al. Matrix extracellular phosphoglycoprotein (MEPE) is highly expressed in osteocytes in human bone. J Bone Miner Metab 2004;22:176-84.

(54) Liu S, Zhou J, Tang W, Menard R, Feng JQ, Quarles LD. Pathogenic role of Fgf23 in Dmp1-null mice. Am J Physiol Endocrinol Metab 2008;295:E254-E261.

(55) Feng JQ, Ward LM, Liu S, Lu Y, Xie Y, Yuan B, et al. Loss of DMP1 causes rickets and osteomalacia and identifies a role for osteocytes in mineral metabolism. Nat Genet 2006;38:1310-5.

(56) Qing H, Bonewald LF. Osteocyte remodeling of the perilacunar and pericanalicular matrix. Int J Oral Sci 2009;1:59-65.

(57) Hai Qing, PaolaDivieti Pajevic, Kevin Barry, Vladimir Dusevich, John Wysolmerski, Lynda Bonewald. PTHR1 in Osteocytes Plays a Major role in Perilacunar Remodeling through the Activation of "Osteoclastic" Genes in Osteocytes. Journal of Bone and Mineral Research 2011;25:s25.

(58) Vaananen HK, Laitala-Leinonen T. Osteoclast lineage and function. Arch Biochem Biophys 2008;473:132-8.

(59) Bar-Shavit Z. The osteoclast: a multinucleated, hematopoietic-origin, bone-resorbing osteoimmune cell. J Cell Biochem 2007;102:1130-9.

(60) Boyle WJ, Simonet WS, Lacey DL. Osteoclast differentiation and activation. Nature 2003;423:337-42.

(61) Boyce BF, Xing L. Functions of RANKL/RANK/OPG in bone modeling and remodeling. Arch Biochem Biophys 2008;473:139-46.

(62) Weir EC, Horowitz MC, Baron R, Centrella M, Kacinski BM, Insogna KL. Macrophage colony-stimulating factor release and receptor expression in bone cells. J Bone Miner Res 1993;8:1507-18.

(63) Teitelbaum SL. Bone resorption by osteoclasts. Science 2000;289:1504-8.

(64) Takayanagi H. Mechanistic insight into osteoclast differentiation in osteoimmunology. J Mol Med 2005;83:170-9.

(65) Miyamoto T, Ohneda O, Arai F, Iwamoto K, Okada S, Takagi K, et al. Bifurcation of osteoclasts and dendritic cells from common progenitors. Blood 2001;98:2544-54.

(66) Jones DH, Kong YY, Penninger JM. Role of RANKL and RANK in bone loss and arthritis. Ann Rheum Dis 2002;61 Suppl 2:ii32-ii39.

(67) Kong YY, Yoshida H, Sarosi I, Tan HL, Timms E, Capparelli C, et al. OPGL is a key regulator of osteoclastogenesis, lymphocyte development and lymph-node organogenesis. Nature 1999;397:315-23.

(68) Horowitz MC, Xi Y, Wilson K, Kacena MA. Control of osteoclastogenesis and bone resorption by members of the TNF family of receptors and ligands. Cytokine Growth Factor Rev 2001;12:9-18.

(69) Pfeilschifter J, Chenu C, Bird A, Mundy GR, Roodman GD. Interleukin-1 and tumor necrosis factor stimulate the formation of human osteoclastlike cells in vitro. J Bone Miner Res 1989;4:113-8.

(70) Lacey DL, Erdmann JM, Teitelbaum SL, Tan HL, Ohara J, Shioi A. Interleukin 4, interferon-gamma, and prostaglandin E impact the osteoclastic cell-forming potential of murine bone marrow macrophages. Endocrinology 1995;136:2367-76.

(71) Jilka RL. Cytokines, bone remodeling, and estrogen deficiency: a 1998 update. Bone 1998;23:75-81.

(72) Yan T, Riggs BL, Boyle WJ, Khosla S. Regulation of osteoclastogenesis and RANK expression by TGF-beta1. J Cell Biochem 2001;83:320-5.

(73) Suda T, Nakamura I, Jimi E, Takahashi N. Regulation of osteoclast function. J Bone Miner Res 1997;12:869-79.

(74) Lerner UH. Osteoclast formation and resorption. Matrix Biol 2000;19:107-20.

(75) Noble BS, Peet N, Stevens HY, Brabbs A, Mosley JR, Reilly GC, et al. Mechanical loading: biphasic osteocyte survival and targeting of osteoclasts for bone destruction in rat cortical bone. Am J Physiol Cell Physiol 2003;284:C934-C943.

(76) Jurdic P, Saltel F, Chabadel A, Destaing O. Podosome and sealing zone: specificity of the osteoclast model. Eur J Cell Biol 2006;85:195-202.

(77) Chabadel A, Banon-Rodriguez I, Cluet D, Rudkin BB, Wehrle-Haller B, Genot E, et al. CD44 and beta3 integrin organize two functionally distinct actin-based domains in osteoclasts. Mol Biol Cell 2007;18:4899-910.

(78) Teitelbaum SL, Abu-Amer Y, Ross FP. Molecular mechanisms of bone resorption. J Cell Biochem 1995;59:1-10.

(79) Sundquist KT, Leppilampi M, Jarvelin K, Kumpulainen T, Vaananen HK. Carbonic anhydrase isoenzymes in isolated rat peripheral monocytes, tissue macrophages, and osteoclasts. Bone 1987;8:33-8.

(80) Blair HC, Teitelbaum SL, Ghiselli R, Gluck S. Osteoclastic bone resorption by a polarized vacuolar proton pump. Science 1989;245:855-7.

(81) Vaananen HK, Karhukorpi EK, Sundquist K, Wallmark B, Roininen I, Hentunen T, et al. Evidence for the presence of a proton pump of the vacuolar H(+)-ATPase type in the ruffled borders of osteoclasts. J Cell Biol 1990;111:1305-11.

(82) Teti A, Blair HC, Teitelbaum SL, Kahn JA, Carano A, Grano M, et al. Cytoplasmic pH is regulated in isolated avian osteoclasts by a Cl-/HCO3- exchanger. Boll Soc Ital Biol Sper 1989;65:589-95.

(83) Schaller S, Henriksen K, Sorensen MG, Karsdal MA. The role of chloride channels in osteoclasts: ClC-7 as a target for osteoporosis treatment. Drug News Perspect 2005;18:489-95.

(84) Gowen M, Lazner F, Dodds R, Kapadia R, Feild J, Tavaria M, et al. Cathepsin K knockout mice develop osteopetrosis due to a deficit in matrix degradation but not demineralization. J Bone Miner Res 1999;14:1654-63.

(85) Vaananen K. Mechanism of osteoclast mediated bone resorption--rationale for the design of new therapeutics. Adv Drug Deliv Rev 2005;57:959-71.

(86) Hayman AR, Macary P, Lehner PJ, Cox TM. Tartrate-resistant acid phosphatase (Acp 5): identification in diverse human tissues and dendritic cells. J Histochem Cytochem 2001;49:675-84.

(87) Hayman AR, Cox TM. Tartrate-resistant acid phosphatase knockout mice. J Bone Miner Res 2003;18:1905-7.

(88) Goldring MB. Update on the biology of the chondrocyte and new approaches to treating cartilage diseases. Best Pract Res Clin Rheumatol 2006;20:1003-25.

(89) Cole AG. A review of diversity in the evolution and development of cartilage: the search for the origin of the chondrocyte. Eur Cell Mater 2011;21:122-9.

(90) Hall BK, Miyake T. All for one and one for all: condensations and the initiation of skeletal development. Bioessays 2000;22:138-47.

(91) Karsenty G, Wagner EF. Reaching a genetic and molecular understanding of skeletal development. Dev Cell 2002;2:389-406.

(92) Bi W, Deng JM, Zhang Z, Behringer RR, de Crombrugghe B. Sox9 is required for cartilage formation. Nat Genet 1999;22:85-9.

(93) Ng LJ, Wheatley S, Muscat GE, Conway-Campbell J, Bowles J, Wright E, et al. SOX9 binds DNA, activates transcription, and coexpresses with type II collagen during chondrogenesis in the mouse. Dev Biol 1997;183:108-21.

(94) Lefebvre V, Li P, de Crombrugghe B. A new long form of Sox5 (L-Sox5), Sox6 and Sox9 are coexpressed in chondrogenesis and cooperatively activate the type II collagen gene. EMBO J 1998;17:5718-33.

(95) Yoshida CA, Yamamoto H, Fujita T, Furuichi T, Ito K, Inoue K, et al. Runx2 and Runx3 are essential for chondrocyte maturation, and Runx2 regulates limb growth through induction of Indian hedgehog. Genes Dev 2004;18:952-63.

(96) Rosen ED, MacDougald OA. Adipocyte differentiation from the inside out. Nat Rev Mol Cell Biol 2006;7:885-96.

(97) Tamori Y, Masugi J, Nishino N, Kasuga M. Role of peroxisome proliferator-activated receptor-gamma in maintenance of the characteristics of mature 3T3-L1 adipocytes. Diabetes 2002;51:2045-55.

(98) Snyder F. Fatty acid oxidation in irradiated bone marrow cells. Nature 1965;206:733.

(99) Naveiras O, Nardi V, Wenzel PL, Hauschka PV, Fahey F, Daley GQ. Bone-marrow adipocytes as negative regulators of the haematopoietic microenvironment. Nature 2009;460:259-63.

(100) Sugimura R, Li L. Shifting in balance between osteogenesis and adipogenesis substantially influences hematopoiesis. J Mol Cell Biol 2010;2:61-2.

(101) Linsenmayer TF, Chen QA, Gibney E, Gordon MK, Marchant JK, Mayne R, et al. Collagen types IX and X in the developing chick tibiotarsus: analyses of mRNAs and proteins. Development 1991;111:191-6.

(102) White A, Wallis G. Endochondral ossification: a delicate balance between growth and mineralisation. Curr Biol 2001;11:R589-R591.

(103) Ortega N, Behonick DJ, Werb Z. Matrix remodeling during endochondral ossification. Trends Cell Biol 2004;14:86-93.

(104) Hirao M, Tamai N, Tsumaki N, Yoshikawa H, Myoui A. Oxygen tension regulates chondrocyte differentiation and function during endochondral ossification. J Biol Chem 2006;281:31079-92.

(105) Lewinson D, Silbermann M. Chondroclasts and endothelial cells collaborate in the process of cartilage resorption. Anat Rec 1992;233:504-14.

(106) Salle BL, Rauch F, Travers R, Bouvier R, Glorieux FH. Human fetal bone development: histomorphometric evaluation of the proximal femoral metaphysis. Bone 2002;30:823-8.

(107) Nilsson O, Baron J. Fundamental limits on longitudinal bone growth: growth plate senescence and epiphyseal fusion. Trends Endocrinol Metab 2004;15:370-4.

(108) Gilbert SF. Osteogenesis: The Development of Bones. Developmental Biology. 6th ed. Sunderland (MA): Sinauer Associates; 2000.

(109) Bonucci E. Bone mineralization. Front Biosci 2012;17:100-28.

(110) Primer on the Metabolic Bone Diseases and Disorders of Mineral Metabolism. 7th ed. The American Society for Bone and Mineral Research.; 2008.

(111) Golub EE. Role of matrix vesicles in biomineralization. Biochim Biophys Acta 2009;1790:1592-8.

(112) Golub EE. Biomineralization and matrix vesicles in biology and pathology. Semin Immunopathol 2011;33:409-17.

(113) Orimo H. The mechanism of mineralization and the role of alkaline phosphatase in health and disease. J Nihon Med Sch 2010;77:4-12.

(114) Rosen CJ. Breaking into bone biology: serotonin's secrets. Nat Med 2009;15:145-6.

(115) Hill PA. Bone remodelling. Br J Orthod 1998;25:101-7.

(116) Hadjidakis DJ, Androulakis II. Bone remodeling. Ann N Y Acad Sci 2006;1092:385-96.

(117) Meikle MC, Bord S, Hembry RM, Compston J, Croucher PI, Reynolds JJ. Human osteoblasts in culture synthesize collagenase and other matrix metalloproteinases in response to osteotropic hormones and cytokines. J Cell Sci 1992;103 (Pt 4):1093-9.

(118) Proff P, Romer P. The molecular mechanism behind bone remodelling: a review. Clin Oral Investig 2009;13:355-62.

(119) Hsu H, Lacey DL, Dunstan CR, Solovyev I, Colombero A, Timms E, et al. Tumor necrosis factor receptor family member RANK mediates osteoclast differentiation and activation induced by osteoprotegerin ligand. Proc Natl Acad Sci U S A 1999;96:3540-5.

(120) Umeda S, Takahashi K, Naito M, Shultz LD, Takagi K. Neonatal changes of osteoclasts in osteopetrosis (op/op) mice defective in production of functional macrophage colony-stimulating factor (M-CSF) protein and effects of M-CSF on osteoclast development and differentiation. J Submicrosc Cytol Pathol 1996;28:13-26.

(121) Lakkakorpi PT, Horton MA, Helfrich MH, Karhukorpi EK, Vaananen HK. Vitronectin receptor has a role in bone resorption but does not mediate tight sealing zone attachment of osteoclasts to the bone surface. J Cell Biol 1991;115:1179-86.

(122) Roodman GD. Advances in bone biology: the osteoclast. Endocr Rev 1996;17:308-32.

(123) Parikka V, Lehenkari P, Sassi ML, Halleen J, Risteli J, Harkonen P, et al. Estrogen reduces the depth of resorption pits by disturbing the organic bone matrix degradation activity of mature osteoclasts. Endocrinology 2001;142:5371-8.

(124) Lerner UH. Bone remodeling in post-menopausal osteoporosis. J Dent Res 2006;85:584-95.

(125) Zaidi M. "Calcium receptors" on eukaryotic cells with special reference to the osteoclast. Biosci Rep 1990;10:493-507.

(126) Pfeilschifter J, Wolf O, Naumann A, Minne HW, Mundy GR, Ziegler R. Chemotactic response of osteoblastlike cells to transforming growth factor beta. J Bone Miner Res 1990;5:825-30.

(127) Pfeilschifter J, Bonewald L, Mundy GR. Characterization of the latent transforming growth factor beta complex in bone. J Bone Miner Res 1990;5:49-58.

(128) Mundy GR, Rodan SB, Majeska RJ, DeMartino S, Trimmier C, Martin TJ, et al. Unidirectional migration of osteosarcoma cells with osteoblast characteristics in response to products of bone resorption. Calcif Tissue Int 1982;34:542-6.

(129) Sutherland MK, Geoghegan JC, Yu C, Turcott E, Skonier JE, Winkler DG, et al. Sclerostin promotes the apoptosis of human osteoblastic cells: a novel regulation of bone formation. Bone 2004;35:828-35.

(130) Jilka RL, Weinstein RS, Bellido T, Parfitt AM, Manolagas SC. Osteoblast programmed cell death (apoptosis): modulation by growth factors and cytokines. J Bone Miner Res 1998;13:793-802.

(131) Teti A. Bone development: overview of bone cells and signaling. Curr Osteoporos Rep 2011;9:264-73.

(132) Garcia RA, Inwards CY, Unni KK. Benign bone tumors--recent developments. Semin Diagn Pathol 2011;28:73-85.

(133) Lee EH, Shafi M, Hui JH. Osteoid osteoma: a current review. J Pediatr Orthop 2006;26:695-700.

(134) Mungo DV, Zhang X, O'Keefe RJ, Rosier RN, Puzas JE, Schwarz EM. COX-1 and COX-2 expression in osteoid osteomas. J Orthop Res 2002;20:159-62.

(135) Mylona S, Patsoura S, Galani P, Karapostolakis G, Pomoni A, Thanos L. Osteoid osteomas in common and in technically challenging locations treated with computed tomography-guided percutaneous radiofrequency ablation. Skeletal Radiol 2010;39:443-9.

(136) Lucas DR. Osteoblastoma. Arch Pathol Lab Med 2010;134:1460-6.

(137) Berry M, Mankin H, Gebhardt M, Rosenberg A, Hornicek F. Osteoblastoma: a 30-year study of 99 cases. J Surg Oncol 2008;98:179-83.

(138) DiCaprio MR, Enneking WF. Fibrous dysplasia. Pathophysiology, evaluation, and treatment. J Bone Joint Surg Am 2005;87:1848-64.

(139) Dorfman HD. New knowledge of fibro-osseous lesions of bone. Int J Surg Pathol 2010;18:62S-5S.

(140) Chapurlat RD, Orcel P. Fibrous dysplasia of bone and McCune-Albright syndrome. Best Pract Res Clin Rheumatol 2008;22:55-69.

(141) Romeo S, Hogendoorn PC, Dei Tos AP. Benign cartilaginous tumors of bone: from morphology to somatic and germ-line genetics. Adv Anat Pathol 2009;16:307-15.

(142) Bovee JV, Hogendoorn PC, Wunder JS, Alman BA. Cartilage tumours and bone development: molecular pathology and possible therapeutic targets. Nat Rev Cancer 2010;10:481-8.

(143) Yamaguchi T, Suzuki S, Ishiiwa H, Shimizu K, Ueda Y. Benign notochordal cell tumors: A comparative histological study of benign notochordal cell tumors, classic chordomas, and notochordal vestiges of fetal intervertebral discs. Am J Surg Pathol 2004;28:756-61.

(144) Yamaguchi T, Suzuki S, Ishiiwa H, Ueda Y. Intraosseous benign notochordal cell tumours: overlooked precursors of classic chordomas? Histopathology 2004;44:597-602.

(145) Hameed M, Dorfman H. Primary malignant bone tumors--recent developments. Semin Diagn Pathol 2011;28:86-101.

(146) Posthumadeboer J, Witlox MA, Kaspers GJ, van Royen BJ. Molecular alterations as target for therapy in metastatic osteosarcoma: a review of literature. Clin Exp Metastasis 2011;28:493-503.

(147) Klein MJ, Siegal GP. Osteosarcoma: anatomic and histologic variants. Am J Clin Pathol 2006;125:555-81.

(148) McNairn JD, Damron TA, Landas SK, Ambrose JL, Shrimpton AE. Inheritance of osteosarcoma and Paget's disease of bone: a familial loss of heterozygosity study. J Mol Diagn 2001;3:171-7.

(149) Ragland BD, Bell WC, Lopez RR, Siegal GP. Cytogenetics and molecular biology of osteosarcoma. Lab Invest 2002;82:365-73.

(150) Ferrari S, Briccoli A, Mercuri M, Bertoni F, Picci P, Tienghi A, et al. Postrelapse survival in osteosarcoma of the extremities: prognostic factors for long-term survival. J Clin Oncol 2003;21:710-5.

(151) Kempf-Bielack B, Bielack SS, Jurgens H, Branscheid D, Berdel WE, Exner GU, et al. Osteosarcoma relapse after combined modality therapy: an analysis of unselected patients in the Cooperative Osteosarcoma Study Group (COSS). J Clin Oncol 2005;23:559-68.

(152) Paulussen M, Bielack S, Jurgens H, Casali PG. Ewing's sarcoma of the bone: ESMO clinical recommendations for diagnosis, treatment and follow-up. Ann Oncol 2009;20 Suppl 4:140-2.

(153) Gurney JG, Severson RK, Davis S, Robison LL. Incidence of cancer in children in the United States. Sex-, race-, and 1-year age-specific rates by histologic type. Cancer 1995;75:2186-95.

(154) Aurias A, Rimbaut C, Buffe D, Dubousset J, Mazabraud A. [Translocation of chromosome 22 in Ewing's sarcoma]. C R Seances Acad Sci III 1983;296:1105-7.

(155) Balamuth NJ, Womer RB. Ewing's sarcoma. Lancet Oncol 2010;11:184-92.

(156) Cotterill SJ, Ahrens S, Paulussen M, Jurgens HF, Voute PA, Gadner H, et al. Prognostic factors in Ewing's tumor of bone: analysis of 975 patients from the European Intergroup Cooperative Ewing's Sarcoma Study Group. J Clin Oncol 2000;18:3108-14.

(157) Bacci G, Ferrari S, Longhi A, Donati D, De PM, Forni C, et al. Therapy and survival after recurrence of Ewing's tumors: the Rizzoli experience in 195 patients treated with adjuvant and neoadjuvant chemotherapy from 1979 to 1997. Ann Oncol 2003;14:1654-9.

(158) Soldatos T, McCarthy EF, Attar S, Carrino JA, Fayad LM. Imaging features of chondrosarcoma. J Comput Assist Tomogr 2011;35:504-11.

(159) Jamil N, Howie S, Salter DM. Therapeutic molecular targets in human chondrosarcoma. Int J Exp Pathol 2010;91:387-93.

(160) Lin PP, Moussallem CD, Deavers MT. Secondary chondrosarcoma. J Am Acad Orthop Surg 2010;18:608-15.

(161) Dorfman HD, Czerniak B. Bone cancers. Cancer 1995;75:203-10.

(162) Papagelopoulos PJ, Galanis E, Frassica FJ, Sim FH, Larson DR, Wold LE. Primary fibrosarcoma of bone. Outcome after primary surgical treatment. Clin Orthop Relat Res 2000;88-103.

(163) Raab MS, Podar K, Breitkreutz I, Richardson PG, Anderson KC. Multiple myeloma. Lancet 2009;374:324-39.

(164) Cohen HJ, Crawford J, Rao MK, Pieper CF, Currie MS. Racial differences in the prevalence of monoclonal gammopathy in a community-based sample of the elderly. Am J Med 1998;104:439-44.

(165) Raje N, Roodman GD. Advances in the biology and treatment of bone disease in multiple myeloma. Clin Cancer Res 2011;17:1278-86.

(166) Terpos E, Sezer O, Croucher P, Dimopoulos MA. Myeloma bone disease and proteasome inhibition therapies. Blood 2007;110:1098-104.

(167) Edwards CM, Zhuang J, Mundy GR. The pathogenesis of the bone disease of multiple myeloma. Bone 2008;42:1007-13.

(168) Lichtenstein A, Berenson J, Norman D, Chang MP, Carlile A. Production of cytokines by bone marrow cells obtained from patients with multiple myeloma. Blood 1989;74:1266-73.

(169) Lee JW, Chung HY, Ehrlich LA, Jelinek DF, Callander NS, Roodman GD, et al. IL-3 expression by myeloma cells increases both osteoclast formation and growth of myeloma cells. Blood 2004;103:2308-15.

(170) Kawano M, Hirano T, Matsuda T, Taga T, Horii Y, Iwato K, et al. Autocrine generation and requirement of BSF-2/IL-6 for human multiple myelomas. Nature 1988;332:83-5.

(171) Pearse RN, Sordillo EM, Yaccoby S, Wong BR, Liau DF, Colman N, et al. Multiple myeloma disrupts the TRANCE/ osteoprotegerin cytokine axis to trigger bone destruction and promote tumor progression. Proc Natl Acad Sci U S A 2001;98:11581-6.

(172) Farrugia AN, Atkins GJ, To LB, Pan B, Horvath N, Kostakis P, et al. Receptor activator of nuclear factor-kappaB ligand expression by human myeloma cells mediates osteoclast formation in vitro and correlates with bone destruction in vivo. Cancer Res 2003;63:5438-45.

(173) Greipp PR, San MJ, Durie BG, Crowley JJ, Barlogie B, Blade J, et al. International staging system for multiple myeloma. J Clin Oncol 2005;23:3412-20.

(174) Machado M, Cruz LS, Tannus G, Fonseca M. Efficacy of clodronate, pamidronate, and zoledronate in reducing morbidity and mortality in cancer patients with bone metastasis: a meta-analysis of randomized clinical trials. Clin Ther 2009;31:962-79.

(175) Mundy GR. Metastasis to bone: causes, consequences and therapeutic opportunities. Nat Rev Cancer 2002;2:584-93.

(176) Sterling JA, Edwards JR, Martin TJ, Mundy GR. Advances in the biology of bone metastasis: how the skeleton affects tumor behavior. Bone 2011;48:6-15.

(177) Langley RR, Fidler IJ. The seed and soil hypothesis revisited--the role of tumor-stroma interactions in metastasis to different organs. Int J Cancer 2011;128:2527-35.

(178) Cancer Facts and Figures, 2007. 1913.

(179) Tubiana-Hulin M. Incidence, prevalence and distribution of bone metastases. Bone 1991;12 Suppl 1:S9-10.

(180) Suva LJ, Washam C, Nicholas RW, Griffin RJ. Bone metastasis: mechanisms and therapeutic opportunities. Nat Rev Endocrinol 2011;7:208-18.

(181) Kozlow W, Guise TA. Breast cancer metastasis to bone: mechanisms of osteolysis and implications for therapy. J Mammary Gland Biol Neoplasia 2005;10:169-80.

(182) Coleman RE. Metastatic bone disease: clinical features, pathophysiology and treatment strategies. Cancer Treat Rev 2001;27:165-76.

(183) Lipton A. Future treatment of bone metastases. Clin Cancer Res 2006;12:6305s-8s.

(184) van der Linden YM, Dijkstra SP, Vonk EJ, Marijnen CA, Leer JW. Prediction of survival in patients with metastases in the spinal column: results based on a randomized trial of radiotherapy. Cancer 2005;103:320-8.

(185) Paget S. The distribution of secondary growths in cancer of the breast. Lancet 1889;1:571-3.

(186) Ewing J. Neoplastic Diseases. 3rd ed. Philadelphia: 1928.

(187) Chaffer CL, Weinberg RA. A perspective on cancer cell metastasis. Science 2011;331:1559-64.

(188) Coghlin C, Murray GI. Current and emerging concepts in tumour metastasis. J Pathol 2010;222:1-15.

(189) van der Pluijm G. Epithelial plasticity, cancer stem cells and bone metastasis formation. Bone 2011;48:37-43.

(190) Thiery JP, Acloque H, Huang RY, Nieto MA. Epithelial-mesenchymal transitions in development and disease. Cell 2009;139:871-90.

(191) Kalluri R, Weinberg RA. The basics of epithelial-mesenchymal transition. J Clin Invest 2009;119:1420-8.

(192) Ota I, Li XY, Hu Y, Weiss SJ. Induction of a MT1-MMP and MT2-MMP-dependent basement membrane transmigration program in cancer cells by Snail1. Proc Natl Acad Sci U S A 2009;106:20318-23.

(193) Huang CH, Yang WH, Chang SY, Tai SK, Tzeng CH, Kao JY, et al. Regulation of membrane-type 4 matrix metalloproteinase by SLUG contributes to hypoxia-mediated metastasis. Neoplasia 2009;11:1371-82.

(194) Orlichenko LS, Radisky DC. Matrix metalloproteinases stimulate epithelial-mesenchymal transition during tumor development. Clin Exp Metastasis 2008;25:593-600.

(195) Bonnomet A, Brysse A, Tachsidis A, Waltham M, Thompson EW, Polette M, et al. Epithelial-to-mesenchymal transitions and circulating tumor cells. J Mammary Gland Biol Neoplasia 2010;15:261-73.

(196) Bruce Alberts, Alexander Johnson, Julian Lewis, Martin Raff, Keith Roberts, Peter Walter. Molecular Biology of the Cell. 4th ed. New York: Garland Science; 2002.

(197) Suva LJ, Griffin RJ, Makhoul I. Mechanisms of bone metastases of breast cancer. Endocr Relat Cancer 2009;16:703-13.

(198) Coleman RE. Skeletal complications of malignancy. Cancer 1997;80:1588-94.

(199) Charhon SA, Chapuy MC, Delvin EE, Valentin-Opran A, Edouard CM, Meunier PJ. Histomorphometric analysis of sclerotic bone metastases from prostatic carcinoma special reference to osteomalacia. Cancer 1983;51:918-24.

(200) Roudier MP, Morrissey C, True LD, Higano CS, Vessella RL, Ott SM. Histopathological assessment of prostate cancer bone osteoblastic metastases. J Urol 2008;180:1154-60.

(201) Coleman RE. Conclusion: Bone markers in metastatic bone disease. Cancer Treat Rev 2006;32 Suppl 1:27-8.

(202) Karaplis AC, Goltzman D. PTH and PTHrP effects on the skeleton. Rev Endocr Metab Disord 2000;1:331-41.

(203) Thomas RJ, Guise TA, Yin JJ, Elliott J, Horwood NJ, Martin TJ, et al. Breast cancer cells interact with osteoblasts to support osteoclast formation. Endocrinology 1999;140:4451-8.

(204) Guise TA. The vicious cycle of bone metastases. J Musculoskelet Neuronal Interact 2002;2:570-2.

(205) Guise TA, Mohammad KS, Clines G, Stebbins EG, Wong DH, Higgins LS, et al. Basic mechanisms responsible for osteolytic and osteoblastic bone metastases. Clin Cancer Res 2006;12:6213s-6s.

(206) Van SC, Wang G, Anderson MG, Trask OJ, Lesniewski R, Semizarov D. Endothelin signaling in osteoblasts: global genome view and implication of the calcineurin/NFAT pathway. Mol Cancer Ther 2007;6:253-61.

(207) Ikeda T, Kasai M, Utsuyama M, Hirokawa K. Determination of three isoforms of the receptor activator of nuclear factor-kappaB ligand and their differential expression in bone and thymus. Endocrinology 2001;142:1419-26.

(208) Wong BR, Rho J, Arron J, Robinson E, Orlinick J, Chao M, et al. TRANCE is a novel ligand of the tumor necrosis factor receptor family that activates c-Jun N-terminal kinase in T cells. J Biol Chem 1997;272:25190-4.

(209) Anderson DM, Maraskovsky E, Billingsley WL, Dougall WC, Tometsko ME, Roux ER, et al. A homologue of the TNF receptor and its ligand enhance T-cell growth and dendritic-cell function. Nature 1997;390:175-9.

(210) Sobacchi C, Frattini A, Guerrini MM, Abinun M, Pangrazio A, Susani L, et al. Osteoclast-poor human osteopetrosis due to mutations in the gene encoding RANKL. Nat Genet 2007;39:960-2.

(211) Franzoso G, Carlson L, Xing L, Poljak L, Shores EW, Brown KD, et al. Requirement for NF-kappaB in osteoclast and B-cell development. Genes Dev 1997;11:3482-96.

(212) Dougall WC, Glaccum M, Charrier K, Rohrbach K, Brasel K, De Smedt T, et al. RANK is essential for osteoclast and lymph node development. Genes Dev 1999;13:2412-24.

(213) Fata JE, Kong YY, Li J, Sasaki T, Irie-Sasaki J, Moorehead RA, et al. The osteoclast differentiation factor osteoprotegerin-ligand is essential for mammary gland development. Cell 2000;103:41-50.

(214) Wada T, Nakashima T, Hiroshi N, Penninger JM. RANKL-RANK signaling in osteoclastogenesis and bone disease. Trends Mol Med 2006;12:17-25.

(215) Kapur RP, Yao Z, Iida MH, Clarke CM, Doggett B, Xing L, et al. Malignant autosomal recessive osteopetrosis caused by spontaneous mutation of murine Rank. J Bone Miner Res 2004;19:1689-97.

(216) Simonet WS, Lacey DL, Dunstan CR, Kelley M, Chang MS, Luthy R, et al. Osteoprotegerin: a novel secreted protein involved in the regulation of bone density. Cell 1997;89:309-19.

(217) Yasuda H, Shima N, Nakagawa N, Mochizuki SI, Yano K, Fujise N, et al. Identity of osteoclastogenesis inhibitory factor (OCIF) and osteoprotegerin (OPG): a mechanism by which OPG/OCIF inhibits osteoclastogenesis in vitro. Endocrinology 1998;139:1329-37.

(218) Bennett BJ, Scatena M, Kirk EA, Rattazzi M, Varon RM, Averill M, et al. Osteoprotegerin inactivation accelerates advanced atherosclerotic lesion progression and calcification in older ApoE-/- mice. Arterioscler Thromb Vasc Biol 2006;26:2117-24.

(219) Van Campenhout A, Golledge J. Osteoprotegerin, vascular calcification and atherosclerosis. Atherosclerosis 2008.

(220) Mizuno A, Amizuka N, Irie K, Murakami A, Fujise N, Kanno T, et al. Severe osteoporosis in mice lacking osteoclastogenesis inhibitory factor/osteoprotegerin. Biochem Biophys Res Commun 1998;247:610-5.

(221) Riches PL, McRorie E, Fraser WD, Determann C, van't Hof R, Ralston SH. Osteoporosis associated with neutralizing autoantibodies against osteoprotegerin. N Engl J Med 2009;361:1459-65.

(222) Daroszewska A, Ralston SH. Mechanisms of disease: genetics of Paget's disease of bone and related disorders. Nat Clin Pract Rheumatol 2006;2:270-7.

(223) Cundy T, Hegde M, Naot D, Chong B, King A, Wallace R, et al. A mutation in the gene TNFRSF11B encoding osteoprotegerin causes an idiopathic hyperphosphatasia phenotype. Hum Mol Genet 2002;11:2119-27.

(224) Hofbauer LC, Schoppet M. Clinical implications of the osteoprotegerin/RANKL/RANK system for bone and vascular diseases. JAMA 2004;292:490-5.

(225) Lomaga MA, Yeh WC, Sarosi I, Duncan GS, Furlonger C, Ho A, et al. TRAF6 deficiency results in osteopetrosis and defective interleukin-1, CD40, and LPS signaling. Genes Dev 1999;13:1015-24.

(226) Iotsova V, Caamano J, Loy J, Yang Y, Lewin A, Bravo R. Osteopetrosis in mice lacking NF-kappaB1 and NF-kappaB2. Nat Med 1997;3:1285-9.

(227) Ruocco MG, Maeda S, Park JM, Lawrence T, Hsu LC, Cao Y, et al. I{kappa}B kinase (IKK){beta}, but not IKK{alpha}, is a critical mediator of osteoclast survival and is required for inflammation-induced bone loss. J Exp Med 2005;201:1677-87.

(228) Gallet M, Sevenet N, Dupont C, Brazier M, Kamel S. Breast cancer cell line MDA-MB 231 exerts a potent and direct anti-apoptotic effect on mature osteoclasts. Biochem Biophys Res Commun 2004;319:690-6.

(229) Yang Y, Ren Y, Ramani VC, Nan L, Suva LJ, Sanderson RD. Heparanase enhances local and systemic osteolysis in multiple myeloma by upregulating the expression and secretion of RANKL. Cancer Res 2010;70:8329-38.

(230) Sabbota AL, Kim HR, Zhe X, Fridman R, Bonfil RD, Cher ML. Shedding of RANKL by tumor-associated MT1-MMP activates Src-dependent prostate cancer cell migration. Cancer Res 2010;70:5558-66.

(231) Nannuru KC, Futakuchi M, Sadanandam A, Wilson TJ, Varney ML, Myers KJ, et al. Enhanced expression and shedding of receptor activator of NF-kappaB ligand during tumor-bone interaction potentiates mammary tumor-induced osteolysis. Clin Exp Metastasis 2009;26:797-808.

(232) Jones DH, Nakashima T, Sanchez OH, Kozieradzki I, Komarova SV, Sarosi I, et al. Regulation of cancer cell migration and bone metastasis by RANKL. Nature 2006;440:692-6.

(233) Storga D, Pecina-Slaus N, Pavelic J, Pavelic ZP, Pavelic K. c-fms is present in primary tumours as well as in their metastases in bone marrow. Int J Exp Pathol 1992;73:527-33.

(234) Santini D, Schiavon G, Vincenzi B, Gaeta L, Pantano F, Russo A, et al. Receptor activator of NF-kB (RANK) expression in primary tumors associates with bone metastasis occurrence in breast cancer patients. PLoS One 2011;6:e19234.

(235) Maier CS, Yan X, Harder ME, Schimerlik MI, Deinzer ML, Pasa-Tolic L, et al. Electrospray ionization Fourier transform ion cyclotron resonance mass spectrometric analysis of the recombinant human macrophage colony stimulating factor beta and derivatives. J Am Soc Mass Spectrom 2000;11:237-43.

(236) Cerretti DP, Wignall J, Anderson D, Tushinski RJ, Gallis BM, Stya M, et al. Human macrophage-colony stimulating factor: alternative RNA and protein processing from a single gene. Mol Immunol 1988;25:761-70.

(237) Arai F, Miyamoto T, Ohneda O, Inada T, Sudo T, Brasel K, et al. Commitment and differentiation of osteoclast precursor cells by the sequential expression of c-Fms and receptor activator of nuclear factor kappaB (RANK) receptors. J Exp Med 1999;190:1741-54.

(238) McGill GG, Horstmann M, Widlund HR, Du J, Motyckova G, Nishimura EK, et al. Bcl2 regulation by the melanocyte master regulator Mitf modulates lineage survival and melanoma cell viability. Cell 2002;109:707-18.

(239) Douglass TG, Driggers L, Zhang JG, Hoa N, Delgado C, Williams CC, et al. Macrophage colony stimulating factor: not just for macrophages anymore! A gateway into complex biologies. Int Immunopharmacol 2008;8:1354-76.

(240) Yoshida H, Hayashi S, Kunisada T, Ogawa M, Nishikawa S, Okamura H, et al. The murine mutation osteopetrosis is in the coding region of the macrophage colony stimulating factor gene. Nature 1990;345:442-4.

(241) Wiktor-Jedrzejczak W, Ratajczak MZ, Ptasznik A, Sell KW, Ahmed-Ansari A, Ostertag W. CSF-1 deficiency in the op/op mouse has differential effects on macrophage populations and differentiation stages. Exp Hematol 1992;20:1004-10.

(242) Usuda H, Naito M, Umeda S, Takahashi K, Shultz LD. Ultrastructure of macrophages and dendritic cells in osteopetrosis (op) mutant mice lacking macrophage colony-stimulating factor (M-CSF/CSF-1) activity. J Submicrosc Cytol Pathol 1994;26:111-9.

(243) Sapi E. The role of CSF-1 in normal physiology of mammary gland and breast cancer: an update. Exp Biol Med (Maywood) 2004;229:1-11.

(244) Mancino AT, Klimberg VS, Yamamoto M, Manolagas SC, Abe E. Breast cancer increases osteoclastogenesis by secreting M-CSF and upregulating RANKL in stromal cells. J Surg Res 2001;100:18-24.

(245) Guise TA, Yin JJ, Taylor SD, Kumagai Y, Dallas M, Boyce BF, et al. Evidence for a causal role of parathyroid hormone-related protein in the pathogenesis of human breast cancer-mediated osteolysis. J Clin Invest 1996;98:1544-9.

(246) Burton DW, Geller J, Yang M, Jiang P, Barken I, Hastings RH, et al. Monitoring of skeletal progression of prostate cancer by GFP imaging, X-ray, and serum OPG and PTHrP. Prostate 2005;62:275-81.

(247) Bundred NJ, Walker RA, Ratcliffe WA, Warwick J, Morrison JM, Ratcliffe JG. Parathyroid hormone related protein and skeletal morbidity in breast cancer. Eur J Cancer 1992;28:690-2.

(248) Powell GJ, Southby J, Danks JA, Stillwell RG, Hayman JA, Henderson MA, et al. Localization of parathyroid hormone-related protein in breast cancer metastases: increased incidence in bone compared with other sites. Cancer Res 1991;51:3059-61.

(249) Yin JJ, Pollock CB, Kelly K. Mechanisms of cancer metastasis to the bone. Cell Res 2005;15:57-62.

(250) Zhang M, Xie R, Hou W, Wang B, Shen R, Wang X, et al. PTHrP prevents chondrocyte premature hypertrophy by inducing cyclin-D1-dependent Runx2 and Runx3 phosphorylation, ubiquitylation and proteasomal degradation. J Cell Sci 2009;122:1382-9.

(251) Goltzman D. Studies on the mechanisms of the skeletal anabolic action of endogenous and exogenous parathyroid hormone. Arch Biochem Biophys 2008;473:218-24.

(252) Miao D, He B, Jiang Y, Kobayashi T, Soroceanu MA, Zhao J, et al. Osteoblast-derived PTHrP is a potent endogenous bone anabolic agent that modifies the therapeutic efficacy of administered PTH 1-34. J Clin Invest 2005;115:2402-11.

(253) Tam CS, Heersche JN, Murray TM, Parsons JA. Parathyroid hormone stimulates the bone apposition rate independently of its resorptive action: differential effects of intermittent and continuous administration. Endocrinology 1982;110:506-12.

(254) Nishida S, Yamaguchi A, Tanizawa T, Endo N, Mashiba T, Uchiyama Y, et al. Increased bone formation by intermittent parathyroid hormone administration is due to the stimulation of proliferation and differentiation of osteoprogenitor cells in bone marrow. Bone 1994;15:717-23.

(255) Attisano L, Wrana JL. Signal transduction by the TGF-beta superfamily. Science 2002;296:1646-7.

(256) Dennler S, Goumans MJ, ten DP. Transforming growth factor beta signal transduction. J Leukoc Biol 2002;71:731-40.

(257) Lin SJ, Lerch TF, Cook RW, Jardetzky TS, Woodruff TK. The structural basis of TGF-beta, bone morphogenetic protein, and activin ligand binding. Reproduction 2006;132:179-90.

(258) Drabsch Y, ten DP. TGF-beta signaling in breast cancer cell invasion and bone metastasis. J Mammary Gland Biol Neoplasia 2011;16:97-108.

(259) Li J, Zhu H, Chen T, Dai G, Zou L. TGF-beta1 and BRCA2 expression are associated with clinical factors in breast cancer. Cell Biochem Biophys 2011;60:245-8.

(260) Kang Y, He W, Tulley S, Gupta GP, Serganova I, Chen CR, et al. Breast cancer bone metastasis mediated by the Smad tumor suppressor pathway. Proc Natl Acad Sci U S A 2005;102:13909-14.

(261) Alarmo EL, Parssinen J, Ketolainen JM, Savinainen K, Karhu R, Kallioniemi A. BMP7 influences proliferation, migration, and invasion of breast cancer cells. Cancer Lett 2009;275:35-43.

(262) Jo M, Lester RD, Montel V, Eastman B, Takimoto S, Gonias SL. Reversibility of epithelial-mesenchymal transition (EMT) induced in breast cancer cells by activation of urokinase receptor-dependent cell signaling. J Biol Chem 2009;284:22825-33.

(263) Christofori G. New signals from the invasive front. Nature 2006;441:444-50.

(264) Figueroa JD, Flanders KC, Garcia-Closas M, Anderson WF, Yang XR, Matsuno RK, et al. Expression of TGF-beta signaling factors in invasive breast cancers: relationships with age at diagnosis and tumor characteristics. Breast Cancer Res Treat 2010;121:727-35.

(265) Yin JJ, Selander K, Chirgwin JM, Dallas M, Grubbs BG, Wieser R, et al. TGF-beta signaling blockade inhibits PTHrP secretion by breast cancer cells and bone metastases development. J Clin Invest 1999;103:197-206.

(266) Deckers M, van DM, Buijs J, Que I, Lowik C, van der Pluijm G, et al. The tumor suppressor Smad4 is required for transforming growth factor beta-induced epithelial to mesenchymal transition and bone metastasis of breast cancer cells. Cancer Res 2006;66:2202-9.

(267) Korpal M, Yan J, Lu X, Xu S, Lerit DA, Kang Y. Imaging transforming growth factor-beta signaling dynamics and therapeutic response in breast cancer bone metastasis. Nat Med 2009;15:960-6.

(268) Stover DG, Bierie B, Moses HL. A delicate balance: TGF-beta and the tumor microenvironment. J Cell Biochem 2007;101:851-61.

(269) Henderson MA, Danks JA, Slavin JL, Byrnes GB, Choong PF, Spillane JB, et al. Parathyroid hormone-related protein localization in breast cancers predict improved prognosis. Cancer Res 2006;66:2250-6.

(270) Mundy GR. The effects of TGF-beta on bone. Ciba Found Symp 1991;157:137-43.

(271) Chenu C, Pfeilschifter J, Mundy GR, Roodman GD. Transforming growth factor beta inhibits formation of osteoclast-like cells in long-term human marrow cultures. Proc Natl Acad Sci U S A 1988;85:5683-7.

(272) Noda M, Camilliere JJ. In vivo stimulation of bone formation by transforming growth factor-beta. Endocrinology 1989;124:2991-4.

(273) Yoneda T, Hiraga T. Crosstalk between cancer cells and bone microenvironment in bone metastasis. Biochem Biophys Res Commun 2005;328:679-87.

(274) Pollak MN, Schernhammer ES, Hankinson SE. Insulin-like growth factors and neoplasia. Nat Rev Cancer 2004;4:505-18.

(275) Sachdev D, Yee D. Disrupting insulin-like growth factor signaling as a potential cancer therapy. Mol Cancer Ther 2007;6:1-12.

(276) Werner H, Leroith D. The role of the insulin-like growth factor system in human cancer. Adv Cancer Res 1996;68:183-223.

(277) Werner H, Bruchim I. The insulin-like growth factor-I receptor as an oncogene. Arch Physiol Biochem 2009;115:58-71.

(278) Baglietto L, English DR, Hopper JL, Morris HA, Tilley WD, Giles GG. Circulating insulin-like growth factor-I and binding protein-3 and the risk of breast cancer. Cancer Epidemiol Biomarkers Prev 2007;16:763-8.

(279) Shi R, Berkel HJ, Yu H. Insulin-like growth factor-I and prostate cancer: a meta-analysis. Br J Cancer 2001;85:991-6.

(280) Rubin J, Fan X, Rahnert J, Sen B, Hsieh CL, Murphy TC, et al. IGF-I secretion by prostate carcinoma cells does not alter tumor-bone cell interactions in vitro or in vivo. Prostate 2006;66:789-800.

(281) van Golen CM, Schwab TS, Kim B, Soules ME, Su OS, Fung K, et al. Insulin-like growth factor-I receptor expression regulates neuroblastoma metastasis to bone. Cancer Res 2006;66:6570-8.

(282) Lee HL, Pienta KJ, Kim WJ, Cooper CR. The effect of bone-associated growth factors and cytokines on the growth of prostate cancer cells derived from soft tissue versus bone metastases in vitro. Int J Oncol 2003;22:921-6.

(283) Rubin J, Chung LW, Fan X, Zhu L, Murphy TC, Nanes MS, et al. Prostate carcinoma cells that have resided in bone have an upregulated IGF-I axis. Prostate 2004;58:41-9.

(284) Doerr ME, Jones JI. The roles of integrins and extracellular matrix proteins in the insulin-like growth factor I-stimulated chemotaxis of human breast cancer cells. J Biol Chem 1996;271:2443-7.

(285) Perrini S, Laviola L, Carreira MC, Cignarelli A, Natalicchio A, Giorgino F. The GH/IGF1 axis and signaling pathways in the muscle and bone: mechanisms underlying age-related skeletal muscle wasting and osteoporosis. J Endocrinol 2010;205:201-10.

(286) Desbois-Mouthon C, Cadoret A, Blivet-Van Eggelpoel MJ, Bertrand F, Cherqui G, Perret C, et al. Insulin and IGF-1 stimulate the beta-catenin pathway through two signalling cascades involving GSK-3beta inhibition and Ras activation. Oncogene 2001;20:252-9.

(287) Giustina A, Mazziotti G, Canalis E. Growth hormone, insulin-like growth factors, and the skeleton. Endocr Rev 2008;29:535-59.

(288) Langdahl BL, Kassem M, Moller MK, Eriksen EF. The effects of IGF-I and IGF-II on proliferation and differentiation of human osteoblasts and interactions with growth hormone. Eur J Clin Invest 1998;28:176-83.

(289) Nakasaki M, Yoshioka K, Miyamoto Y, Sasaki T, Yoshikawa H, Itoh K. IGF-I secreted by osteoblasts acts as a potent chemotactic factor for osteoblasts. Bone 2008;43:869-79.

(290) Zhang M, Xuan S, Bouxsein ML, von SD, Akeno N, Faugere MC, et al. Osteoblast-specific knockout of the insulin-like growth factor (IGF) receptor gene reveals an essential role of IGF signaling in bone matrix mineralization. J Biol Chem 2002;277:44005-12.

(291) Hill PA, Reynolds JJ, Meikle MC. Osteoblasts mediate insulin-like growth factor-I and -II stimulation of osteoclast formation and function. Endocrinology 1995;136:124-31.

(292) Mochizuki H, Hakeda Y, Wakatsuki N, Usui N, Akashi S, Sato T, et al. Insulin-like growth factor-I supports formation and activation of osteoclasts. Endocrinology 1992;131:1075-80.

(293) Wang Y, Nishida S, Elalieh HZ, Long RK, Halloran BP, Bikle DD. Role of IGF-I signaling in regulating osteoclastogenesis. J Bone Miner Res 2006;21:1350-8.

(294) Lindberg MK, Svensson J, Venken K, Chavoshi T, Andersson N, Moverare SS, et al. Liver-derived IGF-I is permissive for ovariectomy-induced trabecular bone loss. Bone 2006;38:85-92.

(295) Yoneda T, Sasaki A, Mundy GR. Osteolytic bone metastasis in breast cancer. Breast Cancer Res Treat 1994;32:73-84.

(296) Nannuru KC, Singh RK. Tumor-stromal interactions in bone metastasis. Curr Osteoporos Rep 2010;8:105-13.

(297) Hideshima T, Nakamura N, Chauhan D, Anderson KC. Biologic sequelae of interleukin-6 induced PI3-K/Akt signaling in multiple myeloma. Oncogene 2001;20:5991-6000.

(298) Franchimont N, Wertz S, Malaise M. Interleukin-6: An osteotropic factor influencing bone formation? Bone 2005;37:601-6.

(299) Ara T, DeClerck YA. Interleukin-6 in bone metastasis and cancer progression. Eur J Cancer 2010;46:1223-31.

(300) Coleman R, Abrahamsson PA, Hadji P. Handbook of Cancer-Related Bone Disease. BioScientifica; 2011.

(301) Blanchard F, Duplomb L, Baud'huin M, Brounais B. The dual role of IL-6-type cytokines on bone remodeling and bone tumors. Cytokine Growth Factor Rev 2009;20:19-28.

(302) Zhang Y, Fujita N, Oh-hara T, Morinaga Y, Nakagawa T, Yamada M, et al. Production of interleukin-11 in bone-derived endothelial cells and its role in the formation of osteolytic bone metastasis. Oncogene 1998;16:693-703.

(303) Bendre MS, Montague DC, Peery T, Akel NS, Gaddy D, Suva LJ. Interleukin-8 stimulation of osteoclastogenesis and bone resorption is a mechanism for the increased osteolysis of metastatic bone disease. Bone 2003;33:28-37.

(304) Bendre MS, Margulies AG, Walser B, Akel NS, Bhattacharrya S, Skinner RA, et al. Tumor-derived interleukin-8 stimulates osteolysis independent of the receptor activator of nuclear factor-kappaB ligand pathway. Cancer Res 2005;65:11001-9.

(305) Sims NA, Jenkins BJ, Nakamura A, Quinn JM, Li R, Gillespie MT, et al. Interleukin-11 receptor signaling is required for normal bone remodeling. J Bone Miner Res 2005;20:1093-102.

(306) Lehrer S, Diamond EJ, Mamkine B, Stone NN, Stock RG. Serum interleukin-8 is elevated in men with prostate cancer and bone metastases. Technol Cancer Res Treat 2004;3:411-11.

(307) Feng X. Regulatory roles and molecular signaling of TNF family members in osteoclasts. Gene 2005;350:1-13.

(308) Abu-Amer Y, Erdmann J, Alexopoulou L, Kollias G, Ross FP, Teitelbaum SL. Tumor necrosis factor receptors types 1 and 2 differentially regulate osteoclastogenesis. J Biol Chem 2000;275:27307-10.

(309) Macewan DJ. TNF ligands and receptors--a matter of life and death. Br J Pharmacol 2002;135:855-75.

(310) Boyce BF, Li P, Yao Z, Zhang Q, Badell IR, Schwarz EM, et al. TNF-alpha and pathologic bone resorption. Keio J Med 2005;54:127-31.

(311) Nanes MS. Tumor necrosis factor-alpha: molecular and cellular mechanisms in skeletal pathology. Gene 2003;321:1-15.

(312) Hamaguchi T, Wakabayashi H, Matsumine A, Sudo A, Uchida A. TNF inhibitor suppresses bone metastasis in a breast cancer cell line. Biochem Biophys Res Commun 2011;407:525-30.

(313) Lu X, Qian CN, Mu YG, Li NW, Li S, Zhang HB, et al. Serum CCL2 and serum TNF-alpha--two new biomarkers predict bone invasion, post-treatment distant metastasis and poor overall survival in nasopharyngeal carcinoma. Eur J Cancer 2011;47:339-46.

(314) Kishimoto T, Akira S, Narazaki M, Taga T. Interleukin-6 family of cytokines and gp130. Blood 1995;86:1243-54.

(315) Rider CC, Mulloy B. Bone morphogenetic protein and growth differentiation factor cytokine families and their protein antagonists. Biochem J 2010;429:1-12.

(316) Canalis E, Economides AN, Gazzerro E. Bone morphogenetic proteins, their antagonists, and the skeleton. Endocr Rev 2003;24:218-35.

(317) Canalis E. Growth factor control of bone mass. J Cell Biochem 2009;108:769-77.

(318) Buijs JT, Rentsch CA, van der Horst G, van Overveld PG, Wetterwald A, Schwaninger R, et al. BMP7, a putative regulator of epithelial homeostasis in the human prostate, is a potent inhibitor of prostate cancer bone metastasis in vivo. Am J Pathol 2007;171:1047-57.

(319) Dai J, Keller J, Zhang J, Lu Y, Yao Z, Keller ET. Bone morphogenetic protein-6 promotes osteoblastic prostate cancer bone metastases through a dual mechanism. Cancer Res 2005;65:8274-85.

(320) Alarmo EL, Kallioniemi A. Bone morphogenetic proteins in breast cancer: dual role in tumourigenesis? Endocr Relat Cancer 2010;17:R123-R139.

(321) Ye L, Kynaston HG, Jiang WG. Bone metastasis in prostate cancer: molecular and cellular mechanisms (Review). Int J Mol Med 2007;20:103-11.

(322) Russo A, Bronte G, Rizzo S, Fanale D, Di GF, Gebbia N, et al. Anti-endothelin drugs in solid tumors. Expert Opin Emerg Drugs 2010;15:27-40.

(323) Bagnato A, Tecce R, Di C, V, Catt KJ. Activation of mitogenic signaling by endothelin 1 in ovarian carcinoma cells. Cancer Res 1997;57:1306-11.

(324) Guise TA, Yin JJ, Mohammad KS. Role of endothelin-1 in osteoblastic bone metastases. Cancer 2003;97:779-84.

(325) Schipani E, Maes C, Carmeliet G, Semenza GL. Regulation of osteogenesis-angiogenesis coupling by HIFs and VEGF. J Bone Miner Res 2009;24:1347-53.

(326) Zelzer E, Olsen BR. Multiple roles of vascular endothelial growth factor (VEGF) in skeletal development, growth, and repair. Curr Top Dev Biol 2005;65:169-87.

(327) Kitagawa Y, Dai J, Zhang J, Keller JM, Nor J, Yao Z, et al. Vascular endothelial growth factor contributes to prostate cancer-mediated osteoblastic activity. Cancer Res 2005;65:10921-9.

(328) Yang Q, McHugh KP, Patntirapong S, Gu X, Wunderlich L, Hauschka PV. VEGF enhancement of osteoclast survival and bone resorption involves VEGF receptor-2 signaling and beta3-integrin. Matrix Biol 2008;27:589-99.

(329) Yang SY, Yu H, Krygier JE, Wooley PH, Mott MP. High VEGF with rapid growth and early metastasis in a mouse osteosarcoma model. Sarcoma 2007;2007:95628.

(330) Li M, Thompson DD, Paralkar VM. Prostaglandin E(2) receptors in bone formation. Int Orthop 2007;31:767-72.

(331) Gao Q, Xu M, Alander CB, Choudhary S, Pilbeam CC, Raisz LG. Effects of prostaglandin E2 on bone in mice in vivo. Prostaglandins Other Lipid Mediat 2009;89:20-5.

(332) Norrdin RW, Jee WS, High WB. The role of prostaglandins in bone in vivo. Prostaglandins Leukot Essent Fatty Acids 1990;41:139-49.

(333) Jee WS, Ma YF. The in vivo anabolic actions of prostaglandins in bone. Bone 1997;21:297-304.

(334) Dekel S, Lenthall G, Francis MJ. Release of prostaglandins from bone and muscle after tibial fracture. An experimental study in rabbits. J Bone Joint Surg Br 1981;63-B:185-9.

(335) Keller J, Bunger C, Andreassen TT, Bak B, Lucht U. Bone repair inhibited by indomethacin. Effects on bone metabolism and strength of rabbit osteotomies. Acta Orthop Scand 1987;58:379-83.

(336) Akhter MP, Cullen DM, Gong G, Recker RR. Bone biomechanical properties in prostaglandin EP1 and EP2 knockout mice. Bone 2001;29:121-5.

(337) Ma X, Kundu N, Rifat S, Walser T, Fulton AM. Prostaglandin E receptor EP4 antagonism inhibits breast cancer metastasis. Cancer Res 2006;66:2923-7.

(338) Sales KJ, Katz AA, Howard B, Soeters RP, Millar RP, Jabbour HN. Cyclooxygenase-1 is up-regulated in cervical carcinomas: autocrine/paracrine regulation of cyclooxygenase-2, prostaglandin e receptors, and angiogenic factors by cyclooxygenase-1. Cancer Res 2002;62:424-32.

(339) Takita M, Inada M, Maruyama T, Miyaura C. Prostaglandin E receptor EP4 antagonist suppresses osteolysis due to bone metastasis of mouse malignant melanoma cells. FEBS Lett 2007;581:565-71.

(340) Hiraga T, Myoui A, Choi ME, Yoshikawa H, Yoneda T. Stimulation of cyclooxygenase-2 expression by bone-derived transforming growth factor-beta enhances bone metastases in breast cancer. Cancer Res 2006;66:2067-73.

(341) Takahashi T, Uehara H, Bando Y, Izumi K. Soluble EP2 neutralizes prostaglandin E2-induced cell signaling and inhibits osteolytic tumor growth. Mol Cancer Ther 2008;7:2807-16.

(342) Strongin AY. Mislocalization and unconventional functions of cellular MMPs in cancer. Cancer Metastasis Rev 2006;25:87-98.

(343) Krane SM, Inada M. Matrix metalloproteinases and bone. Bone 2008;43:7-18.

(344) Lafleur MA, Drew AF, de Sousa EL, Blick T, Bills M, Walker EC, et al. Upregulation of matrix metalloproteinases (MMPs) in breast cancer xenografts: a major induction of stromal MMP-13. Int J Cancer 2005;114:544-54.

(345) Wiesner C, Bonfil RD, Dong Z, Yamamoto H, Nabha SM, Meng H, et al. Heterogeneous activation of MMP-9 due to prostate cancer-bone interaction. Urology 2007;69:795-9.

(346) Kominsky SL, Doucet M, Thorpe M, Weber KL. MMP-13 is over-expressed in renal cell carcinoma bone metastasis and is induced by TGF-beta1. Clin Exp Metastasis 2008;25:865-70.

(347) Hu F, Wang C, Guo S, Sun W, Mi D, Gao Y, et al. deltaEF1 promotes osteolytic metastasis of MDA-MB-231 breast cancer cells by regulating MMP-1 expression. Biochim Biophys Acta 2011;1809:200-10.

(348) Incorvaia L, Badalamenti G, Rini G, Arcara C, Fricano S, Sferrazza C, et al. MMP-2, MMP-9 and activin A blood levels in patients with breast cancer or prostate cancer metastatic to the bone. Anticancer Res 2007;27:1519-25.

(349) Cheng YY, Huang L, Lee KM, Li K, Kumta SM. Alendronate regulates cell invasion and MMP-2 secretion in human osteosarcoma cell lines. Pediatr Blood Cancer 2004;42:410-5.

(350) Claesson-Welsh L, Heldin CH. Platelet-derived growth factor. Three isoforms that bind to two distinct cell surface receptors. Acta Oncol 1989;28:331-4.

(351) Heldin CH, Westermark B. Mechanism of action and in vivo role of platelet-derived growth factor. Physiol Rev 1999;79:1283-316.

(352) Graham S, Leonidou A, Lester M, Heliotis M, Mantalaris A, Tsiridis E. Investigating the role of PDGF as a potential drug therapy in bone formation and fracture healing. Expert Opin Investig Drugs 2009;18:1633-54.

(353) Sanchez-Fernandez MA, Gallois A, Riedl T, Jurdic P, Hoflack B. Osteoclasts control osteoblast chemotaxis via PDGF-BB/PDGF receptor beta signaling. PLoS One 2008;3:e3537.

(354) Russell MR, Jamieson WL, Dolloff NG, Fatatis A. The alpha-receptor for platelet-derived growth factor as a target for antibody-mediated inhibition of skeletal metastases from prostate cancer cells. Oncogene 2009;28:412-21.

(355) Lev DC, Kim SJ, Onn A, Stone V, Nam DH, Yazici S, et al. Inhibition of platelet-derived growth factor receptor signaling restricts the growth of human breast cancer in the bone of nude mice. Clin Cancer Res 2005;11:306-14.

(356) Russell MR, Liu Q, Fatatis A. Targeting the {alpha} receptor for platelet-derived growth factor as a primary or combination therapy in a preclinical model of prostate cancer skeletal metastasis. Clin Cancer Res 2010;16:5002-10.

(357) Valta MP, Tuomela J, Bjartell A, Valve E, Vaananen HK, Harkonen P. FGF-8 is involved in bone metastasis of prostate cancer. Int J Cancer 2008;123:22-31.

(358) Ornitz DM. FGF signaling in the developing endochondral skeleton. Cytokine Growth Factor Rev 2005;16:205-13.

(359) Rades D, Schild SE, Abrahm JL. Treatment of painful bone metastases. Nat Rev Clin Oncol 2010;7:220-9.

(360) Zou X, Zou L, He Y, Bunger C. Molecular treatment strategies and surgical reconstruction for metastatic bone diseases. Cancer Treat Rev 2008;34:527-38.

(361) Hartsell WF, Scott CB, Bruner DW, Scarantino CW, Ivker RA, Roach M, III, et al. Randomized trial of short- versus long-course radiotherapy for palliation of painful bone metastases. J Natl Cancer Inst 2005;97:798-804.

(362) Bone Pain Trial Working Party. 8 Gy single fraction radiotherapy for the treatment of metastatic skeletal pain: randomised comparison with a multifraction schedule over 12 months of patient follow-up. Radiotherapy and Oncology 1999;52:111-21.

(363) Foro AP, Fontanals AV, Galceran JC, Lynd F, Latiesas XS, de Dios NR, et al. Randomized clinical trial with two palliative radiotherapy regimens in painful bone metastases: 30 Gy in 10 fractions compared with 8 Gy in single fraction. Radiother Oncol 2008;89:150-5.

(364) Amouzegar-Hashemi F, Behrouzi H, Kazemian A, Zarpak B, Haddad P. Single versus multiple fractions of palliative radiotherapy for bone metastases: a randomized clinical trial in Iranian patients. Curr Oncol 2008;15:151.

(365) Gaze MN, Kelly CG, Kerr GR, Cull A, Cowie VJ, Gregor A, et al. Pain relief and quality of life following radiotherapy for bone metastases: a randomised trial of two fractionation schedules. Radiother Oncol 1997;45:109-16.

(366) Coleman RE. Risks and benefits of bisphosphonates. Br J Cancer 2008;98:1736-40.

(367) Redzepovic J, Weinmann G, Ott I, Gust R. Current trends in multiple myeloma management. J Int Med Res 2008;36:371-86.

(368) Blahos J. Treatment and prevention of osteoporosis. Wien Med Wochenschr 2007;157:589-92.

(369) Rodan GA, Fleisch HA. Bisphosphonates: mechanisms of action. J Clin Invest 1996;97:2692-6.

(370) Jung A, Bisaz S, Fleisch H. The binding of pyrophosphate and two diphosphonates by hydroxyapatite crystals. Calcif Tissue Res 1973;11:269-80.

(371) Rogers MJ. New insights into the molecular mechanisms of action of bisphosphonates. Curr Pharm Des 2003;9:2643-58.

(372) Giuliani N, Pedrazzoni M, Negri G, Passeri G, Impicciatore M, Girasole G. Bisphosphonates stimulate formation of osteoblast precursors and mineralized

nodules in murine and human bone marrow cultures in vitro and promote early osteoblastogenesis in young and aged mice in vivo. Bone 1998;22:455-61.

(373) Duque G, Rivas D. Alendronate has an anabolic effect on bone through the differentiation of mesenchymal stem cells. J Bone Miner Res 2007;22:1603-11.

(374) Tobias JH, Chow JW, Chambers TJ. 3-Amino-1-hydroxypropylidine-1-bisphosphonate (AHPrBP) suppresses not only the induction of new, but also the persistence of existing bone-forming surfaces in rat cancellous bone. Bone 1993;14:619-23.

(375) Idris AI, Rojas J, Greig IR, van't Hof RJ, Ralston SH. Aminobisphosphonates cause osteoblast apoptosis and inhibit bone nodule formation in vitro. Calcif Tissue Int 2008;82:191-201.

(376) Orriss IR, Key ML, Colston KW, Arnett TR. Inhibition of osteoblast function in vitro by aminobisphosphonates. J Cell Biochem 2009;106:109-18.

(377) Diel IJ, Bergner R, Grotz KA. Adverse effects of bisphosphonates: current issues. J Support Oncol 2007;5:475-82.

(378) Park IH, Ro J, Nam BH, Kwon Y, Lee KS. Potential antitumor effects of nitrogen-containing bisphosphonate in hormone receptor negative breast cancer patients with bone metastases. BMC Cancer 2009;9:154.

(379) Coleman RE. Bisphosphonates in breast cancer. Ann Oncol 2005;16:687-95.

(380) Winter MC, Holen I, Coleman RE. Exploring the anti-tumour activity of bisphosphonates in early breast cancer. Cancer Treat Rev 2008;34:453-75.

(381) Pageau SC. Denosumab. MAbs 2009;1:210-5.

(382) Stopeck AT, Lipton A, Body JJ, Steger GG, Tonkin K, de Boer RH, et al. Denosumab compared with zoledronic acid for the treatment of bone metastases in patients with advanced breast cancer: a randomized, double-blind study. J Clin Oncol 2010;28:5132-9.

(383) Smith MR, Saad F, Coleman R, Shore N, Fizazi K, Tombal B, et al. Denosumab and bone-metastasis-free survival in men with castration-resistant prostate cancer: results of a phase 3, randomised, placebo-controlled trial. Lancet 2012;379:39-46.

(384) Body JJ. New developments for treatment and prevention of bone metastases. Curr Opin Oncol 2011;23:338-42.

(385) Thomas D, Henshaw R, Skubitz K, Chawla S, Staddon A, Blay JY, et al. Denosumab in patients with giant-cell tumour of bone: an open-label, phase 2 study. Lancet Oncol 2010;11:275-80.

(386) Brown JE, Coleman RE. Denosumab in patients with cancer-a surgical strike against the osteoclast. Nat Rev Clin Oncol 2012;9:110-8.

(387) Matsumine A, Takegami K, Asanuma K, Matsubara T, Nakamura T, Uchida A, et al. A novel hyperthermia treatment for bone metastases using magnetic materials. Int J Clin Oncol 2011;16:101-8.

(388) Saad F, Lipton A. SRC kinase inhibition: targeting bone metastases and tumor growth in prostate and breast cancer. Cancer Treat Rev 2010;36:177-84.

(389) Ahmed SA, Gogal RM, Jr., Walsh JE. A new rapid and simple non-radioactive assay to monitor and determine the proliferation of lymphocytes: an alternative to [3H]thymidine incorporation assay. J Immunol Methods 1994;170:211-24.

(390) van't Hof RJ, Tuinenburg-Bol Raap AC, Nijweide PJ. Induction of osteoclast characteristics in cultured avian blood monocytes; modulation by osteoblasts and 1,25-(OH)2 vitamin D3. Int J Exp Pathol 1995;76:205-14.

(391) Nakayama GR, Caton MC, Nova MP, Parandoosh Z. Assessment of the Alamar Blue assay for cellular growth and viability in vitro. J Immunol Methods 1997;204:205-8.

(392) Serrels A, Macpherson IR, Evans TR, Lee FY, Clark EA, Sansom OJ, et al. Identification of potential biomarkers for measuring inhibition of Src kinase activity in colon cancer cells following treatment with dasatinib. Mol Cancer Ther 2006;5:3014-22.

(393) Geback T, Schulz MM, Koumoutsakos P, Detmar M. TScratch: a novel and simple software tool for automated analysis of monolayer wound healing assays. Biotechniques 2009;46:265-74.

(394) Idris AI. Analysis of signalling pathways by western blotting and immunoprecipitation. Methods Mol Biol 2012;816:223-32.

(395) Wislowska M, Jakubicz D, Stepien K, Cicha M. Serum concentrations of formation (PINP) and resorption (Ctx) bone turnover markers in rheumatoid arthritis. Rheumatol Int 2009;29:1403-9.

(396) van't Hof RJ, Macphee J, Libouban H, Helfrich MH, Ralston SH. Regulation of bone mass and bone turnover by neuronal nitric oxide synthase. Endocrinology 2004;145:5068-74.

(397) Parfitt AM, Drezner MK, Glorieux FH, Kanis JA, Malluche H, Meunier PJ, et al. Bone histomorphometry: standardization of nomenclature, symbols, and units. Report of the ASBMR Histomorphometry Nomenclature Committee. J Bone Miner Res 1987;2:595-610.

(398) Idris AI, Ralston SH, van't Hof RJ. The nitrosylated flurbiprofen derivative HCT1026 inhibits cytokine-induced signalling through a novel mechanism of action. Eur J Pharmacol 2008;602:215-22.

(399) Idris AI, Rojas J, Greig IR, van't Hof RJ, Ralston SH. Aminobisphosphonates cause osteoblast apoptosis and inhibit bone nodule formation in vitro. Calcif Tissue Int 2008;82:191-201.

(400) Collin-Osdoby P, Yu X, Zheng H, Osdoby P. RANKL-mediated osteoclast formation from murine RAW 264.7 cells. Methods Mol Med 2003;80:153-66.

(401) Sudo H, Kodama HA, Amagai Y, Yamamoto S, Kasai S. In vitro differentiation and calcification in a new clonal osteogenic cell line derived from newborn mouse calvaria. J Cell Biol 1983;96:191-8.

(402) American Cancer Society. Cancer Facts and Figures, 2007. Cancer Facts and Figures 2007.

(403) Yu M, Smolen GA, Zhang J, Wittner B, Schott BJ, Brachtel E, et al. A developmentally regulated inducer of EMT, LBX1, contributes to breast cancer progression. Genes Dev 2009;23:1737-42.

(404) Tu YF, Kaipparettu BA, Ma Y, Wong LJ. Mitochondria of highly metastatic breast cancer cell line MDA-MB-231 exhibits increased autophagic properties. Biochim Biophys Acta 2011;1807:1125-32.

(405) Weigel RJ, deConinck EC. Transcriptional control of estrogen receptor in estrogen receptor-negative breast carcinoma. Cancer Res 1993;53:3472-4.

(406) Liu X, Feng R. Inhibition of epithelial to mesenchymal transition in metastatic breast carcinoma cells by c-Src suppression. Acta Biochim Biophys Sin (Shanghai) 2010;42:496-501.

(407) So FV, Guthrie N, Chambers AF, Carroll KK. Inhibition of proliferation of estrogen receptor-positive MCF-7 human breast cancer cells by flavonoids in the presence and absence of excess estrogen. Cancer Lett 1997;112:127-33.

(408) Lou Y, Preobrazhenska O, auf dem KU, Sutcliffe M, Barclay L, McDonald PC, et al. Epithelial-mesenchymal transition (EMT) is not sufficient for spontaneous murine breast cancer metastasis. Dev Dyn 2008;237:2755-68.

(409) Xanthopoulos JM, Romano AE, Majumdar SK. Response of Mouse Breast Cancer Cells to Anastrozole, Tamoxifen, and the Combination. J Biomed Biotechnol 2005;2005:10-9.

(410) Lirdprapamongkol K, Sakurai H, Kawasaki N, Choo MK, Saitoh Y, Aozuka Y, et al. Vanillin suppresses in vitro invasion and in vivo metastasis of mouse breast cancer cells. Eur J Pharm Sci 2005;25:57-65.

(411) Kohler M, Ruttner B, Cooper S, Hengartner H, Zinkernagel RM. Enhanced tumor susceptibility of immunocompetent mice infected with lymphocytic choriomeningitis virus. Cancer Immunol Immunother 1990;32:117-24.

(412) Simpson MA, Reiland J, Burger SR, Furcht LT, Spicer AP, Oegema TR, Jr., et al. Hyaluronan synthase elevation in metastatic prostate carcinoma cells correlates with hyaluronan surface retention, a prerequisite for rapid adhesion to bone marrow endothelial cells. J Biol Chem 2001;276:17949-57.

(413) Vanquelef E, Helesbeux JJ, Duval O, Debiton E, Barthomeuf C, Jarry C, et al. Synthesis and PC3 androgen-independent prostate cells antiproliferative effect of fagaronine derivatives. J Enzyme Inhib Med Chem 2007;22:647-54.

(414) Rucci N, Ricevuto E, Ficorella C, Longo M, Perez M, Di GC, et al. In vivo bone metastases, osteoclastogenic ability, and phenotypic characterization of human breast cancer cells. Bone 2004;34:697-709.

(415) Tao K, Fang M, Alroy J, Sahagian GG. Imagable 4T1 model for the study of late stage breast cancer. BMC Cancer 2008;8:228.

(416) Marton I, Johnson SE, Damjanov I, Currier KS, Sundberg JP, Knowles BB. Expression and immune recognition of SV40 Tag in transgenic mice that develop metastatic osteosarcomas. Transgenic Res 2000;9:115-25.

(417) Sugatani T, Alvarez U, Hruska KA. PTEN regulates R. J Biol Chem 2003;278:5001-8.

(418) Kelley TW, Graham MM, Doseff AI, Pomerantz RW, Lau SM, Ostrowski MC, et al. Macrophage colony-stimulating factor promotes cell survival through Akt/protein kinase B. J Biol Chem 1999;274:26393-8.

(419) Curry JM, Eubank TD, Roberts RD, Wang Y, Pore N, Maity A, et al. M-CSF signals through the MAPK/ERK pathway via Sp1 to induce VEGF production and induces angiogenesis in vivo. PLoS One 2008;3:e3405.

(420) Chen Y, Wang X, Di L, Fu G, Chen Y, Bai L, et al. Phospholipase Cgamma2 mediates RANKL-stimulated lymph node organogenesis and osteoclastogenesis. J Biol Chem 2008;283:29593-601.

(421) Boyde A, Maconnachie E, Reid SA, Delling G, Mundy GR. Scanning electron microscopy in bone pathology: review of methods, potential and applications. Scan Electron Microsc 1986;1537-54.

(422) Mundy GR. Mechanisms of osteolytic bone destruction. Bone 1991;12 Suppl 1:S1-S6.

(423) Nicolin V, Bortul R, Bareggi R, Baldini G, Martinelli B, Narducci P. Breast adenocarcinoma MCF-7 cell line induces spontaneous osteoclastogenesis via a RANK-ligand-dependent pathway. Acta Histochem 2008;110:388-96.

(424) Ramnaraine M, Pan W, Clohisy DR. Osteoclasts direct bystander killing of cancer cells in vitro. Bone 2006;38:4-12.

(425) Ohshiba T, Miyaura C, Inada M, Ito A. Role of RANKL-induced osteoclast formation and MMP-dependent matrix degradation in bone destruction by breast cancer metastasis. Br J Cancer 2003;88:1318-26.

(426) Lau YS, Danks L, Sun SG, Fox S, Sabokbar A, Harris A, et al. RANKL-dependent and RANKL-independent mechanisms of macrophage-osteoclast differentiation in breast cancer. Breast Cancer Res Treat 2007;105:7-16.

(427) Kitazawa S, Kitazawa R. RANK ligand is a prerequisite for cancer-associated osteolytic lesions. J Pathol 2002;198:228-36.

(428) Tumber A, Morgan HM, Meikle MC, Hill PA. Human breast-cancer cells stimulate the fusion, migration and resorptive activity of osteoclasts in bone explants. Int J Cancer 2001;91:665-72.

(429) Grano M, Mori G, Minielli V, Cantatore FP, Colucci S, Zallone AZ. Breast cancer cell line MDA-231 stimulates osteoclastogenesis and bone resorption in human osteoclasts. Biochem Biophys Res Commun 2000;270:1097-100.

(430) Guo Y, Tiedemann K, Khalil JA, Russo C, Siegel PM, Komarova SV. Osteoclast precursors acquire sensitivity to breast cancer derived factors early in differentiation. Bone 2008;43:386-93.

(431) Mercer RR, Miyasaka C, Mastro AM. Metastatic breast cancer cells suppress osteoblast adhesion and differentiation. Clin Exp Metastasis 2004;21:427-35.

(432) Takayanagi H. Mechanistic insight into osteoclast differentiation in osteoimmunology. J Mol Med (Berl) 2005;83:170-9.

(433) Teitelbaum SL. Bone resorption by osteoclasts. Science 2000;289:1504-8.

(434) Lewis EA, Irving JT. An autoradiographic investigation of bone remodelling in the rat calvarium grown in organ culture. Arch Oral Biol 1970;15:769-76.

(435) Ortiz SG, Ma T, Regula D, Smith RL, Goodman SB. Continuous intramedullary polymer particle infusion using a murine femoral explant model. J Biomed Mater Res B Appl Biomater 2008;87:440-6.

(436) Nakajima K, Komiyama Y, Hojo H, Ohba S, Yano F, Nishikawa N, et al. Enhancement of bone formation ex vivo and in vivo by a helioxanthin-derivative. Biochem Biophys Res Commun 2010;395:502-8.

(437) Wu X, Downes S, Watts DC. Evaluation of critical size defects of mouse calvarial bone: An organ culture study. Microsc Res Tech 2010;73:540-7.

(438) Rosol TJ, Tannehill-Gregg SH, LeRoy BE, Mandl S, Contag CH. Animal models of bone metastasis. Cancer 2003;97:748-57.

(439) Henriquez NV, van Overveld PG, Que I, Buijs JT, Bachelier R, Kaijzel EL, et al. Advances in optical imaging and novel model systems for cancer metastasis research. Clin Exp Metastasis 2007;24:699-705.

(440) Frantzias J, Logan JG, Mollat P, Sparatore A, Del SP, Ralston SH, et al. Hydrogen sulphide-releasing diclofenac derivatives inhibit breast cancer-induced osteoclastogenesis in vitro and prevent osteolysis ex vivo. Br J Pharmacol 2012;165:1914-25.

(441) Kang Y, Siegel PM, Shu W, Drobnjak M, Kakonen SM, Cordon-Cardo C, et al. A multigenic program mediating breast cancer metastasis to bone. Cancer Cell 2003;3:537-49.

(442) Garrett I. Assessing Bone Formation Using Mouse Calvarial Organ Cultures. In: Ralston SH, Helfrich M, editors. Bone Research Protocols. 80 ed. 2003. p. 183-98.

(443) Reynolds JJ, Dingle JT. A sensitive in vitro method for studying the induction and inhibition of bone resorption. Calcif Tissue Res 1970;4:339-49.

(444) Reynolds JJ, Minkin C, Morgan DB, Spycher D, Fleisch H. The effect of two diphosphonates on the resorption of mouse calvaria in vitro. Calcif Tissue Res 1972;10:302-13.

(445) Gowen M, Wood DD, Ihrie EJ, McGuire MK, Russell RG. An interleukin 1 like factor stimulates bone resorption in vitro. Nature 1983;306:378-80.

(446) Mundy G, Garrett R, Harris S, Chan J, Chen D, Rossini G, et al. Stimulation of bone formation in vitro and in rodents by statins. Science 1999;286:1946-9.

(447) Traianedes K, Dallas MR, Garrett IR, Mundy GR, Bonewald LF. 5-Lipoxygenase metabolites inhibit bone formation in vitro. Endocrinology 1998;139:3178-84.

(448) Tabuenca A, Mohan S, Garberoglio CA, Borgen PI, Rosol T, Linkhart TA. Parathyroid hormone-related protein: primary osteolytic factor produced by breast tumor cells in vitro? World J Surg 1995;19:292-7.

(449) Yi B, Williams PJ, Niewolna M, Wang Y, Yoneda T. Tumor-derived platelet-derived growth factor-BB plays a critical role in osteosclerotic bone metastasis in an animal model of human breast cancer. Cancer Res 2002;62:917-23.

(450) Huss WJ, Maddison LA, Greenberg NM. Autochthonous mouse models for prostate cancer: past, present and future. Semin Cancer Biol 2001;11:245-60.

(451) Niikura K. Effect of a V-ATPase inhibitor, FR202126, in syngeneic mouse model of experimental bone metastasis. Cancer Chemother Pharmacol 2007;60:555-62.

(452) Safina A, Sotomayor P, Limoge M, Morrison C, Bakin AV. TAK1-TAB2 Signaling Contributes to Bone Destruction by Breast Carcinoma Cells. Mol Cancer Res 2011;9:1042-53.

(453) Garcia T, Jackson A, Bachelier R, Clement-Lacroix P, Baron R, Clezardin P, et al. A convenient clinically relevant model of human breast cancer bone metastasis. Clin Exp Metastasis 2008;25:33-42.

(454) Jones MD, Liu JC, Barthel TK, Hussain S, Lovria E, Cheng D, et al. A proteasome inhibitor, bortezomib, inhibits breast cancer growth and reduces osteolysis by downregulating metastatic genes. Clin Cancer Res 2010;16:4978-89.

(455) Corey E, Quinn JE, Bladou F, Brown LG, Roudier MP, Brown JM, et al. Establishment and characterization of osseous prostate cancer models: intra-tibial injection of human prostate cancer cells. Prostate 2002;52:20-33.

(456) Gordon AH, O'Keefe RJ, Schwarz EM, Rosier RN, Puzas JE. Nuclear factor-kappaB-dependent mechanisms in breast cancer cells regulate tumor burden and osteolysis in bone. Cancer Res 2005;65:3209-17.

(457) Rucci N, Recchia I, Angelucci A, Alamanou M, Del FA, Fortunati D, et al. Inhibition of protein kinase c-Src reduces the incidence of breast cancer metastases and increases survival in mice: implications for therapy. J Pharmacol Exp Ther 2006;318:161-72.

(458) Yang RS, Tang CH, Chuang WJ, Huang TH, Peng HC, Huang TF, et al. Inhibition of tumor formation by snake venom disintegrin. Toxicon 2005;45:661-9.

(459) Zheng Y, Zhou H, Modzelewski JR, Kalak R, Blair JM, Seibel MJ, et al. Accelerated bone resorption, due to dietary calcium deficiency, promotes breast cancer tumor growth in bone. Cancer Res 2007;67:9542-8.

(460) Rucci N, Millimaggi D, Mari M, Del FA, Bologna M, Teti A, et al. Receptor activator of NF-kappaB ligand enhances breast cancer-induced osteolytic lesions through upregulation of extracellular matrix metalloproteinase inducer/CD147. Cancer Res 2010;70:6150-60.

(461) Welch DR, Harms JF, Mastro AM, Gay CV, Donahue HJ. Breast cancer metastasis to bone: evolving models and research challenges. J Musculoskelet Neuronal Interact 2003;3:30-8.

(462) Lorenzo J, Choi Y, Horowitz M, Takayanagi H. Osteoimmunology. First ed. Elsevier; 2011.

(463) Thiolloy S, Halpern J, Holt GE, Schwartz HS, Mundy GR, Matrisian LM, et al. Osteoclast-derived matrix metalloproteinase-7, but not matrix metalloproteinase-9, contributes to tumor-induced osteolysis. Cancer Res 2009;69:6747-55.

(464) Pederson L, Winding B, Foged NT, Spelsberg TC, Oursler MJ. Identification of breast cancer cell line-derived paracrine factors that stimulate osteoclast activity. Cancer Res 1999;59:5849-55.

(465) Weir EC, Horowitz MC, Baron R, Centrella M, Kacinski BM, Insogna KL. Macrophage colony-stimulating factor release and receptor expression in bone cells. J Bone Miner Res 1993;8:1507-18.

(466) Hofbauer LC, Heufelder AE. Role of receptor activator of nuclear factor-kappaB ligand and osteoprotegerin in bone cell biology. J Mol Med (Berl) 2001;79:243-53.

(467) Lloyd SA, Yuan YY, Kostenuik PJ, Ominsky MS, Lau AG, Morony S, et al. Soluble RANKL induces high bone turnover and decreases bone volume, density, and strength in mice. Calcif Tissue Int 2008;82:361-72.

(468) Park HR, Min SK, Cho HD, Kim DH, Shin HS, Park YE. Expression of osteoprotegerin and RANK ligand in breast cancer bone metastasis. J Korean Med Sci 2003;18:541-6.

(469) Nicolin V, Narducci P. Soluble TRAIL could enhance bone destruction acting on Rank-ligand in estrogen-independent human breast cancer cell line MDA-MB-231. Acta Histochem 2010;112:189-92.

(470) Ullrich A, Gray A, Tam AW, Yang-Feng T, Tsubokawa M, Collins C, et al. Insulin-like growth factor I receptor primary structure: comparison with insulin receptor suggests structural determinants that define functional specificity. EMBO J 1986;5:2503-12.

(471) Furstenberger G, Senn HJ. Insulin-like growth factors and cancer. Lancet Oncol 2002;3:298-302.

(472) Slieker LJ, Brooke GS, DiMarchi RD, Flora DB, Green LK, Hoffmann JA, et al. Modifications in the B10 and B26-30 regions of the B chain of human insulin alter affinity for the human IGF-I receptor more than for the insulin receptor. Diabetologia 1997;40 Suppl 2:S54-S61.

(473) Mynarcik DC, Williams PF, Schaffer L, Yu GQ, Whittaker J. Identification of common ligand binding determinants of the insulin and insulin-like growth factor 1 receptors. Insights into mechanisms of ligand binding. J Biol Chem 1997;272:18650-5.

(474) Werner H, Le RD. New concepts in regulation and function of the insulin-like growth factors: implications for understanding normal growth and neoplasia. Cell Mol Life Sci 2000;57:932-42.

(475) Samani AA, Yakar S, Leroith D, Brodt P. The role of the IGF system in cancer growth and metastasis: overview and recent insights. Endocr Rev 2007;28:20-47.

(476) Celil AB, Campbell PG. BMP-2 and insulin-like growth factor-I mediate Osterix (Osx) expression in human mesenchymal stem cells via the MAPK and protein kinase D signaling pathways. J Biol Chem 2005;280:31353-9.

(477) Kawai M, Rosen CJ. Insulin-like growth factor-I and bone: lessons from mice and men. Pediatr Nephrol 2009;24:1277-85.

(478) Bikle D, Majumdar S, Laib A, Powell-Braxton L, Rosen C, Beamer W, et al. The skeletal structure of insulin-like growth factor I-deficient mice. J Bone Miner Res 2001;16:2320-9.

(479) Clemens TL, Chernausek SD. Genetic strategies for elucidating insulin-like growth factor action in bone. Growth Horm IGF Res 2004;14:195-9.

(480) Wagner K, Hemminki K, Forsti A. The GH1/IGF-1 axis polymorphisms and their impact on breast cancer development. Breast Cancer Res Treat 2007;104:233-48.

(481) Tang FY, Su YC, Chen NC, Hsieh HS, Chen KS. Resveratrol inhibits migration and invasion of human breast-cancer cells. Mol Nutr Food Res 2008;52:683-91.

(482) Mulvihill MJ, Cooke A, Rosenfeld-Franklin M, Buck E, Foreman K, Landfair D, et al. Discovery of OSI-906: a selective and orally efficacious dual inhibitor of the IGF-1 receptor and insulin receptor. Future Med Chem 2009;1:1153-71.

(483) Ji QS, Mulvihill MJ, Rosenfeld-Franklin M, Cooke A, Feng L, Mak G, et al. A novel, potent, and selective insulin-like growth factor-I receptor kinase inhibitor blocks insulin-like growth factor-I receptor signaling in vitro and inhibits insulin-like growth factor-I receptor dependent tumor growth in vivo. Mol Cancer Ther 2007;6:2158-67.

(484) Zhang W, Shen X, Wan C, Zhao Q, Zhang L, Zhou Q, et al. Effects of insulin and insulin-like growth factor 1 on osteoblast proliferation and differentiation: differential signalling via Akt and ERK. Cell Biochem Funct 2012.

(485) Canalis E. Insulin like growth factors and the local regulation of bone formation. Bone 1993;14:273-6.

(486) Ohlsson C, Sjogren K, Jansson JO, Isaksson OG. The relative importance of endocrine versus autocrine/paracrine insulin-like growth factor-I in the regulation of body growth. Pediatr Nephrol 2000;14:541-3.

(487) Niu T, Rosen CJ. The insulin-like growth factor-I gene and osteoporosis: a critical appraisal. Gene 2005;361:38-56.

(488) Zhao HY, Liu JM, Ning G, Zhao YJ, Chen Y, Sun LH, et al. Relationships between insulin-like growth factor-I (IGF-I) and OPG, RANKL, bone mineral density in healthy Chinese women. Osteoporos Int 2008;19:221-6.

(489) Lamothe B, Webster WK, Gopinathan A, Besse A, Campos AD, Darnay BG. TRAF6 ubiquitin ligase is essential for RANKL signaling and osteoclast differentiation. Biochem Biophys Res Commun 2007;359:1044-9.

(490) Yang WL, Wang J, Chan CH, Lee SW, Campos AD, Lamothe B, et al. The E3 ligase TRAF6 regulates Akt ubiquitination and activation. Science 2009;325:1134-8.

(491) Kadono Y, Okada F, Perchonock C, Jang HD, Lee SY, Kim N, et al. Strength of TRAF6 signalling determines osteoclastogenesis. EMBO Rep 2005;6:171-6.

(492) Sachdev D, Yee D. The IGF system and breast cancer. Endocr Relat Cancer 2001;8:197-209.

(493) Key TJ, Appleby PN, Reeves GK, Roddam AW. Insulin-like growth factor 1 (IGF1), IGF binding protein 3 (IGFBP3), and breast cancer risk: pooled individual data analysis of 17 prospective studies. Lancet Oncol 2010;11:530-42.

(494) DeLellis K, Ingles S, Kolonel L, McKean-Cowdin R, Henderson B, Stanczyk F, et al. IGF1 genotype, mean plasma level and breast cancer risk in the Hawaii/Los Angeles multiethnic cohort. Br J Cancer 2003;88:277-82.

(495) Rosenzweig SA, Atreya HS. Defining the pathway to insulin-like growth factor system targeting in cancer. Biochem Pharmacol 2010;80:1115-24.

(496) Zhang Y, Ma B, Fan Q. Mechanisms of breast cancer bone metastasis. Cancer Lett 2010;292:1-7.

(497) Yoneda T, Williams PJ, Hiraga T, Niewolna M, Nishimura R. A bone-seeking clone exhibits different biological properties from the MDA-MB-231 parental human breast cancer cells and a brain-seeking clone in vivo and in vitro. J Bone Miner Res 2001;16:1486-95.

(498) Demeure MJ, Bussey KJ, Kirschner LS. Targeted therapies for adrenocortical carcinoma: IGF and beyond. Horm Cancer 2011;2:385-92.

(499) Renehan AG, Zwahlen M, Minder C, O'dwyer ST, Shalet SM, Egger M. Insulin-like growth factor (IGF)-I, IGF binding protein-3, and cancer risk: systematic review and meta-regression analysis. Lancet 2004;363:1346-53.

(500) Li SL, Liang SJ, Guo N, Wu AM, Fujita-Yamaguchi Y. Single-chain antibodies against human insulin-like growth factor I receptor: expression, purification, and effect on tumor growth. Cancer Immunol Immunother 2000;49:243-52.

(501) Mitsiades CS, Mitsiades NS, McMullan CJ, Poulaki V, Shringarpure R, Akiyama M, et al. Inhibition of the insulin-like growth factor receptor-1 tyrosine kinase activity as a therapeutic strategy for multiple myeloma, other hematologic malignancies, and solid tumors. Cancer Cell 2004;5:221-30.

(502) Buck E, Gokhale PC, Koujak S, Brown E, Eyzaguirre A, Tao N, et al. Compensatory Insulin Receptor (IR) Activation on Inhibition of Insulin-Like Growth Factor-1 Receptor (IGF-1R): Rationale for Cotargeting IGF-1R and IR in Cancer. Mol Cancer Ther 2010;9:2652-64.

(503) Mark J Mulvihill, Andrew Cooke, Maryland Rosenfeld-Franklin, Elizabeth Buck, Ken Foreman, Darla Landfair, et al. Discovery of OSI-906: a selective and orally efficacious dual inhibitor of the IGF-1 receptor and insulin receptor. Future Medicinal Chemistry 2009;1:1153-71.

(504) Netchine I, Azzi S, Le BY, Savage MO. IGF1 molecular anomalies demonstrate its critical role in fetal, postnatal growth and brain development. Best Pract Res Clin Endocrinol Metab 2011;25:181-90.

(505) Abuzzahab MJ, Schneider A, Goddard A, Grigorescu F, Lautier C, Keller E, et al. IGF-I receptor mutations resulting in intrauterine and postnatal growth retardation. N Engl J Med 2003;349:2211-22.

(506) Klammt J, Pfaffle R, Werner H, Kiess W. IGF signaling defects as causes of growth failure and IUGR. Trends Endocrinol Metab 2008;19:197-205.

(507) Rodon J, DeSantos V, Ferry RJ, Jr., Kurzrock R. Early drug development of inhibitors of the insulin-like growth factor-I receptor pathway: lessons from the first clinical trials. Mol Cancer Ther 2008;7:2575-88.

(508) Singer FR, Eyre DR. Using biochemical markers of bone turnover in clinical practice. Cleve Clin J Med 2008;75:739-50.

(509) Buck E, Gokhale PC, Koujak S, Brown E, Eyzaguirre A, Tao N, et al. Compensatory Insulin Receptor (IR) Activation on Inhibition of Insulin-Like Growth Factor-1 Receptor (IGF-1R): Rationale for Cotargeting IGF-1R and IR in Cancer. Mol Cancer Ther 2010;9:2652-64.

Appendix 1: Materials, Reagents, Apparatus and Software

1.1 Materials and Reagents used in this study:

Materials and reagents	Supplier
1.5ml eppendorf tubes with cap	Greiner Bio-One Inc, Gloucestershire, UK
10mM dNTP Mix	Invitrogen, Paisley, UK
1ml pasteur pipette	Fisher Scientific, Leicestershire, UK
2-methoxyethyl acetate (MEA)	Sigma Aldrich, Dorset, UK
2-Propanol	Sigma Aldrich, Dorset, UK
4T1	ATCC, Manassas, VA-USA
5X first-strand buffer	Invitrogen, Paisley, UK
99.7-100% AnalaR Ethanol	VWR International LTD, Leicestershire, UK
Acetic Acid Glacial	Sigma Aldrich, Dorset, UK
alamarBlue™ reagent	Invitrogen, Paisley, UK
Alizarin Red S	Sigma Aldrich, Dorset, UK

Amersham Hybond™-P	GE Healthcare Life Sciences, Buckinghamshire, UK
Basic fuchsin	Sigma Aldrich, Dorset, UK
Bicinchoninic acid (BCA) protein assay	Sigma Aldrich, Dorset, UK
Borax	Taab Lab, Berkshire, UK
Boric Acid	Taab Lab, Berkshire, UK
Bovine serum albumin	Sigma Aldrich, Dorset, UK
Bromophenol Blue	BDH Laboratory Supplies, Poole, Dorset, UK
Calcein	Sigma Aldrich, Dorset, UK
Centrifuge tubes (15 and 50ml)	Fisher Scientific, Leicestershire, UK
Cetyl pyridinium chloride monohydrate	Sigma Aldrich, Dorset, UK
Chloroform	Sigma Aldrich, Dorset, UK
Collagenase (type 1A)	Sigma Aldrich, Dorset, UK
Copper (II)-sulfate	Sigma Aldrich, Dorset, UK
Cover slips	Scientific Laboratory supplies Ltd, Hessle, UK
Criterion™ XT pre-cast gels (12% Bis-Tris)	Bio-Rad Laboratories, Hertfordshire, UK
CTX serum assay (RatLaps™ EIA)	Immunodiagnostic Systems Ltd. (IDS), Boldon Colliery, UK
DEPC Treated Water	Invitrogen, Paisley, UK
Dibenzoylperoxide	Leica Microsystems, Milton Keynes, UK
Dibutyl Phthalate	Sigma Aldrich, Dorset, UK
Diethanolamin	Sigma Aldrich, Dorset, UK
DL-Dithiothreitol (DTT)	Sigma Aldrich, Dorset, UK
DMSO	Sigma Aldrich, Dorset, UK
DNA Ladder 1kb	New England Biolabs, Hitchin, Hertfordshire, UK
dNTPs	Promega, Southampton, UK
DPX mounting medium	Sigma Aldrich, Dorset, UK
DTT	Invitrogen, Paisley, UK
EDTA	Sigma Aldrich, Dorset, UK
Electrophoresis power supply	Anachem, Bedfordshire, UK
Embedding baskets	Leica Microsystems, Milton Keynes, UK
Embedding molds	Custom-made by the University workshop
Embedding rings	Leica Microsystems, Milton Keynes, UK
Ethanol Absolute	Fisher Scientific, Leicestershire, UK
EU One-piece, non-skirted thin wall plate natural	Genetic Research Instrumentation Ltd (GRI), Essex, UK
EU One-piece,sub-skirted Thin wall plate white	Genetic Research Instrumentation Ltd (GRI), Essex, UK
EU OP flat cap thin wall 8-cap strip	Genetic Research Instrumentation Ltd (GRI), Essex, UK
Extra thick blot papers	Bio-Rad Laboratories, Hertfordshire, UK

Fetal calf serum (FCS)	Fisher Scientific, Leicestershire, UK
Filter Paper	Fisher Scientific, Leicestershire, UK
Filter Tips Axygen	Thistle Scientific, Glasgow, UK
Forceps watchmaker's	Fisher Scientific, Leicestershire, UK
Fuchsin Acid	Taab Lab, Berkshire, UK
Gelatin	Sigma Aldrich, Dorset, UK
Glycerol 2 phosphate	Sigma Aldrich, Dorset, UK
Glycine	BDH Laboratory Supplies, Poole, Dorset, UK
Hanks buffer (HBSS)	Sigma Aldrich, Dorset, UK
HistoResin Mounting Medium (solution and powder)	Leica Microsystems, Milton Keynes, UK
Human insulin-like growth factor 1	R & D Systems, Abingdon, UK
Hydrochloric acid	BDH Laboratory Supplies, Poole, Dorset, UK
Invisorb® Spin Tissue Mini Kit	Thistle Scientific, Glasgow, UK
Isopropanol	Sigma Aldrich, Dorset, UK
Jackson ImmunoResearch Anti-rabbit secondary ab	Stratech Scientific Unit, Newmarket Suffolk, UK
Kaleidoscope	Bio-Rad Laboratories, Hertfordshire, UK
Kisol foil	Taab Lab, Berkshire, UK
Knife 16cm long tungsten carbide tipped profile D	Leica Microsystems, Milton Keynes, UK
Knife Holder NZ	Leica Microsystems, Milton Keynes, UK
L-Glutamine	Invitrogen, Paisley, UK
Low molecular weight DNA ladder	New England Biolabs, Hitchin, Hertfordshire, UK
Magic Marker	Invitrogen, Paisley, UK
Magnesium chloride	Sigma Aldrich, Dorset, UK
MC3T3-E1	ATCC, Manassas, VA-USA
MC57G	ATCC, Manassas, VA-USA
MCF7	ATCC, Manassas, VA-USA
M-CSF mouse recombinant	R & D Systems, Abingdon, UK
MDA-MB-231	ATCC, Manassas, VA-USA
MDA-MB-231-BS	ATCC, Manassas, VA-USA
Medium density linkage panel	Illumina Inc., California, US
Methanol	Fisher Scientific, Leicestershire, UK
Methyl Methacrylate	Sigma Aldrich, Dorset, UK
Mettler Toledo Titrator	Fisher Scientific, Leicestershire, UK
Microtubes (0.5, 1.5, 2ml)	Sarstedt Ltd, Leicester, UK
N,N-Dimethylformamide	Fisher Scientific, Leicestershire, UK
N,N-dimethyl-p-toluidine	Leica Microsystems, Milton Keynes, UK
Napthol-AS-BI-phosphate	Sigma Aldrich, Dorset, UK

Needles (19, 21 and 25G)	Fisher Scientific, Leicestershire, UK
Neubauer Haemocytometer	Hawksley, Lancing, UK
Nitrile gloves	Fisher Scientific, Leicestershire, UK
Oligo(dt)20 Primer	Invitrogen, Paisley, UK
Orange G loading dye	Sigma Aldrich, Dorset, UK
Paraformaldehyde	Taab Lab, Berkshire, UK
Pararosanilin	Sigma Aldrich, Dorset, UK
PBS tablets	Invitrogen, Paisley, UK
PC3	ATCC, Manassas, VA-USA
PCR lid strip	Fisher Scientific, Leicestershire, UK
PCR microplate 96 well and lids	Fisher Scientific, Leicestershire, UK
PCR primers	Invitrogen, Paisley, UK
PCR microtubes	Fisher Scientific, Leicestershire, UK
Penicillin/Streptomycin	Invitrogen, Paisley, UK
Petri Dishes	Becton Dickinson, Berkshire, UK
Pierce SuperSignal® West Dura Extended Duration Substrate	Fisher Scientific, Leicestershire, UK
PINP serum assay (Rat/Mouse PINP EIA)	Immunodiagnostic Systems Ltd. (IDS), Boldon Colliery, UK
Pipette tips (all sizes)	Starlab, Milton Keynes, UK
p-Nitrophenol	Sigma Aldrich, Dorset, UK
p-Nitrophenol-phosphate	Sigma Aldrich, Dorset, UK
Polysciences Silane coated microscope slides	Park Scientific Ltd., Northampton, UK
PQIP	OSI Pharmaceuticals., Farmingdale, NY-USA
PTH	Sigma Aldrich, Dorset, UK
QIAquick PCR Purification Kit	Qiagen (UK), West Sussex, UK
Quant-iT™ PicoGreen® assay	Invitrogen, Paisley, UK
Rabbit Anti-Actin (AA20-33) IgG	Sigma Aldrich, Dorset, UK
RANKL human recombinant	Gift from Dr. Patrick Mollat (Proskelia SASU)
RNase-free water	Invitrogen, Paisley, UK
RnaseOut Recombinant Rnase Inhibitor	Invitrogen, Paisley, UK
Scalpel, disposable	VWR International LTD, Leicestershire, UK
Scissors (fine points and spring bow handles)	S Murray & Co Ltd, Surrey, UK
SensiMix(dT) Taq polymerase	GC Biotech, Alphen aan den Rijn, The Netherlands
Silver nitrate	Sigma Aldrich, Dorset, UK
Slide press cover slips	Taab Lab, Berkshire, UK
Sodium acetate anhydrous	Sigma Aldrich, Dorset, UK
Sodium barbiturate	BDH Laboratory Supplies, Poole, Dorset, UK
Sodium chloride	Sigma Aldrich, Dorset, UK
Sodium dodecyl sulphate (SDS)	Bio-Rad Laboratories, Hertfordshire, UK

Sodium hydroxide	VWR International LTD, Leicestershire, UK
Sodium phosphate	Sigma Aldrich, Dorset, UK
Sodium tartrate dibasic dihydrate	Sigma Aldrich, Dorset, UK
Sodium tetraborate	BDH Laboratory Supplies, Poole, Dorset, UK
Steel Knife 16cm "c"	Leica Microsystems, Milton Keynes, UK
Sterile filter (0.45µm)	Sartorius Mechatronics UK Ltd., Epsom Surrey, UK
Stripettes (5, 10, 25 and 50ml)	Sarstedt Ltd, Leicester, UK
SuperScript III Reverse Transcriptase	Invitrogen, Paisley, UK
SYBR Safe DNA gel stain	Invitrogen, Paisley, UK
SYBR Safe	Invitrogen, Paisley, UK
Syngene BIO imaging system	Fisher Scientific, Leicestershire, UK
Syringes (all sizes)	Becton Dickinson, Berkshire, UK
Taq DNA Polymerase	Invitrogen, Paisley, UK
TaqMan® Gene Expression Assay Mix for 18S rRNA	Applied Biosystems, Cheshire, UK
TBE buffer 10X	Invitrogen, Paisley, UK
Tissue culture 75cm^2 flasks	Fisher Scientific, Leicestershire, UK
Tissue culture microplates (6, 12, 24, 48 and 96-well plates)	Fisher Scientific, Leicestershire, UK
Toluidine Blue	Sigma Aldrich, Dorset, UK
Tris	Bio-Rad Laboratories, Hertfordshire, UK
Tris-EDTA buffer	Sigma Aldrich, Dorset, UK
Triton X-100^{TM}	Sigma Aldrich, Dorset, UK
Trizol reagent	Invitrogen, Paisley, UK
Trypsin/EDTA	Sigma Aldrich, Dorset, UK
Tween-20	Bio-Rad Laboratories, Hertfordshire, UK
Ultraclear Xylene	Taab Lab, Berkshire, UK
UPL probes	Roche Diagnostics Ltd., East Sussex, UK
UV 96 well plates for plate reader	Fisher Scientific, Leicestershire, UK
Vacuum desiccator	Fisher Scientific, Leicestershire, UK
Vitamin C (Ascorbic acid)	BDH Laboratory Supplies, Poole, Dorset, UK
xCELLigence System	Roche Diagnostics Ltd., East Sussex, UK
XT-MOPS	Bio-Rad Laboratories, Hertfordshire, UK
Xylene	Sigma Aldrich, Dorset, UK
Minimum Essential Medium (αMEM)	Sigma Aldrich, Dorset, UK
β-glycerophosphate disodium	Sigma Aldrich, Dorset, UK

1.2 Apparatus used in this thesis:

Apparatus	Supplier
AA Hoefer® protein transfer apparatus	Fisher Scientific, Leicestershire, UK
Astec Bioquell Monair 5 fume cabinet	Jencons PLS, East Grinstead, UK
Automatic tissue processor	Leica Microsystems, Milton Keynes, UK
AxioImager A1 upright research microscope	Carl Zeiss Ltd., Hertfordshire, UK
Axiovert 200 inverted research Microcope	Carl Zeiss Ltd., Hertfordshire, UK
Axiovert 40 CFL inverted microscope	Carl Zeiss Ltd., Hertfordshire, UK
Balancer Fisherbrand	Fisher Scientific, Leicestershire, UK
Bench-top centrifuge	SciQuip, Shropshire, UK
Bench-top Eppendorf centrifuge	Fisher Scientific, Leicestershire, UK
Bio-Tek Synergy HT plate reader	Fisher Scientific, Leicestershire, UK
Envair Bio2 safety cabinets	H&V Commissioning Services Ltd., Ayrshire, UK
Grant OLS 200 water bath	Thistle Scientific, Glasgow, UK
Horizontal electrophoresis tanks	Fisher Scientific, Leicestershire, UK
Hotplate/stirrer	Thistle Scientific, Glasgow, UK
Ika Vortex	Thistle Scientific, Glasgow, UK
MJ Research Chromo 4 Real Time PCR thermocycler	Genetic Research Instrumentation Ltd (GRI), Essex, UK
MJ Research Tetrad Thermal cycler	Genetic Research Instrumentation Ltd (GRI), Essex, UK
Nichiryo America Inc. Pipettes (2, 10, 100, 200 and 1000µl)	Thistle Scientific, Glasgow, UK
NoAir Class II Biological safety cabinet	TripleRed Ltd., Buckinghamshire, UK
Origo PSU-400/200 power supply for electrophoresis	Anachem, Bedfordshire, UK
PowerPac basic™	Bio-Rad Laboratories, Hertfordshire, UK
QImaging Retiga 4000R CCD camera	Media Cybernetics UK, Berkshire, UK
Rotary Microtome	Leica Microsystems, Milton Keynes, UK
Rotary tool	Dremel UK, Uxbridge, UK
SkyScan 1172 X-ray Microtomography system	SKYSCAN, Kontich, Belgium
SkyScan 1176 in-vivo micro-CT	SKYSCAN, Kontich, Belgium
Syngene GeneGenius Gel Bio-Imaging system	Fisher Scientific, Leicestershire, UK
SynSyngene GeneGnome Bio-Imaging system for chemiluminescence	Fisher Scientific, Leicestershire, UK
Vertical Criterion™ gel tanks	Bio-Rad Laboratories, Hertfordshire, UK

1.3 Software used in this thesis:

Software	Supplier
Aphelion Image Analysis tool kit	ADCIS, Hérouville-Saint-Clair, France
Bio-Tek Gen5^{TM} plate reader software	Fisher Scientific, Leicestershire, UK
GraphPad Prism (version 4)	GraphPad Software Inc., CA-US
ImageJ	U. S. National Institutes of Health Bethesda, MA-US
Opticon Monitor analysis software version 3	Genetic Research Instrumentation Ltd (GRI), Essex, UK
QCapture Pro software	Media Cybernetics UK, Berkshire, UK
Skyscan 1172 MicroCT software	SKYSCAN, Kontich, Belgium
Skyscan CTAn analysis software	SKYSCAN, Kontich, Belgium
Skyscan CTVol software	SKYSCAN, Kontich, Belgium
Skyscan NRecon reconstruction system	SKYSCAN, Kontich, Belgium
SPSS version 13	SPSS Ltd. UK, Surrey, UK
Syngene GeneSnap software	Fisher Scientific, Leicestershire, UK
Syngene GeneTool software	Fisher Scientific, Leicestershire, UK
TScratch	ETH Zürich, Switzerland

Appendix 2 : Solutions and Recipes

Appendix 2.1 Solutions for TRAcP staining

Naphthol-AS-BI-phosphate

10 mg/ml Naphthol-AS-BI-phosphate in Dimethylformamide

Veronal buffer

1.17 g sodium acetate anhydrous and 2.94g sodium barbiturate both dissolved in 100 ml of dH_2O

Acetate buffer

0.82 g sodium acetate anhydrous dissolved in 100 ml of dH_2O and pH adjusted to 5.2 with 0.6 ml glacial acetic acid made up to 100 ml with dH_2O

Pararosanilin

1 g Pararosanilin dissolved in 20 ml of dH_2O and 5 ml of 5M HCl added to it

The solution was heated carefully whilst stirring and filtered after cooling.

TRAcP Staining Solution

The TRAcP staining solution was freshly prepared by mixing solution A and B as outlined below.

Solution A

150 ml of Napthol-AS-BI-phosphate

750 ml of Veronal buffer

900 ml Acetate buffer

900 ml Acetate buffer with 100 mM Sodium Tartate

Solution B

120 ml of Pararosanilin

120 ml of Sodium Nitrate (4% w/v)

Appendix 2.2 Solutions for ALP assay

Diethanolamine (DEA)/$MgCl_2$ buffer

1 M DEA and 1 M $MgCl_2$ made up in 100 ml dH_2O and pH adjusted to 9.8. Left at room temperature for 24 hours

ALP Lysis buffer

0.05% Triton X-100 added to DEA/$MgCl_2$ buffer

p-Nitrophenol standard solution

p-Nitrophenol standards (1.25 – 30 nM) prepared in lysis buffer

Substrate solution

20 mM p-nitrophenol-phopshate made up in DEA/$MgCl_2$ buffer and pH adjusted to 9.8

Appendix 2.3 Solution for cell Lysis

RIPA Lysis buffer

1% Triton 100X, 0.5% (w/v) Sodium Deoxycholate, 0.1% (w/v) Sodium Dodecyl Sulphate (SDS), 50 mM Tris-HCl (pH 7.4) and 150 mM Sodium Chloride were dissolved in dH_2O.

Appendix 2.4 Solutions for PAGE and western blot

Electrophoresis running buffer

50 ml of XT-MOPS (20X) in 1000 ml of dH2O

Samples loading protein buffer (5X stock)

5.2 ml of 1M Tris-HCl pH adjusted to 6.8, 1 g of DL-Dithiothreitol (DTT), 3 g SDS, 6.5 ml glycerol and 130 □l of 10% (w/v) Bromophenol Blue. Stored at -20□C.

Transfer buffer

3.63 g of Tris, 14.4g of Glycine, 200 ml of Methanol and 3.75 ml of 10% (w/v) SDS made up to 1000 ml with dH_2O. Stored at room temperature.

TBS

1 M of Tris and 1 M Tris-HCl. pH adjusted to 7.9 prior to addition of 3 M Sodium Chloride. Stored at room temperature.

TBST

0.1% (v/v) Tween-20 in TBS. Stored at room temperature.

Stripping buffer

1 mM DTT, 2% (w/v) SDS and 62.5 mM Tris-HCl (pH 6.7). Stored at room temperature.

Appendix 2.5 Solutions for Histology

Infiltrating solution

89 g MMA, 10 g Dibutyl phthalate, 1 g Perkadox 16, and 0.01 g Novoscave for 100 g of infiltration solution

Embedding solution

Same as infiltration solution but 1 week old

Paragon staining solution

0.625 g basic fuchsin and 1.875 g toluidine blue in 250 ml 30% (v/v) ethanol

Borax buffer

6 g boric acid and 2 g sodium tetraborate in 500 ml dH_2O

Appendix 3: qPCR Primers and Probes

Gene (all human unless stated)	Forward Primer	Reverse Primer	Taqman Probe
18s	N.A. part of kit	N.A. part of kit	N.A. part of kit
C-Fms	gcagcgttgatgttaactttgat	gttgagggattgcgagctta	10
GAPDH	agccacatcgctcagacac	gcccaatacgaccaaatcc	60
GAPDH (mouse)	cctgaattttaagctacacacagc	ctggcactgcacaagaagat	84
IGF-1	tgtggagacaggggctttta	atccacgatgcctgtctga	67
IGF-1 (mouse)	caaaagcagcccgctcta	tgcacttcctctacttgtgttctt	104
IGF-1R	aaaaaccttcgcctcatcc	tggttgtcgaggacgtagaa	55
IGF-1R (mouse)	gagaatttccttcacaattccatc	cacttgcatgacgtctctcc	104
IL-1β	agctgatggccctaaacaga	tcggagattcgtagctggat	12
M-CSF	gcaagaactgcaacaacagc	agttgcaatcaggcttggtc	19
MMP9	gaaccaatctcaccgacagg	gccacccgagtgtaaccata	6
OPG (mouse)	atgaacaagtggctgtgctg	cagtttctgggtcataatgcaa	69
PTHrP	ctcggtggagggtctcag	tggatggacttccccttgt	17
RANK	gaacatcatgggacagagaaatc	ggcaagtaaacatggggttc	53
RANKL	tgattcatgtaggagaattaaacagg	gatgtgctgtgatccaacga	17
RANKL (mouse)	tgaagacacactacctgactcctg	ccacaatgtgttgcagttcc	88
TGFβ	actactacgccaaggaggtcac	tgcttgaacttgtcatagatttcg	31
TNFα	agcccatgttgtagcaaacc	tctcagctccacgccatt	79
UPa	ttgctcaccacaacgacatt	ggcaggcagatggtctgtat	46

Appendix 4 : Publications from Thesis